



A methodological framework for assessing and reducing temporal uncertainty in paleovegetation mapping from late-Quaternary pollen records

Jessica L. Blois ^{a,*}, John W. Williams ^a, Eric C. Grimm ^b, Stephen T. Jackson ^c, Russell W. Graham ^d

^a Department of Geography and the Center for Climatic Research, University of Wisconsin-Madison, 1225 W. Dayton St., Madison, WI 53706, USA

^b Research and Collections Center, Illinois State Museum, Springfield, IL 62703, USA

^c Department of Botany and Program in Ecology, University of Wyoming, Laramie, WY 82071, USA

^d Earth and Mineral Sciences Museum, Pennsylvania State University, University Park, PA 16802, USA

ARTICLE INFO

Article history:

Received 9 February 2011

Received in revised form

23 April 2011

Accepted 25 April 2011

Available online 11 June 2011

Keywords:

Neotoma

Age model

Quaternary

Paleoecology

Pollen core

ABSTRACT

Mapping past vegetation dynamics from heterogeneous databases of fossil-pollen records must face the challenge of temporal uncertainty. The growing collection of densely sampled fossil-pollen records with accurate and precise chronologies allows us to develop new methods to assess and reduce this uncertainty. Here, we test our methods in the context of vegetation changes in eastern North America during the abrupt climate changes of the last deglaciation. We use the network of fossil-pollen records in the Neotoma Paleoecology Database (www.neotomadb.org) and data contributed by individual investigators. Because many of these records were collected decades before the current generation of ¹⁴C and age-model technologies, we first developed a framework to assess the overall reliability of ¹⁴C chronologies by systematically evaluating individual ¹⁴C ages and associated chronologies. We developed a qualitative ranking scheme for individual ¹⁴C ages that combines information about their accuracy and precision. 'Benchmark' pollen records were defined to have at least one ¹⁴C age with an accuracy within 250 years and a precision less than 500 years that is within 1000 years of the time interval of interest, and at least five pollen samples per 1000 years across this time period. Only 22 of >350 late-Pleistocene pollen cores in eastern North America met the benchmark criteria. We then used Bayesian change-point analysis to identify widespread ecological events (*Picea* decline, *Quercus* rise, and *Alnus* decline), and interpolated the ages of these events from the benchmark sites to non-benchmark sites. Leave-one-out cross-validation analyses with the benchmark sites indicated that the spatial error associated with interpolation was less for inverse distance-weighting (IDW) than thin-plate splines (TPS) and was about 500 years for the three biotic events. By comparison, the difference between the original ages of events at poorly constrained sites and the biostratigraphic ages interpolated from the benchmark sites was close to 1000 years, suggesting that the use of biostratigraphic ages can significantly improve the age models for poorly constrained sites. Overall, these analyses suggest that the temporal resolution of multi-site syntheses of late-Pleistocene fossil-pollen data in eastern North America is about 500 years, a resolution that allows analysis of ecological responses to millennial-scale climate change during the last deglaciation.

© 2011 Elsevier Ltd. All rights reserved.

1. Introduction

Future climates are projected to warm substantially and rapidly (Solomon et al., 2007) and how species and communities will respond to these changes is still uncertain. The paleoecological record of past vegetation change is a powerful source of data for

understanding potential responses. The rates and magnitudes of abrupt climate changes such as the initiation of the Bølling-Allerød event 14.5 thousand calendar years ago (ka) and the initiation and termination of the Younger Dryas event (12.9–11.5 ka) (Denton et al., 2010) approximate those projected for the 21st century (Overpeck et al., 2003; Williams et al., 2011); these time periods are thus critical for studying ecological responses to abrupt climate change. Integrative analyses of paleoecological records can help to answer questions about the velocity of species migration and population expansion, changes in vegetation composition, ecological resilience

* Corresponding author. Tel.: +1 650 804 2934; fax: +1 608 263 4190.

E-mail address: blois@wisc.edu (J.L. Blois).

to climate change, and ecosystem responses to abrupt climate change (Flessa and Jackson, 2005; Willis et al., 2010; Dietl and Flessa, 2011).

Mapped networks of fossil-pollen and plant-macrofossil data are the primary source of information about spatial responses of plant species and communities to late-Quaternary climate change. Thousands of pollen records from the late Quaternary have been collected globally and are incorporated into public databases (APSA Members, 2007; Grimm et al., 2007; Binney et al., 2008; Fyfe et al., 2009). Syntheses of these records have provided fundamental insights into the relative sequence and nature of vegetation change over the past 21,000 years (e.g. Firbas, 1950; Davis, 1976; Huntley and Birks, 1983; Williams et al., 2004). Increasingly, these datasets are used to determine the timing and rate of vegetation responses to rapid climate change (e.g. Shuman et al., 2002; Peros et al., 2008). At local to regional scales, sites with paired vegetation and climate records demonstrate that shifts in vegetation composition occurred within decades or less of abrupt climate change (e.g. Birks and Ammann, 2000; Williams et al., 2002; Yu, 2007). At sub-continental scales, late-Quaternary vegetation has been mapped at 1000-year intervals (Williams et al., 2004). These maps summarize the spatial patterns of vegetation dynamics when forced by climate at orbital to millennial timescales, while rate-of-change analyses based on these datasets show elevated rates of community turnover associated with the Younger Dryas and Pleistocene/Holocene transition (Jacobson et al., 1987; Grimm and Jacobson, 1992; Williams et al., 2004; Shuman et al., 2005).

These mapped syntheses, however, are critically limited by the accuracy and precision of the ^{14}C ages and age models of the constituent pollen records (Grimm and Jacobson, 2003), which limits their utility for studying climate-driven vegetation dynamics at sub-millennial scales. Most pollen records used in these syntheses were developed before current methods of ^{14}C dating were available and are based on sparse, inaccurate, and/or imprecise ^{14}C ages. Nevertheless, these records contain unique information about local vegetation history and so there is value in retaining them in integrative analyses.

An emerging challenge is to use the relatively precise chronological information available in a small but growing set of fossil-pollen records with highly accurate and precise chronologies, while also taking advantage of the spatial density of the full pollen databases. One way forward is to use ecological events from the well-dated records as biostratigraphic markers to update the age models of other, more poorly constrained pollen records. We first review sources of temporal uncertainty in paleovegetation mapping, then outline a conceptual framework for ranking the quality of individual ^{14}C ages and site chronologies that assesses both the random and systematic sources of error (Section 2). In Section 3, we apply this framework to identify the best pollen records (which we term ‘benchmark’ sites). We then use Bayesian change-point analysis (Barry and Hartigan, 1993; Emerson and Erdman, 2007) to determine the timing of widespread ecological events for the benchmark sites (the end-Pleistocene *Picea* decline, *Quercus* rise, and *Alnus* decline). We reassess the timing of these ecological events at poorly constrained sites by spatially interpolating the event ages from the benchmark sites to all sites across the region. Although conceptually similar to using pollen-zone boundaries as a tool for stratigraphic correlation (e.g., Deevey, 1939; von Post, 1946), the use of events linked to individual taxa rather than to overall pollen assemblages is preferable because taxa respond individualistically and their changes can be tracked over larger areas than pollen zones, which are often definable only for limited spatial regions. Additionally, our method neither assumes nor rejects synchrony of biological events (Blaauw, 2010b), but only assumes that these events spatially propagate in a smooth manner. Maps of these events also

provide an opportunity to study the spatial velocity of major biotic changes. Finally, we quantify the temporal uncertainty associated with individual sites and the spatial interpolation of ecological events and assess the impact of the new biostratigraphic age estimates on the poorly constrained chronologies. These analyses lay the foundation for a new generation of maps and other syntheses designed to understand sub-millennial vegetation responses to rapid climate changes.

2. Sources of temporal uncertainty in paleovegetation mapping

Multiple sources of temporal uncertainty affect paleovegetation mapping. The quality of a chronology for a site depends on the density of independent age controls, the accuracy and precision of individual ^{14}C ages and other age controls, uncertainties in the ^{14}C calibration curve, and uncertainties in age models. If biostratigraphic events are used as age controls, additional uncertainty arises from the assumptions built into the spatial interpolation of ecological events among sites. Simple assumptions that biostratigraphic events are synchronous are particularly problematic (Smith and Pilcher, 1973; Blaauw, 2010b). Temporal uncertainties for individual site chronologies accumulate when assembling data from many irregularly distributed sites having chronologies of varying quality (Bennett, 1994; Bennett and Fuller, 2002). In order to build and critically evaluate syntheses of past vegetation dynamics, all sources of temporal uncertainty must be quantified and minimized.

We focus here on ^{14}C ages because these are by far the most common form of radiometric dating for late-Quaternary pollen records. The quality of a ^{14}C age comprises two components: precision and accuracy. Precision refers to the temporal width of the probability density function (pdf) of a radiometric age. Here we define precision as the two-sigma or 95% highest posterior density region of the calibrated ^{14}C age or other absolute age control. For ^{14}C ages, precision depends on analytical precision and the shape of the calibration curve. The major constraint on analytical precision is the amount of carbon in the sample and its age (Bronk Ramsey, 2008), which is why small and old materials tend to have the worst precision. Analytical precision is also affected by the dating method, particularly between conventional radiometric versus accelerator mass spectrometry (AMS) ^{14}C dating. As technologies have improved, precision has increased (Santos et al., 2007). For a ^{14}C age of a given analytical precision, the precision of the calibrated age is highly dependent upon the shape of the calibration curve where intercepted by the ^{14}C -age pdf. Because of variations in atmospheric ^{14}C through time (Damon et al., 1978), the calibration curve is irregular and non-monotonic (e.g. Reimer et al., 2009). Wiggles in the curve usually cause the pdfs of calibrated ages to be broader than their ^{14}C -age pdfs. However, if the ^{14}C pdf intercepts a steep portion of the calibration curve, the calibrated ^{14}C age may be more precise than the original measurement.

The accuracy of an age control is defined as the magnitude of any offset between the true age and estimated age of an event. A ^{14}C age may be precisely measured, but inaccurate if the age of the dated material does not correspond with the age of deposition. Accuracy depends upon the type and amount of material chosen for ^{14}C dating, as well as stratigraphic integrity and depositional processes. For a ^{14}C age to accurately estimate the true age, $\Delta^{14}\text{C}$ in the dated sample must represent atmospheric $\Delta^{14}\text{C}$ at the time of deposition. Contamination in the field or laboratory can bias the results, producing either too old or too young ^{14}C ages. Ages on small amounts of material are more susceptible to contamination and thus inaccurate ages (Bronk Ramsey, 2008). Perhaps an even more serious problem is that carbon in lake sediments can be redeposited

or derived from older sources. The well known “hardwater effect” results from aquatic organisms such as algae and submersed aquatic plants incorporating ^{14}C -depleted carbon derived from groundwater dissolution of carbonate rocks such as limestone and dolomite (e.g. Deevey Jr et al., 1954; Andree et al., 1986; MacDonald et al., 1991; Grimm et al., 2009). The hardwater effect is generally a problem with bulk-sediment ages, but also with shells from ostracodes and mollusks, for example. On some landscapes, old carbon derived from extensive peatlands (Lowe et al., 1988) may bias ^{14}C ages, and on some geological settings old carbon from carbonaceous rocks such as shales and lignite may severely bias bulk-sediment ^{14}C ages—by as much as 8000 years (Grimm et al., 2009).

Given these problems with bulk-sediment ages, terrestrial plant macrofossils are preferred now for dating. However, terrestrial plant macrofossils may also provide inaccurate ages. Wood and wood charcoal, although in principle excellent materials for ^{14}C dating, may exhibit “in-built” ages because they may be derived from long-lived or long-dead trees (Gavin, 2001). Wood and wood charcoal are resistant to decay and physical destruction and may persist for a long time before transport to lake sediments (Barnekow et al., 1998; Gavin, 2001; Oswald et al., 2005). In contrast, charcoal from short-lived herbaceous plants is much more delicate and may, in general, provide more accurate ^{14}C ages (Grimm et al., 2009). But even terrestrial plant macrofossils well suited for dating, such as small seeds and conifer needles, may be redeposited, perhaps from shallower lake sediments (Turney et al., 2000; Grimm, 2011).

In most cases, accuracy cannot be determined directly because the true ages are not known. However, accuracy can be qualitatively assessed based on expert knowledge of potential sources of systematic bias. This assessment considers two sets of processes: those preceding the death or excision of the material (i.e., residence time of the dated material in the living organism) and those occurring from the time of death to deposition (i.e., residence time in the environment). For example, residence times of seeds on a tree are on the order of one or at most a few years, while stem wood may be derived from tissue formed from 10^0 to 10^3 years prior to tree death. Once the tree's tissues are released to the environment (e.g. through seedfall or tree death), taphonomic processes determine the residence time before the material is transported and permanently deposited in a sedimentary archive. Typical environmental residence times range from 10^0 to 10^3 years, depending on the material and the depositional setting. For example, transport and burial of an intact seed in lake sediments may have occurred within a year, whereas wood fragments in a fluvial setting may have been deposited, reworked, and redeposited for decades to centuries—or even millennia—before final deposition. Accuracy will be highest when pre- and post-death residence times are minimal. With a sufficient number of ^{14}C ages from a sedimentary sequence, large inaccuracies in any single age will usually be evident. More difficult to detect are small errors of a few decades or centuries.

Major strides have been made in the past decade toward understanding the best material and methods for dating pollen cores, for improving the precision of ^{14}C calibration curves (e.g. Bronk Ramsey, 2008), and for constructing age models (e.g. Parnell et al., 2008; Blaauw, 2010a). A new generation of fossil-pollen records with high-precision ^{14}C ages on carefully chosen organic carbon has been collected over the last decade [e.g., Kettle Lake (Clark et al., 2002; Brown et al., 2005; Grimm, 2011), White Lake (Yu, 2007)]. However, many records contain very few (or no) radiometric ages, and many of the existing radiometric ages may be inaccurate. One option is to simply discard these records, but this practice eliminates considerable information because each site is a unique record of vegetation history at a particular locale. Alternatively, the

age models for these records can be reassessed and refined by using non-radiometric age controls such as biostratigraphic events. In this approach, the ages of major ecological events at well-dated sites are spatially interpolated to other sites and used as age controls for the chronologies of these sites. This procedure introduces new complications, particularly that age models based on biostratigraphic ages are no longer fully independent of age models from other sites and thus incorporate assumptions about spatiotemporal propagation of ecological events (Blaauw, 2010b). Furthermore, many methods are available for spatially interpolating events between sites, and interpolation precision may vary based on technique, so a new source of uncertainty emerges when transferring ages of ecological events at individual sites to nearby sites: error due to the method of spatial interpolation.

2.1. Conceptual framework for determining benchmark chronologies

The framework developed here explicitly accounts for and limits many of the above sources of error. There are three main elements: 1) a system for ranking the quality of individual ages, based on their accuracy and precision, 2) a system for identifying benchmark chronologies, and 3) methods for identifying major ecological events, interpolating the ages of events to other sites, and quantifying the error of spatial interpolation for the resultant biostratigraphic ages. We outline the criteria used to rank ^{14}C ages and identify benchmark sites here, then develop the interpolation methods in Section 3.

Our framework for ranking the quality of individual ages (Table 1) jointly addresses the issues of accuracy and precision outlined above. Because accuracy is rarely known, we developed a qualitative ranking scheme (Table 1) and assigned ranks to individual ^{14}C ages based on their material and depositional setting (Appendix A). We also converted precision into a qualitative ranking, scaled to be comparable to the accuracy rankings. Our ranking categories capture a wide range of possible accuracies and precisions and can be extended further as needed.

After each ^{14}C age was coded for accuracy and precision, we developed a set of criteria to identify benchmark sites, i.e. sites with the most accurate and precise temporal resolution. The density and quality of ages and sampling resolution varies within sites, so some sites may be benchmarks for one time period, but not another. Because our objective is to map sub-millennial-scale ecological phenomena, we defined a benchmark site according to the following criteria: a) the chronology contained, within 1000 years of the time period of interest, at least one AMS ^{14}C age with an accuracy rank ≤ 4 (i.e., on terrestrial material with a short residence time, such as seeds, twigs, and cones) and precision rank ≤ 5 (a calibrated 95% confidence interval <500 years) (Table 1); b) the time period contained at least 5 pollen samples per 1000 years. The

Table 1

Accuracy and precision ranks assigned to each ^{14}C age. Benchmark sites had at least one ^{14}C age within 1000 years of the time period of interest with accuracy less than or equal to rank 4 and precision less than or equal to rank 5.

Rank	Accuracy	Precision
	The true age of event and estimated age may be systematically offset by:	The calibrated age range is:
1	≤ 1 years	≤ 1 years
2	≤ 10 years	≤ 10 years
3	≤ 100 years	≤ 100 years
4	≤ 250 years	≤ 250 years
5	≤ 500 years	≤ 500 years
6	≤ 1000 years	≤ 1000 years
7	≤ 5000 years	≤ 5000 years
8	>5000 years	>5000 years

only non-radiometric ages allowed in benchmark chronologies were core tops and the ages of the European settlement (e.g. marked by a rise in *Ambrosia* pollen), though these markers were largely irrelevant here since this paper focuses on the late Pleistocene. This definition of a benchmark was designed for our specific research objectives and may be too restrictive (or too loose) for other applications.

3. Materials and methods

3.1. The Neotoma paleoecology database

We focus on lake-sediment records from eastern North America in the Neotoma paleoecology database (www.neotomadb.org). Neotoma is a multiproxy relational database that stores fossil data for the past 5 million years (the Pliocene and Quaternary). The fossil-pollen component of Neotoma currently comprises over 4200 sites globally, with almost 400 additional sites submitted and awaiting data upload. We limited our search to records with pollen data between 21 and 11.5 ka; we will soon extend our effort to the Holocene. Overall, 371 sediment cores were included in this analysis (Fig. 1).

3.2. Ranking the quality of individual ages and defining benchmark sites

We assessed the quality of all ^{14}C ages and defined benchmark sites according to the criteria outlined in 2.1. Each ^{14}C age was assigned an accuracy ranking based on the type of the dated material (Table 1, Appendix A). The precision of each ^{14}C age was calculated based on the 95% confidence interval of the calibrated age and converted into a qualitative ranking (Table 1). All ages were calibrated in Calib 6.0 (Stuiver and Reimer, 1993) using the IntCal09 calibration curve (Reimer et al., 2009). For non-radiometric ages, such as core tops or cultural associations, the precision rank was calculated from the author-determined age range.

3.3. Age models

Except where noted (Section 3.7), we relied on the default Neotoma chronologies, particularly regarding the shape of the age model (e.g., linear interpolation vs polynomial) and decisions about which ^{14}C ages were rejected or averaged. Neotoma's defaults were developed by either the original researchers, previous working groups, or by the Neotoma data steward upon data upload. These chronologies are based largely on radiometric ages (mostly ^{14}C) from diverse source materials and biostratigraphic markers. Neotoma stores age estimates but not age-model uncertainty for each sample within a pollen record. We estimated the chronology error for samples by assigning the maximum 2-sigma calibrated age range of the age controls bracketing each pollen sample to the estimated sample ages and assumed a uniform error distribution within this age range.

We explicitly chose not to override the expert knowledge that went into creating the original age model at a site, unless we had information not available to the original authors (e.g. the IntCal09 calibration curve). However, we tested the effect of simply updating the default age model to IntCal09 versus constructing a Bayesian age model by comparing the Neotoma chronologies with chronologies constructed in Bchron (Supplementary Discussion, Supplementary Figs. 1 and 2; Haslett and Parnell, 2008; Parnell et al., 2008). The expected values of the original and Bayesian models generally show only small differences (<200 years), mainly because Bayesian approaches have little impact unless the pdfs of the calibrated radiocarbon ages overlap enough to constrain each

other (Supplementary Fig. 1). There were also no systematic differences in uncertainty surrounding the event ages between the two types of chronologies, although a few sites showed larger uncertainties in the Bayesian estimates of age ranges at some ecological events (Supplementary Fig. 1).

3.4. Determining significant biostratigraphic events

We used a combination of Bayesian change-point analysis and visual analysis to identify biostratigraphic events at all cores. Five end-Pleistocene biostratigraphic events were selected *a priori*, based on their widespread occurrence in eastern North America: *Picea* decline, *Alnus* rise and decline, *Pinus* rise, and *Quercus* rise (Mayle et al., 1993a; Williams et al., 2004). For example, we scanned each time series of *Picea* pollen abundance at benchmark sites to determine if there was a change-point associated with the final decline in *Picea* near the end of the Pleistocene (Fig. 2). Not all sites manifest each event. We used the R package BCP (Emerson and Erdman, 2007) to determine change points. BCP implements a Bayesian analysis (Barry and Hartigan, 1993) that partitions the time series of relative-abundance data into segments such that the mean relative abundance is constant within segments. We used 1000 Markov Chain Monte Carlo (MCMC) iterations with a burn-in period of 100 iterations, and set the prior variance equal to the observed variance for the entire core. For each sample in the time series, BCP determines the posterior probability that the sample is a change point, i.e. a point of significant change in abundance between two segments of different mean abundances. The change-point analyses typically find a few intervals with a high probability of being a change point and most with a low probability (Fig. 2).

For benchmark sites, we set an initial threshold of ≥ 0.80 posterior probability to identify change points and visually inspected the relative abundance plot to determine which change point, if any, was associated with a particular biostratigraphic event. We relaxed the 0.80 threshold for a few cases in which we were both visually confident of an event and the BCP analysis detected a lower probability change point, which happened for several time series for each ecological event (>0.6 probability threshold for the *Alnus* decline at Splan Pond, and the *Quercus* rise at Clear Pond, Hiscock Site, Sutherland Pond, and White Lake, and >0.3 probability threshold at Chase Pond for the *Alnus* decline; Supplementary Information). Our identification of change points is thus primarily determined by statistical methods but unavoidably includes some degree of judgment. So that others can review our decisions, Supplementary Fig. 3 shows the relative-abundance diagrams for the relevant pollen types for all benchmark sites, with our decisions about which change points were associated with an event at each site. For non-benchmark sites, we used the same change-point analysis procedure to determine the depths of the biostratigraphic events, but adhered to a strict 0.80 posterior probability threshold.

3.5. Spatially interpolating the ages of biostratigraphic events to other sites

We inferred the mean age of an ecological event at each poorly constrained site by interpolation among benchmark sites. We compared the performance of two spatial interpolation techniques: inverse distance-weighting (IDW) and thin-plate spline (TPS) interpolation. For IDW, inverse distance power was set to 2. For TPS, we set the appropriate smoothing parameter (lambda) by generalized cross-validation. For both IDW and TPS, we experimented with two sets of spatial parameters for the interpolation: latitude and longitude (which we call 2d), and latitude, longitude, and altitude (3d). All latitude and longitude coordinates were

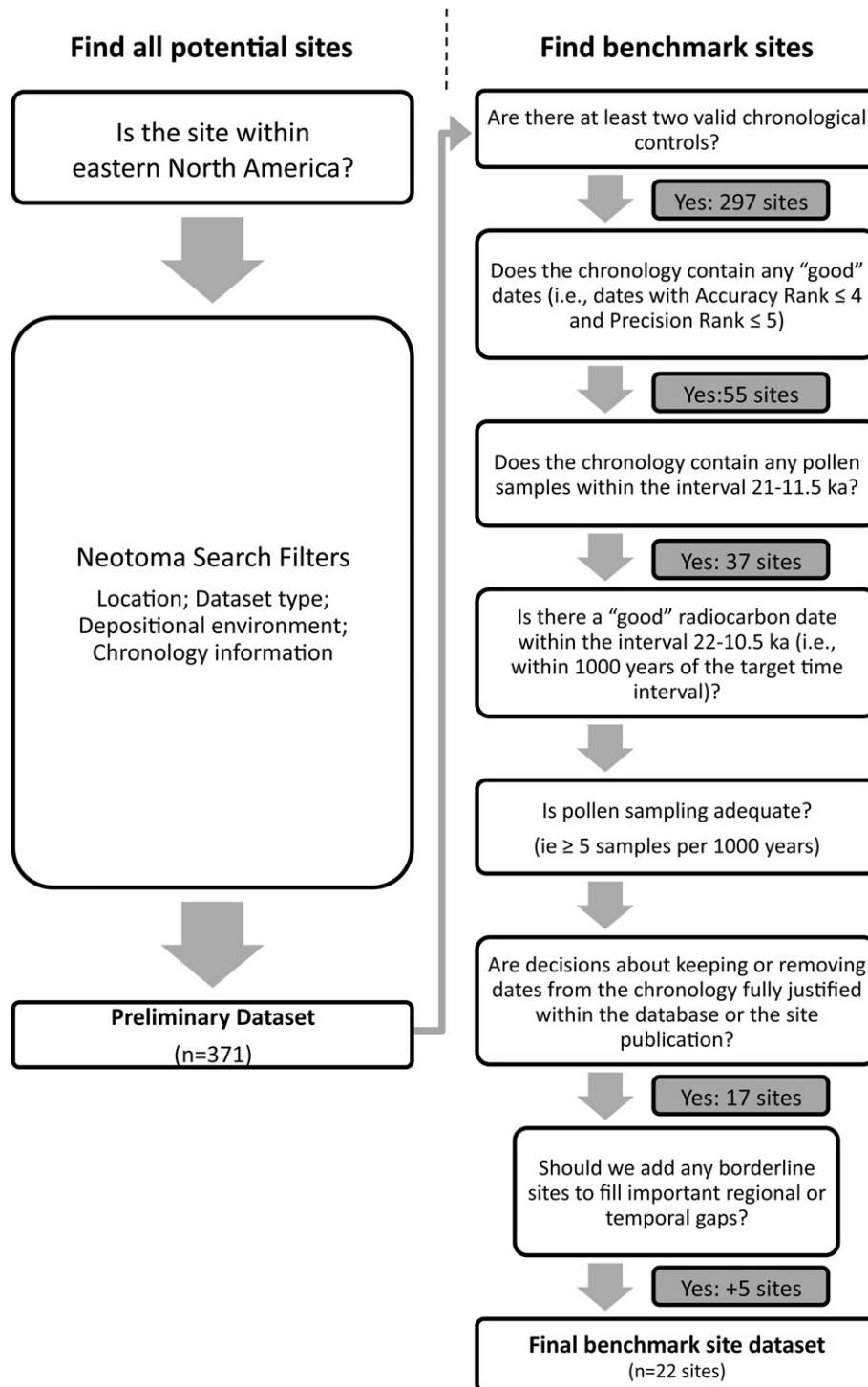


Fig. 1. Flow chart outlining the search criteria within Neotoma used to identify the initial list of potential benchmark sites in eastern North America (left hand column), and the criteria used to narrow the initial list down to benchmark sites. The specific Neotoma search filters included: 1) Location. Sites within the United States or Canada east of -111° longitude, excluding sites within the states/provinces of Arizona, Northwest Territories, Nunavut, New Mexico. 2) Dataset type = pollen. 3) We excluded sites from the following depositional environments*: Biological (ID #6), Estuarine (ID #16), Playa (ID #47), Coastal (ID #52), Fluvial (ID #77), Stream-cut Exposure (ID #92), Terrestrial (ID #103), Cave (ID #109), Soil (ID #127), Other (ID #136), Unknown (ID #137). 4) Chronology information: We relied on the default chronology, restricting the AgeBoundYounger to $\leq 22,000$ years. All terms and IDs are as in the Neotoma database.

converted to North America Albers Equal Area Conic projection (Origin: 40°N , 96°W , standard parallels: 20°N , 60°N). Altitude was upweighted in the 3d interpolation by using a scaling factor set to the approximate ratio of the temperature lapse rate across latitude versus elevation in eastern North America (1-km elevation ≈ 600 -km latitudinal distance) ([Hopkins, 1920](#); [MacArthur, 1972](#)).

Because the sample depth of each ecological event in the benchmark sites was associated with an age plus estimated uncertainty (see Section 3.3), we randomly drew an age of the change point from the uniform age range associated with the event depth and repeated the IDW and TPS analyses 1000 times to calculate mean interpolated ages.

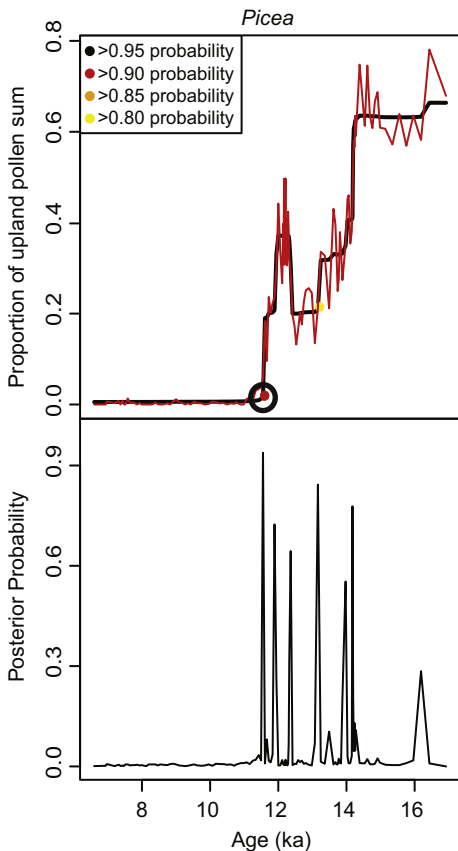


Fig. 2. Change point diagram for *Picea* at Crystal Lake, IL (Gonzales and Grimm, 2009). The upper graph shows the original relative abundance, as a proportion of the upland pollen sum (red line) and the posterior mean probability relative abundance (black line). Probable change points (based on BCP analysis) are indicated in filled circles and the change point that we identified as corresponding to each biostratigraphic event is circled. The bottom graph shows the posterior probability of a change point occurring at a given sampling age. (For interpretation of the references to color in this figure legend, the reader is referred to the web version of this article.)

3.6. Cross-validation

To estimate error in the benchmark sites associated with spatial interpolation, we used a leave-one-out cross-validation analysis in which we sequentially dropped each benchmark site from the dataset and used the remaining benchmark sites to estimate the mean event age at the dropped site. We used the same bootstrapping procedure with 1000 replicates as in Section 3.5. We then calculated the site cross-validation error by determining the difference between the original age of the event estimated by change point analysis and the mean interpolated age of the event at the dropped site. We used mean absolute error (MAE) to summarize cross-validation error across all sites. Additionally, sites were classified as interpolation or extrapolation sites based on whether they were located within or on the boundary of a minimum convex polygon around all sites. (During cross-validation, removing a site that lies on this boundary forces the interpolation technique to extrapolate to it from the other remaining sites.) We recalculated MAE for the boundary and internal sites separately, which provided measures of extrapolation and interpolation error. Interpolation error is the most relevant diagnostic, because biostratigraphic ages were only assigned to non-benchmark sites if they lay within the minimum convex polygon (i.e., we did not allow extrapolation). We also examined the error statistics for systematic bias by correlating the site cross-validation error with five site characteristics: the

original age of the event, temporal sampling resolution at the time of the event, latitude, longitude, and altitude. For each event, we also determined the influence of potential outliers on interpolation reliability.

3.7. Impact of the new biostratigraphic age estimates on chronologies

To assess the influence of the new biostratigraphic age estimates on chronologies, for each site we compared the mean age of an event based on interpolation between the benchmark sites to the age estimate based on the original chronology. In order to strictly limit this comparison to the effects of the interpolation, we slightly modified the original chronologies by recalibrating all age controls within the Neotoma default age model to the IntCal09 calibration curve and recalculated ages at individual sampling depths. For this comparative analysis, we only used cores with at least two ^{14}C ages and we removed all non- ^{14}C -based ages (such as deglaciation ages, or age of the *Tsuga* decline) from the analysis except for core top and *Ambrosia* rise/European settlement. The form of the age model (e.g., linear interpolation, polynomial) was unchanged from the original age model. Once the age model was updated, we extracted the ages associated with the change point depths.

All analyses (change-point detection, interpolation and cross-validation) were done using the statistical package R (R Development Core Team, 2010). Copies of the scripts used for change-point determination and event age interpolation and cross-validation are provided in the Supplementary Information.

4. Results

4.1. Determining benchmark sites

We searched Neotoma for all North American pollen records east of the Rocky Mountains with ^{14}C ages, focusing on lake and mire depositional environments (Figs. 1 and 3). This search provided a list of initial sites ($n = 371$) with over 3150 associated ^{14}C ages (Appendix B). Of these sites, 297 sites had sufficient chronological information for this project (e.g. at least 2 valid age controls to interpolate ages to undated samples), but only 17 sites met all criteria for being a benchmark site for at least part of the late Pleistocene (Fig. 1). To this list, we added three sites because their chronologies nearly met the benchmark site criteria, and they filled important regional or temporal gaps: Brown's Pond, Cottonwood Lake, and Sharkey Lake. The chronology for Brown's Pond, VA (Kneller and Peteet, 1993) did not meet the age precision criterion; it had one good age (accuracy rank = 2, precision rank = 5) at 8.5 ka, among other lower-quality ages. However, this site clearly fills an important spatial gap (Fig. 3). Cottonwood Lake, SD (Barnosky et al., 1987; Grimm et al., 2009) also fails the precision threshold, with one good age at 8.6 ka, but this site increases site density in the sparsely sampled western region of the dataset (Fig. 3). Sharkey Lake, MN (Camill et al., 2003) did not meet the sampling density criterion (roughly 4 samples per 1000 years rather than 5), but this site bridges a gap between sites close to Great Lakes and sites farther west so we retained this site as well (Fig. 3). Additionally, two sites met most criteria, but their sampling did not extend into the late Pleistocene (21–11.5 ka) [Blackwoods Hollow, ME (Schauffler and Jacobson Jr., 2002) and Steel Lake, MN (Wright et al., 2004; Tian et al., 2005)]. These sites were used in cases when ecological events extended into the early Holocene. Overall, we identified 22 benchmark sites (Figs. 1 and 3). Even given the expanded final list of benchmark sites, the spatial and temporal density of these sites varied greatly (Fig. 3).

The highest density of benchmark sites was found in the time period 12.9–11.5 ka (22 sites), and benchmark sites for other late-

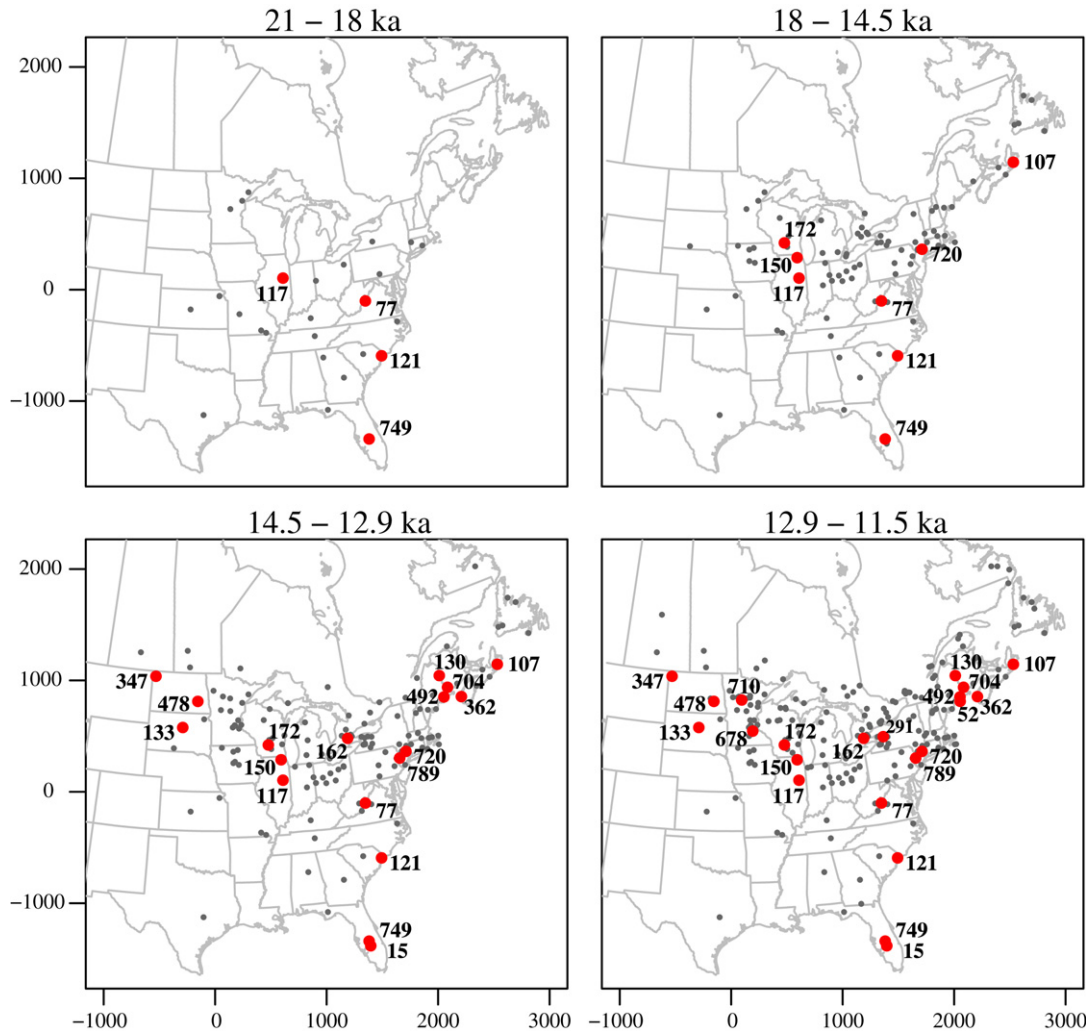


Fig. 3. Pollen sites in eastern North America during four different late-Pleistocene time periods. All sites in eastern North America that at least partially overlap the time period are shown in black, and the benchmark sites for each time period are shown in red. The number corresponds to the site name: 15, Lake Annie (Watts, 1975); 52, Blackwoods Hollow (Schaufler and Jacobson Jr, 2002); 77, Browns Pond (Kneller and Peteet, 1993); 107, Chase Pond (Mayle et al., 1993b); 117, Chatsworth Bog (Nelson et al., 2006; Grimm et al., 2009); 121, Clear Pond (Hussey, 1993); 130, Conroy Lake (Doner, 1995; Borns Jr et al., 2004); 133, Cottonwood Lake (Barnosky et al., 1987; Grimm et al., 2009); 150, Crystal Lake (Gonzales and Grimm, 2009); 162, Decoy Lake (Szeicz and MacDonald, 1991); 172, Devil's Lake (Baker et al., 1992; Grimm et al., 2009; Maher Jr, 2009); 291, Hiscock Site (McAndrews, 2003); 347, Kettle Lake (Clark et al., 2002; Brown et al., 2005; Grimm, 2011); 362, Lac a Magie (Mayle et al., 1993b); 478, Moon Lake (Laird et al., 1996a,b); 492, Mud Pond (Borns Jr et al., 2004; Doner, 1995); 678, Sharkey Lake (Camil et al., 2003); 704, Splan Pond (Mayle et al., 1993b; Mott et al., 1986); 710, Steel Lake, MN (Wright et al., 2004); 720, Sutherland Pond (Maenza-Gmelch, 1997a; Maenza-Gmelch, 1997b); 749, Lake Tulane (Grimm et al., 2006); 789, White Lake (Yu, 2007). ka: thousand years before present. (For interpretation of the references to color in this figure legend, the reader is referred to the web version of this article.)

Pleistocene time periods were subsets of this list (Fig. 3). The number of benchmark sites declined with increasing age (14.5–12.9 ka: 18 sites; 18–14.5 ka: 8 sites; 21–18 ka: 4 sites). The percentage of benchmark sites ranged from 8.5% to 14% among the four time periods (12.9–11.5 ka: 22/223 sites; 14.5–12.9 ka: 18/153 sites; 18–14.5 ka: 8/94 sites; 21–18 ka: 4/28 sites). Given the paucity of sites in the earlier time periods, we focused exclusively on the latest Pleistocene (12.9–11.5 ka) in examining biostratigraphic events.

4.2. Biostratigraphic events and cross-validation

Of the five ecological events initially examined (*Alnus* rise, *Alnus* decline, the end of *Picea* decline, *Pinus* rise, and *Quercus* rise), we eliminated the *Pinus* rise because not all researchers discriminated between *P. strobus* (subg. *Strobus*) and *P. banksiana/resinosa* (subg. *Pinus*), and the *Alnus* rise because spatial cross-validation error indicated it was a poorly constrained event. Thus, our final analysis included *Alnus* decline, *Picea* decline, and *Quercus* rise. For all three

events and across all interpolation methods, error was significantly correlated with the original age of the event at sites, indicating that the interpolated ages are smoothed and hence have less variance than the original ages (Table 2). Error was not consistently correlated with temporal sampling resolution, nor with spatial attributes such as latitude, longitude, or altitude (Table 2). Additionally, for both the IDW and TPS interpolation techniques, using altitude did not significantly increase interpolation accuracy and in some cases worsened it, so for simplicity we present results for interpolation using latitude and longitude only (e.g. IDW-2d and TPS-2d). We applied the interpolated ages to all poorly constrained sites within a minimum convex polygon that spanned the benchmark sites used for interpolation.

Across all events, IDW-2d interpolation had a smaller cross-validation error than TPS-2d interpolation (e.g., 574 years Interpolation MAE vs 746 years Interpolation MAE for *Picea* decline; Table 3). TPS-2d smoothed the pollen signal more strongly and was more highly influenced by individual sites (Fig. 4). The means of the interpolated ages did not substantially differ between IDW-2d and

TPS-2d, though in general IDW-2d error was less than TPS-2d error: *Picea* decline, -150 ± 256 (mean and standard deviation of the difference between IDW-2d and TPS-2d ages, for both the benchmark and poorly constrained sites); *Alnus* decline, 18 ± 170 ; *Quercus* rise, -102 ± 392 . When using the IDW-2d interpolation method, cross-validation interpolation error was less than 600 years for each event and lower than 400 years for *Alnus* decline (Table 3), Interpolation MAE). The error estimates are highly influenced by a few 'outlier' sites [i.e. Clear Pond (Hussey, 1993) for all three events, plus Brown's Pond (Kneller and Peteet, 1993) for *Alnus* decline; Table 3]. When outlier sites are removed, spatial interpolation error (for the IDW-2d method) declines to 530 years for the *Picea* decline and 327 years for the *Alnus* decline, and increases to 614 years for the *Quercus* rise (Table 3). These outlier sites generally occur in the south-central US in areas of low sampling density. The high cross-validation errors for these sites are likely caused by a combination of time-transgressive ecological events that are difficult to reproduce accurately when sites from low-density regions are removed during the cross-validation, and possibly also errors in the age models for these sites (Jackson and Whitehead, 1993; Jackson et al., 2000). Thus, these outlier sites cannot be well predicted during the cross-validation analyses but, because they are in areas of low site density, are essential to estimating biostratigraphic ages for the non-benchmark sites. We report error estimates with and without these outlier sites (Table 3) and retain them in subsequent analyses.

4.3. Comparison with original event ages

The timing of biostratigraphic events estimated from the original chronologies of non-benchmark sites varied widely (Table 4, Fig. 5), and was often very different than age estimates based on interpolation. For all events, the mean absolute age difference between interpolated ages (IDW-2d) and original ages of the non-benchmark sites was approximately twice as much as the Interpolation MAE of the cross-validation for the benchmark sites (Tables 3, 4): 845 vs 574 years for *Picea* decline, 858 vs 352 years for *Alnus* decline, 1106 vs 573 years for *Quercus* rise. This discrepancy indicates that error is built into many of the original site chronologies and the interpolation of biostratigraphic ages can substantially improve these chronologies.

4.4. Ecological patterns

Although the primary focus of this paper is methodological, maps of the spatial propagation of major biotic events reveal highly individualistic ecological dynamics (Figs. 4 and 6). For example, the *Picea* decline and the *Quercus* rise both originated at southern sites between 16–18 ka and propagated northward. However, the *Picea* decline spread rapidly across the southern Great Lakes region between 11.5 and 11 ka and then propagated west and northeast until the final declines around 10.1 ka. On the other hand, the rise in *Quercus* abundances spread rapidly through the northeast starting

Table 3

Cross-validation and correlation statistics for three biostratigraphic events, for benchmark sites only. For the *Alnus* decline, the southern sites are defined as Clear Pond, SC and Browns Pond, VA. ME: Mean error; RMSE: Root mean square error; MAE: Mean Absolute Error; Extrapolation MAE: MAE at sites at the boundary of the interpolation range; Interpolation MAE: MAE at sites within the boundary of the interpolation range. Interpolation MAE is the most appropriate metric of interpolation error (see text).

a. <i>Picea</i> Decline	All sites		CLEARPOND removed	
	IDW-2d	TPS-2d	IDW-2d	TPS-2d
MAE	842	1038	450	453
Extrapolation MAE	1582	1843	307	439
Interpolation MAE	574	746	530	461
b. <i>Alnus</i> decline	All sites		Southern sites removed	
	IDW-2d	TPS-2d	IDW-2d	TPS-2d
MAE	367	720	325	563
Extrapolation MAE	398	1416	323	794
Interpolation MAE	352	372	327	410
c. <i>Quercus</i> Rise	All sites		CLEARPOND removed	
	IDW-2d	TPS-2d	IDW-2d	TPS-2d
MAE	1012	947	637	743
Extrapolation MAE	2110	1697	664	784
Interpolation MAE	573	647	614	709

around 12 ka, but did not begin around the Great Lakes and westward until after 11 ka. It did not rise at some sites until 9.1 ka. Thus, the temporal relationship between *Picea* decline and *Quercus* rise varies spatially, in which the temporal offset increases toward the northwest (Fig. 6). In contrast to both events, the *Alnus* decline originated much later (11.6 ka) than the other two events and occurred first in the northeast, then spread south and west within a few hundred years. In New England and Maritime Canada, the *Alnus* decline is an indicator of the end of the Younger Dryas (Mayle et al., 1993a), but these maps suggest that across eastern North America, the *Alnus* decline is a rapid but time-transgressive event.

5. Discussion

Spatial networks of well-dated fossil-pollen records are critically needed to understand spatial vegetation dynamics during periods of abrupt change. We have 1) developed a methodological framework that presents a standard ranking scheme for assessing the quality of ^{14}C ages and outlines criteria for identifying benchmark sites, 2) applied this framework to identify benchmark fossil-pollen records in eastern North America, and 3) used these benchmark sites to interpolate the ages of key biostratigraphic events to other, less-well dated sites. We explicitly tested the strengths and limits of this approach, focusing on late-Pleistocene pollen datasets from eastern North America. Our cross-validation analyses show a mean error of roughly 500 years associated with the spatial interpolation of key biostratigraphic events, suggesting that 500 years is effectively the temporal limit to maps and other inter-site syntheses relying on late-Pleistocene pollen records from

Table 2

The correlation between the site-specific cross-validation age error with the original age of the event, original age range, latitude, longitude, and altitude, for *Picea* decline, *Alnus* decline, and *Quercus* rise. The r-value is listed first, followed by the P-value. Significant correlations are shown in bold.

	<i>Picea</i> Decline		<i>Alnus</i> Decline		<i>Quercus</i> Rise	
	IDW-2d	TPS-2d	IDW-2d	TPS-2d	IDW-2d	TPS-2d
Original age	-0.976; 0	-0.847; 0	-0.847; 0.001	-0.503; 0.096	-0.948; 0	-0.832; 0.000
Age range	-0.411; 0.128	-0.277; 0.317	0.437; 0.155	0.425; 0.169	-0.567; 0.035	-0.362; 0.203
Latitude	0.596; 0.019	0.391; 0.150	-0.002; 0.996	0.462; 0.131	0.601; 0.023	0.401; 0.156
Longitude	-0.147; 0.602	-0.230; 0.312	-0.083; 0.798	-0.118; 0.716	-0.096; 0.745	-0.031; 0.916
Altitude	0.434; 0.106	0.633; 0.011	0.681; 0.015	0.589; 0.044	0.412; 0.143	0.404; 0.152

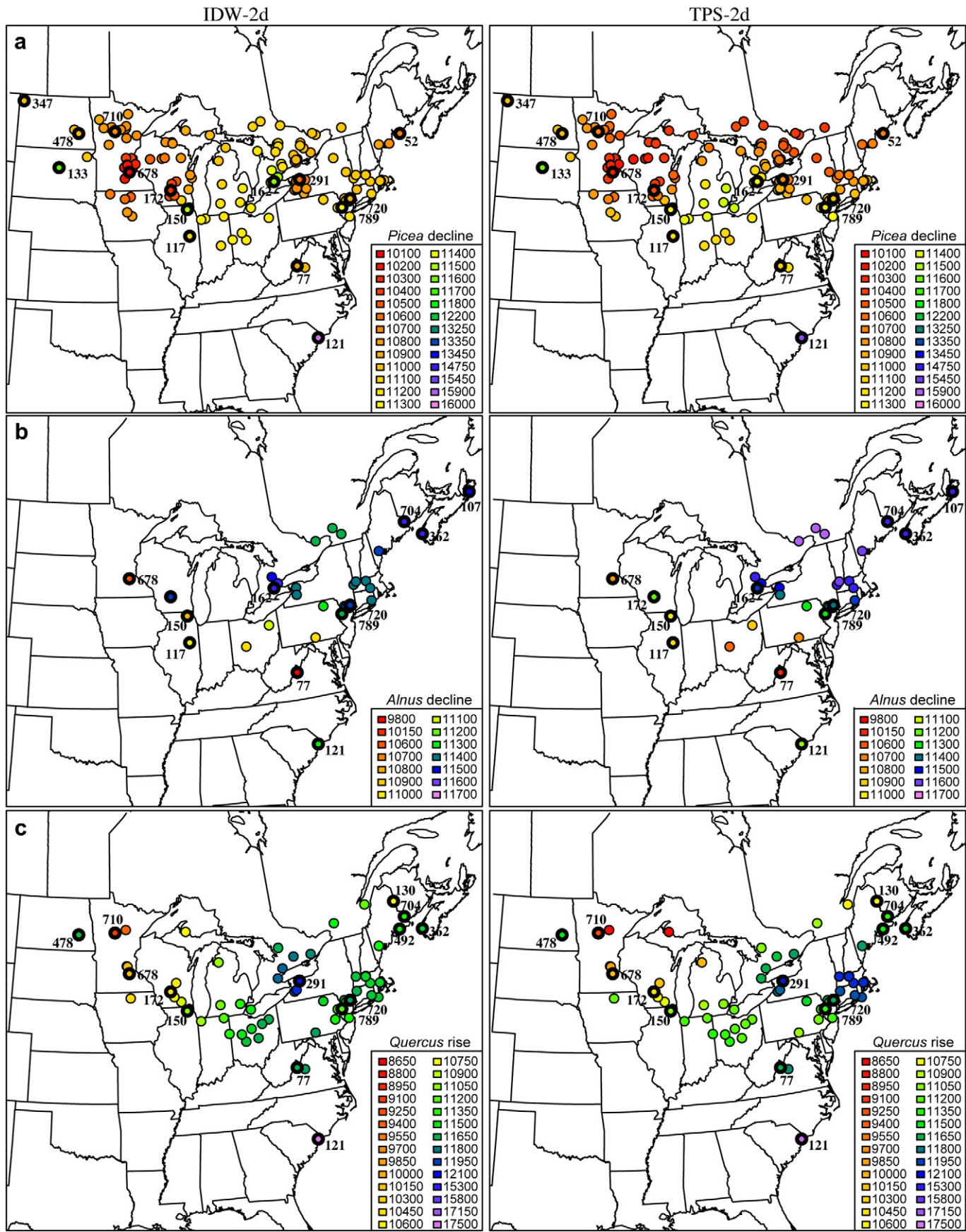


Fig. 4. Interpolated ages of each event for two different methods, inverse distance-weighting (IDW-2d) and thin-plate splines (TPS-2d). a) *Picea* decline; b) *Alnus* decline; c) *Quercus* rise. Benchmark sites are circled in a thick black line and labeled as in Fig. 3.

Table 4

Comparison of biostratigraphic versus original ages, for all sites. All statistics are calculated on the difference between the original age of an event estimated by change-point analysis and the event age estimated by interpolation (IDW-2d).

	Mean	Standard Deviation	Minimum	Maximum	Mean Absolute Difference
<i>Picea</i> decline	-287	1134	-4353	2889	845
<i>Alnus</i> decline	33	1532	-4059	4566	858
<i>Quercus</i> rise	-287	1650	-3676	4842	1106

eastern North America. To reduce error further and better understand the spatial responses of plant taxa and communities to the abrupt climate changes accompanying the last deglaciation, additional pollen records with high-resolution chronologies are critically needed. In the meantime, this approach provides a simple yet rigorous way of assessing temporal uncertainty and studying vegetation changes at sub-millennial timescales.

5.1. Benchmark chronologies

Many formal and informal approaches have been developed to evaluate reliability of individual ^{14}C ages (Meltzer and Mead, 1983; Stafford Jr et al., 1987; Pettitt et al., 2003) and chronologies (Jackson et al., 2000; Williams et al., 2004). We integrated information from various sources into a comprehensive ranking scheme that is applied here to ^{14}C dating, but in principle is widely applicable to different proxy types and dating methods.

The main elements of our framework are a) a qualitative scale that assesses both precision and accuracy, b) a definition of benchmark sites that is tied to this scale, and c) standards for sample density and age proximity. Other research groups have developed frameworks that contain similar elements. For example, the European Pollen Database (EPD) has implemented a system whereby each individual sample in a stratigraphic sequence is classified according to its temporal uncertainty (Thomas Giesecke, pers. comm.). The EPD system takes into account the proximity of ages to samples, as well as the overall shape of the age model in the region surrounding the sample. The uncertainty of samples is estimated by linear interpolation of error at the bounding ages, but accuracy and precision of the underlying ^{14}C ages are not formally assessed. The main distinction between approaches is that the EPD is mainly concerned with characterizing the temporal uncertainty of samples within a sequence, whereas we have focused on both assessing the uncertainty of individual age controls and chronologies and narrowing that uncertainty by incorporating biostratigraphic age estimates for poorly constrained chronologies. Our approach is closer to that outlined in Williams et al. (2004), where individual sites were excluded or down-weighted for mapping purposes by the age controls and sampling quality associated with the site.

After evaluating all late-Pleistocene pollen datasets from eastern North America in the Neotoma database, we found that only 22 of the several hundred datasets fulfilled the criteria for benchmark sites (Figs. 1 and 3). This estimate is undoubtedly conservative. For example, we have assigned an accuracy ranking of 5 (<500 years) to all ages obtained from bulk-sediment samples, due to concerns about potential hardwater contamination, but in regions without known hardwater effects, some sites that use AMS dating on bulk lake sediments may have accurate chronologies (e.g., Blood Lake; Oswald et al., 2007). Our ranking assignments for individual dates will be stored in Neotoma, so future workers can review and revise as appropriate. The distribution of late-Pleistocene benchmark sites in eastern North America is heavily concentrated in the upper Midwest and Northeast, in part because of the large number of lakes in these regions. However, suitable sites with good late-Pleistocene records do exist in other regions that should be a priority for re-dating [e.g. the southeastern United States (Watts, 1980; Jackson and Whitehead, 1993)]. The geographic bias of

benchmark sites limits our ability to accurately infer the rates and patterns of vegetation change across eastern North America and points to the need for new sediment cores or new ages from existing cores in the undersampled regions.

5.2. Quantifying and minimizing temporal error

After accounting for both chronologic and interpolation error, the error associated with mapping each ecological event was on the order of 500 years. This value indicates that the temporal resolution of mapping can be improved to 500-year intervals for some periods of the late Pleistocene, which is sufficient to detect ecological change before and after major events such as the Bølling-Allerød and Younger Dryas oscillations. However, it also points to a temporal limit to current synoptic mapping efforts, set by the site-specific variability of ecological events and by error due to factors such as ^{14}C dating, calibration, and sampling resolution (both within core and across landscape). The accumulated error during syntheses is too large to detect phenomena that can be seen in individual well-dated records, e.g. the 300–400 year lag between local climate changes at Crystal Lake, Illinois (Gonzales and Grimm, 2009) and the timing of Bølling-Allerød and Younger Dryas oscillations in North Atlantic records. (However, leads and lags could be calculated from individual well-dated records, then their spatial distribution mapped, which would aid understanding of the teleconnections between North Atlantic and North American climate).

The assignment of ages to biostratigraphic events at poorly constrained sites using IDW interpolation clearly improved over the original age estimates for most of the original chronologies (Table 4, Fig. 5). For example, the mean absolute difference between the age of the *Picea* decline based on interpolation versus its age from the original chronology is 845 years, with individual differences ranging from interpolated ages 4353 years older than the original chronology to 2889 years younger than the original chronology (Table 4). Some of this error is due to interpolation, but the fact that the mean absolute age difference is substantially larger than the mean cross-validation error for all events (Tables 3, 4) indicates that the use of biostratigraphic ages roughly halves the temporal uncertainty inherent in the original chronologies of some of the non-benchmark sites.

Critically, our method does not assume synchrony of biological events (Smith and Pilcher, 1973; Blaauw, 2010b), but rather assumes that these events spatially propagate in a smooth manner. A key innovation used here is change-point analysis, which offers a formal tool for determining if and where particular biotic events occur in pollen records. This method avoids setting arbitrary relative-abundance thresholds for particular events and instead focuses on the pattern of change in each taxon within the context of the local site. Moreover, using change-point detection for individual taxa, rather than pollen zonation based on the entire assemblage, is a better way of accommodating individualistic species dynamics in data syntheses at sub-continental and broader scales. Our use of biostratigraphic ages does build in assumptions about the spatial smoothness of ecological change. Thus, the full dataset is appropriate for some synthetic applications—e.g. data-model comparisons to vegetation models driven by global climate models—but we must restrict ourselves to the benchmark sites and their

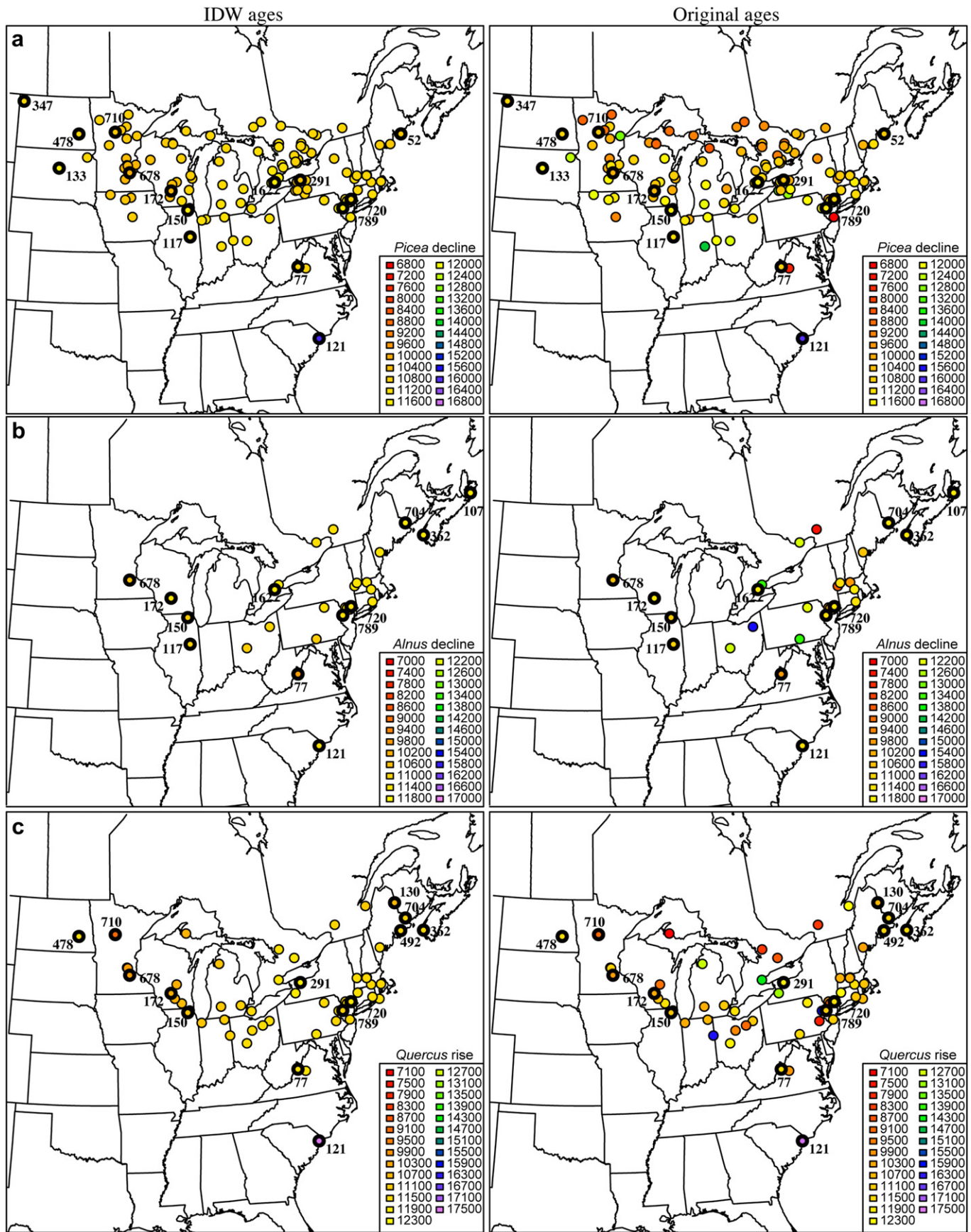


Fig. 5. Comparison of age of each event (based on IDW-2d interpolation) versus the age of the event designated by the default chronology in the Neotoma database. a) *Picea* decline; b) *Alnus* decline; c) *Quercus* rise. Benchmark sites are circled in a thick black line and labeled as in Fig. 3.

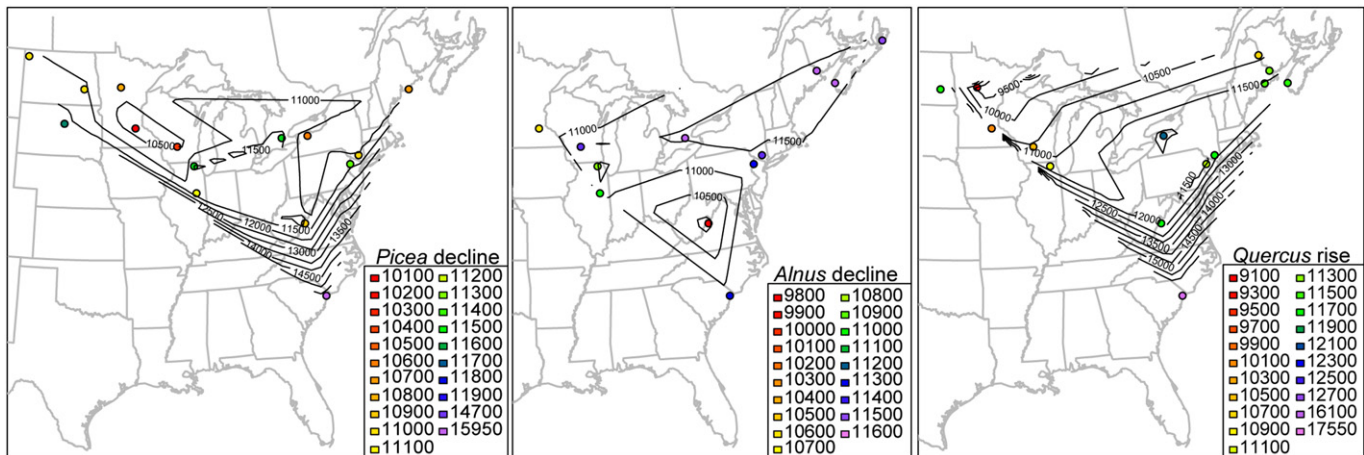


Fig. 6. Contour plots of ecological events, based on linear interpolation of event ages between the benchmark sites. The contours are spaced at 500-year intervals on all three panels.

independent age models when testing hypotheses about spatio-temporal patterns within the taxa used as biostratigraphic markers.

Our treatment of the sample-level temporal uncertainty resulting from age models was simple—we assigned the maximum age range from the bracketing ages to a sample and assumed a uniform age distribution around this sample (see Section 3.3). New Bayesian age-modeling tools (Parnell et al., 2008) allow integration of the age-calibration step with age-model construction and provide posterior estimates of the age error of undated samples. The functionality to store these estimates of sample-level age uncertainty is currently being built into the Neotoma database. Because our estimates of sample-level uncertainty are intentionally conservative (i.e. they likely overestimate uncertainty), incorporation of these new tools should reduce the estimates of temporal uncertainty.

5.3. Spatial patterns in major biotic events during the last deglaciation

The events mapped here are broadly concordant with patterns identified previously (Williams et al., 2004), yet refine key details of vegetation changes around abrupt climate events such as the end of the Younger Dryas Chronozone. (It is difficult to compare strictly these maps with those in Williams et al. (2004) because we are mapping different phenomena [pollen isochrones in this paper versus isopolls in Williams et al. (2004)].) Both sets of maps show that the final decline of *Picea* was time-transgressive, occurring first in the southern US, then very rapidly propagating across in the northeastern US and eastern Great Plains (Figs. 4 and 6). Ages for this event among the benchmark sites ranged from 16 ka at Clear Pond (Hussey, 1993) in the south to 10.15 ka at Sharkey Lake (Camill et al., 2003) in the Upper Midwest.

Similarly, our mapping of the *Quercus* rise based on change-point detection (Figs. 4 and 6) is broadly consistent with the Williams et al. (2004) maps but provides additional detail, showing that the *Quercus* rise began in the northern US in western New York ca. 12 ka at the Hiscock Site (McAndrews, 2003), then propagated through New England and Maritime Canada between 11.75 and 10.7 ka and westward through the Great Lakes between 11.9 ka and 9.1 ka. The value of the improved sub-millennial temporal resolution is most notable for the *Alnus* decline. The rise and decline of *Alnus* along the northeastern US and maritime Canada is effectively a synchronous event that has been used as a biological indicator for the Younger Dryas Chronozone (Mayle et al., 1993a). Our results confirm the synchrony of the *Alnus* decline along the east coast

around 11.5 ka, but also show that the *Alnus* decline then propagated westward very quickly within a 1000 year interval (Figs. 4 and 6), reaching Sharkey Lake (Camill et al., 2003) by 10.6 ka. This pattern suggests additional complexity to an ecological event that previously had been linked simply to a single abrupt climate event. However, additional taxonomic resolution may potentially reveal an even more complex event. In the maritime provinces of Canada and highland areas of New England, the *Alnus* peak is primarily *A. viridis*-type, whereas it is mainly *A. incana*-type at lowland sites (Mayle et al., 1993a). In the Midwest, the *Alnus* peak is virtually all *A. incana*-type (e.g. Cushing, 1967; Gonzales and Grimm, 2009). In addition, in the Northeast *A. incana*-type includes both *A. incana* and *A. serrulata* with *A. serrulata* having a more southern distribution. Thus, it is unclear whether the *Alnus*-peak represents a single event or multiple events closely spaced in time involving different species. Unfortunately, *Alnus* is not consistently separated into the *A. viridis* and *A. incana* types at many sites, making it difficult to resolve this question with existing data. Nevertheless, the *Alnus* types are easily distinguished (Mayle et al., 1993a) and future efforts to separate the pollen types may reveal important paleoecological patterns on a synoptic scale. Plant macrofossils could also help determine particular species involved in important ecological events (Jackson et al., 1997), and could be used in some cases to subdivide pollen taxa into higher-resolution units (e.g., species). We have not yet explored such application. It poses new problems (e.g., subdividing pollen when two or more species are represented by macrofossils; deciding whether the same species are represented locally by macrofossils and regionally by pollen). These problems are surmountable, but would require an additional set of decision rules beyond the scope of our study.

Across all three ecological events, the slowest rates of ecological change occurred in the region bordering the mid-Atlantic. The *Quercus* rise and *Picea* decline spread at similar rates, with the slowest rates of event propagation in the south, trending northwest, then speeding up in the northeast and upper Midwest. The *Alnus* decline occurred almost simultaneously throughout the northeast, then slowed toward the mid-Atlantic region. Across all three events, the fastest rates of change occurred at the end of the Younger Dryas Chronozone (Fig. 6).

6. Conclusions

Our conceptual framework for ranking ages and our use of benchmark sites as the basis for refined chronologies offers

a simple yet rigorous approach to assessing and improving the temporal resolution of mapped vegetation changes. Our error analyses suggest that the effective temporal limit to multi-site syntheses of late-Pleistocene vegetation dynamics from fossil-pollen records is about 500 years. This resolution is suitable for answering questions at the synoptic scale such as how species and communities responded to abrupt climate change at millennial and, to some degree, sub-millennial timescales. For example, both the Bølling-Allerød and Younger Dryas climatic oscillations lasted over 1000 years, so synoptic patterns of ecological change can be compared before and after rapid climate change at the boundaries of these events. These methods also provide a foundation for a reassessment of how the ecological responses to these climatic changes propagated across large spatial regions. Finally, our identification of benchmark sites helps identify where such sites are sparse and illustrates high-priority regions for future field campaigns. As more benchmark sites and more accurate and precise ages are added, especially in the undersampled regions, the methodological framework established here can be easily used to assess the new limits of mapping and narrow the temporal resolution of future syntheses even further.

Acknowledgments

We would like to thank Maarten Blaauw, Simon Brewer, Paul Buckland, Phil Buckland, Thomas Giesecke, Allan Hall, and Alison Smith for discussion of age models, precision, and accuracy. The paper benefitted from comments by Simon Brewer, Thomas Giesecke, Rachel Jones, Mark Lesser, Yao Liu, and two anonymous reviewers. Funding for this project comes from NSF (EAR-0844223, EAR-0843831). A workshop on age models and analysis and visualization tools for the Neotoma Database and related projects was held in Umeå, Sweden in Fall 2010 and funded by The Swedish Research Council, Umeå University Humanities Faculty, and The SEAD Project. Pollen records were obtained from the Neotoma paleoecological database.

Appendix and Supplementary data

Supplementary data associated with this article can be found, in the online version, at doi:10.1016/j.quascirev.2011.04.017.

References

- Andree, M., Oeschger, H., Siegenthaler, U., Riesen, T., Moell, M., Ammann, B., Tobolski, K., 1986. 14C dating of plant macrofossils in lake sediment. Radiocarbon 28, 411–416.
- APSA Members, 2007. The Australasian Pollen and Spore Atlas V1.0. Australian National University, Canberra. <http://apsa.anu.edu.au/>.
- Baker, R., Maher, L., Chumbley, C., Van Zant, K., 1992. Patterns of Holocene environmental change in the midwestern United States. Quaternary Research 37, 379–389.
- Barnekow, L., Possnert, G., Sandgren, P., 1998. AMS 14C chronologies of Holocene lake sediments in the Abisko area, northern Sweden – a comparison between dated bulk sediment and macrofossil samples. GFF 120, 59–67.
- Barnosky, C., Grimm, E., Wright, H., 1987. Towards a postglacial history of the northern Great Plains: a review of the paleoecologic problems. Annals of the Carnegie Museum 56, 259–273.
- Barry, D., Hartigan, J., 1993. A Bayesian analysis for change point problems. Journal of the American Statistical Association 88, 309–319.
- Bennett, K., 1994. Confidence intervals for age estimates and deposition times in late-Quaternary sediment sequences. The Holocene 4, 337–348.
- Bennett, K., Fuller, J., 2002. Determining the age of the mid-Holocene *Tsuga canadensis* (hemlock) decline, eastern North America. The Holocene 12, 421–429.
- Binney, H., Edwards, M.E., Willis, K.J., 2008. Establishing a Northern Eurasian paleoecological database: The pollen data. PAGES News 16, 34.
- Birks, H., Ammann, B., 2000. Two terrestrial records of rapid climatic change during the glacial-Holocene transition (14,000–9,000 calendar years B.P. from Europe. Proceedings of the National Academy of Sciences USA 97, 1390–1394.
- Blaauw, M., 2010a. Methods and code for ‘classical’ age-modelling of radiocarbon sequences. Quaternary Geochronology 5, 512–518.
- Blaauw, M., 2010b. Out of tune: the dangers of aligning proxy archives. Quaternary Science Reviews. doi:10.1016/j.quascirev.2010.11.012.
- Borns Jr., H.W., Doner, L.A., Dorion, C.C., Jacobson Jr., G.L., Kaplan, M.R., Kreutz, K.J., Lowell, T.V., Thompson, W.B., Weddle, T.K., Ehlers, J., Gibbard, P.L., 2004. The Deglaciation of Maine, U.S.A.: Developments in Quaternary Science. Elsevier, pp. 89–109.
- Bronk Ramsey, C., 2008. Radiocarbon dating: revolutions in understanding. Archaeometry 50, 249–275.
- Brown, K.J., Clark, J., Grimm, E., Donovan, J., Mueller, P., Hansen, B., Stefanova, I., 2005. Fire cycles in North American interior grasslands and their relation to prairie drought. Proceedings of the National Academy of Sciences USA 102, 8865–8870.
- Camill, P., Umbanhowar Jr., C., Teed, R., Geiss, C., Aldinger, J., Dvorak, L., Kenning, J., Limmer, J., Walkup, K., 2003. Late-glacial and Holocene climatic effects on fire and vegetation dynamics at the prairie-forest ecotone in south-central Minnesota. Journal of Ecology 91, 822–836.
- Clark, J., Grimm, E.C., Donovan, J.J., Fritz, S., Engstrom, D., Almendinger, J., 2002. Drought cycles and landscape responses to past aridity on prairies of the northern Great Plains, USA. Ecology 83, 595–601.
- Cushing, E.J., 1967. Late-Wisconsin pollen stratigraphy in the glacial sequence in Minnesota. In: Cushing, E.J., Wright, H.E., Jr (Eds.), Quaternary Paleocology. Yale University Press, New Haven, pp. 59–88.
- Damon, P.E., Lerman, J.C., Long, A., 1978. Temporal fluctuations of atmospheric 14C: causal factors and implications. Annual Review of Earth and Planetary Sciences 6, 457–494.
- Davis, M.B., 1976. Pleistocene biogeography of temperate deciduous forests. Geoscience and Man XIII, 13–26.
- Deevey Jr., E.S., 1939. Studies on Connecticut lake sediments. I. A postglacial climatic chronology for southern New England. American Journal of Science 237, 691–724.
- Deevey Jr., E.S., Gross, M.S., Hutchinson, G.E., Kraybill, H.L., 1954. The natural C14 contents of materials from hard-water lakes. Proceedings of the National Academy of Sciences USA 40, 285–288.
- Denton, G.H., Anderson, R.S., Toggweiler, J.R., Edwards, R.L., Schaefer, J.M., Putnam, A.E., 2010. The last glacial termination. Science 328, 1652–1656.
- Dietl, G.P., Flessa, K.W., 2011. Conservation paleobiology: putting the dead to work. Trends in Ecology & Evolution.
- Doner, L.A., 1995. Late-Pleistocene Environments in Maine and the Younger Dryas Dilemma. University of Maine, Orono, Maine, USA.
- Emerson, J.W., Erdman, C., 2007. bcp: an R package for performing a Bayesian analysis of change point problems. Journal of Statistical Software 23, 1–13.
- Firbas, F., 1950. The Late-Glacial vegetation of central Europe. New Phytologist 49, 163–173.
- Flessa, K.W., Jackson, S.T., 2005. The Geological Record of Ecological Dynamics: Understanding the Biotic Effects of Future Environmental Change. National Academy Press, Washington, D.C.
- Fyfe, R., de Beaulieu, J.L., Binney, H., Bradshaw, R., Brewer, S., Le Flao, A., Finsinger, W., Gaillard, M., Giesecke, T., Gil-Romera, G., 2009. The European Pollen Database: past efforts and current activities. Vegetation History and Archaeobotany 18, 417–424.
- Gavin, D., 2001. Estimation of inbuilt age in radiocarbon ages of soil charcoal for fire history studies. Radiocarbon 43, 27–44.
- Gonzales, L.M., Grimm, E., 2009. Synchronization of late-glacial vegetation changes at Crystal Lake, Illinois, USA with the North Atlantic event stratigraphy. Quaternary Research 72, 234–245.
- Grimm, E., 2011. High-resolution age model based on AMS radiocarbon ages for Kettle Lake, North Dakota, USA. Radiocarbon 53.
- Grimm, E., Jacobson, G., 2003. Late-Quaternary vegetation history of the eastern United States. In: Gillespie, A.R., Porter, S.C., Atwater, B.F. (Eds.), The Quaternary Period in the United States. Elsevier, Amsterdam, pp. 381–402.
- Grimm, E., Maher Jr., L., Nelson, D., 2009. The magnitude of error in conventional bulk-sediment radiocarbon dates from central North America. Quaternary Research 72, 301–308.
- Grimm, E., Watts, W., Jacobson Jr., G., Hansen, B., Almqvist, H., Dieffenbacher-Krall, A., 2006. Evidence for warm wet Heinrich events in Florida. Quaternary Science Reviews 25, 2197–2211.
- Grimm, E.C., Jacobson Jr., G.L., 1992. Fossil-pollen evidence for abrupt climate changes during the past 18 000 years in eastern North America. Climate Dynamics 6, 179–184.
- Grimm, E.C., Keltner, J., Cheddadi, R., Hicks, S., Lézine, A.-M., Berrio, J.C., Williams, J.W., 2007. Pollen databases and their application. In: Elias, S.A. (Ed.), Encyclopedia of Quaternary Science. Elsevier, Amsterdam, pp. 2522–2530.
- Haslett, J., Parnell, A., 2008. A simple monotone process with application to radiocarbon-dated depth chronologies. Journal of the Royal Statistical Society: Series C (Applied Statistics) 57, 399–418.
- Hopkins, A.D., 1920. The bioclimatic law. Monthly Weather Review 48, 355.
- Huntley, B., Birks, H.J.B., 1983. An Atlas of Past and Present Pollen Maps for Europe: 0–13000 Years Ago. Cambridge University Press, Cambridge.
- Hussey, T.C., 1993. A 20,000 year History of Vegetation and Climate at Clear Pond, Northeastern South Carolina. University of Maine, Orono, Maine, USA.
- Jackson, S., Whitehead, D., 1993. Pollen and macrofossils from Wisconsinan interstadial sediments in northeastern Georgia. Quaternary Research 39, 99–106.
- Jackson, S.T., Webb, R.S., Anderson, K.H., Overpeck, J.T., Webb III, T., Williams, J.W., Hansen, B., 2000. Vegetation and environment in eastern North America during the Last Glacial Maximum. Quaternary Science Reviews 19, 489–508.
- Jackson, S.T., Overpeck, J.T., Webb III, T., Keatitch, S.E., Anderson, K.H., 1997. Mapped plant-macrofossil and pollen records of late Quaternary vegetation change in eastern North America. Quaternary Science Reviews 16, 1–70.

- Jacobson Jr., G.L., Webb III, T., Grimm, E.C., 1987. Patterns and rates of vegetation change during the deglaciation of eastern North America. In: Ruddiman, W.F., Wright Jr., H.E. (Eds.), North America and Adjacent Oceans during the Last Deglaciation. Geological Society of America, Boulder, pp. 277–288.
- Kneller, M., Peteet, D., 1993. Late-Quaternary climate in the Ridge and Valley of Virginia, U.S.A.: changes in vegetation and depositional environment. *Quaternary Science Reviews* 12, 613–628.
- Laird, K., Fritz, S., Grimm, E., Mueller, P., 1996a. Century-scale paleoclimatic reconstruction from Moon Lake, a closed-basin lake in the northern Great Plains. *Limnology and Oceanography* 41, 890–902.
- Laird, K.R., Fritz, S.C., Maasch, K., Cumming, B.F., 1996b. Greater drought intensity and frequency before AD 1200 in the Northern Great Plains, USA. *Nature* 384, 552–554.
- Lowe, J.J., Lowe, S., Fowler, A.J., Hedges, R.E.M., Austin, T.J.F., 1988. Comparison of accelerator and radiometric ^{14}C measurements obtained from Late Devensian lateglacial lake sediments from Llyn Gwernan, North Wales, UK. *Boreas* 17, 355–369.
- MacArthur, R.H., 1972. *Geographical Ecology: Patterns in the Distribution of Species*. Harper and Row, New York.
- MacDonald, G.M., Beukens, R.P., Kieser, W.E., 1991. Radiocarbon dating of limnic sediments: a comparative analysis and discussion. *Ecology* 72, 1150–1155.
- Maenza-Gmelch, T., 1997a. Late-glacial-early Holocene vegetation, climate, and fire at Sutherland Pond, Hudson Highlands, southeastern New York, USA. *Canadian Journal of Botany* 75, 431–439.
- Maenza-Gmelch, T.E., 1997b. Holocene vegetation, climate, and fire history of the Hudson Highlands, southeastern New York, USA. *The Holocene* 7, 25–37.
- Maher Jr., L.J., 2009. The palynology of Devils Lake, Sauk County, Wisconsin. In: Knox, J.C., Clayton, L., Mickelson, D.M. (Eds.), *Quaternary History of the Driftless Area: Wisconsin geological and natural history survey field trip guide B*, pp. 119–135.
- Mayle, F., Levesque, A., Cwynar, L., 1993a. *Alnus* as an indicator taxon of the Younger Dryas cooling in eastern North America. *Quaternary Science Reviews* 12, 295–305.
- Mayle, F.E., Levesque, A., Cwynar, L.C., 1993b. Accelerator-mass-spectrometer ages for the Younger Dryas event in Atlantic Canada. *Quaternary Research* 39, 355–360.
- McAndrews, J.H., 2003. Postglacial ecology of the Hiscock Site. In: Laub, R.S. (Ed.), *The Hiscock Site: Late Pleistocene and Holocene Paleoenvironment and Archaeology of Western New York State*. Bulletin of the Buffalo Society of Natural Sciences, Buffalo, NY, pp. 190–198.
- Meltzer, D.J., Mead, J.I., 1983. The timing of late Pleistocene mammalian extinctions in North America. *Quaternary Research* 19, 130–135.
- Mott, R., Grant, D., Stea, R., Occhietti, S., 1986. Late-glacial climatic oscillation in Atlantic Canada equivalent to the Allerød/Younger Dryas event. *Nature* 323, 247–250.
- Nelson, D., Hu, F., Grimm, E., Curry, B., Slate, J., 2006. The influence of aridity and fire on Holocene prairie communities in the eastern Prairie Peninsula. *Ecology* 87, 2523–2536.
- Oswald, W., Faison, E., Foster, D., Doughty, E., Hall, B., Hansen, B., 2007. Post-glacial changes in spatial patterns of vegetation across southern New England. *Journal of Biogeography* 34, 900–913.
- Oswald, W.W., Anderson, P.M., Brown, T.A., Brubaker, L.B., Hu, F.S., Lozhkin, A.V., Tinner, W., Kaltenrieder, P., 2005. Effects of sample mass and macrofossil type on ^{14}C dating of arctic and boreal lake sediments. *The Holocene* 15, 758–767.
- Overpeck, J.T., Whitlock, C., Huntley, B., 2003. Terrestrial biosphere dynamics in the climate system: past and future. In: Bradley, R.S., Pedersen, T.F., Alverson, K.D., Bergmann, K.F. (Eds.), *Paleoclimate, Global Change and the Future*. Springer-Verlag, Berlin, pp. 81–103.
- Parnell, A., Haslett, J., Allen, J., Buck, C., Huntley, B., 2008. A flexible approach to assessing synchronicity of past events using Bayesian reconstructions of sedimentation history. *Quaternary Science Reviews* 27, 1872–1885.
- Peros, M.C., Gajewski, K., Vial, A.E., 2008. Continental-scale tree population response to rapid climate change, competition and disturbance. *Global Ecology and Biogeography* 17, 658–669.
- Pettitt, P., Davies, W., Gamble, C., Richards, M., 2003. Palaeolithic radiocarbon chronology: quantifying our confidence beyond two half-lives. *Journal of Archaeological Science* 30, 1685–1693.
- R Development Core Team, 2010. R: a Language and Environment for Statistical Computing. R Foundation for Statistical Computing, Vienna, Austria.
- Reimer, P., Baillie, M., Bard, E., Bayliss, A., Beck, J., Blackwell, P., Ramsey, C., Buck, C., Burr, G., Edwards, R., Friedrich, M., Grootes, P.M., Guilderson, T.P., Hajdas, I., Heaton, T.J., Hogg, A.G., Hughen, K.A., Kaiser, K.F., Kromer, B., McCormac, F.G., Manning, S.W., Reimer, R.W., Richards, D.A., Southon, J.R., Talamo, S., Turney, C.S.M., van der Plicht, J., Weyhenmeyer, C.E., 2009. IntCal09 and Marine09 radiocarbon age calibration curves, 0–50,000 years cal BP. *Radiocarbon* 51, 1111–1150.
- Santos, G.M., Southon, J.R., Griffin, S., Beaupre, S.R., Druffel, E.R.M., 2007. Ultra small-mass AMS ^{14}C sample preparation and analyses at KCCAMS/UCI Facility. *Nuclear Instruments and Methods in Physics Research B* 259, 293–302.
- Schauffer, M., Jacobson Jr., G., 2002. Persistence of coastal spruce refugia during the Holocene in northern New England, USA, detected by stand-scale pollen stratigraphies. *Journal of Ecology* 90, 235–250.
- Shuman, B., Bartlein, P., Webb III, T., 2005. The magnitudes of millennial-and orbital-scale climatic change in eastern North America during the Late Quaternary. *Quaternary Science Reviews* 24, 2194–2206.
- Shuman, B., Webb III, T., Bartlein, P., Williams, J.W., 2002. The anatomy of a climatic oscillation: vegetation change in eastern North America during the Younger Dryas chronozone. *Quaternary Science Reviews* 21, 1777–1791.
- Smith, A., Pilcher, J., 1973. Radiocarbon dates and vegetational history of the British Isles. *New Phytologist* 72, 903–914.
- Solomon, S., Qin, D., Manning, M., Chen, Z., Marquis, M., Averyt, K.B., Tignor, M., Miller, H.L., 2007. *Climate Change 2007: The Physical Science Basis. Contribution of Working Group I to the Fourth Assessment Report of the Intergovernmental Panel on Climate Change*. Cambridge University Press, New York.
- Stafford Jr., T., Jull, A., Brendel, K., Duhamel, R., Donahue, D., 1987. Study of bone radiocarbon dating accuracy at the University of Arizona NSF Accelerator Facility for Radioisotope Analysis. *Radiocarbon* 29, 24–44.
- Stuiver, M., Reimer, P.J., 1993. Extended ^{14}C database and revised CALIB radiocarbon calibration program. *Radiocarbon* 35, 215–230.
- Szeicz, J., MacDonald, G., 1991. Postglacial vegetation history of oak savanna in southern Ontario. *Canadian Journal of Botany* 69, 1507–1519.
- Tian, J., Brown, T., Hul, F., 2005. Comparison of varve and ^{14}C chronologies from Steel Lake, Minnesota, USA. *The Holocene* 15, 510.
- Turney, C., Coope, G., Harkness, D., Lowe, J., Walker, M., 2000. Implications for the dating of Wisconsinan (Weichselian) Late-Glacial events of systematic radiocarbon age differences between terrestrial plant macrofossils from a site in SW Ireland. *Quaternary Research* 53, 114–121.
- von Post, L., 1946. The prospect for pollen analysis in the study of Earth's climatic history. *New Phytologist* 45, 193–217.
- Watts, W.A., 1975. A late Quaternary record of vegetation from Lake Annie, south-central Florida. *Geology* 3, 344–346.
- Watts, W.A., 1980. The late Quaternary vegetation history of the southeastern United States. *Annual Review of Ecology and Systematics* 11, 387–409.
- Williams, J., Post, D.M., Cwynar, L.C., Lotter, A.F., Levesque, A.J., 2002. Rapid and widespread vegetation responses to past climate change in the North Atlantic region. *Geology* 30, 971–974.
- Williams, J.W., Blois, J.L., Shuman, B.N., 2011. Extrinsic and intrinsic forcing of abrupt ecological change: case studies from the late Quaternary. *Journal of Ecology* 99, 664–677.
- Williams, J.W., Shuman, B., Webb III, T., Bartlein, P.J., Leduc, P.L., 2004. Late-Quaternary vegetation dynamics in North America: scaling from taxa to biomes. *Ecological Monographs* 74, 309–334.
- Willis, K., Bailey, R., Bhagwat, S., Birks, H., 2010. Biodiversity baselines, thresholds and resilience: testing predictions and assumptions using palaeoecological data. *Trends in Ecology & Evolution* 25, 583–591.
- Wright, H., Stefanova, I., Tian, J., Brown, T.A., Hu, F.S., 2004. A chronological framework for the Holocene vegetational history of central Minnesota: the Steel Lake pollen record. *Quaternary Science Reviews* 23, 611–626.
- Yu, Z., 2007. Rapid response of forested vegetation to multiple climatic oscillations during the last deglaciation in the northeastern United States. *Quaternary Research* 67, 297–303.

Appendix A

Material (as in the Geochronology table of the Neotoma database)	Accuracy Rank	Notes
2 Sagittaria seeds; 1 Picea seed; charcoal	3	weighted towards seeds (between 2=seed, 5=charcoal)
Picea needle; 2 Betula seeds; Larix needle; Picea seed wing	2	
"cedar" type wood	5	
(NaOH insoluble fraction)	5	uncertain material; assigned 5 as default
(NaOH soluble fraction)	5	uncertain material; assigned 5 as default
(organic fraction)	5	uncertain material; assigned 5 as default
(shell fraction)	6	
1 Alnus seed	2	
1 Betula and 1 Cyperaceae seed	2	
1 Betula seed	2	
1 black Schoenoplectus seed, 2 yellow Schoenoplectus seeds	2	
1 bud	2	
1 Cladium, 5 yellow Schoenoplectus seeds	2	
1 Cyperaceae seed	2	
1 Dirca seed, 5 yellow Schoenoplectus	2	
1 ml bulk sediment	5	
1 Polygonaceae seed	2	
1 sedge node, 1 Eleocharis seed	2	
1 seed	2	
1 seed bract	2	
10.5 Schoenoplectus seeds	2	
15 Schoenoplectus seeds	2	
1st extraction humic acid	5	uncertain material; assigned 5 as default
2 Betula seeds	2	
2 Betula/Alnus seeds	2	
2 black Schoenoplectus seeds	2	
2 bud scales, charcoal	4	weighted towards charcoal (between 2=bud scales, 5=charcoal)
2 Cenchrus longispinus seeds	2	
2 charcoal stems	5	
2 charcoalized Picea needle tips, charcoal	4	weighted towards charcoal (between 2=needle tips, 5=charcoal)
2 Cyperaceae seeds	2	
2 Heliotropium seeds/charcoal	3	weighted towards seeds (between 2=seed, 5=charcoal)
2 Picea needles, 1 Picea seed	2	
2 Polygonum seeds	2	
2 Sagittaria seeds, 1 Picea seed, charcoal	3	weighted towards seeds (between 2=seed, 5=charcoal)
2 Schoenoplectus nodes	2	
2 Schoenoplectus seeds	2	
2 sedge nodes, 1 woody fragment	3	midway between ranks of sedge nodes (rank=2) and woody fragments (rank=4)

Material (as in the Geochronology table of the Neotoma database)	Accuracy Rank	Notes
2 sedge nodes, 2 woody fragments	3	midway between ranks of sedge nodes (rank=2) and woody fragments (rank=4)
20 picea, 40 larix needles	2	
21 Polygonum seeds	2	
2nd extraction humic acid	5	uncertain material; assigned 5 as default
2nd extraction humin	5	uncertain material; assigned 5 as default
3 Betula seeds	2	
3 Carex seeds	2	
3 charcoal pieces, 1 Schoenoplectus seed	4	weighted towards charcoal (between 2=seed, 5=charcoal)
3 Eleocharis seeds, 1 white Carex seed	2	
3 larix, 1 betula bract, charc	3	weighted towards bract (between 2=bract, 5=charcoal)
3 Schoenoplectus seeds	2	
30 dryas and 26 salix leaves	2	
30 pinus strobus needles	2	
36 Polygonum seeds	2	
3rd extraction humic acid	5	uncertain material; assigned 5 as default
3rd extraction humin	5	uncertain material; assigned 5 as default
4 black Schoenoplectus seeds	2	
4 picea and 1 larix needle	2	
5 Heliotropium seeds	2	
57 Chenopodium-type seeds	2	
6 black Schoenoplectus seeds	2	
7 black Schoenoplectus seeds	2	
9 picea needles and a seed	2	
90 dryas and 15 salix leaves	2	
90 ml bulk sediment	5	
Abies cf. lasiocarpa wood	5	
Abies cone scale	2	
Abies needle	2	
Abies seed	2	
acorn fragments	2	
Alces alces bone	6	
algal clayey gyttja	5	
algal copropel	5	
Algal gyttja	5	
algal gyttja	5	
algal-calcareous gyttja	5	
Algal-clayey gyttja	5	
Alkali-soluble humus	5	
Alkali-soluble humus (1)	5	
alluvial silt	5	
Alnus twig	2	
Alnus twigs	2	
Alnus wood	5	
also sample number BETA-59381	5	material not specified

Material (as in the Geochronology table of the Neotoma database)	Accuracy Rank	Notes
also sample number BETA-61558	5	material not specified
also sample number BETA-61559	5	material not specified
amberat sample #7865	4	assigned this as a default- probably better than wood?
amberat sample #7866	4	assigned this as a default- probably better than wood?
amberat sample #7867	4	assigned this as a default- probably better than wood?
amberat sample #7868	4	assigned this as a default- probably better than wood?
amberat sample #7869	4	assigned this as a default- probably better than wood?
amberat sample #7870	4	assigned this as a default- probably better than wood?
amberat sample #7871	4	assigned this as a default- probably better than wood?
amberat sample #7872	4	assigned this as a default- probably better than wood?
amberat sample #7873	4	assigned this as a default- probably better than wood?
Ambrosia seed	2	
Angiosperm wood	5	
Antler	6	
aquatic moss	6	
aquatic moss peat and wood	5	
aquatic mosses	6	
Arctodus simus bone	6	
Arctodus simus bone collagen	5	
Artiodactyla bone	6	
Aster seeds, wood	4	weighted towards wood (between 2=seed, 5=wood)
bark	3	
Bark	3	
Bark and bract	3	Weighted towards bark (between 2=bract, 3=bark)
Bark and charcoal	4	Weighted between bark (3) and charcoal (5)
Bark and plant fragments	3	between 3=plant matter/fragments/material, 3=bark)
bark fragment	3	
Bark, needles	3	Weighted towards bark (between 2=needles, 3=bark)
Bark,seeds,insect parts	3	weighted towards bark (between 2=seed, 3=bark)
Basal clayey gyttja	5	
basal peat moss	6	
base soluble bulk sediment	5	

Material (as in the Geochronology table of the Neotoma database)	Accuracy Rank	Notes
bat dung	2	
beaver-gnawed wood	5	
beetle parts	2	
beetle, probably aquatic	3	penalized one rank because 'probably aquatic'
Betuaceae frts and catkin scls	2	
Betula and Larix twigs	2	
Betula fruits	2	
Betula fruits and bracts	2	
Betula lenta seed and stem frgs	2	
Betula nana twig	2	
Betula sect. Albae bark and wood	4	weighted between wood and bark, not sure what "sect" refers to (between wood=5, bark=3)
Betula seed and bract	2	
Betula seed; moss stem	4	weighted towards mosses (between 2=seed, 6=mosses)
Betula seeds and pinus scales	2	
Betula twig	2	
Betula twigs	2	
Betula/Viola seeds, picea ndls	2	
Betulaceae frts, Lrx lf nd twg	2	
Biomphalaria gastropod shells	6	
Birch	5	
Birch seed	2	
Birch twigs	2	
bird bone	6	
Bison antiquus bone	6	
Bison antiquus bone amino acid	5	
Bison bison	6	
Bison bison bone	6	
Bison bison bone collagen	5	
Bison bison hoof	6	
Bison bison horn sheath	6	
Bison bone	6	
Bison bone apatite/carbonate	6	
Bison bone collagen	5	
Bison occidentalis bone	6	
Bivalve	6	
bivalve	6	
black and gray silty clay	5	
Black clay	5	
Black detritus gyttja	5	
Black gyttja	5	
Black highly humified peat	5	
Black lake mud	5	
black muck	5	

Material (as in the Geochronology table of the Neotoma database)	Accuracy Rank	Notes
Black mud	5	
black organic clay	5	
black peat	5	
Black peat	5	
black silt	5	
black silty clay	5	
black, gelatinous gyttja	5	
Black, highly humified peat	5	
Blackish decomposed <i>Alnus</i> peat	5	
blue-grey silty clay	5	
Bog-forest peat	5	
Bone	6	
bone	6	
Bone (phalanx)	6	
bone amino acid	5	
bone apatite/carbonate	6	
bone collagen	5	
<i>Bootherium bombifrons</i> bone	6	
<i>Bos taurus</i> bone	6	
Bovidae bone	6	
bract, seed, twig, and leaf frgs	2	
branch fragment	4	
branch of shrub	4	
<i>Brasenia</i> seeds	2	
Brown dark clay	5	
brown fibrous peat	5	
brown gyttja	5	
Brown gyttja	5	
Brown moss	6	
Brown peat	5	
Brown peat with <i>Phragmites</i>	5	
Brown peat, shell, <i>Phragmites</i> , wood	5	weighted towards wood/peat
Brown peat, with abundant <i>Phragmites</i> rhizomes	5	
Brown, coarse detritus gyttja	5	
Brownclay with peat admixture	5	
Bryophyte macrofossil	2	
bryophyte peat	5	
bryophytes	5	
Bryophytes (<i>sphagnum</i>)	5	
Bryophytes (unidentified)	5	
bryophytic peat	5	
bulk	5	
Bulk	5	
Bulk carbon in sediment	5	
bulk clay sample	5	
bulk clay sediment	5	

Material (as in the Geochronology table of the Neotoma database)	Accuracy Rank	Notes
bulk date	5	
bulk date (carbonate)	5	
bulk lake sediment	5	
Bulk marine sediment	5	
Bulk mud	5	
bulk organic in clay matrix	5	
Bulk organic sediment	5	
bulk organics	5	
bulk peat	5	
Bulk peat	5	
bulk peat sample	5	
bulk peaty material	5	
Bulk peaty sediment	5	
bulk sediment	5	
Bulk sediment	5	
Bulk sediment - gyttja w/ detritus	5	
Bulk sediment - marly gyttja	5	
bulk sediment (clay)	5	
bulk sediment (marly gyttja)	5	
bulk sediment: needles, wood	4	weighted towards wood (5) and bulk (5), away from needles (2)
bulk sediment:detrtus gyttja	5	
bulk;gyttja	5	
bulk:gyttja	5	
Buried peat	5	
Buried peat lower limit	5	
Buried soils	5	
burned log	5	
Calc with sand	5	
Calcareous	5	
Calcareous clay gyttja	5	
calcareous detritus gyttja	5	
Calcareous fraction	5	
Calcareous fraction (39%)	5	
Calcareous fraction (47%)	5	
Calcareous gyttia	5	
calcareous gyttja	5	
Calcareous gyttja	5	
calcareous organic silt	5	
calcareous sand	5	
calcareous silt	5	
Calcareous silt	5	
calcareous silty gyttja	5	
calcareous silty muck	5	
calcareous-ferrous gyttja	5	
Camelops bone	6	
Camelops hesternus bone	6	

Material (as in the Geochronology table of the Neotoma database)	Accuracy Rank	Notes
Camelops hesternus bone amino acid	5	
Carbon in loamy sand	5	
Carbon in sandy clay loam	5	
carbonate	5	
Carbonate - lacustrine lime	5	
Carbonate fen	5	
Carbonate-rich horizon with shell fragments and lime mud. Organic carbon: 0.75%; CaCO ₃ : 16.2%.	5	weighted towards mud
Carbonized spruce needle, inse	4	unclear what the complete material is weighted towards wood (between 2=twig, 5=wood)
Carbonized twigs and wood frag	4	
Carex	2	
Carex - gyttja	5	
Carex peat	5	
Carex with Carex peat	5	
Carex-Sphagnum peat	5	
Castoroides ohioensis bone collagen	5	
cedar type wood	5	
Cellulose	2	
Cervalces scotti bone	6	
Cervalces scotti bone collagen	5	
Cervidae bone	6	
Cervus bone	6	
Cervus canadensis bone	6	
cf. Quercus leaf and twig	2	
Chalk with shells	6	
Charcoal	5	
charcoal	5	
Charcoal (25 mg)	5	
Charcoal and 1 Larix needle	4	weighted towards charcoal (between 2=needle, 5=charcoal)
charcoal and Schoenoplectus seeds	4	weighted towards charcoal (between 2=seed, 5=charcoal)
charcoal and wood	5	
charcoal flakes	5	
charcoal fragments	5	
Charcoal, 1 Cyperaceae seed	4	weighted towards charcoal (between 2=seed, 5=charcoal)
charcoal, 1 Schoenoplectus seed	4	weighted towards charcoal (between 2=seed, 5=charcoal)
Charcoal, leaf fragment	4	weighted towards charcoal (between 2=leaf, 5=charcoal)
Charcoal, picea needle	4	weighted towards charcoal (between 2=needle, 5=charcoal)
charcoal, Poaceae seed, Cyperaceae seed	4	weighted towards charcoal (between 2=seed, 5=charcoal)

Material (as in the Geochronology table of the Neotoma database)	Accuracy Rank	Notes
charcoal, Schoenoplectus seed	4	weighted towards charcoal (between 2=seed, 5=charcoal)
charcoal, Schoenoplectus seed, Chenopodium seed	4	weighted towards charcoal (between 2=seed, 5=charcoal)
charcoal, Typha seed	4	weighted towards charcoal (between 2=seed, 5=charcoal)
charcoal, wood	5	
charcoal, wood, leaf	4	weighted towards wood/charcoal (between 2=leaf, 5=charcoal/wood)
Charcoal; wood; leaf	4	weighted towards wood/charcoal (between 2=leaf, 5=charcoal/wood)
charred bone	6	
charred grass	2	
charred Juniperus wood	5	
Charred macrofossils	5	no information on which type of macrofossil
Charred material	5	
Charred material, bark	5	
Charred material, twig	3	Penalized one rank for "charred material"
charred plant matter	3	
charred wood	5	
Chenopod seeds	2	
Chenopodium seeds	2	
clay	5	
Clay	5	
clay gyttja	5	
Clay gyttja	5	
clay gyttya	5	
Clay mud	5	
Clay w/ fine organic detritus	5	
Clay with fen peat	5	
Clay with humus	5	
Clay with low organic content. Almost no carbonate.	5	
clay with organic traces from 5 m below shell layer.	5	
Clay with plant remains	5	
clay-gyttja	5	
clay-silt fine-detritus gyttja	5	
clay/gyttja	5	
Clayey	5	
clayey copropel	5	
clayey fine sand	5	
Clayey gyttja	5	
clayey gyttja	5	
Clayey gyttja lower limit	5	
Clayey gyttja upper limit	5	

Material (as in the Geochronology table of the Neotoma database)	Accuracy Rank	Notes
clayey medium sand	5	
clayey mud	5	
clayey organic lake sediments	5	
clayey peat	5	
Clayey peat	5	
clayey sandy silt	5	
clayey silt	5	
clayey silt with macrofossils	5	
Clayey-gyttja	5	
clayish fine sand	5	
Clays of low organic content. Almost no carbonate.	5	
Clethrionomys gapperi bone amino acid	5	
coarse detritus gyttja	5	
Coarse detritus gyttja	5	
Coarse detritus mud	5	
coarse sand and plant frags	5	
collagen from eight partial thoracic vertebrae from a single individual of Symbos cavifons	5	
compressed peat	5	
Conifer charcoal	5	
Conifer cone bract, bark	3	Weighted towards bark (between 2=bract, 3=bark)
Conifer cone scales, bark	3	Weighted towards bark (between 2=scales, 3=bark)
conifer needle fragments	2	
Conifer needles	2	
conifer needles	2	
Conifer twig	2	
Conifer twigs	2	
conifer wood	5	
conifer-wood fragment	5	
copropel	5	
copropelic moss peat	5	
copropelic silty clay	5	
Coquilles	6	
core 180-1	6	
core 180-2	6	
core 180-3	6	
Cornus drummondii seed	2	
course detritus gyttja	5	
course gyttja	5	
course Sphagnum peat	5	
course-detritus gyttja	5	
Cyperaceae achenes	2	
Cyperaceae seed	2	

Material (as in the Geochronology table of the Neotoma database)	Accuracy Rank	Notes
Cyperaceae seeds	2	
Daphnia eggs	5	uncertain about hardwater contamination?
		uncertain about hardwater contamination?
Daphnia eggs; aquatic plant frags	5	Ranked between eggs (5) and aquatic plants (6)
Dark brown detritus peat	5	
dark brown dy	5	
dark brown humus-rich gyttja	5	
Dark clay	5	
dark gray organic silt	5	
dark gray silt with rootlets	5	
Dark gray soil zone with finely divided organic matter. Organic carbon: 1.94%; CaCO ₃ : 1.68%.	5	
dark gray to black silty clay	5	
Dark gyttja	5	
dark olive clay	5	
dark peat	5	
Dark sediment	5	
Darkish sands with pale layer. Almost no carbonate.	5	
Decalcified sediment	5	
Deciduous leaf	2	
deciduous wood	5	
decomposed peat	5	
detrital gyttja	5	
detrital mollusc shell frags	6	
detrital peat	5	
detritus gyttja	5	
Detritus gyttja	5	
detritus gyttja, wood frags	5	
detritus mud	5	
Detritus mud	5	
Detritus mud with wood	5	
detritus peat	5	
Detritus peat	5	
Detritus with clay	5	
Detritus with kaolin + gravel	5	
Detritus with sand and silt	5	
Detritus with woody fragments	5	
Dichelyma capillaceum	6	
Dicroidium bone amino acid	5	
Drepanocladus	6	
Drepanocladus cf. vernicosus	6	
Drepanocladus crassicostatus	6	
Drepanocladus/Calliergon	6	

Material (as in the Geochronology table of the Neotoma database)	Accuracy Rank	Notes
Dryas and salix leaves	2	
dung	2	
Duplicated run on sample# 1	5	material not specified
elk bone collagen	5	
Elphidium	5	uncertain material; assigned 5 as default
Equus bone	6	
Equus bone amino acid	5	
Equus bone apatite/carbonate	6	
Equus hoof	6	
Equus occidentalis bone amino acid	5	
Erythizon dorsatum dung	2	
Eriophorum-Sphagnum peat	5	
Eriophorum-Sphagnum-woody peat	5	
Eriophorum-woody peat	5	
feature or structure	5	uncertain material; assigned 5 as default
Fen	5	
Fen peat + organic rich sand	5	
ferrous gyttja	5	
fibrous artifact	5	uncertain material; assigned 5 as default
fibrous gyttja	5	
Fibrous peat	5	
fibrous peat	5	
fibrous peat with wood frags	5	
Fibrous sedge peat	5	
fibrous sedge peat	5	
Fine aragonite pellets	5	
Fine detrital sapropel	5	
fine detritus gyttja	5	
Fine detritus gyttja	5	
fine detritus mud	5	
Fine detritus mud	5	
fine detritus mud, gray silt	5	
Fine detritus with macros	4	weighted between macros and detritus (5)
Fine detritus wood	5	
Fine fraction of reed-swamp	5	
fine gyttja	5	
Fine gyttja	5	
Fine organic detritus w/ clay	5	
Fine particulate peat fraction	5	
Fine particule of peat	5	
fine sand	5	
fine sand/organic clayey silt	5	
fine-detritus gyttja	5	
fine-grained peat, org clay	5	

Material (as in the Geochronology table of the Neotoma database)	Accuracy Rank	Notes
Finely divided organic matter in zone affected by weak pedogenesis. Organic carbon: 1.45%; CaCO ₃ : 0.41%.	5	
flocculent organic gyttja	5	
Fluid gyttja	5	
fossil Sphagnum peat	5	
fossil tooth	5	
Four charred spruce needle fragments, four conifer seed wing fragments, three birth nutlets	2	
fragment of <i>Betula</i> leaf	2	
fragmented mollusc shells	6	
<i>Fraxinus nigra</i> wood	5	
Ga2, Ag2, Dh+, Dg+	5	
Ga2, Ld2, Lc+, Ag+	5	
gelatin from KOH-extracted collagen from <i>Dasypus bellus</i> bone	3	
gelatin from KOH-extracted collagen from <i>Felis onca</i> bone	3	
gelatin from KOH-extracted collagen from <i>Mammut americanum</i> bone	3	
gelatin from KOH-extracted collagen from <i>Platygonus compressus</i> bone	3	
gelatin from KOH-extracted collagen from reptile bone	3	
gelatin from untreated collagen from <i>Mammuthus columbi</i> bone	4	
<i>Glossotherium harlani</i> bone	6	
<i>Glossotherium harlani</i> bone amino acid	5	
<i>Glossotherium harlani</i> bone apatite/carbonate	6	
graminoid stems	2	
graminoid, terr. plant frags	3	between graminoid (2) and terr. plant fragments (3)
Grass or sedge stem	2	
Grass spikelets	2	
gray silt	5	
gray silt and fine sand	5	
gray silty clay	5	
gray silty mud	5	
gray-green silt	5	
greenish brown gyttja	5	
greenish gray silty gyttja	5	
greenish gyttja	5	
Grey clay mud.	5	
Grey detritus gyttja	5	
Grey silt	5	

Material (as in the Geochronology table of the Neotoma database)	Accuracy Rank	Notes
Grey-brown silt	5	
Gymnogyps californianus bone	6	
Gymnosperm wood	5	
gyttja	5	
Gyttja	5	
Gyttja - clay gyttja	5	
Gyttja - Equisetum	5	
gyttja (2nd core)	5	
Gyttja and Carex peat	5	
Gyttja and clay	5	
Gyttja and detritus.	5	
Gyttja clay	5	
Gyttja clay, silt	5	
Gyttja clayey silt	5	
Gyttja with calc	5	
gyttja with clay	5	
Gyttja with diatoms	5	
gyttja with marl banding	5	
Gyttja with plant remains	5	
gyttja with Vivianite	5	
gyttja, coarse plant fragments	5	
gyttja, silt	5	
gyttja, wood, charcoal	5	
gyttja/clay transition	5	
gyttja/moss	5	
gyttja/silt	5	
gyttja/silt-clay	5	
gytya	5	
hearth	5	uncertain material; assigned 5 as default
herb peat	5	
herbaceous detritus gyttja	5	
herbaceous peat	5	
Highly humified Sphagnum peat	5	
Homo sapiens bone	6	
Homo sapiens bone amino acid	5	
Homo sapiens bone apatite/carbonate	6	
Homo sapiens bone collagen	5	
Homo sapiens dung	2	
horn sheath	6	
humates	5	uncertain rank; assigned 5 as default
humic acid	5	uncertain material; assigned 5 as default
Humic acid extract	5	
Humic acids	5	uncertain material; assigned 5 as default
humic acids	5	uncertain material; assigned 5 as default
humic acids from paleosols	5	
humic gyttja	5	
Humic-amorphous peats	5	

Material (as in the Geochronology table of the Neotoma database)	Accuracy Rank	Notes
Humic-fibrous peats	5	
Humic-organic muds	5	
Humic-silty clay	5	
Humidic acids from peat	5	
Humidic acids from the peat	5	
humified copropel	5	
humified peat	5	
Humified peat	5	
humified peat, becoming muddy	5	
humified sphagnum peat	5	
humified Sphagnum peat	5	
Humin-amorphous peats	5	
Humin-fibrous peats	5	
Humin-organic muds	5	
Humin-silty clay	5	
humins	5	uncertain material; assigned 5 as default
Humus	5	
Humus peat	5	
Hydromorphic soils	5	
Hygrohypnum spp.	6	
Immature conifer strobilus	2	
in situ wood fragment	5	
inorganic clay	5	
inorganic fraction bulk sed.	5	
inorganic lake sediment	5	
insect parts	2	
insects, probably aquatic	3	penalized one rank because 'probably aquatic'
Insects, wood fragments	4	weighted towards wood (between 2=insects, 5=wood)
insol. fraction bulk sediment	5	
invertebrate egg cases	5	uncertain about hardwater contamination?
Ivory	6	
Jatropha seeds	2	
Juniperus twig	2	
lacustrine bulk sediment	5	
Lacustrine lime	5	
Lacustrine lime- CO ₃ fraction	5	
lacustrine silt	5	
Lake deposit	5	
lake mud	5	
Lake mud	5	
Lake sediment	5	
lake sediment	5	
Laminated clayey gyttja	5	
laminated gyttja	5	

Material (as in the Geochronology table of the Neotoma database)	Accuracy Rank	Notes
laminated marl and gyttja	5	
laminated sediments	5	
laminated silty gyttja	5	
Larch needle + blackened organic fragments	3	Penalized one rank for "blackened organic fragments"
Larix and Picea needle fragments, Picea seed wing fragment	2	
Larix and Picea needle fragments, Picea seed wing fragment	2	
Larix cone	2	
Larix leaf, charcoal	4	weighted towards charcoal (between 2=leaf, 5=charcoal)
Larix leaf,charcoal,unid leaf	4	weighted towards charcoal (between 2=leaf, 5=charcoal)
Larix leaves	2	
Larix leaves, twig	2	
Larix lf, Betula or Alnus seed	2	
Larix lf;semiwoody;plant frags	3	weighted towards wood (between 2=leaf, 3=plant matter/fragments/material/litter/detritus, 4=semi-woody)
Larix needle	2	
Larix needle fragments, Picea seed wing	2	
Larix needle fragments, Picea seed wing	2	
Larix needle, moss, insects	4	weighted towards mosses (between 2=needle, 6=mosses)
Larix needle, unident seed	2	
Larix needle; unid leaf frags	2	
Larix needle;unid.terr.plants	3	Penalized one rank for "unid.terr.plants"
Larix needles	2	
Larix needles, Betula papyrifera seed and fruit scale	2	
Larix needles, charred scales	2	
Larix needles, Picea seed wing	2	
Larix needles; Betula papyrifera seed and fruit scale	2	
Larix needles; Picea seed wing	2	
Larix needles; wood fragment	4	weighted towards wood (between 2=needle, 5=wood)
Larix root	3	
Larix seed, Picea seed, Larix needles	2	
Larix twig	2	
Larix twig/cone	2	
Larix wood	5	
Larix wood pieces	5	
Larix; unident. plant material	3	
late glacial clay	5	

Material (as in the Geochronology table of the Neotoma database)	Accuracy Rank	Notes
late glacial clay	5	
Lateral bud + 13 deciduous leaf fragments	2	
Ld2, Ag2, Ga+, Dh+, Dg+	5	
Ld2, Dg2, Dh+	5	
Ld2, Dg2, Dh+, Ag+	5	
Ld2, Dh1, Dg1	5	
Ld2, Ga2, Dg+, Dh+	5	
Ld2, Lc1, Ag1, Ga+, Dg+	5	
Ld2, Lso2, Dg+, Dh+, Ag+, Ga+	5	
Ld3, Ag1, Ga+, Dh+, Dg+	5	
Ld3, Dg1, Dh+	5	
Ld3, Dg1, Dh+, Ga+	5	
Ld3, Dh1, Dg+	5	
Ld3, Ga1, Ag+	5	
Ld3, Ga1, Dg+, Ag+	5	
Ld4, Ag+, Dh+, Dg+	5	
Ld4, Dh+, Dg+	5	
Leaf	2	
leaf	2	
Leaf and bark	3	Weighted towards bark (between 2=leaf, 3=bark)
leaf and twig fragments	2	
Leaf fragments	2	
Leaves of Dryas octopetala	2	
Lepidoptera mandibles	2	
Lepus americanus bone	6	
light brown organic silt	5	
light brown peat	5	
light-brown sandy silt	5	
Lime mud	5	
Limestone	5	
limnic peat	5	
Loam	5	
Loamy sand	5	
Loch sediment	5	
log (Abies)	5	
log (Picea)	5	
loose fibrous organic debris	5	no information on which part
macrofossil fragments	5	
Male cone	2	
Male cone/needles/wood	3	weighted towards needles/cone (between 2=needles, 5=wood)
Male cone/seeds	2	
mammoth bone collagen	5	
mammoth skin	2	
mammoth skin and muscle	2	

Material (as in the Geochronology table of the Neotoma database)	Accuracy Rank	Notes
mammoth tusk	5	
mammoth tusk collagen	5	
Mammut americanum	6	
Mammut americanum bone	6	
Mammut americanum bone apatite/carbonate	6	
Mammut americanum bone collagen	5	
Mammut bone	6	
Mammuthus bone	6	
Mammuthus bone apatite/carbonate	6	
Mammuthus bone collagen	5	
Mammuthus columbi bone	6	
Mammuthus columbi bone apatite/carbonate	6	
Mammuthus columbi bone collagen	5	
Mammuthus columbi carbonate	6	
Mammuthus columbi XAD-resin-purified hydrolyzate from KOH-extracted gelatin	2	
Mammuthus dung	2	
Mammuthus exilis bone	6	
Mammuthus exilis bone collagen	5	
Mammuthus imperator bone collagen	5	
Mammuthus jeffersonii bone	6	
Mammuthus jeffersonii tooth enamel	5	
Mammuthus tooth enamel	5	
marine mollusc shells	6	
Marine shell fragments in sand	6	
marl	5	
Marl	5	
marl and detritus	5	
marl carbonate fraction	5	
marl CO3	5	
Marl mixed with some peat	5	
Marl with moss	6	
Marl with organic matter	5	
marly copropel	5	
marly detritus gyttja	5	
marly gyttja	5	
Marly organic mud	5	
Marly peat	5	
Marly sediment	5	
marly sediment	5	
marly, organic gyttja	5	
marly, silty gyttja	5	
Marmota flaviventris bone collagen	5	
marsh sediments	5	
matrix	5	

Material (as in the Geochronology table of the Neotoma database)	Accuracy Rank	Notes
medium-detritus gyttja	5	
Megalonyx bone	6	
Micro mud	5	
Microtus bone amino acid	5	
Microtus bone collagen	5	
Microtus ochrogaster bone	6	
Midden debris	5	material not specified
Milodon faeces	2	
mixed gastropod shell	6	
Mixed plant material	3	
Mixed wood and bark	4	weighted between wood=5, bark=3
mod. humified fibrous peat	5	
mollusc shell	6	
Mollusc shell	6	
mollusc shells	6	
molluscs	6	
Mollusk	6	
mollusk shell	6	
Monocot frags	2	probably not aquatic?
moss	6	
moss fragments	6	
moss fragments P. wahlenbergii	6	
moss fragments; leaf, stem	4	
moss in clay	6	
moss leaves; Betula seed	4	
Moss peat	5	
moss pieces, plant remains	4	between plant remains (3) and moss (5)
moss stems	6	
moss stems and leaves	6	
moss-rich organic silt	6	
moss, possibly aquatic	6	
Mosses	6	
Mosses and organic matter	6	
Mosses-total fraction	6	
mud	5	
Mud	5	
Mud and silt	5	
Muddy peat	5	
Muddy sapropel	5	
Muddy silty clay	5	
Mulinia lateralis	6	
muscle	2	
muscle and skin of mammoth	2	
Mushroom	2	
NA	6	no information
NaOH insoluble	5	
NaOH insoluble algal gyttja	5	

Material (as in the Geochronology table of the Neotoma database)	Accuracy Rank	Notes
NaOH soluble	5	
NaOH soluble algal gyttja	5	
NaOH soluble peaty/sandy layer	5	
NaOH soluble portion	5	uncertain material; assigned 5 as default
NaOH-insoluble fraction	5	
NaOH-soluble fraction	5	
NaOH-soluble fraction-sediment	5	
needle fragment	2	
Needles	2	
Needles, cone scale, catkin	2	
Needles, wood, seeds, leaves	3	weighted towards needles/seeds/leaves (between 2=seed, 5=wood)
Needles; wood; seeds; leaves	3	weighted towards needles/seeds (between 2=seed, 5=wood)
Needles/seeds/wood	3	weighted towards needles/seeds (between 2=seed, 5=wood)
Needles/wood	4	weighted towards wood (between 2=needle, 5=wood)
Neotoma cinerea dung	2	
Neotoma dung	2	
Neotoma floridana bone amino acid	5	
Neotoma pellets	2	
Nothrotheriops dung	2	
Nothrotheriops shastense bone collagen	5	
Nothrotheriops shastense dung	2	
Nymphaea seeds	2	
Oak leaf fragments	2	
Ochotona princeps dung	2	
Odocoileus antler	6	
Odocoileus bone	6	
Odocoileus dung	2	
Odocoileus virginianus bone	6	
olive-gray gyttja	5	
olive-gray marl-gyttja	5	
Oreamnos harringtoni	6	
Oreamnos harringtoni dung	2	
Oreamnos harringtoni horn sheath	6	
Org.mat in sand	5	
Org.mat.in salty sand	5	
Org.mat.in salty silt	5	
Org.material in salty sand	5	
Org.material in salty silt	5	
Org.material in sand	5	
organic	5	
organic bulk date	5	
Organic carbon fraction.	5	
organic clay	5	

Material (as in the Geochronology table of the Neotoma database)	Accuracy Rank	Notes
Organic clay	5	
organic clay gyttja	5	
Organic copropel	5	
Organic detrit	5	
organic detritus	5	
organic fine sand	5	
organic fine sandy silt	5	
organic fraction	5	
Organic fraction	5	
Organic fraction of marly sed	5	
organic fraction, bulk sed.	5	
organic gyttja	5	
organic lake sediment	5	
Organic lake sediment	5	
organic loamy clay	5	
organic marl	5	
Organic material	5	
organic material in black clay layer	5	
organic matter	5	
organic micaceous silt	5	
organic mud	5	
Organic mud	5	
Organic mud w/ sand	5	
Organic mud, humic acid treatment	5	
organic rich moss layer	6	
organic sand	5	
Organic sand	5	
organic sediment	5	
Organic sediment	5	
Organic sediment inc.carbonate	5	
organic silt	5	
Organic silt	5	
organic silt and marl	5	
Organic silts	5	
organic silty clay	5	
organic silty clay and marl	5	
organic-clay gyttja	5	
Organic-rich sand	5	
organics	5	
organics in clay	5	
ostracod rich gyttja	5	
ostracodes	5	uncertain shell chemistry?
Ovis bone	6	
Ovis canadensis dung	2	
Ovis canadensis horn sheath	6	
Ovis horn sheath	6	
Oyster	6	

Material (as in the Geochronology table of the Neotoma database)	Accuracy Rank	Notes
Particulate matter	5	
Particulate matter (1)	5	
Particulate matter (2)	5	
Particulate matter (3)	5	
Particulate matter <250 micron	5	
Particulate matter >250 micron	5	
partly decayed, uncarb. wood	5	
peat	5	
Peat	5	
PEAT	5	
peat (adjacent to log)	5	
peat (adjacent to wood)	5	
peat and gyttja	5	
peat and wood	5	
Peat fibers	5	
Peat material	5	
Peat Material	5	
Peat materials	5	
Peat moderately decayed	5	
Peat slightly decayed	5	
Peat slightly decayed and wood	5	
Peat with clay, Alnus fragments	5	
Peat with mollusc shells	5	weighted towards peat
Peat with Phragmites rhizomes	5	
peat with Picea needles	4	weighted towards peat (between Picea needles (2) and peat (5))
Peat with shell remains	5	weighted towards peat
peat with silt	5	
peat with wood	5	
Peat with Wood	5	
peat with wood remains	5	
peat, decomposed	5	
Peat, herbacea, Alnus fragments	5	
PEAT, WOOD	5	
Peat/gyttja	5	
peat/sand	5	
peat/sediment	5	
Peat/silt-peat transition	5	
Peaty gyttja	5	
Peaty chalk	5	
Peaty chalk with shells	5	
peaty detritus gyttja	5	
peaty detritus mud	5	
peaty gyttja	5	
Peaty gyttja	5	
peaty gyttja	5	
peaty organics	5	

Material (as in the Geochronology table of the Neotoma database)	Accuracy Rank	Notes
Peaty sand	5	
peaty sands	5	
Peaty sapropel	5	
peaty silt	5	
Peaty silt	5	
Peaty silt with mollusc shells	5	weighted towards silt
peaty/gyttja	5	
Phragmites Carex peat	5	
Phragmites peat/peaty gyttja	5	
Picea plant matter	4	Weighted towards Picea (between 3=plant matter/fragments/material, 5=wood)
Picea wood	5	
Picea and Larix needle fragments	2	
Picea and Larix needle fragments, 3 Picea seed wings	2	
Picea and Larix needle fragments, Picea seed wing	2	
Picea charcoal	5	
Picea cone	2	
Picea cones	2	
Picea frags, Cyperaceae seeds	2	
Picea glauca cones	2	
Picea macrofossils	5	no information on which part
picea mariana needles and twig	2	
Picea needle	2	
Picea needle and seed	2	
Picea needle fragments	2	
Picea needle fragments, Picea seed wing, Larix needle fragment	2	
Picea needle, 2 Betula seeds, Larix needle, Picea seed wing	2	
Picea needle, Picea seed wing	2	
Picea needle; 2 Betula seeds; Larix needle; Picea seed wing	2	
Picea needles	2	
Picea needles, 3 Rubus seeds	2	
Picea needles, charcoal	4	weighted towards charcoal (between 2=needles, 5=charcoal)
Picea needles, charred twigs	2	
Picea needles, wood	4	weighted between needles (between needle=2, charcoal=5)
Picea needles,seed; Rubus seed	2	
Picea seed wing, Picea seed, Larix needle, 3 charcoalized Picea needle fragments, charcoal	3	weighted towards plant fragments (between 2=seed/needles, 5=charcoal)

Material (as in the Geochronology table of the Neotoma database)	Accuracy Rank	Notes
Picea seed, 2 needle fragments, 2 charcoal particles, 2 seed wings	3	weighted towards plant fragments (between 2=seed/needles, 5=charcoal)
Picea seed, Cyperaceae leaves	2	
Picea seed, Drepanocladus	6	weighted between seed (2) and moss (6)
Picea seed; 2 needle fragments; 2 charcoal particles; 2 seed wings	3	weighted towards needles/seeds (between 2=seed, 5=charcoal)
Picea wood	5	
Picea, Sparganium, Menyanthes	5	no information on which part, Picea=5, Sparganium= aquatic plant = 6, and Menyanthes? (occurs in bogs and marshes)
Picea/Larix needles, charcoal	3	weighted toward needles (between needle=2, charcoal=5)
Picea/Pinus needles	2	
Piece of wood	5	
Pieces of wood	5	
Pine bark	3	
pine ndls, birch seeds, wood	3	weighted towards needles/seeds (between 2=seed, 5=wood)
pine needles	2	
Pine stump	5	
Pinus contorta twigs and needles	2	
Pinus needle	2	
Pinus needles; unident. plant	3	
Pinus resinosa needle	2	
Pinus scales	2	
Pinus strobus needle frgs (6)	2	
Pinus strobus wood	5	
Pinus sylvestris wood	5	
Pisidium sp.	6	
Pistia stratiotes seeds	2	
plant debris	3	
plant detritus	3	
PLANT DETRITUS	3	
Plant fragment	3	
plant fragment	3	
Plant fragments	3	
plant fragments	3	
Plant fragments and wood	4	between wood (5) and plant frags (3)
Plant fragments, twig	3	
plant macrofossils	3	
plant matter	3	
plant remains	3	
Plant remains	3	
Plant remains (washed peat)	5	
Plant remains in tephra V<~900	3	
Plant remains in tephra V^~900	3	

Material (as in the Geochronology table of the Neotoma database)	Accuracy Rank	Notes
Plant remains in tephra Vö~900	3	
plant stem (<i>Scirpus</i> ?)	2	
Plant tissue	3	
Plastic blue-grey clay	5	
Plastic clay with traces of organic matter and carbonate.	5	
<i>Platygonus compressus</i> bone	6	
<i>Platygonus compressus</i> bone collagen	5	
Poaceae;unidentified plant mat	3	
pollen	4	rationale: not as good as macrofossils, better than wood
Pollen	4	rationale: not as good as macrofossils, better than wood
pond mud	5	
Populus twig	2	
Populus wood	5	
Porous chalk	5	
Potamogeton seeds	2	
Potamogeton,Ruppia,Carex seeds	2	
pottery	5	uncertain material; assigned 5 as default
Proboscidean bone	6	
Quercus charcoal	5	
Quercus wood	5	
Rangifer tarandus bone	6	
Reed swamp peat	5	
reptile bone	6	
reptile bone collagen	5	
residue	5	uncertain material; assigned 5 as default
residue (minus humates)	5	uncertain material; assigned 5 as default
Rodentia bone	6	
Rodentia bone apatite/carbonate	6	
Rodentia bone collagen	5	
root and branch of shrubs	4	
Roots	3	
roots and shrub branches	4	
roots of tree Betula	3	
Rosa seed	2	
Ruppia seeds	2	
Salix (?) twig	2	
Salix and Dryas twigs/leaves	2	
Salix branches	4	
Salix bud scale;moss;unid seed	4	weighted towards mosses (between 2=seed, 6=mosses)
Salix herbacea leaves	2	
Salix herbacea leaves, wood	4	weighted towards wood (5), away from leaves (2)
Salix remains	5	no information on which part

Material (as in the Geochronology table of the Neotoma database)	Accuracy Rank	Notes
Salix undifferentiated wood	5	
Salix wood	5	
sand	5	
sand and clay	5	
sand and gravel	5	
Sand with clay	5	
sand, low in organic matter	5	
Sands with organic fragments. Organic carbon: 2.08%; CaCO3: 0.22%.	5	
sandy calcareous gyttja	5	
sandy clay	5	
Sandy clay with organic matter as small black specks. Organic carbon: 1.66%; CaCO3: 0.90%.	5	
Sandy clay with organic specks. Organic carbon: 1.21%; CaCO3: 0.03%.	5	
sandy gyttja	5	
sandy olive-gray gyttja	5	
Sandy organic mud	5	
sandy peat	5	
Sandy peat	5	
sandy silt	5	
Sandy silt	5	
sandy silty clay	5	
sandy, clay-marl	5	
Sapropel	5	
Sapropel mud	5	
Scenedesmus gyttja	5	
Schoenoplectus stem	2	
Scirpus achenes	2	
Scirpus seeds	2	
Sedge	2	
sedge	2	
sedge peat	5	
Sedge peat	5	
sedge peat (Carex)	5	
Sedge peat with wood	5	
sedge peat with wood fragments	5	
Sedge-Sphagnum	5	
Sediment	5	
sediment	5	
sediment and clay (2nd core)	5	
seed	2	
seed of Betula or Alnus	2	
seed, moss stem	4	weighted towards mosses (between 2=seed, 6=mosses)
seeds	2	

Material (as in the Geochronology table of the Neotoma database)	Accuracy Rank	Notes
Seeds	2	
Seeds, bark	3	weighted towards bark (between 2=seed, 3=bark)
Seeds, wood, insect elytra	3	weighted towards seeds/insects (between 2=seed, 5=wood)
Several pieces of picked wood	5	
shell	6	
shell organics	6	
shrub branch	4	
shrub fragments	4	
Shrub-sedge peat	5	
Sieved charcoal fragments	5	
Silt	5	
silt	5	
silt or clay	5	
Silt with fine detritus	5	
Silt with limey layers	5	
Silt with plant detritus	5	
Silt with roots	5	
silt with wood detritus	5	
Silt/Clay	5	
silty clay	5	
Silty clay	5	
silty clay with stones	5	
silty copropel	5	
Silty detritus	5	
silty fine sand	5	
Silty gyttja	5	
silty gyttja	5	
Silty gyttja/Clayey-gyttja	5	
silty mud	5	
Silty mud	5	
silty organic gyttja	5	
Silty organic lake sediment	5	
silty organic mud	5	
silty peat	5	
silty sand	5	
silty-sandy colluvium	5	
silty, marly gyttja	5	
Single piece of picked wood	5	
skin, intestines	2	
skin, large intestines	2	
skin, muscles, intestines	2	
Slightly calcareous lake sdmt.	5	
slightly sandy silty clay	5	
slightly silty clay	5	
Small conifer twigs	2	

Material (as in the Geochronology table of the Neotoma database)	Accuracy Rank	Notes
Smilodon fatalis bone amino acid	5	
Smilodon floridanus bone apatite/carbonate	6	
Smilodon floridanus bone collagen	5	
soil	5	
soil (humic acids)	5	
soil with wood	5	
soil, wood	5	
Soluble humus fraction	5	
some peat in fine detritus mud	5	
speleothem	5	
Spermophilus bone collagen	5	
Sphagnum	5	
Sphagnum - Carex	5	
Sphagnum - Equisetum	5	
Sphagnum - Eriophorum	5	
Sphagnum + charcoal	5	
Sphagnum + Eriophorum	5	
Sphagnum + wood	5	
Sphagnum peat	5	
Sphagnum peat fine fraction	5	
Sphagnum-Carex peat	5	
Spilogale putorius	6	
Spruce needle	2	
Spruce needle fragment, birch nutlet, + blackened organic fragments	3	Penalized one rank for "blackened organic fragments"
Spruce needles and wood frags	4	weighted towards wood (between 2=needle, 5=wood)
Spruce twig	2	
Spruce wood	5	
spruce wood	5	
Stick	2	ranked same as twig
Stockoceros onusrosagris bone	6	
stone artifact	5	uncertain material; assigned 5 as default
Subfossil soil	5	
Symbos bone collagen	5	
Symbos cavifrons bone apatite/carbonate	6	
Symbos cavifrons bone collagen	5	
Synaptomys borealis bone collagen	5	
Tadarida brasiliensis dung	2	
Tapirus bone	6	
Taxidea taxus bone	6	
Taxodium leaflet	2	
Telmatic (marsh) peat	5	
terrestrial macrofossil	5	no information on which part
terrestrial macros	5	no information on which part

Material (as in the Geochronology table of the Neotoma database)	Accuracy Rank	Notes
terrestrial moss	2	
terrestrial moss stems	2	
terrestrial moss, leaves, stems	2	
terrestrial moss, conifer leave	2	
terrestrial moss, wood, insects	3	between 2=leaf, 2=terrestrial mosses weighted towards mosses (2) and insects (2), away from wood (5)
terrestrial plant remains	3	
tissue from skull of <i>Gymnogyps californianus</i>	2	
tissue of <i>Gymnogyps californianus</i>	2	
tooth enamel	5	
top of claygyttja	5	
Tourbe	5	
transitional	5	uncertain material; assigned 5 as default
Transitional gyttja	5	
trash (wood, needles, moss)	5	weighted towards wood/moss (needles=2, wood=5, moss=6)
Tree	5	
Tree or shrub bark	3	
<i>Tsuga mertensiana</i> needles	2	
<i>Tsuga</i> needles (10)	2	
<i>Tsuga</i> wood	5	
<i>Tsuga/Pinus</i> needles and bark	3	Weighted towards bark (between 2=needles, 3=bark)
tusk of <i>Mammuthus primigenius</i>	5	
twig	2	
Twig	2	
twig and charcoal fragment	4	weighted towards charcoal (between 2=twig, 5=charcoal)
twig and conifer needles	2	
twig and needle frgs spr twig	2	
twig fragment	2	
Twig fragments	2	
twig fragments	2	
twig fragments, spruce needles	2	
twig, Larix leaf	2	
twig, leaf and spruce ndle fgs	2	
twig, leaf fragments	2	
twig, leaf, Lar and Pic frags	3	weighted towards twig/leaf (between 2=twig, 5=wood)
twig, leaves	2	
Twigs	2	
twigs	2	
twigs and bark	3	Weighted towards bark (between 2=twig, 3=bark)
twigs, leaves	2	

Material (as in the Geochronology table of the Neotoma database)	Accuracy Rank	Notes
twigs, seeds, and mosses	4	weighted towards mosses (between 2=seed, 6=mosses)
twigs,leaves	2	
Ulmus wood	5	
Undecomposed peat	5	
Undifferentiated leaves	2	
unhumified sphagnum peat	5	
unhumified Sphagnum peat	5	
unid. terrest. plant remains	3	
unident. plant remains	3	
unident. semi-woody material	4	weighted towards wood (between 3=plant matter/fragments/material/litter/detritus, 5=wood)
unidentified plant fragments	3	
unidentified plant material	3	
unidentified plant remains	3	
Unknown	5	
unknown plant remains	3	
Upland wood	5	
Upper clay	5	
Ursidae bone	6	
Ursus americanus bone	6	
Ursus americanus bone collagen	5	
Ursus arctos bone	6	
Ursus arctos bone collagen	5	
very calcareous gyttja	5	
very humified fibrous peat	5	
volcanic ash	5	
Water soluble humus	5	
Water-soluble humus	5	
white pine needle	2	
whole peat	5	
Whole sample	5	material dated not specified
Whole sample - mean	5	material dated not specified
Whole sample (1)	5	material dated not specified
Whole sample (2)	5	material dated not specified
Wood	5	
wood	5	
WOOD	5	
wood (from alluvium)	5	
Wood (oak)	5	
Wood (Pinus sylvestris).	5	
wood (shrub)	5	
wood and herb peat	5	
wood and leaf fragments	4	weighted towards wood (between 2=leaf, 5=wood)

Material (as in the Geochronology table of the Neotoma database)	Accuracy Rank	Notes
wood and plant fragments	4	weighted towards wood (between 3=plant matter/fragments/material, 5=wood)
wood and spruce macrofossils	5	
Wood charcoal	5	
wood charcoal	5	
wood chips	5	
Wood fragment	5	
wood fragment	5	
wood fragment Abies sp.	5	
wood fragment Picea sp.	5	
Wood fragment, seeds	4	weighted towards wood (between 2=seed, 5=wood)
wood fragment; charcoal	5	
wood fragments	5	
Wood fragments and Carex	5	
wood fragments and peat	5	
wood fragments Picea sp.	5	
wood fragments Salix sp.	5	
Wood frags	5	
Wood from peat.	5	
wood from tree Betula	5	
wood of Larix	5	
Wood peat	5	
Wood peat with many roots	5	
Wood stems	5	
Wood with bark	4	weighted between wood=5, bark=3
wood within basal peat	5	
wood within top peat	5	
wood, charcoal	5	
Wood, charred material	5	
wood, conifer leaf	4	weighted towards wood (5)
wood, conifer needle	4	weighted towards wood (between 2=needle, 5=wood)
Wood, flower bract	4	weighted towards wood (between 2=bract, 5=wood)
wood, insect parts	4	weighted towards wood (5)
wood, large chunks of decayed wood, with some nut fragments	4	weighted towards wood (5)
wood, leaf	4	weighted towards wood (between 2=leaf, 5=wood)
wood, needles, and roots	3	weighted towards needles/root (between 2=needle, 5=wood)
Wood, plant fragments	4	weighted towards wood (between 3=plant matter/fragments/material, 5=wood)
wood, seed	4	weighted towards wood (between 2=seed, 5=wood)

Material (as in the Geochronology table of the Neotoma database)	Accuracy Rank	Notes
Wood, twigs	4	weighted towards wood (between 2=twig, 5=wood)
Wood; leaf	4	weighted towards wood (between 2=leaf, 5=wood)
wood;insect parts;unid. plants	4	weighted towards wood (between 3=plant matter/fragments/material, 5=wood)
Wooded peat	5	
woody Carex peat	5	
woody detritus	4	weighted towards wood (between 3=plant matter/fragments/material/litter/detritus, 5=wood)
Woody fibrous peat	5	
woody fragments	5	
woody litter	4	weighted towards wood (between 3=plant matter/fragments/material/litter/detritus, 5=wood)
Woody long stem	5	
Woody peat	5	
woody peat	5	
woody plant detritus	4	weighted towards wood (between 3=plant matter/fragments/material/litter/detritus, 5=wood)
Woody sedge peat	5	
woody terrestrial material	4	weighted towards wood (between 3=plant matter/fragments/material/litter/detritus, 5=wood)
Woody twig	2	
woody twig	2	
woody twigs	2	
XAD-resin-purified hydrolyzate from KOH extracted gelatin from <i>Arctodus simus</i> bone	2	
XAD-resin-purified hydrolyzate from KOH extracted gelatin from <i>Bison antiquus</i> bone	2	
XAD-resin-purified hydrolyzate from KOH extracted gelatin from <i>Bison</i> bone	2	
XAD-resin-purified hydrolyzate from KOH extracted gelatin from <i>Camelops</i> bone	2	
XAD-resin-purified hydrolyzate from KOH extracted gelatin from <i>Equus</i> bone	2	
XAD-resin-purified hydrolyzate from KOH extracted gelatin from <i>Mammut americanum</i> bone	2	
XAD-resin-purified hydrolyzate from KOH extracted gelatin from <i>Mammuthus</i> bone	2	

Material (as in the Geochronology table of the Neotoma database)	Accuracy Rank	Notes
XAD-resin-purified hydrolyzate from KOH extracted gelatin from <i>Mammuthus columbi</i> bone	2	
XAD-resin-purified hydrolyzate from KOH extracted gelatin from <i>Mammuthus primigenius</i> bone	2	
XAD-resin-purified hydrolyzate from KOH extracted gelatin from <i>Nothrotheriops shshastensis</i> bone	2	
XAD-resin-purified hydrolyzate from KOH extracted gelatin from <i>Oreamnos harringtoni</i> bone	2	
XAD-resin-purified hydrolyzate from KOH extracted gelatin from <i>Ovis canadensis</i> bone	2	
XAD-resin-purified hydrolyzate from KOH extracted gelatin from <i>Rangifer tarandus</i> bone	2	
XAD-resin-purified hydrolyzate from KOH extracted gelatin from reptile bone	2	
<i>Zea mays</i> kernal charcoal	2	
<blank>	6	no information

Appendix B

Site ID	Site Name	Handle (km, Albers)	Longitude (km, Albers)	Latitude (km, Albers)	Altitude (km, scaled)	Altitude (m, original)	Country
3	Alexis Lake	ALEXISLK	2455.491439	1986.401508	120	200	Canada
6	Aliuk Pond	ALIUK	2340.60689	2198.004612	15	25	Canada
10	Anderson Lake	ANDERSLK	237.610822	762.159559	NA	NA	United States
11	Anderson Pond	ANDERSON	893.83754	-417.067548	183	305	United States
14	Lac à l'Ange	ANGE	1777.535125	1122.473861	388.8	648	Canada
15	Lake Annie	ANNIE	1395.9227193	-1382.638198	20.22	33.7	United States
16	Appleman Lake	APPLEMAN	843.373316	239.708818	176.4	294	United States
17	Arrington Marsh	ARRINGTO	38.344058	-59.458932	168	280	United States
20	Lac des Atocas	ATO	1651.117188	853.401214	68.4	114	Canada
21	Axe Lake	AXELAKE	1208.778691	740.998791	193.8	323	Canada
24	Ballston Lake	BALLSTON	1683.545074	546.776037	45.6	76	United States
25	Balsam Lake	BALSAM	1651.825713	426.905827	457.2	762	United States
27	Barry Lake	BARRY	1348.41865	636.967747	100.2	167	Canada
28	Baseball Bog	BASEBALL	1151.990583	952.825122	175.2	292	Canada
31	Lac Bastien	BASTIEN	1230.215535	867.223736	183	305	Canada
33	Battaglia Bog	BATTAGLI	1153.765293	224.467461	201	335	United States
35	Bear Bog	BEARBOG	1126.237601	942.444699	182.4	304	Canada
40	Belmont Bog	BELMONT	1394.358163	399.065989	298.2	497	United States
42	Berry Pond	BERRYPND	1735.958914	503.899135	360	600	United States
45	Big Pond	BIGPOND	1399.751474	101.672346	380.4	634	United States
48	Binnewater Pond	BINNEWTR	1672.304899	356.801929	153.6	256	United States
49	Bishops Falls	BISHOPSF	2719.737565	1644.93024	45	75	Canada
50	Black Gum Swamp	BLACKGUM	1820.294669	530.128411	214.8	358	United States
52	Blackwoods Hollow	BLACKWDS	2053.902154	812.646991	18	30	United States
54	BL-Tombigbee	BILBIGBEE	664.169631	-729.025861	29.4	49	United States
56	Blood Pond	BLOOD	1849.914973	481.388918	128.4	214	United States
57	Blue Mounds Creek	BLUMOUND	469.106623	379.336355	201	335	United States
60	Bog D	BOGD	59.523667	848.788087	274.2	457	United States
61	Bondi Section	BONDI	1035.881572	319.663909	126.6	211	Canada
62	Boney Spring	BONEYSPR	217.795035	-219.435835	126	210	United States
64	Boniack Bog	BORIACKB	-103.902682	-1126.554259	85.8	143	United States
70	Brandreth Bog	BRANDRET	1595.859405	642.84141	360	600	United States

Site ID	Site Name	Handle	Younger Age Bound	Older Age Bound	21-18 ka	18-14.5 ka	14.5-12.9 ka	12.9-11.5 ka	Source
3	Alexis Lake	ALEXISLK	30	9890	n	n	n	n	access
6	Aliuk Pond	ALIUK	2250	9970	n	n	n	n	access
10	Anderson Lake	ANDERSLK	10050	10750	n	n	n	y	access
11	Anderson Pond	ANDERSON	0	24000	y	y	y	y	access
14	Lac à l'Ange	ANGE	0	10560	n	n	y	y	access
15	Lake Annie	ANNIE	210	13690	n	n	y	y	excel
16	Appleman Lake	APPLEMAN	7500	17000	n	y	y	y	excel
17	Arrington Marsh	ARRINGTO	15970	24890	y	n	n	n	access
20	Lac des Atocas	ATO	0	10250	n	n	n	y	access
21	Axe Lake	AXELAKE	-20	9900	n	n	n	n	access
24	Ballston Lake	BALLSTON	1710	12700	n	n	y	y	excel
25	Balsam Lake	BALSAM	-30	14810	n	y	y	y	excel
27	Barry Lake	BARRY	-20	10310	n	n	y	y	access
28	Baseball Bog	BASEBALL	-30	10470	n	n	y	y	access
31	Lac Bastien	BASTIEN	-40	9500	n	n	n	n	access
33	Battaglia Bog	BATTAGLI	10000	15970	y	y	y	y	access
35	Bear Bog	BEARBOG	3560	10000	n	n	n	n	access
40	Belmont Bog	BELMONT	0	13000	n	y	y	y	access
42	Berry Pond	BERRYPND	0	12500	n	y	y	y	access
45	Big Pond	BIGPOND	0	11000	n	n	y	y	access
48	Binnewater Pond	BINNEWTR	-40	15670	n	y	y	y	excel
49	Bishops Falls	BISHOPSF	100	10610	n	n	n	y	access
50	Black Gum Swamp	BLACKGUM	-40	13550	n	n	y	y	excel
52	Blackwoods Hollow	BLACKWDS	910	11410	n	n	n	n	access
54	BL-Tombigbee	BLBIGBEE	0	10000	n	n	n	n	access
56	Blood Pond	BLOOD	-50	15000	n	y	y	y	private
57	Blue Mounds Creek	BLUMOUND	0	10000	n	n	n	n	access
60	Bog D	BOGD	-20	10300	n	n	y	y	access
61	Bondi Section	BONDI	13130	13240	n	y	n	n	access
62	Boney Spring	BONEYSPR	17000	27500	y	n	n	n	access
64	Boniack Bog	BORIACKB	0	16210	y	y	y	y	access
70	Brandreth Bog	BRANDRET	30	10490	n	n	n	y	access

72	Brier Island Bog MS-85-22	BRIERISL	2189.424737	851.709651	9	15	Canada
77	Browns Pond	BROWNSPD	1347.749936	-100.673521	372	620	United States
80	Bucyrus Bog	BUCYRUS	1034.042907	165.455065	190.8	318	United States
84	Byron-Bergen Swamp (Site 2)	BYRONMRL	1368.705227	495.924637	108	180	United States
86	Cahaba Pond	CAHABA	835.707434	-721.02255	122.4	204	United States
90	Saint-Calixte	CAL	1599.911095	891.861147	156.6	261	Canada
91	Camel Lake	CAMEL	1012.408352	-1079.235889	12	20	United States
92	Camp 11 Lake	CAMP11LK	574.693523	811.769957	329.4	549	United States
95	Canyon Lake	CANYON	579.86143	831.950749	156	260	United States
99	Lac Caribou	CARIB	2140.604678	1321.968573	69.6	116	Canada
100	Caribou Bog	CARIBBOG	1960.403119	984.508101	22.2	37	United States
102	Carter Site	CARTER	904.645682	79.634245	183	305	United States
103	Lac Castor	CAS	1643.029837	981.638222	132	220	Canada
104	Cedar Bog Lake	CEDARBLK	206.355652	642.327522	165	275	United States
105	Chance Harbour Lake	CHANCEHA	2397.726136	1096.914009	7.2	12	Canada
107	Chase Pond	CHASE	2531.073003	1144.776065	9	15	Canada
108	Chesapeake Bay, main branch (MD99-2207)	CHES2207	1626.91589	-61.673075	0	0	United States
112	Cheyenne Bottoms	CHEYENNE	-219.398887	-177.622932	328.2	547	United States
114	Chippewa Bog	CHIPPEWA	972.952508	434.522841	162	270	United States
117	Chatsworth Bog	CHAT2003	608.335554	104.329646	131.4	219	United States
119	Clear Lake (US:Iowa)	CLEARLIA	202.579834	374.867293	224.4	374	United States
121	Clear Pond	CLEARPND	1493.003797	-593.370673	6	10	United States
125	Colo Marsh	COLOMSH	212.538929	241.555237	197.4	329	United States
127	Compass Pond	COMPASS	2623.51771	1743.109459	141.6	236	Canada
130	Conroy Lake	CONROYME	2010.475712	1043.688505	82.2	137	United States
131	Lac Ctt	COT	2045.159428	1385.562911	549	915	Canada
133	Cottonwood Lake	COTTONWWD	-290.367541	577.314291	329.4	549	United States
136	Cranberry Lake	CRANBER	1339.349022	611.153306	102	170	Canada
138	Cranberry Glades	CRANGLDS	1292.520825	-104.708919	617.4	1029	United States
140	Crawford Bog	CRAWFBOG	1215.195939	513.203639	160.8	268	Canada

72	Brier Island Bog MS-85-22	BRIERISL	11480	14400	n	n	y	y	excel
77	Browns Pond	BROWNSPD	0	17350	y	y	y	y	access
80	Bucyrus Bog	BUCYRUS	8360	14500	n	y	y	y	access
84	Byron-Bergen Swamp (Site 2)	BYRONMRL	-20	12970	n	n	y	y	excel
86	Cahaba Pond	CAHABA	650	12000	n	n	y	y	access
90	Saint-Calixte	CAL	80	10560	n	n	n	y	access
91	Camel Lake	CAMEL	0	32000	y	y	y	y	access
92	Camp 11 Lake	CAMP11LK	0	10000	n	n	n	n	access
95	Canyon Lake	CANYON	110	10830	n	n	n	y	access
99	Lac Caribou	CARIB	80	9590	n	n	n	n	access
100	Caribou Bog	CARIBBOG	60	9570	n	n	n	n	access
102	Carter Site	CARTER	11690	14700	n	y	y	n	access
103	Lac Castor	CAS	130	9540	n	n	n	n	access
104	Cedar Bog Lake	CEDARBLK	-10	11060	n	n	y	y	access
105	Chance Harbour Lake	CHANCEHA	-40	15910	n	y	y	y	access
107	MS-85-16 Chase Pond	CHASE	10377	17068	n	y	y	y	access
108	Chesapeake Bay, main branch (MD99-2207)	CHES2207	930	10500	n	n	n	n	excel
112	Cheyenne Bottoms	CHEYENNE	0	29740	y	y	y	y	access
114	Chippewa Bog	CHIPPEWA	1000	9500	n	n	n	n	access
117	Chatsworth Bog	CHAT2003	2540	19990	y	y	y	y	excel
119	Clear Lake (US:Iowa)	CLEARLIA	-30	13050	n	y	y	y	access
121	Clear Pond	CLEARPND	-40	20380	y	y	y	y	access
125	Colo Marsh	COLOMSH	0	13500	n	y	y	y	access
127	Compass Pond	COMPASS	-20	13300	n	y	y	y	access
130	Conroy Lake	CONROYME	10260	13000	n	y	y	y	excel
131	Lac Ctt	COT	0	9710	n	n	n	n	access
133	Cottonwood Lake	COTTONWDL	-20	12330	n	n	y	y	access
136	Cranberry Lake	CRANBER	-30	12250	n	n	y	y	access
138	Cranberry Glades	CRANGLDS	0	12500	n	y	y	y	access
140	Crawford Bog	CRAWFBOG	-30	16250	n	y	y	y	excel

141	Crawford Lake [CA:Ontario]	CRAWFDC	1215.052805	512.912589	166.8	278	Canada
145	Crider's Pond	CRIDERS	1474.417033	139.999383	174	290	United States
	Crooked Lake (Northwest Basin)	CROOKEDN	486.651656	755.23946	311.4	519	United States
147	Crystal Lake	CRYSTAL	591.929384	287.786121	163.8	273	United States
150	Cupola Pond	CUPOLA	413.14534	-365.991768	146.4	244	United States
153	South Dansville buried peat	DANSVILL	1410.420841	432.097217	343.2	572	United States
157	Devil's Bathtub	DBATHTUB	1402.780432	493.956016	118.8	198	United States
160	Decoy Lake	DECOY	1188.218993	480.083113	156	260	Canada
162	Deer Lake Bog	DEER	1801.384297	707.308915	795	1325	United States
165	Demont Lake	DEMONT	830.197856	462.385184	160.8	268	United States
168	Devils Lake	DEVILSWI	477.191546	420.610073	176.4	294	United States
172	Lac du Diable	DIAB	2035.693555	1375.521467	296.4	494	Canada
174	Disterhaft Farm Bog	DISTRHFT	515.440595	481.274435	146.4	244	United States
177	Divers Lake	DIVERS	1340.319442	483.94712	143.4	239	United States
178	Duck Pond	DUCKPOND	2001.918933	504.445803	1.2	2	United States
184	Lac Dufresne	DUFRESNE	1851.941597	943.207596	390	650	Canada
185	Eagle Lake Bog	EAGLE	1809.5333371	725.730514	765	1275	United States
188	Eagle Lake	EAGLELK	2332.955064	2024.816959	240	400	Canada
190	E Lake	ELAKE68	-245.323436	1265.917477	441	735	Canada
196	Emrick Lake	EMRICK	484.210426	465.233252	162	270	United States
198	Lake Erie	ERIE	1029.211443	298.668979	100.8	168	Canada
199	Lac a la Fourche	ESPOIR	1778.261072	1138.329128	183	305	Canada
202	East Twin Lake	ETWINOH	1152.401148	230.79479	193.2	322	United States
203	Fawn Lake (CA:Ontario)	FAWN	1216.867385	746.024701	199.8	333	Canada
209	Frains Lake	FRAINSLK	955.67651	337.564449	162.6	271	United States
218	Hayes Lake	FRBLAKE	153.992587	1132.977857	234.6	391	Canada
219	Fresh Pond	FRESHPND	1906.782211	383.724264	16.8	28	United States
223	Fudger Lake	FUDGER	997.631533	77.488189	192	320	United States
224	Gass Lake	GASS	621.962462	505.553041	126.6	211	United States
227	Little Salt Spring (GDF 141)	GDF141	1320.423184	-1408.474109	3.6	6	United States
232							

141	Crawford Lake [CA:Ontario]	CRAWFDC	-50	11010	n	n	n	n	excel
145	Crider's Pond	CRIDERS	0	15000	y	y	y	y	access
	Crooked Lake								
147	(Northwest Basin)	CROOKDN	-10	11780	n	n	n	y	excel
150	Crystal Lake	CRYSTAL	6500	17000	n	y	y	y	excel
153	Cupola Pond	CUPOLA	0	17330	y	y	y	y	access
	South Dansville buried peat								
157	Dansville	DANSVILL	1250	18640	y	y	y	y	excel
160	Devil's Bathtub	DBATHTUB	1740	13430	n	n	y	y	excel
162	Decoy Lake	DECOY	0	13615	n	n	y	y	access
165	Deer Lake Bog	DEER	0	13500	n	y	y	y	access
168	Demont Lake	DEMONT	10	13320	n	y	y	y	excel
172	Devils Lake	DEVILSWI	9550	14747	n	y	y	y	access
174	Lac du Diable	DIAB	0	10660	n	n	n	y	access
177	Disterhaft Farm Bog	DISTRHFT	500	13960	n	y	y	y	access
178	Divers Lake	DIVERS	-50	16030	n	y	y	y	excel
184	Duck Pond	DUCKPOND	0	12000	n	n	y	y	access
185	Lac Dufresne	DUFRESNE	0	11000	n	n	n	y	access
188	Eagle Lake Bog	EAGLE	0	10500	n	n	y	y	access
190	Eagle Lake	EAGLELK	20	11530	n	n	y	y	access
196	E Lake	ELAKE68	-20	13530	n	n	y	y	access
198	Emrick Lake	EMRICK	-60	13490	n	n	y	y	excel
199	Lake Erie	ERIE	-20	13030	n	y	y	y	access
202	Lac a la Fourche	ESPOIR	0	9450	n	n	n	n	access
203	East Twin Lake (US:Ohio)	ETWINOH	40	11660	n	n	y	y	access
209	Fawn Lake [CA:Ontario]	FAWN	-30	10730	n	n	n	y	access
218	Frains Lake	FRAINSLK	0	13000	n	y	y	y	access
219	Hayes Lake	FRBLAKE	100	10000	n	n	n	n	access
223	Fresh Pond	FRESHPND	-40	13020	n	y	y	y	access
224	Fudger Lake	FUDGER	-20	14600	n	y	y	y	access
227	Gass Lake	GASS	0	12000	n	n	y	y	access
232	Little Salt Spring (GDF 141)	GDF141	0	11390	n	n	n	n	excel

235	Lac Geai	GEAI	1590.114519	893.752968	219	365	Canada
237	Lac a St-Germain	GER	1564.614081	881.71277	283.8	473	Canada
244	Glenboro Lake Site	GLENBORO	-225.300146	1117.424038	270	450	Canada
246	Glimmerglass Lake	GLIMMER	484.911196	751.647821	313.2	522	United States
250	Gould Pond	GOULD	1953.050255	865.424247	53.4	89	United States
252	Graham Lake	GRAHAM	1369.729389	747.534452	228.6	381	Canada
256	Green Lake	GREENLK	806.789532	623.27397	183	305	United States
270	Hack Pond	HACK	1401.715066	-111.388081	281.4	469	United States
271	Hafichuk Site	HAFICHUK	-666.291917	1252.470109	444	740	Canada
272	Hams Lake	HAMSLAKE	1184.639689	479.887822	180.6	301	Canada
273	Hanson Marsh	HANSON	480.98881	421.544662	228.6	381	United States
275	Lac Harriman	HARR	2079.328383	1306.399145	39	65	Canada
285	Helmetta Bog	HELMETTA	1708.401628	240.399319	9	15	United States
290	High Lake	HIGHLAKE	1440.067278	681.443583	115.2	192	Canada
291	Hiscock Site	HISCOCK	1363.984194	495.243899	113.4	189	United States
297	Houghton Bog	HOUGHTON	1330.646654	422.102021	256.8	428	United States
305	Hyde Park	HYDEPARK	1714.260775	413.376606	44.4	74	United States
309	Indian Lake	INDIAN	370.513445	1298.424709	229.8	383	Canada
310	Inglesby Lake	INGLESBY	1407.897511	670.824542	100.2	167	Canada
312	Irvin Lake	IRVIN	168.436952	844.983495	286.8	478	United States
315	Itasca Bison Kill Site	ITASCAMB	55.365415	850.365162	268.2	447	United States
322	Jack Lake	JACKLAKE	1010.499602	940.257064	258	430	Canada
323	Jackson Pond	JACKSON	857.083889	-255.797962	157.2	262	United States
330	Jewell Site	JEWELL	178.381433	269.016614	190.2	317	United States
331	Joes Pond	JOES3	2578.071554	1493.439341	60	100	Canada
338	Kellys Hollow	KELLHOL1	416.579201	638.566278	282	470	United States
339	Kellys Hollow	KELLHOL2	416.579201	638.566278	282	470	United States
340	Kellners Lake	KELLNERS	61.1.443341	526.951772	156.6	261	United States
347	Kettle Lake	KETTLE	-530.516785	1037.653452	363	605	United States
349	Kimble Pond	KIMBLE	162.374889	500.374951	186.6	311	United States
350	Kinsman Pond	KINSMAN	1805.682322	720.647976	684	1140	United States
351	Kirchner Marsh	KIRCHNR1	214.317135	567.056794	171.6	286	United States
354	Kotiranta Lake	KOTIRANT	243.327111	798.190619	231.6	386	United States
357	Kylen Lake	KYLENLK	299.031878	874.811663	291	485	United States
359	Lac Colin	LACCOLIN	1828.058628	1042.781626	394.8	658	Canada
362	Lac a Magie	LACMAGIE	2208.933747	855.219404	36	60	Canada

235	Lac Geai	GEAI	0	10390	n	n	n	y	access
237	Lac a St-Germain	GER	70	10410	n	n	n	y	access
244	Glenboro Lake Site	GLENBORO	0	12000	n	y	y	y	access
246	Glimmerglass Lake	GLIMMER	40	11870	n	y	y	y	excel
250	Gould Pond	GOULD	-30	12260	n	y	y	y	access
252	Graham Lake	GRAHAM	0	10050	n	y	y	y	access
256	Green Lake	GREENLK	200	12500	n	y	y	y	access
270	Hack Pond	HACK	0	12720	n	y	y	y	access
271	Hafichuk Site	HAFICHUK	11930	13680	n	y	y	y	access
272	Hams Lake	HAMSLAKE	-30	11360	n	y	y	y	access
273	Hanson Marsh	HANSON	10020	11030	n	y	y	y	access
275	Lac Harriman	HARR	0	11680	n	n	y	y	access
285	Helmetta Bog	HELMETTA	0	10000	n	n	n	y	access
290	High Lake	HIGHLAKE	0	9490	n	n	n	y	access
291	Hiscock Site	HISCOCK	140	12850	n	n	n	y	excel
297	Houghton Bog	HOUGHTON	-20	11900	n	n	y	y	access
305	Hyde Park	HYDEPARK	-40	14180	n	y	y	y	excel
309	Indian Lake	INDIAN	5110	9660	n	n	n	y	access
310	Inglesby Lake	INGLESBY	500	10470	n	n	y	y	access
312	Irvin Lake	IRVIN	-40	10710	n	n	y	y	access
315	Itasca Bison Kill Site	ITASCAMB	9870	10690	n	n	n	y	excel
322	Jack Lake	JACKLAKE	20	11730	n	n	y	y	access
323	Jackson Pond	JACKSON	-30	20460	y	y	y	y	access
330	Jewell Site	JEWELL	1050	12000	n	n	y	y	access
331	Joes Pond	JOES3	-20	13640	n	y	y	y	access
338	Kellys Hollow	KELLHOL1	-30	10000	n	n	n	y	access
339	Kellys Hollow	KELLHOL2	-30	10740	n	n	y	y	access
340	Kellners Lake	KELLNERS	-30	10750	n	n	n	y	access
347	Kettle Lake	KETTLE	-50	12980	n	n	y	y	excel
349	Kimble Pond	KIMBLE	-50	12390	n	n	y	y	excel
350	Kinsman Pond	KINSMAN	0	11000	n	n	y	y	access
351	Kirchner Marsh	KIRCHNR1	180	11790	n	n	y	y	access
354	Kotiranta Lake	KOTIRANT	150	14970	y	y	y	y	access
357	Kylen Lake	KYLENLK	8500	15500	y	y	y	y	access
359	Lac Colin	LACCOLIN	0	11000	n	n	y	y	access
362	Lac a Magie	LACMAGIE	10462	13993	n	n	y	y	access

364	Lake Sixteen	LAKE16	855.393831	714.370606	129.6	216	United States
366	Lake A	LAKEA	-620.729578	1590.266474	264	440	Canada
368	Lake Ann	LAKEANNF	170.226741	642.994119	174.6	291	United States
370	Lake B	LAKEB	-636.322523	1657.553729	331.8	553	Canada
383	Lake Mary	LAKEMARY	442.4998099	752.606934	292.8	488	United States
384	Lake QC	LAKEQC	1094.969357	895.201225	199.8	333	Canada
391	Leading Ticks	LEADINGT	2695.688255	1703.14411	63	105	Canada
395	Lily Lake (US:Minnesota)	LILYLAKE	235.179732	600.5461	154.8	258	United States
396	Lily Lake [US:Michigan]	LILYMI	486.999517	952.374979	180.6	301	United States
398	Lima Bog	LIMABOG	550.898196	351.551151	181.2	302	United States
400	Little Bass Lake	LITTBASS	171.112339	862.488985	234.6	391	United States
406	Lake Annie	LKANNIE	1395.927193	-1382.638198	20.4	34	United States
407	Lake of the Clouds (US:Minnesota)	LKCLDSH	343.697933	953.673391	277.2	462	United States
409	Lake Hope Simpson	LKHOPE	2494.246819	1994.952962	177	295	Canada
410	Little Lake (CA:Nova Scotia)	LLAKE	2345.234118	951.874302	24	40	Canada
412	Lockport Gulf Section	LOCKPORT	1313.731467	494.095588	65.4	109	United States
414	Lonesome Lake	LONESOME	1807.827468	722.024422	498.6	831	United States
415	Longswamp	LONGSWMP	1609.740795	230.329003	115.2	192	United States
420	Lost Pond	LOSTPOND	1837.267435	742.890721	375	625	United States
421	Lake Louise	LOUISE-D	1166.479481	-1006.478049	29.4	49	United States
423	Lovesick Lake (core 1)	LOVESIC1	1322.08686	664.014767	145.2	242	Canada
425	Lovesick Lake (core 3)	LOVESIC3	1322.08686	664.014767	145.2	242	Canada
438	Maplehurst Lake	MPLHRST	1166.300549	475.471964	180	300	Canada
439	Lac Marcotte	MARC	1739.10979	1062.782452	301.8	503	Canada
444	Wapizagonke	MAU3	1637.606707	993.976186	138	230	Canada
445	Sud du Lac du Noyer	MAU5	1649.324653	1004.350371	162	270	Canada
446	Mayflower Lake	MAYFLOWR	2171.406773	972.122829	30	50	Canada
461	Lake Mendota	MENDOTAD	503.334581	383.609947	154.2	257	United States
462	Mermaid Bog	MERMAID	2345.698396	1150.495484	9	15	Canada
468	Lac Mimi	MIMI	1798.215484	1130.036348	253.8	423	Canada

364	Lake Sixteen	LAKE16	2200	10870	n	n	y	access
366	Lake A	LAKEA	0	11000	n	n	y	access
368	Lake Ann	LAKEANNF	790	10550	n	n	y	access
370	Lake B	LAKEB	0	10000	n	n	n	access
383	Lake Mary	LAKEMARY	200	10350	n	n	y	access
384	Lake QC	LAKEQC	0	10930	n	n	y	access
391	Leading Tickles	LEADINGT	-40	12670	n	y	y	access
395	Lily Lake (US:Minnesota)	LILYLAKE	0	12000	n	n	y	access
396	Lily Lake [US:Michigan]	LILYMI	980	10660	n	n	n	excel
398	Lima Bog	LIMABOG	-20	11740	n	n	y	excel
400	Little Bass Lake	LITTBASS	0	10500	n	n	y	access
406	Lake Annie	LKANNIE	0	13000	n	y	y	access
407	Lake of the Clouds (US:Minnesota)	LKCLDSH	490	9590	n	n	n	access
409	Lake Hope Simpson	LKHOPE	200	10500	n	n	y	access
410	Little Lake (CA:Nova Scotia)	LLAKE	9610	11850	n	n	y	access
412	Lockport Gulf Section	LOCKPORT	8340	11080	n	n	y	access
414	Lonesome Lake	LONESOME	430	10530	n	n	y	access
415	Longswamp	LONGSWMP	9000	12500	n	y	y	access
420	Lost Pond	LOSTPOND	20	13480	n	y	y	access
421	Lake Louise	LOUISE-D	0	10650	n	n	y	access
423	Lovesick Lake (core 1)	LOVESIC1	-50	10800	n	n	n	excel
425	Lovesick Lake (core 3)	LOVESIC3	-50	10800	n	n	n	excel
438	Maplehurst Lake	MPLHRST	0	12500	n	y	y	access
439	Lac Marcotte	MARC	0	9820	n	n	n	access
444	Wapizagonke	MAU3	770	9730	n	n	n	access
445	Sud du Lac du Noyer	MAU5	230	9590	n	n	n	access
446	Mayflower Lake	MAYFLOWR	9390	12520	n	y	y	access
461	Lake Mendota	MENDOTAD	0	14000	n	y	y	access
462	Mermaid Bog	MERMAID	-30	9720	n	n	n	access
468	Lac Mimi	MIMI	960	10930	n	n	y	access

470	Lake Minnie	MINNIEO	70.643844	855.580183	257.4	429	United States
472	Makepeace Cedar Swamp	MKPEACEA	1945.087858	490.589427	24	40	United States
474	Makepeace Cedar Swamp	MKPEACED	1945.087858	490.589427	24	40	United States
475	Mohawk Pond	MOHAWK	1757.624458	426.075678	216	360	United States
478	Moon Lake	MONLAKE	-155.028011	811.845331	266.4	444	United States
480	Moraine Lake	MORAINE	2406.293639	1933.551457	231	385	Canada
481	Mordsger Lake	MORDSGER	115.880898	1343.264751	240	400	Canada
484	MS7812X Island Lake	MS7812X	2071.496851	1253.482056	174	290	Canada
485	Pye Lake	MS9011	2462.309252	1033.312058	3	5	Canada
492	Mud Pond	MUDPOND	2052.464926	851.837778	62.4	104	United States
494	Muscotah Marsh	MUSCOTAA	39.403017	-55.327141	168	280	United States
496	Myrtle Lake	MYRTLE	184.278399	945.398369	235.8	393	United States
502	Neville Marsh	NEVILLE	967.024623	126.544555	183	305	United States
504	Nichols Brook Site	NICHOLS2	1345.109139	425.158011	262.8	438	United States
505	Nina Lake	NINA	1042.169813	859.546311	228	380	Canada
506	No Bottom Pond	NOBOTTOM	2006.933635	426.18289	3.6	6	United States
508	North Pond	NORTHPND	1751.719363	526.020445	351.6	586	United States
512	Nutt Lake	NUTTLAKE	1216.484364	722.75955	183	305	Canada
515	Lake West Okoboji	OKOBOJI	60.980983	393.962783	255.6	426	United States
517	Oliver Pond	OLIVER	466.196158	1010.980856	150	250	Canada
522	Lake O' Pines	OPINES	490.223977	743.003732	308.4	514	United States
523	Otisville	OTISVILL	1672.993563	364.487447	138	230	United States
526	Lac Ouellet	OUEL	1894.846421	1161.992576	180	300	Canada
528	Panther Run Pond	PANTHER	1465.781852	238.535802	380.4	634	United States
529	Paradise Lake	PARADISE	2388.455992	2025.10148	108	180	Canada
534	Pass Lake	PASSLAKE	505.65161	1030.153425	150	250	Canada
537	Patschke Bog	PATSCHKE	-103.022278	-1125.794547	85.2	142	United States
539	Pawelski Farm	PAWELSKI	1684.011097	351.384315	73.2	122	United States
542	Peatsah Section	PEATSAH	1227.430624	498.313784	55.2	92	Canada
552	Pickerel Lake (US:South Dakota)	PICKEREL	-97.784583	650.464798	237	395	United States
554	Pilot Mound Site	PILOTMND	163.13445	256.843361	211.2	352	United States
559	Pine Lake	PINEWI	547.795885	643.309012	234	390	United States
560	Pinhook Bog	PINHOOK	716.024582	225.353125	145.8	243	United States

470	Lake Minnie	MINNIEO	0	11580	n	n	y	y	access
472	Makepeace Cedar Swamp	MKPEACEA	10	13540	n	n	y	y	excel
474	Makepeace Cedar Swamp	MKPEACED	-10	11960	n	n	n	y	excel
475	Mohawk Pond	MOHAWK	200	15780	y	y	y	y	access
478	Moon Lake	MONLAKE	-35	13675	n	n	y	y	access
480	Moraine Lake	MORAINE	0	10000	n	n	n	n	access
481	Mordsger Lake	MORDSGER	20	9310	n	n	n	n	access
484	MS7812X Island Lake	MS7812X	10	11350	n	n	n	n	excel
485	Pye Lake	MS9011	-40	14590	n	y	y	y	excel
492	Mud Pond	MUDPOND	11280	13500	n	n	y	y	excel
494	Muscotah Marsh	MUSCOTAA	50	23040	y	y	y	y	access
496	Myrtle Lake	MYRTLE	0	11000	n	n	y	y	access
502	Neville Marsh	NEVILLE	8950	12440	n	y	y	y	access
504	Nichols Brook Site	NICHOLS2	9080	12640	n	y	y	y	access
505	Nina Lake	NINA	10	10150	n	n	y	y	access
506	No Bottom Pond	NOBOTTOM	-40	14440	n	y	y	y	access
508	North Pond	NORTHPND	0	11000	n	n	n	y	access
512	Nutt Lake	NUTTLAKE	-30	9640	n	n	n	n	access
515	Lake West Okoboji	OKOBOJI	0	14000	n	y	y	y	access
517	Oliver Pond	OLIVER	-20	10320	n	n	y	y	access
522	Lake O' Pines	OPINES	-40	12510	n	y	y	y	excel
523	Otisville	OTISVILL	-40	17100	n	y	y	y	excel
526	Lac Ouellet	OUEL	100	10540	n	n	y	y	access
528	Panther Run Pond	PANTHER	0	12500	n	y	y	y	access
529	Paradise Lake	PARADISE	0	10980	n	n	y	y	access
534	Pass Lake	PASSLAKE	0	10000	n	n	n	n	access
537	Patschke Bog	PATSCHKE	190	17360	y	y	y	y	access
539	Pawelski Farm	PAWELSKI	-50	15470	n	y	y	y	excel
542	Peatsah Section	PEATSAH	9040	12460	n	y	y	y	access
552	(US:South Dakota) Pickerel Lake	PICKEREL	0	11140	n	n	y	y	access
554	Pilot Mound Site	PILOTMND	0	13500	n	y	y	y	access
559	Pine Lake	PINEWI	-30	12670	n	n	y	y	excel
560	Pinhook Bog	PINHOOK	-20	14020	n	n	y	y	excel

561	Pink Lake	PINKLAKE	1474.158717	803.759198	97.2	162	Canada
566	Pogonia Bog Pond	POGONIA	175.368491	596.827014	175.2	292	United States
567	Poland Spring Pond	POLAND	1909.321421	736.340537	56.4	94	United States
569	Porqui Pond	PORQUI2	1198.235627	685.185909	112.8	188	Canada
570	Portage Lake	PORTAGE	134.993059	837.842639	237.6	396	United States
571	Portage Marsh	PORTAGE1	687.320905	217.897855	113.4	189	United States
574	Potts Mountain Pond	POTTSMTN	1316.499634	-172.246564	504	840	United States
580	Protection Bog	PROTECTN	1344.352381	434.334204	258	430	United States
581	Point Escuminac	PTESCUMI	2192.688465	1199.864988	3.6	6	Canada
584	Powers Fort Swale	PWFITSWAL	458.003829	-387.060583	54.6	91	United States
585	Pyle Site	PYLE	882.301583	130.457885	150	250	United States
587	Qually Pond	QUALLY	-14.146129	907.693338	212.4	354	United States
589	Quicksand Pond	QUICKSND	971.035745	-609.272906	171	285	United States
590	Quillin Site	QUILLIN	1106.469702	200.065108	183	305	United States
591	Radtko Lake	RADTKE	600.836143	426.635232	164.4	274	United States
595	Ramsay Lake	RAMSAYLK	1449.966579	814.341523	120	200	Canada
596	Rattle Lake	RATTLE	226.78555	1107.673804	276	460	Canada
621	Vallée de l'Albion	REDRIVER	1788.622567	904.062638	192	320	Canada
623	Reidel Lake	REIDEL	51.996847	734.06788	265.8	443	United States
626	Rhule Fen	RHULEFEN	823.542266	39.129137	160.8	268	United States
632	Rice Lake (marsh core 3)	RICEMSH3	1331.35006	621.427243	111.6	186	Canada
633	Rice Lake [CA:Ontario]	RICEON	1339.779926	631.226522	111.6	186	Canada
637	Lac a Robin	ROBIN	2124.344921	1298.336378	30	50	Canada
638	Robinson's Pond	ROBPPOND	2540.935481	1480.493871	19.2	32	Canada
640	Rockyhock Bay	ROCKYHOC	1633.201475	-284.013133	3.6	6	United States
641	Rogers Lake	ROGERSLK	1859.271868	396.773917	54.6	91	United States
644	Rose Swamp	ROSE1	1238.505426	602.23429	136.8	228	Canada
645	Rosebud	ROSEBUDA	-370.059665	390.858757	NA	NA	United States
646	Rosebud	ROSEBUDB	-370.059665	390.858757	NA	NA	United States
648	Rossburg Bog	ROSSBURG	173.203348	779.912878	223.2	372	United States
649	Ross Pond	ROSSPOND	1981.124539	742.890178	22.2	37	United States
650	Rostock Mammoth Site	ROSTOCK1	1135.526564	503.430813	199.8	333	Canada
655	Rutz Lake	RUTZLAKE	158.268451	577.113927	188.4	314	United States

561	Pink Lake	PINKLAKE	-30	11760	n	n	y	y	access
566	Pogonia Bog Pond	POGONIA	-30	11120	n	n	y	y	access
567	Poland Spring Pond	POLAND	-30	13030	n	y	y	y	access
569	Porqui Pond	PORQUI2	-20	13500	n	y	y	y	access
570	Portage Lake	PORTAGE	10	11780	n	n	y	y	access
571	Portage Marsh	PORTAGE1	770	10880	n	n	n	y	access
574	Potts Mountain Pond	POTTSMTN	70	11300	n	n	y	y	access
580	Protection Bog	PROTECTN	-20	11430	n	n	y	y	access
581	Point Escuminac	PTESCUMI	0	10710	n	n	n	y	access
584	Powers Fort Swale	PWFSTSWAL	-40	18070	y	y	y	y	access
585	Pyle Site	PYLE	8250	14500	n	y	y	y	access
587	Qually Pond	QUALLY	1560	13690	n	n	y	y	excel
589	Quicksand Pond	QUICKSND	13400	20160	y	y	n	n	access
590	Quillin Site	QUILLIN	3980	13400	n	y	y	y	access
591	Radtko Lake	RADTKE	0	11500	n	n	y	y	access
595	Ramsay Lake	RAMSAYLK	-30	10940	n	n	n	y	access
596	Rattle Lake	RATTLE	5750	11400	n	n	y	y	access
621	VallTe de l'Albion	REDRIVER	150	10880	n	n	n	y	access
623	Reidel Lake	REIDEL	-30	11610	n	n	y	y	access
626	Rhule Fen	RHULEFEN	9440	13120	n	y	y	y	access
632	Rice Lake (marsh core 3)	RICEMSH3	4650	11650	n	n	n	y	excel
633	Rice Lake [CA:Ontario]	RICEON	-30	11730	n	n	n	y	excel
637	Lac a Robin	ROBIN	470	9440	n	n	n	n	access
638	Robinson's Pond	ROBPOND	-20	14210	n	y	y	y	access
640	Rockyhock Bay	ROCKYHOC	0	26000	y	y	y	y	access
641	Rogers Lake	ROGERSLK	0	15160	y	y	y	y	access
644	Rose Swamp	ROSE1	7160	10740	n	n	n	y	access
645	Rosebud	ROSEBUDA	11790	12420	n	y	y	n	access
646	Rosebud	ROSEBUDB	12570	12630	n	y	n	n	access
648	Rossburg Bog	ROSSBURG	2000	10270	n	n	n	y	access
649	Ross Pond	ROSSPOND	-20	12510	n	y	y	y	access
650	Rostock Mammoth Site	ROSTOCK1	10790	12940	n	y	y	y	access
655	Rutz Lake	RUTZLAKE	-10	11840	n	n	y	y	access

658	Lac a Sam	SAM	1643.267557	986.595137	144	240	Canada
661	Sandy Run Creek	SANDYRUN	1155.821268	-789.781407	48	80	United States
663	Lac Manitou	SAV1	1554.804453	893.011662	272.4	454	Canada
664	Lac aux Quenouilles	SAV2	1556.803948	907.313702	241.8	403	Canada
665	Lake Site South Burin Peninsula	SBURIN	2811.210774	1425.451291	68.4	114	Canada
676	Shady Valley Bog	SHADYVAL	1186.986082	-320.723637	229.8	383	United States
678	Sharkey Lake	SHARKEY	193.257704	545.332232	183	305	United States
680	Mont Shefford	SHE	1708.235784	845.152721	169.2	282	Canada
683	Shouldice Lake	SHOULD1	1074.354549	691.22407	123.6	206	Canada
687	Silver Lake (CA:Nova Scotia)	SILVERNS	2370.1937	947.569208	41.4	69	Canada
691	Sioux Pond	SIOUX	301.417841	1179.309835	246	410	Canada
693	Smoot Lake Bog	SMOOTLK	1082.313168	101.755161	175.2	292	United States
702	Spirit Lake (US:Michigan)	SPIRIT	652.872747	795.499242	121.8	203	United States
703	Spiritwood Lake	SPIRITWD	-185.131329	838.10806	262.2	437	United States
704	Splian Pond	SPLANPD	2084.541639	938.529634	63.6	106	Canada
705	Spring Lake (US:Pennsylvania)	SPRINGLK	1527.502968	356.485806	205.2	342	United States
706	Spruce Pond	SPRUCE	1703.20314	342.957104	133.8	223	United States
710	Steel Lake	STEELMN	94.340494	824.483055	249	415	United States
716	Stotzel-Leis Site	STOTZEL	903.938732	79.549462	185.4	309	United States
717	Stewart's Dark Lake	STWDARK2	335.545235	634.202589	201	335	United States
718	Sugarloaf Pond	SUGRLOAF	2966.013126	1589.584475	60	100	Canada
720	Sutherland Pond	SUTHRLND	1711.852619	3633.422995	228	380	United States
721	Swan Lake (US:Nebraska)	SWANLAKE	-508.805552	220.689878	NA	NA	United States
723	Szabo Pond	SZABOPND	1704.066618	241.415678	17.4	29	United States
726	Tannersville Bog	TANNERSV	1626.819287	300.56648	166.2	277	United States
728	Taupawhas Bog	TAUPAW	2018.579632	428.41998	8.4	14	United States
733	Terhell Pond	TERHELL	16.388202	849.070678	265.2	442	United States
734	Petit Lac Terrien	TERRIEN	1810.114379	1021.090987	242.4	404	Canada
740	Titicut Swamp	TITICUT1	1923.753596	485.023309	12	20	United States
743	Tom Swamp	TOMSWAMP	1818.233366	526.508874	138.6	231	United States
744	Tonawa Lake	TONAWA	1390.184362	711.457936	164.4	274	Canada

658	Lac a Sam	SAM	370	9350	n	n	n	n	access
661	Sandy Run Creek	SANDYRUN	100	25490	y	y	y	y	excel
663	Lac Manitou	SAV1	60	10100	n	n	y	y	access
664	Lac aux Quenouilles	SAV2	50	10750	n	n	y	y	access
665	Lake Site South Burin Peninsula	SBURIN	10500	13500	n	y	y	y	access
676	Shady Valley Bog	SHADYVAL	300	10000	n	n	n	n	access
678	Sharkey Lake	SHARKEY	630	12020	n	n	n	y	excel
680	Mont Shefford	SHE	70	11400	n	n	y	y	access
683	Shouldice Lake	SHOULD1	10	9910	n	n	n	n	access
687	Silver Lake (CA:Nova Scotia)	SILVERNS	0	10000	n	n	n	n	access
691	Sioux Pond	SIOUX	3120	10100	n	n	y	y	access
693	Smoot Lake Bog	SMOOTLK	9340	14540	n	y	y	y	access
702	Spirit Lake (US:Michigan)	SPIRIT	-20	11770	n	n	y	y	access
703	Spiritwood Lake	SPIRITWWD	-20	10500	n	n	y	y	access
704	Splian Pond	SPLANPD	9903	13497	n	n	y	y	access
705	Spring Lake (US:Pennsylvania)	SPRINGLK	0	12880	n	y	y	y	access
706	Spruce Pond	SPRUCE	120	12410	n	n	y	y	access
710	Steel Lake	STEELMN	-50	11290	n	n	n	n	excel
716	Stotzel-Leis Site	STOTZEL	30	15130	y	y	y	y	access
717	Stewart's Dark Lake	STWDARK2	500	10500	n	n	y	y	access
718	Sugarloaf Pond	SUGRLOAF	-30	9520	n	n	n	n	access
720	Sutherland Pond	SUTHRLND	0	14902	n	y	y	y	access
721	Swan Lake (US:Nebraska)	SWANLAKE	30	9370	n	n	n	n	access
723	Szabo Pond	SZABOPND	-30	11150	n	n	y	y	access
726	Tannersville Bog	TANNERSV	0	13000	n	y	y	y	access
728	Taupawshas Bog	TAUPAW	-30	10860	n	n	y	y	access
733	Terhell Pond	TERHELL	-10	10490	n	n	y	y	access
734	Petit Lac Terrien	TERRIEN	0	12000	n	n	y	y	access
740	Titicut Swamp	TITICUT1	-20	11810	n	n	y	y	access
743	Tom Swamp	TOMSWAMP	200	13850	n	y	y	y	access
744	Tonawa Lake	TONAWA	-30	12000	n	n	y	y	access

746	Torren's Bog	TORNSBOG	1078.694325	119.955836	181.2	302	United States
749	Lake Tulane	TULANEGL	1381.335571	-1340.548791	20.4	34	United States
753	Lac Turcotte	TUR	2050.428715	1410.929379	268.2	447	Canada
756	Twiss Marl Pond	TWISMARL	1215.130254	510.327709	153.6	256	Canada
759	Upper Mallot Lake	UPMALLOT	834.727046	915.032063	253.2	422	Canada
761	Upper Wallface Pond	UPWALLFC	1635.899423	680.015736	568.8	948	United States
763	Van Nostrand Lake	VANNOSTR	1246.657824	582.069463	178.2	297	Canada
766	Volo Bog	VOLOBOG	604.637079	302.557216	137.4	229	United States
776	Weslemkoon Lake	WESLEM1	1367.137122	728.946679	189.6	316	Canada
780	White Pond	WHITEPND	1328.066831	-578.140742	54	90	United States
781	Whitney's Gulch	WHITGLCH	2485.974052	1872.382059	58.8	98	Canada
787	Winneconnet Pond	WINNE	1916.96992	485.236677	12	20	United States
788	Wintergreen Lake	WINTERGR	819.907763	329.35551	162.6	271	United States
789	White Lake	WL02-1	1655.316198	303.165453	82.8	138	United States
790	Winter Gulf Site	WNTRGULF	1310.214953	420.690393	148.8	248	United States
791	Wolf Creek	WOLFCRK	137.016785	723.981326	225	375	United States
792	Wolsfeld Lake	WOLSFELD	180.408409	593.014315	174.6	291	United States
793	Wolverine Lake	WOLVERIN	746.717805	800.279593	155.4	259	United States
795	Wood Lake	WOODLAKE	435.970137	643.696567	278.4	464	United States
798	Wylde Bog	WYLDDEBOG	1172.799341	557.402917	290.4	484	Canada
799	Wylde Lake	WYLDELK	1172.605704	558.568981	290.4	484	Canada
802	Zuehl Farm Site	ZUEHL	163.154606	359.685139	213.6	356	United States

746	Torren's Bog	TORNSBOG	0	10500	n	n	y	excel
749	Lake Tulane	TULANEGL	870	60740	y	y	y	excel
753	Lac Turcotte	TUR	0	10350	n	n	y	access
756	Twiss Marl Pond	TWISMARL	-50	13040	n	y	y	excel
759	Upper Mallot Lake	UPMALLOT	0	10500	n	n	y	access
761	Upper Wallface Pond	UPWALLFC	200	12500	n	y	y	access
763	Van Nostrand Lake	VANNOSTR	0	11000	n	n	y	access
766	Volo Bog	VOLOBOG	0	11000	n	n	y	access
776	Weslemkoon Lake	WESLEM1	5420	9770	n	n	n	access
780	White Pond	WHITEPND	0	19000	y	y	y	access
781	Whitney's Gulch	WHITGLCH	-30	10360	n	n	y	access
787	Winneconnet Pond	WINNE	0	13360	n	y	y	access
788	Wintergreen Lake	WINTERGR	0	12500	n	y	y	access
789	White Lake	WL02-1	8200	14190	n	n	y	excel
790	Winter Gulf Site	WNTRGULF	12490	12780	n	y	n	access
791	Wolf Creek	WOLFCRK	9000	20500	y	y	y	access
792	Wolsfeld Lake	WOLSFELD	120	13870	n	y	y	access
793	Wolverine Lake	WOLVERIN	100	10000	n	n	n	access
795	Wood Lake	WOODLAKE	0	13110	n	y	y	access
798	Wylde Bog	WYLDEBOG	60	12280	n	y	y	access
799	Wylde Lake	WYLDDELK	-30	12460	n	y	y	access
802	Zuehl Farm Site	ZUEHL	0	13000	n	y	y	access

Supplementary Information Table of Contents

Supplementary Discussion: Age models.....	2
Supplementary Figure 1.....	4
Supplementary Figure 2.....	6
Supplementary Figure 3.....	24
Supplementary Code.....	93

Supplementary Discussion: Age models.

We explicitly chose to rely on the default chronology stored in Neotoma (updated to IntCal09) rather than inferring new chronologies using programs such as clam (Blaauw, 2010) or Bchron (Haslett and Parnell, 2008; Parnell et al., 2008). Our decision to rely on the Neotoma chronologies is based on the reasoning that the site analyst has access to information not yet available to the Bayesian model, e.g. about type of material, size of sample, stratigraphic context, etc. We tested how much of a difference this made for the benchmark sites by constructing age models in Bchron (Haslett and Parnell, 2008; Parnell et al., 2008) using all of the original age controls, but with no rejecting or averaging of dates. In some cases (e.g., Crystal Lake, Devil's Lake, Hiscock Site, and Sutherland Pond), the parameters of the Bchron age model did not converge, even with a “super-long” MCMC run (10,000,000 iterations). Since the inferred age model was not markedly different between the standard (100,000 iterations, 10,000 burn-in period), long (200,000 iterations, 20,000 burn-in period), and super-long (10,000,000 iterations, 2,000,000 burn-in period) MCMC runs, we took the super-long MCMC results as the final age model. Because of this, our age-model comparison should be considered tentative for these four sites. We then examined the estimated age and uncertainty across all depths and at particular biostratigraphic event depths in the two sets of chronologies to determine the influence of our choice of age model.

For the majority of event depths, the different age estimates were within 200 years of each other (Supplementary Figure 1, top panel). The generally small differences between the original and Bayesian age models are because very few radiocarbon dates are close enough that their probability density functions (pdfs) overlap. Bayesian models add the most value relative to traditional age models when they can use overlapping pdfs to constrain the range of possible

age models. When age estimates were larger than 200 years, this was generally due to dates that were rejected in the Bayesian model and kept in the original model (Supplementary Figure 2).

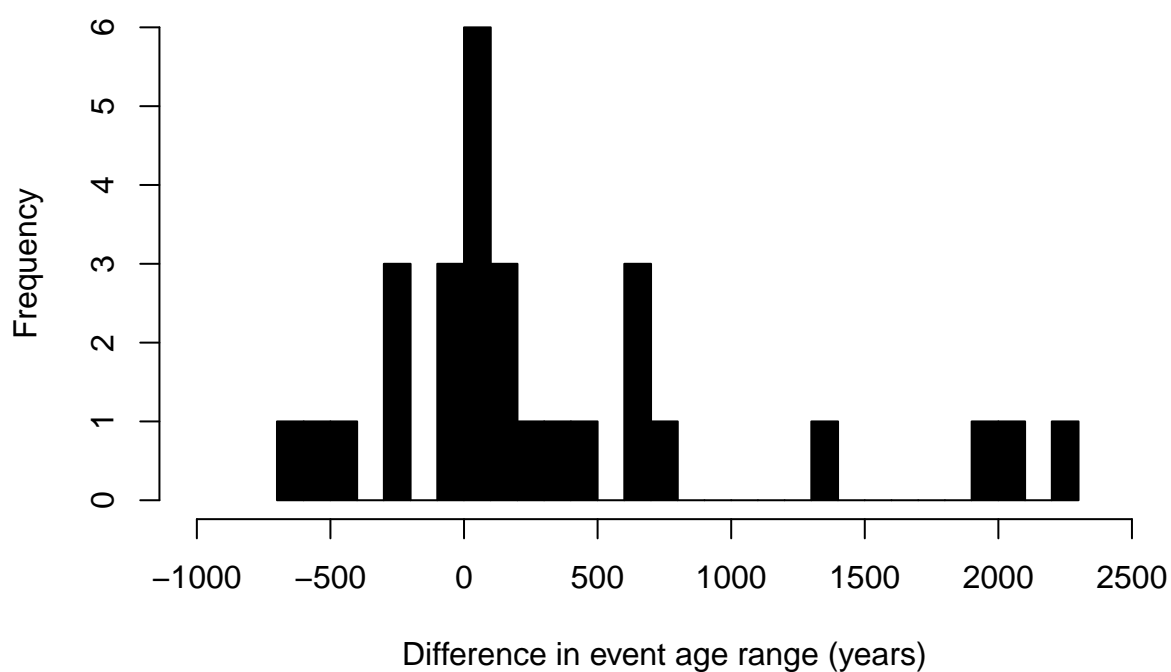
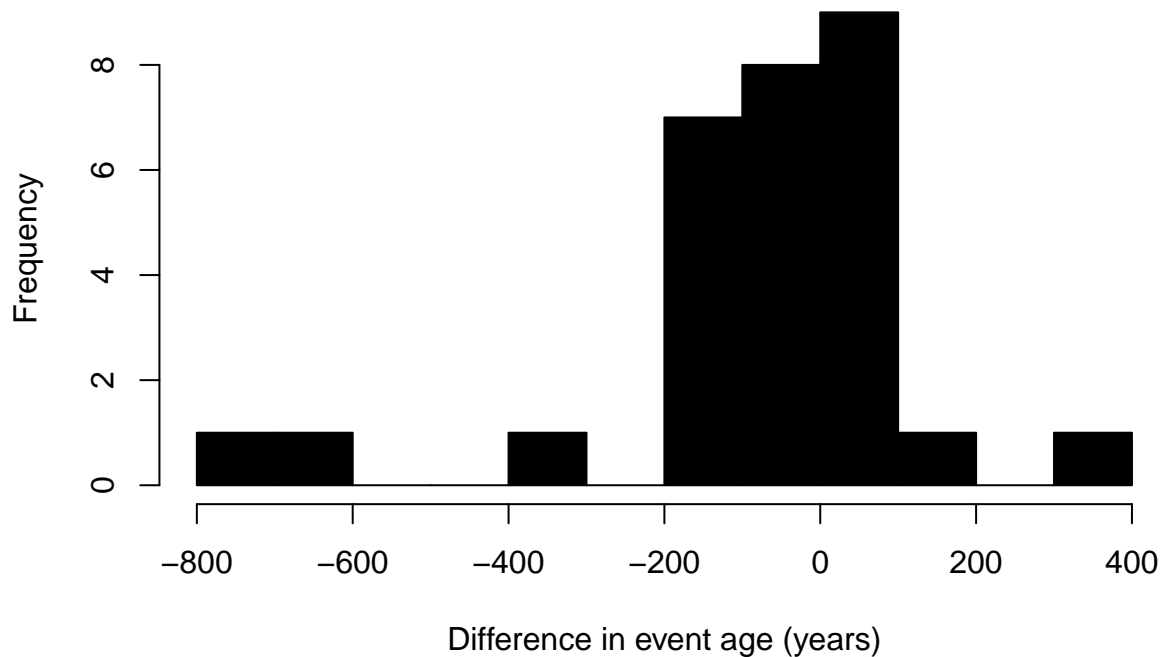
The event age ranges for the different types of age models were generally within 500 years of one another (Supplementary Figure 1, bottom panel) and showed very little systematic offsets in uncertainty, with the median difference 88 years. A few sites show larger uncertainties in the Bayesian estimates (Supplementary Figure 1).

Literature Cited

- Blaauw, M., 2010. Methods and code for 'classical' age-modelling of radiocarbon sequences. Quaternary Geochronology 5, 512-518.
- Haslett, J., Parnell, A., 2008. A simple monotone process with application to radiocarbon-dated depth chronologies. Journal of the Royal Statistical Society: Series C (Applied Statistics) 57, 399-418.
- Parnell, A., Haslett, J., Allen, J., Buck, C., Huntley, B., 2008. A flexible approach to assessing synchronicity of past events using Bayesian reconstructions of sedimentation history. Quaternary Science Reviews 27, 1872-1885.

Supplementary Figure 1.

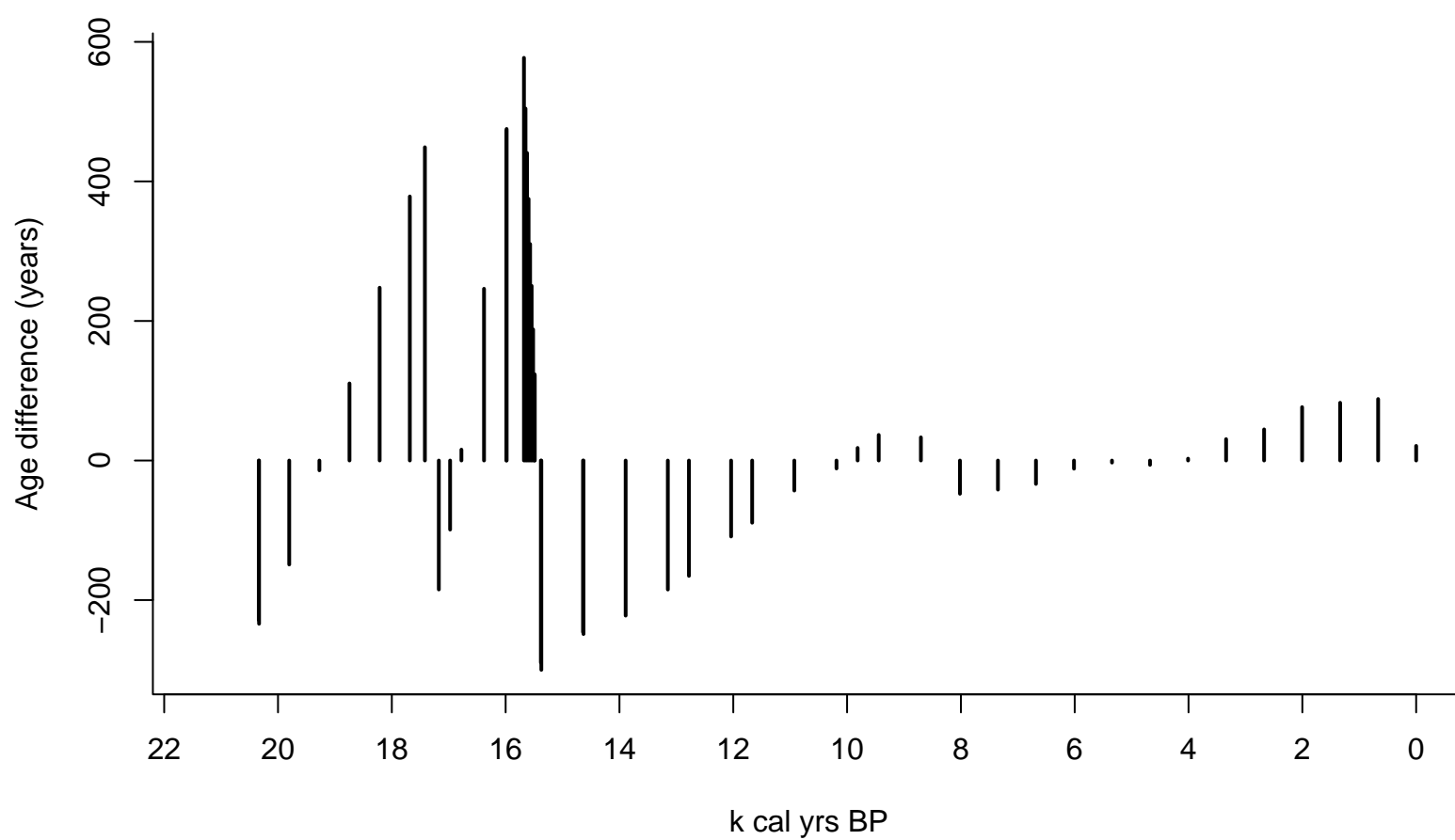
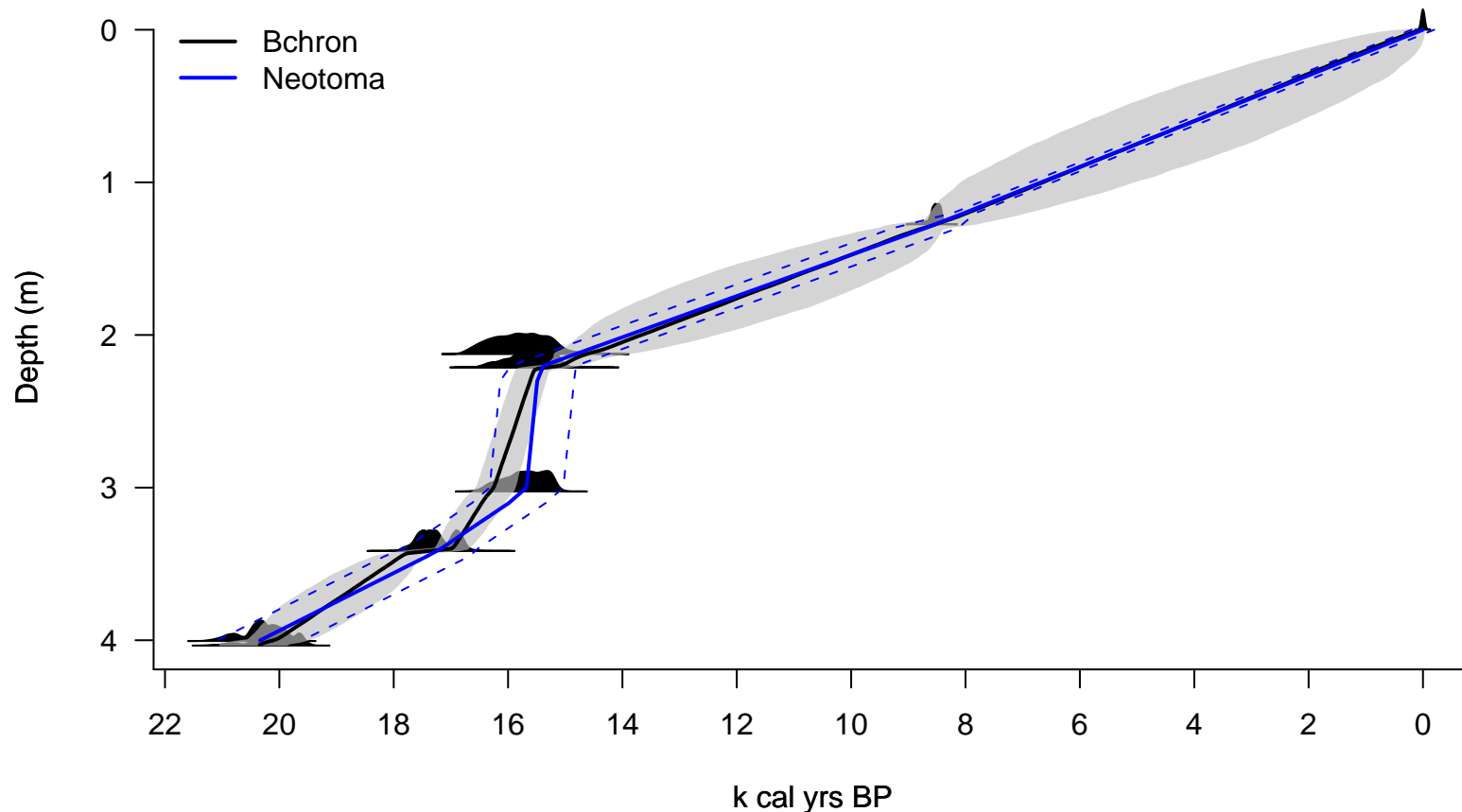
Histogram of the difference in event age (top panel) and event age range (bottom panel) across benchmark sites. The difference is calculated as Bchron - Neotoma. All events and all sites are included, except for events detected at Kettle Lake, ND and Steel Lake, MN, which do not have Bchron chronologies.

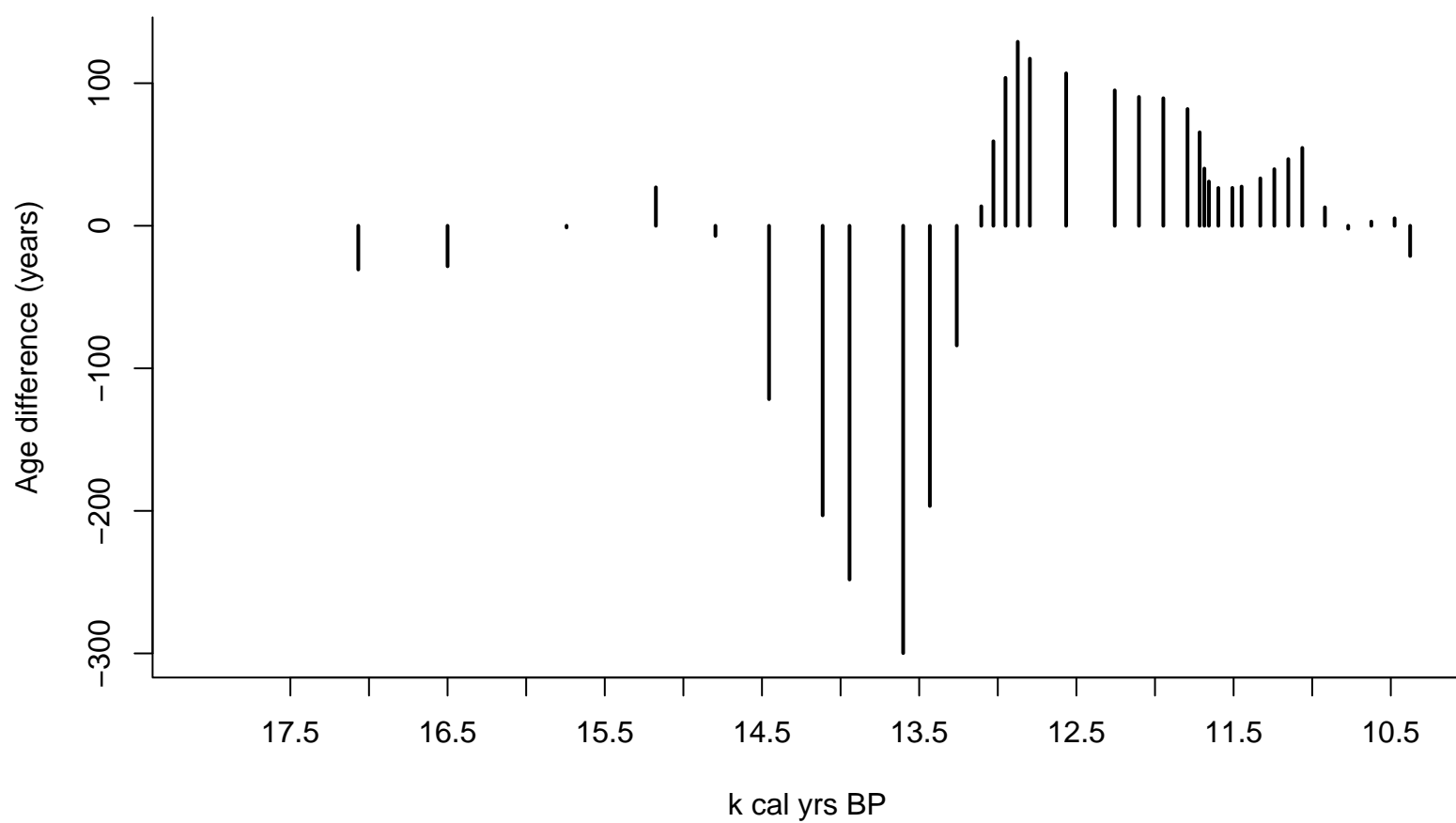
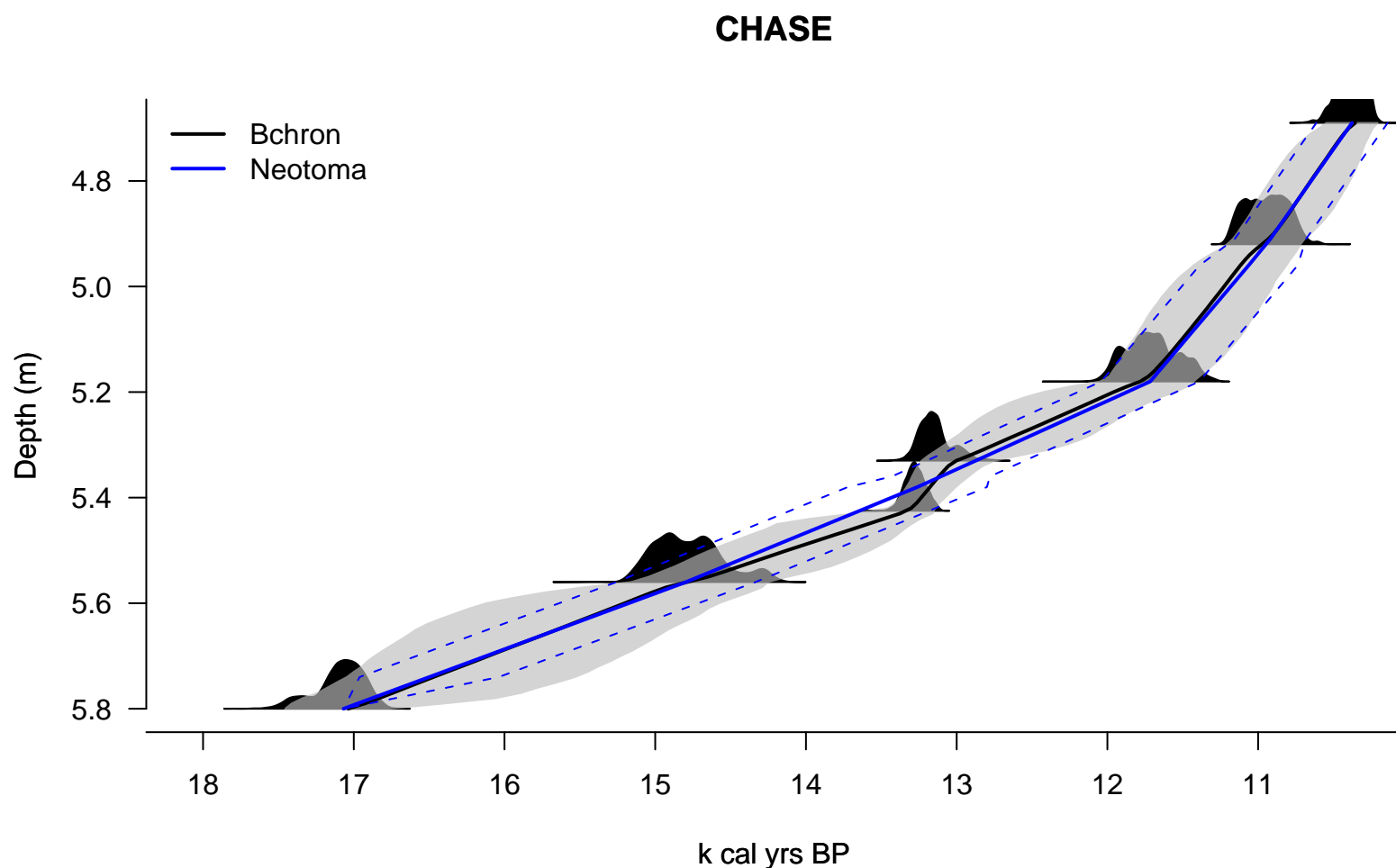


Supplementary Figure 2.

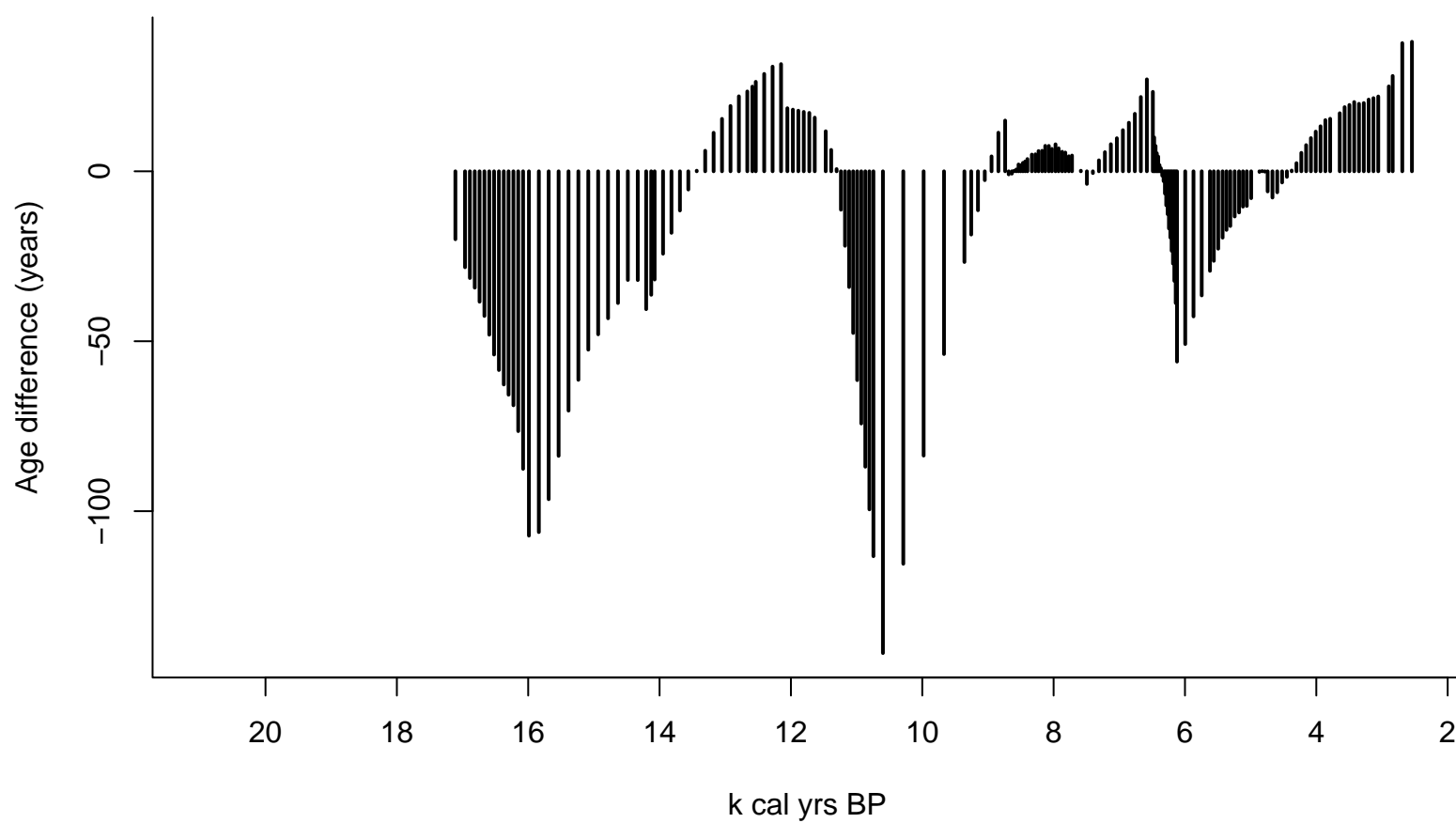
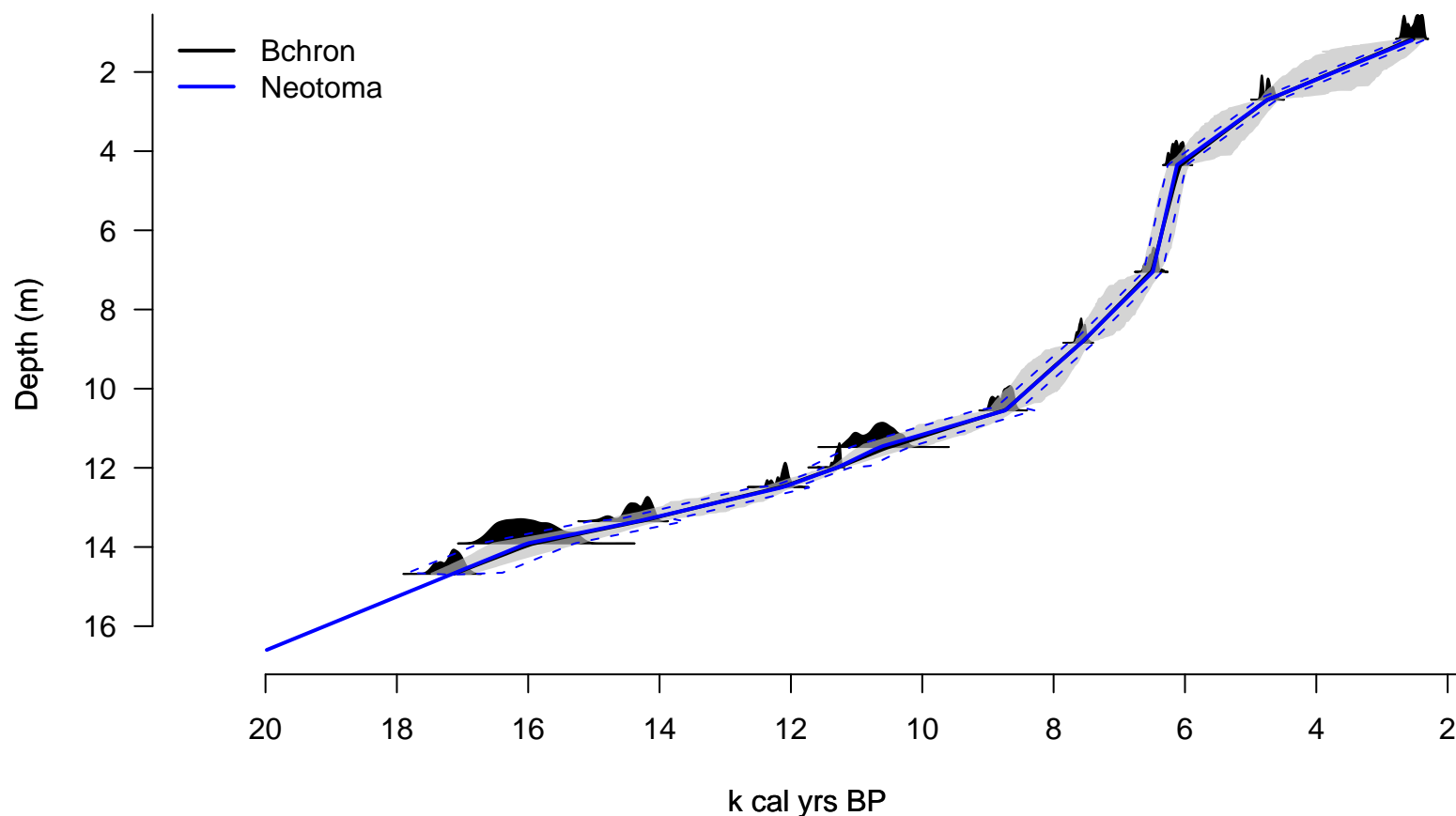
Upper panel: Age models for each benchmark site. The probability density function of the original radiocarbon dates and other age controls are shown in black. The black line indicates the median age as inferred by Bchron, with the 95% probability range shaded in gray. The solid blue line indicates the median age as inferred by the default Neotoma chronology, with the dashed blue lines indicating our estimate of uncertainty at each depth. Dates shown in red are ones that Bchron flagged as outliers. Lower panel: The difference in inferred age at each sample depth, calculated as Median age (Bchron) – Median Age (Neotoma).

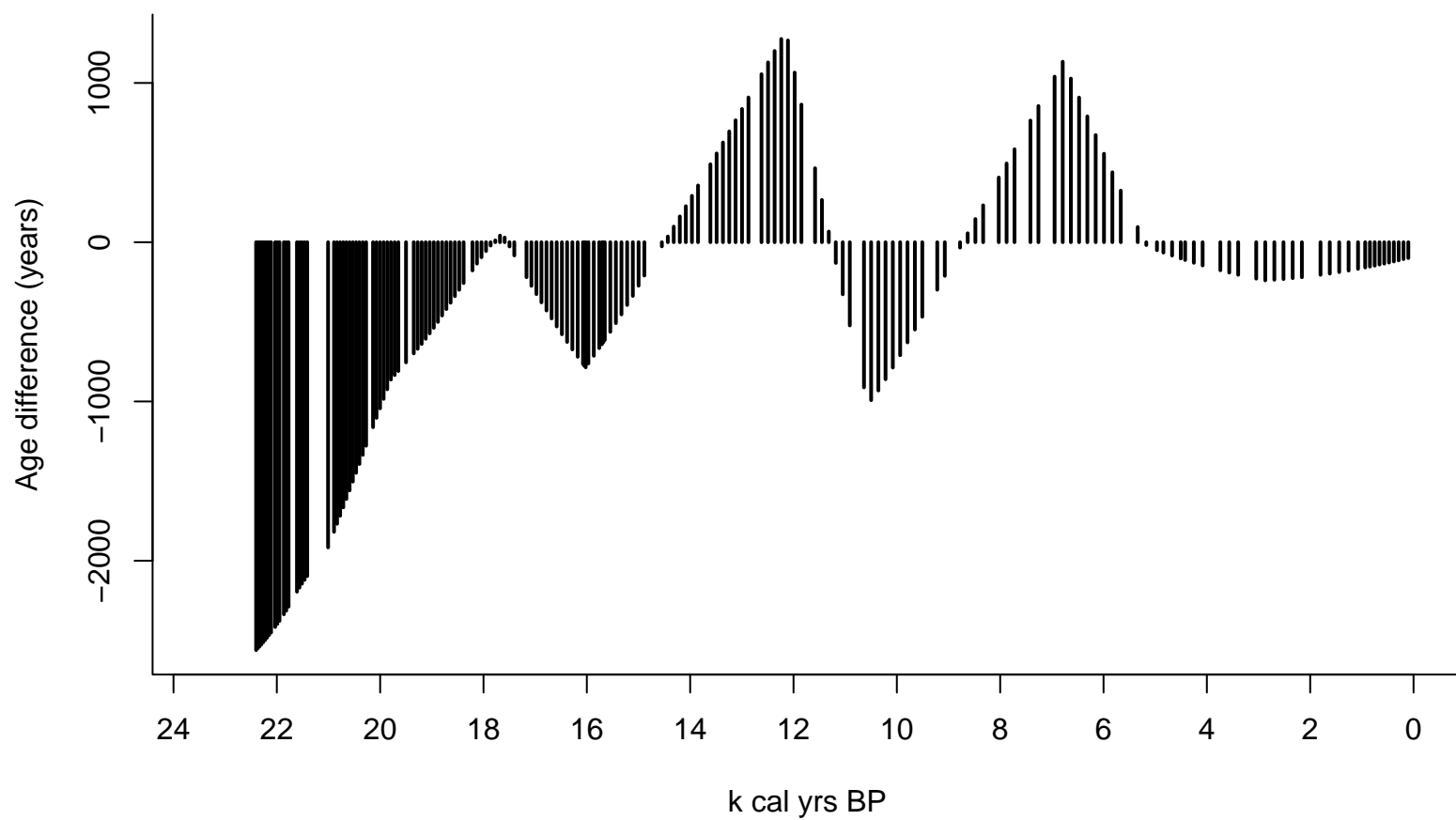
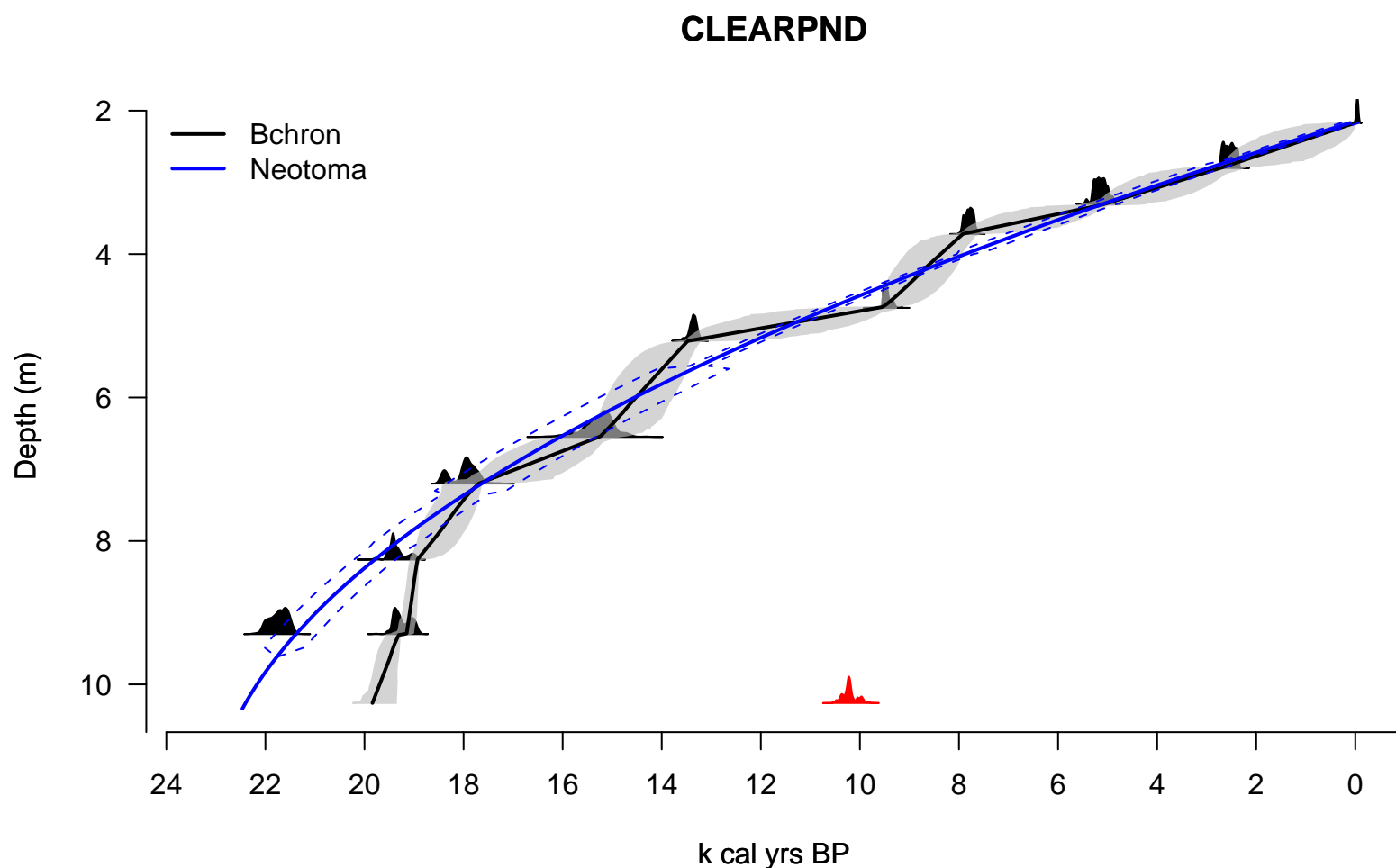
BROWNSPD

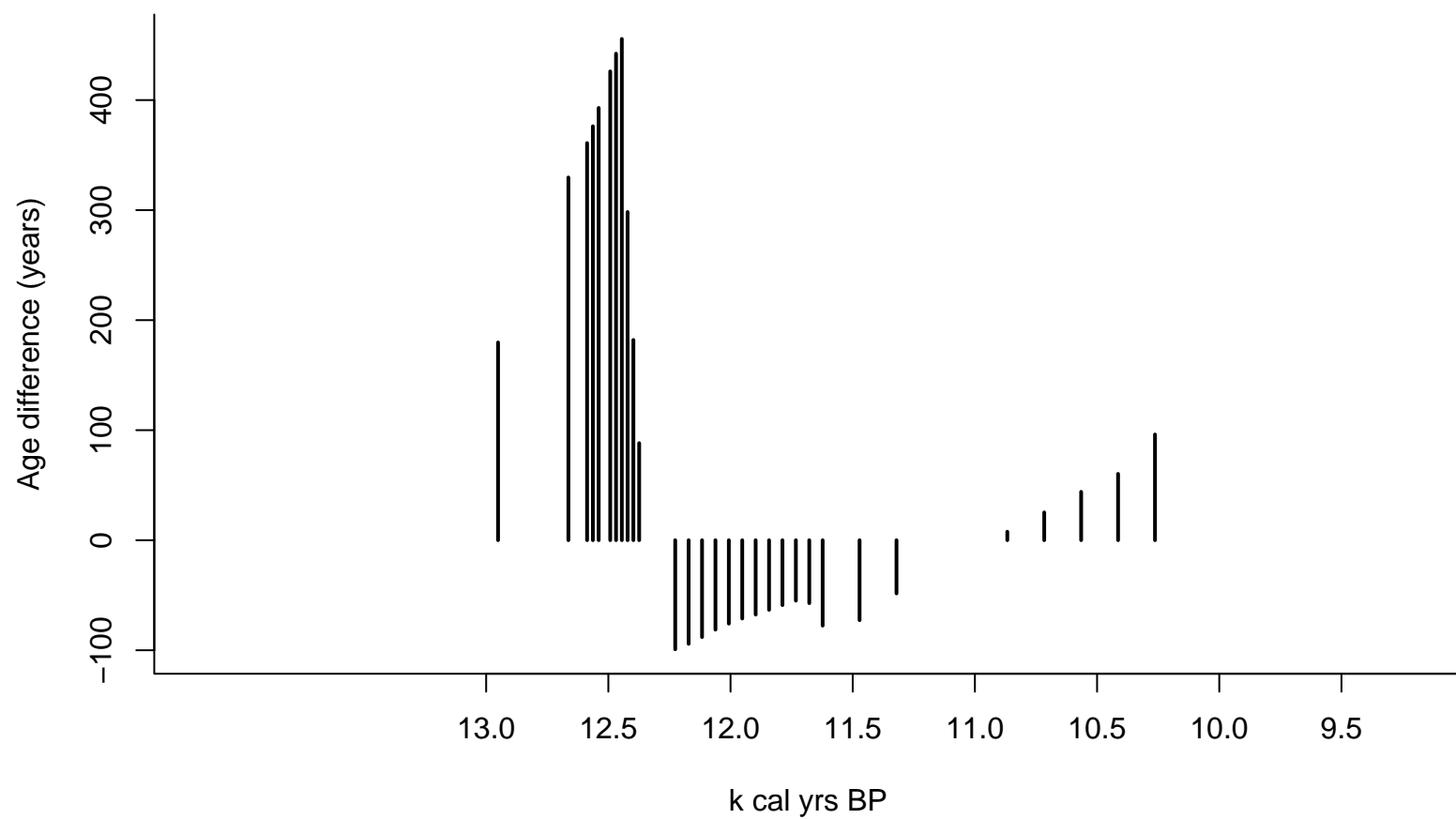
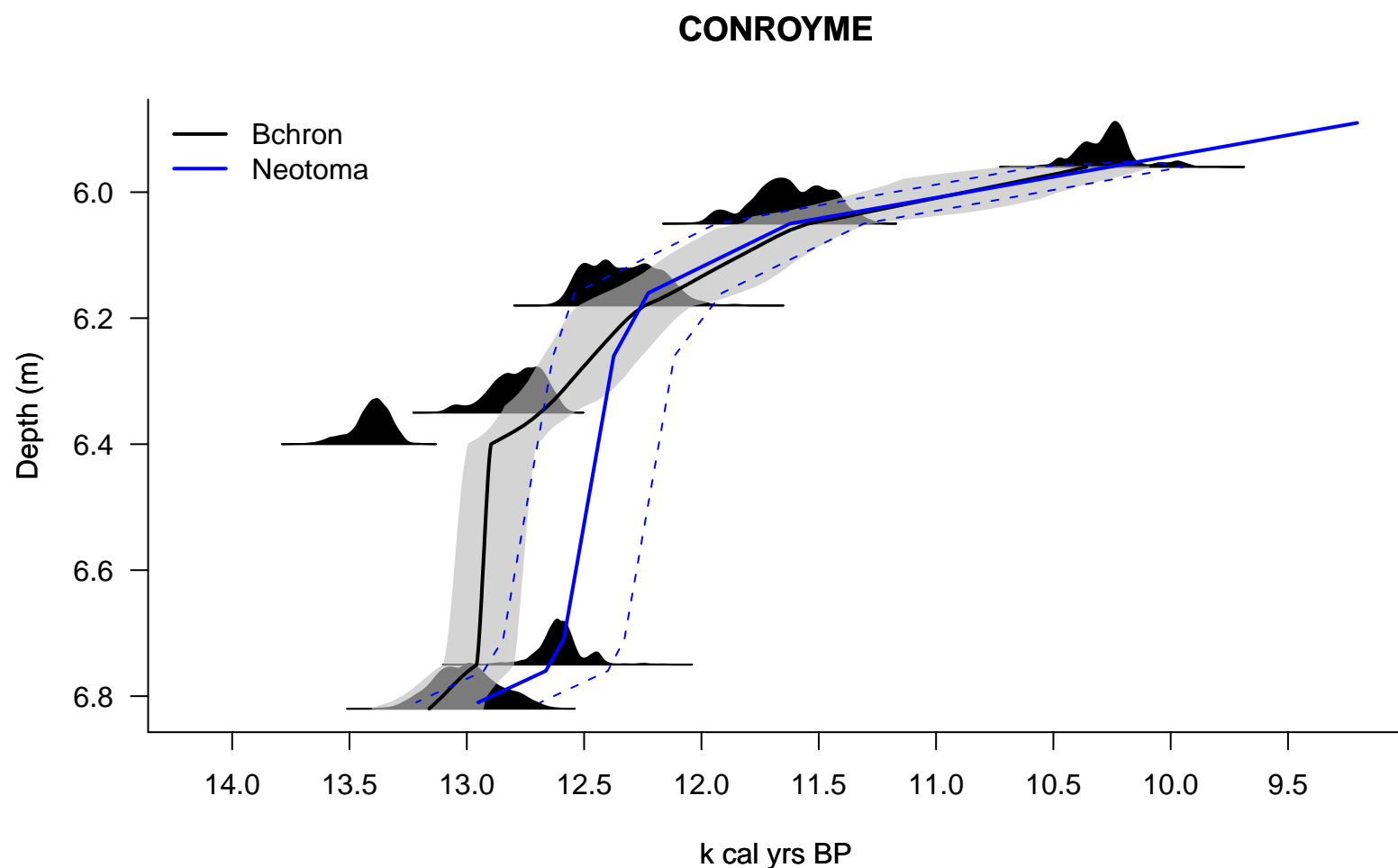


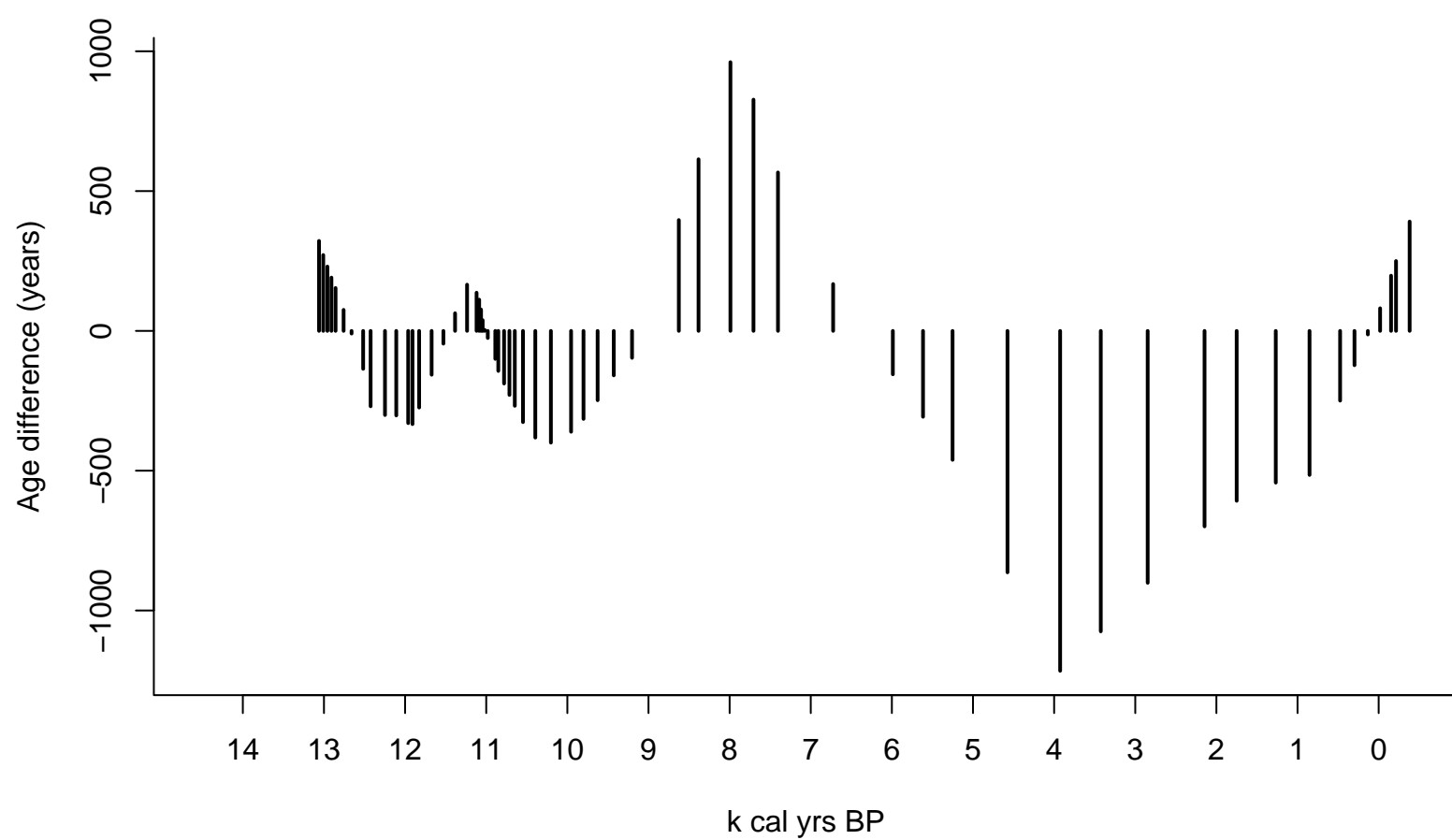
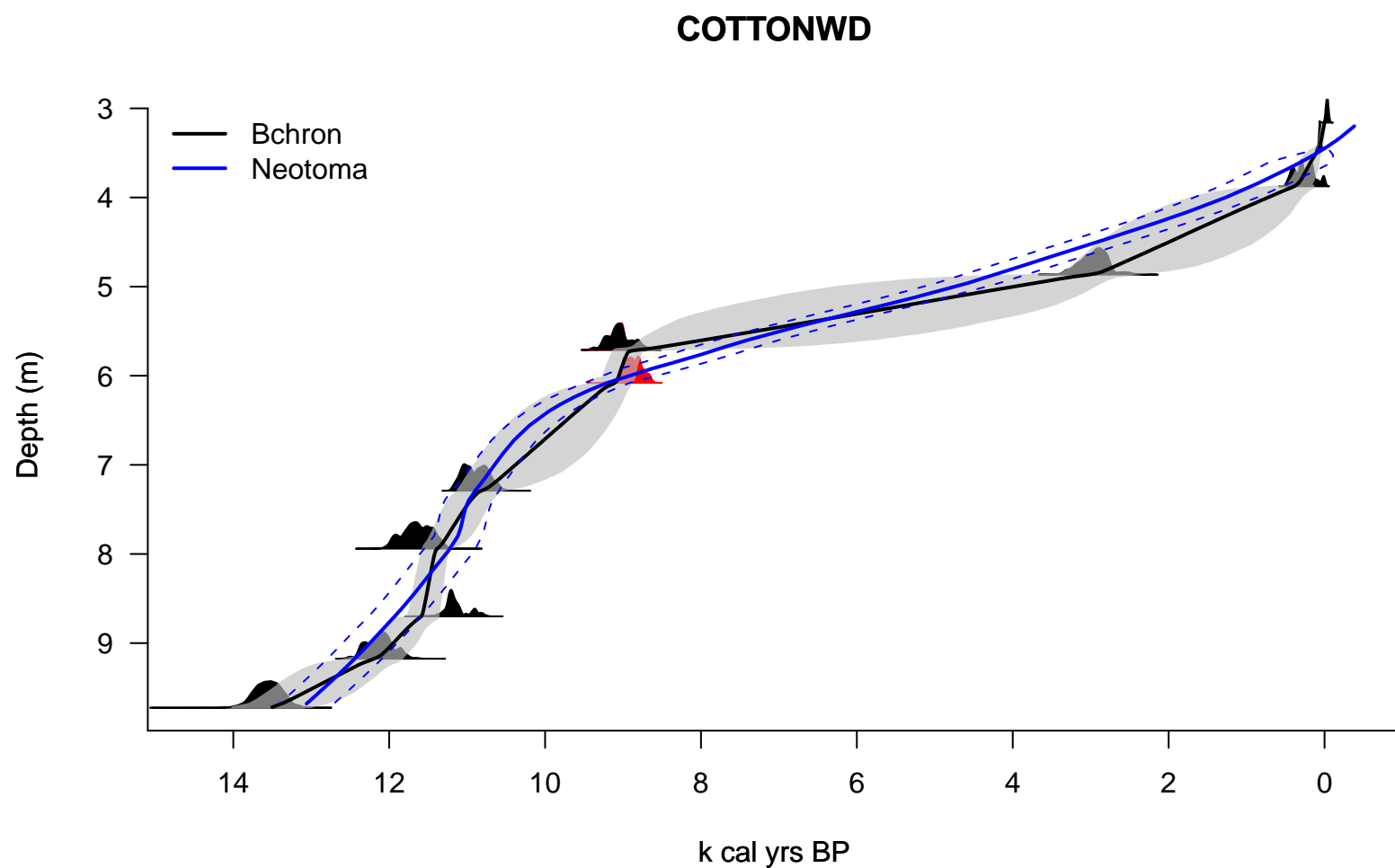


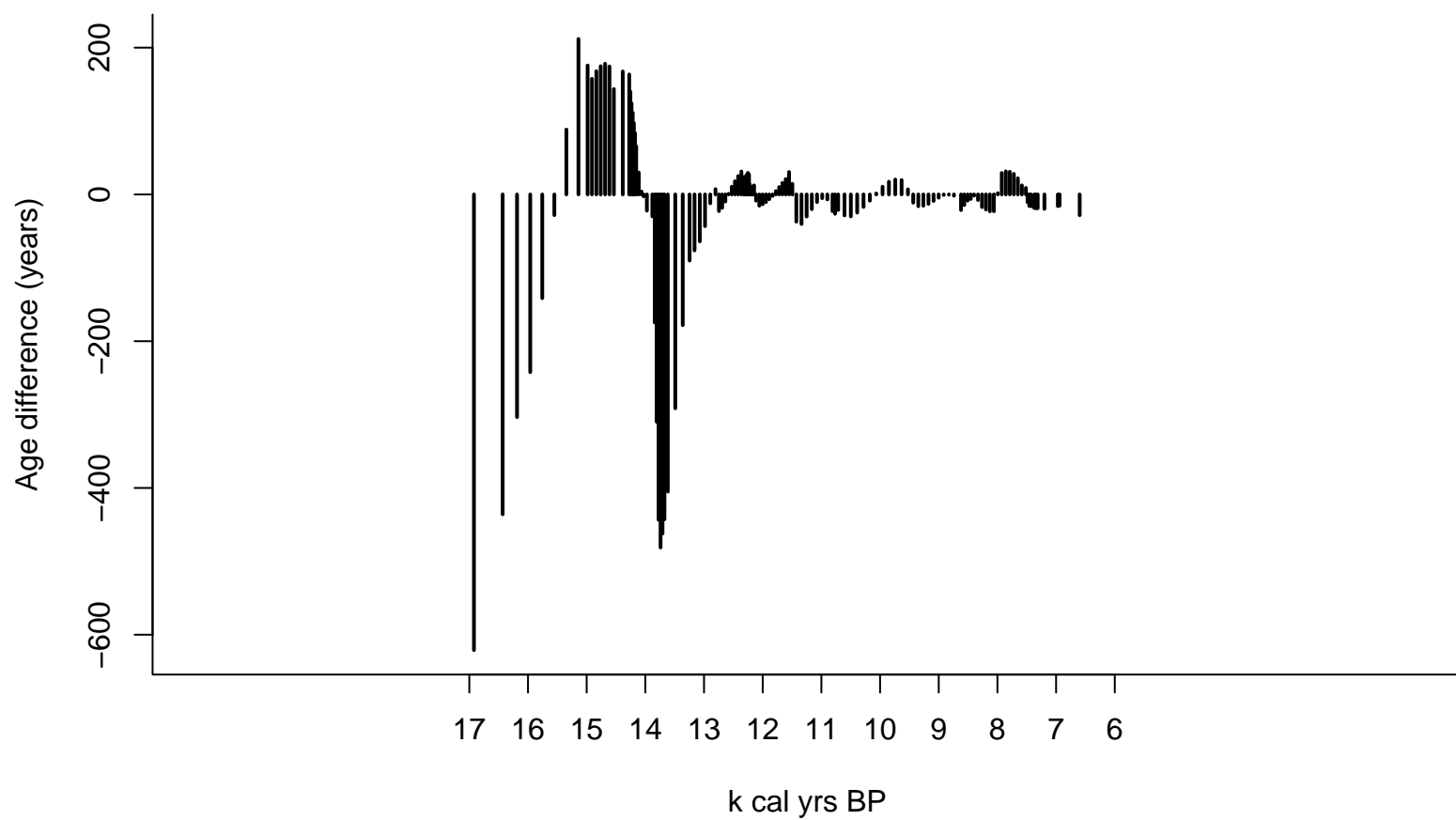
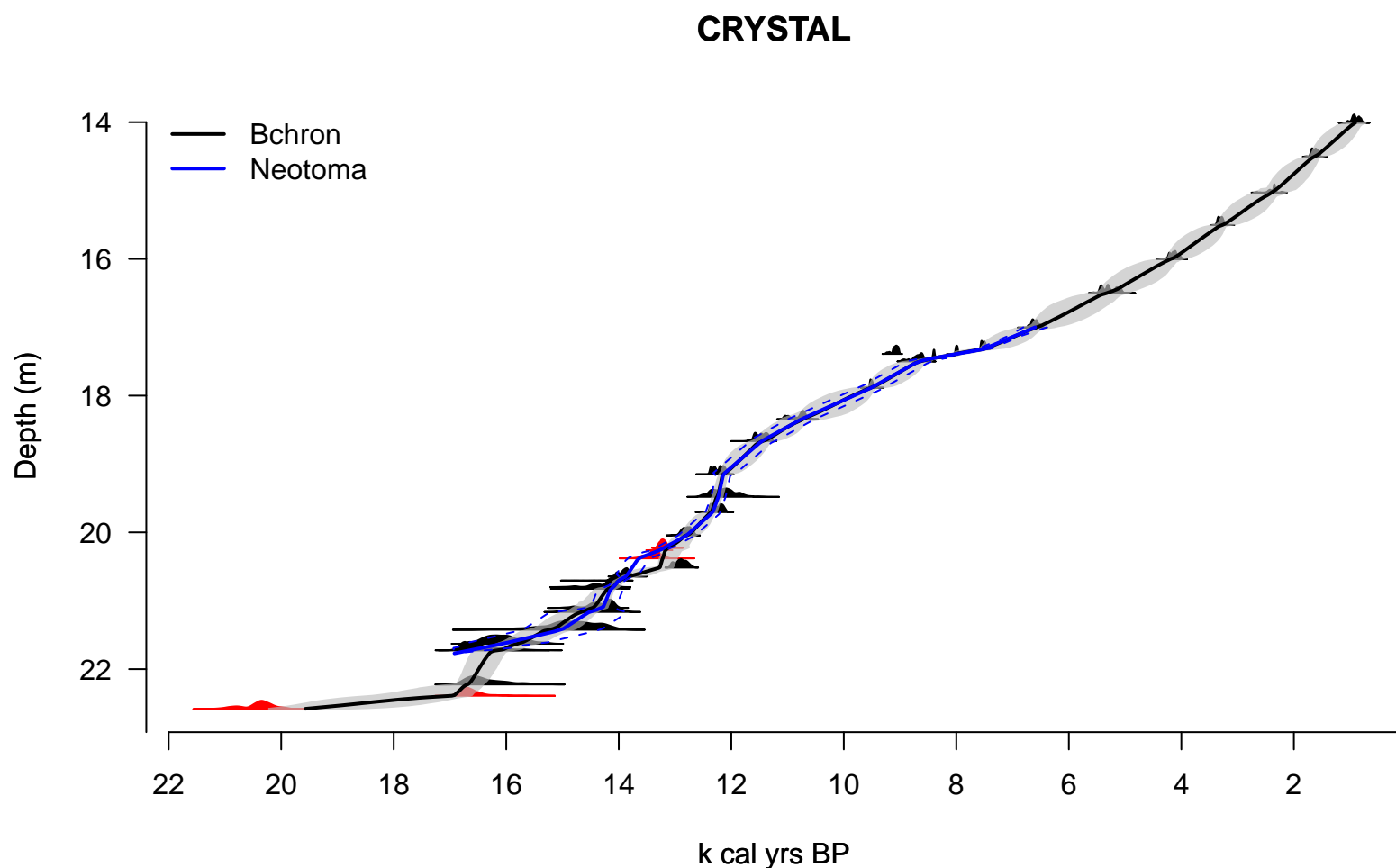
CHAT2003

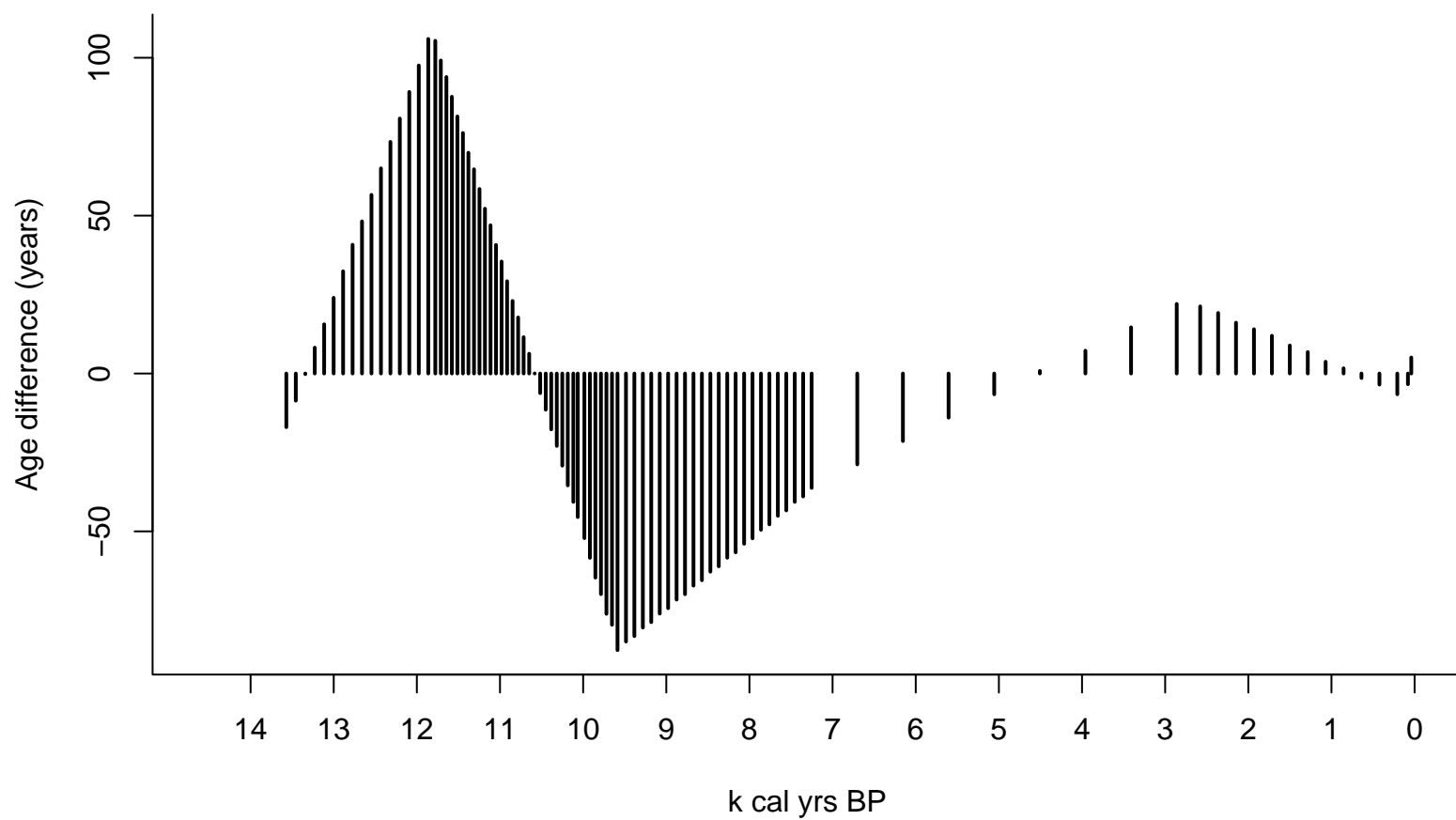
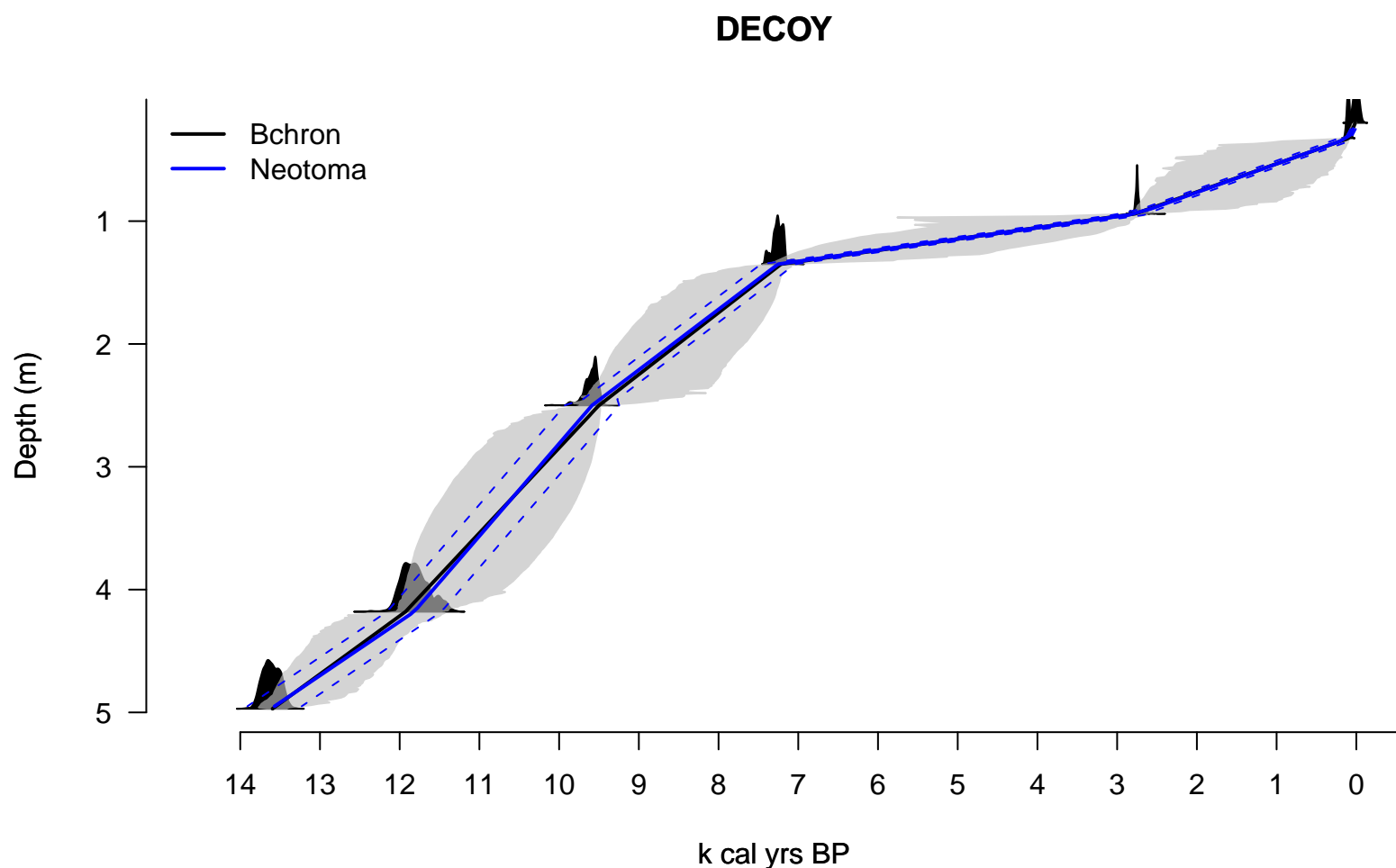


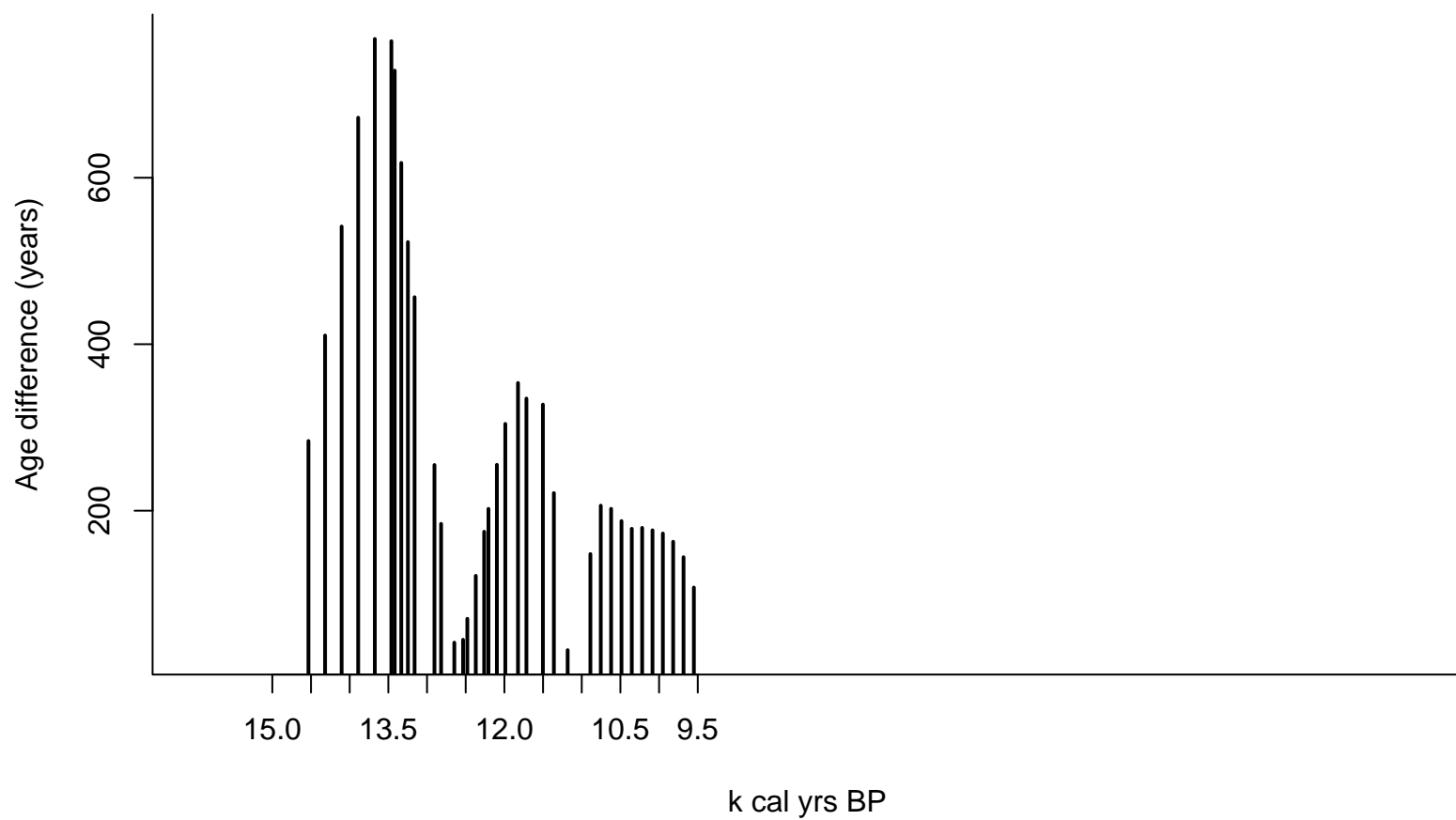
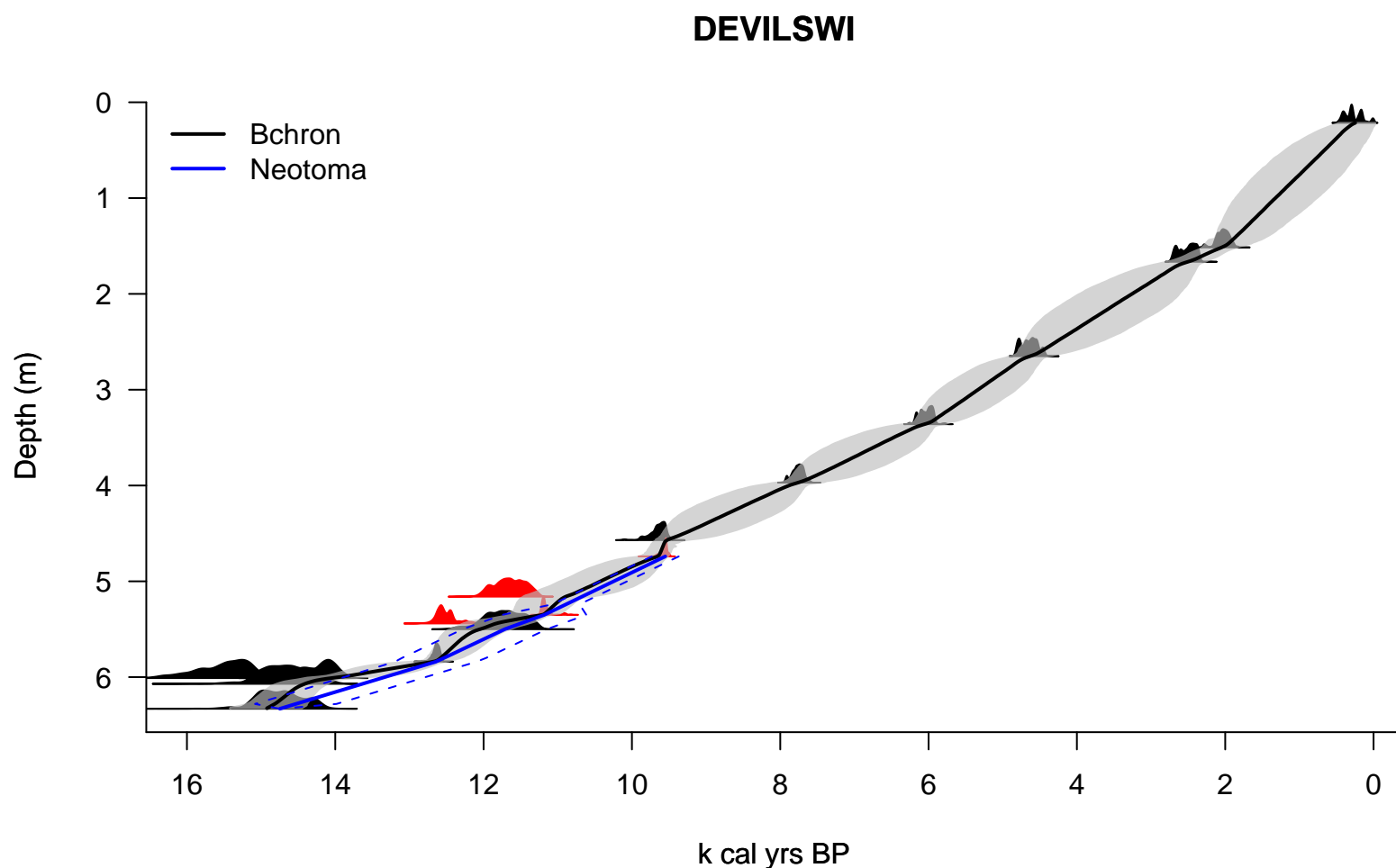




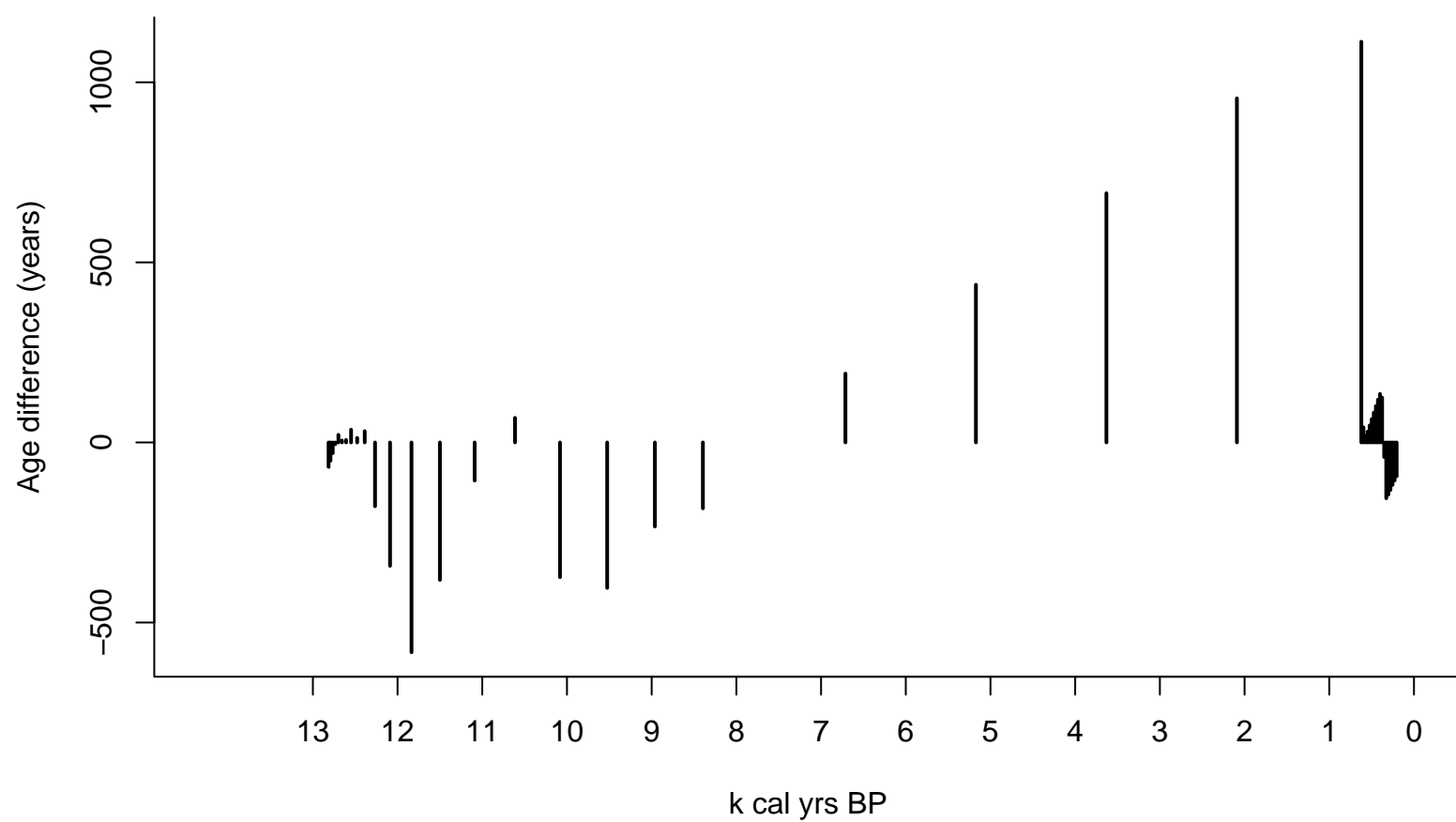
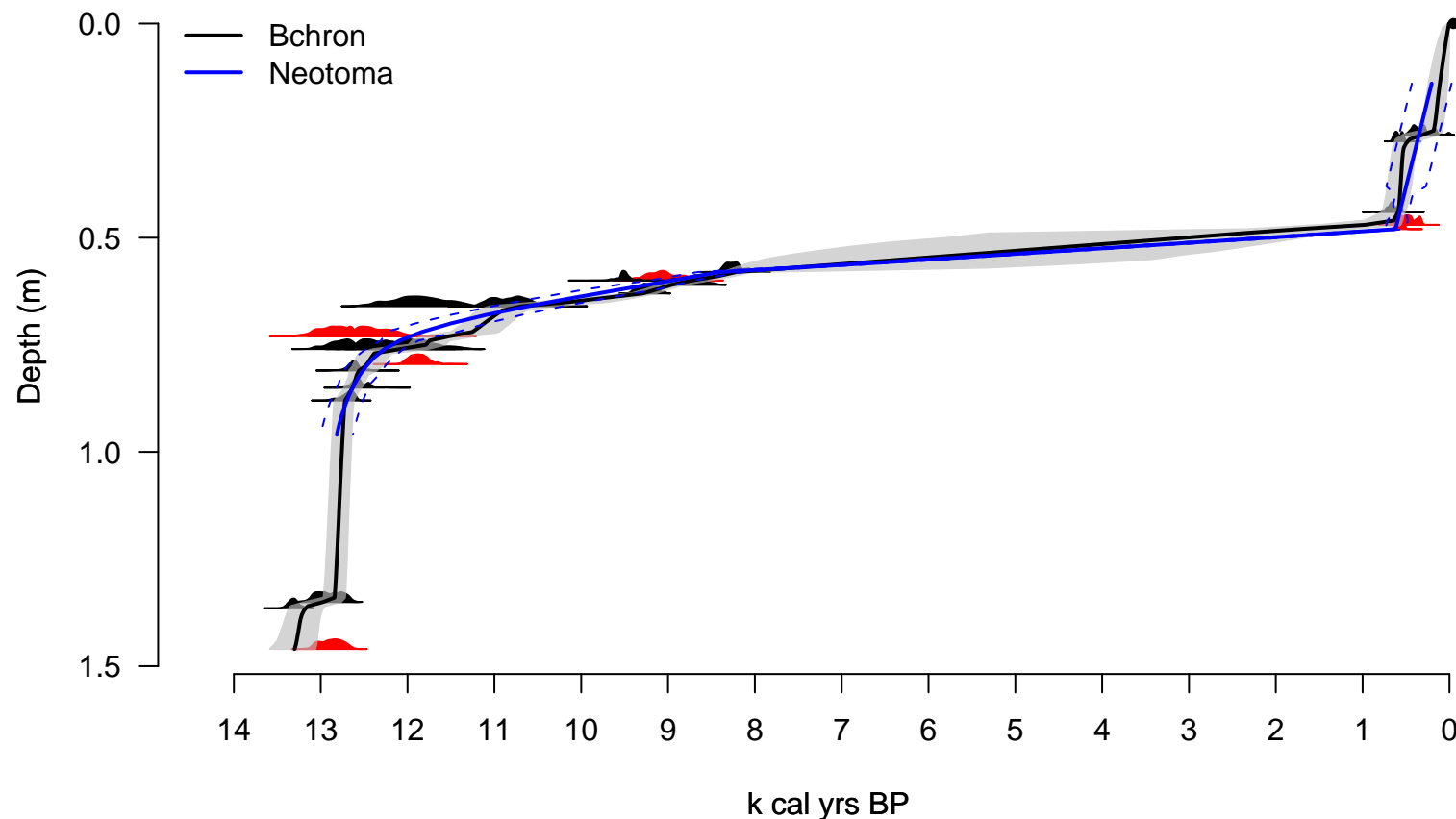


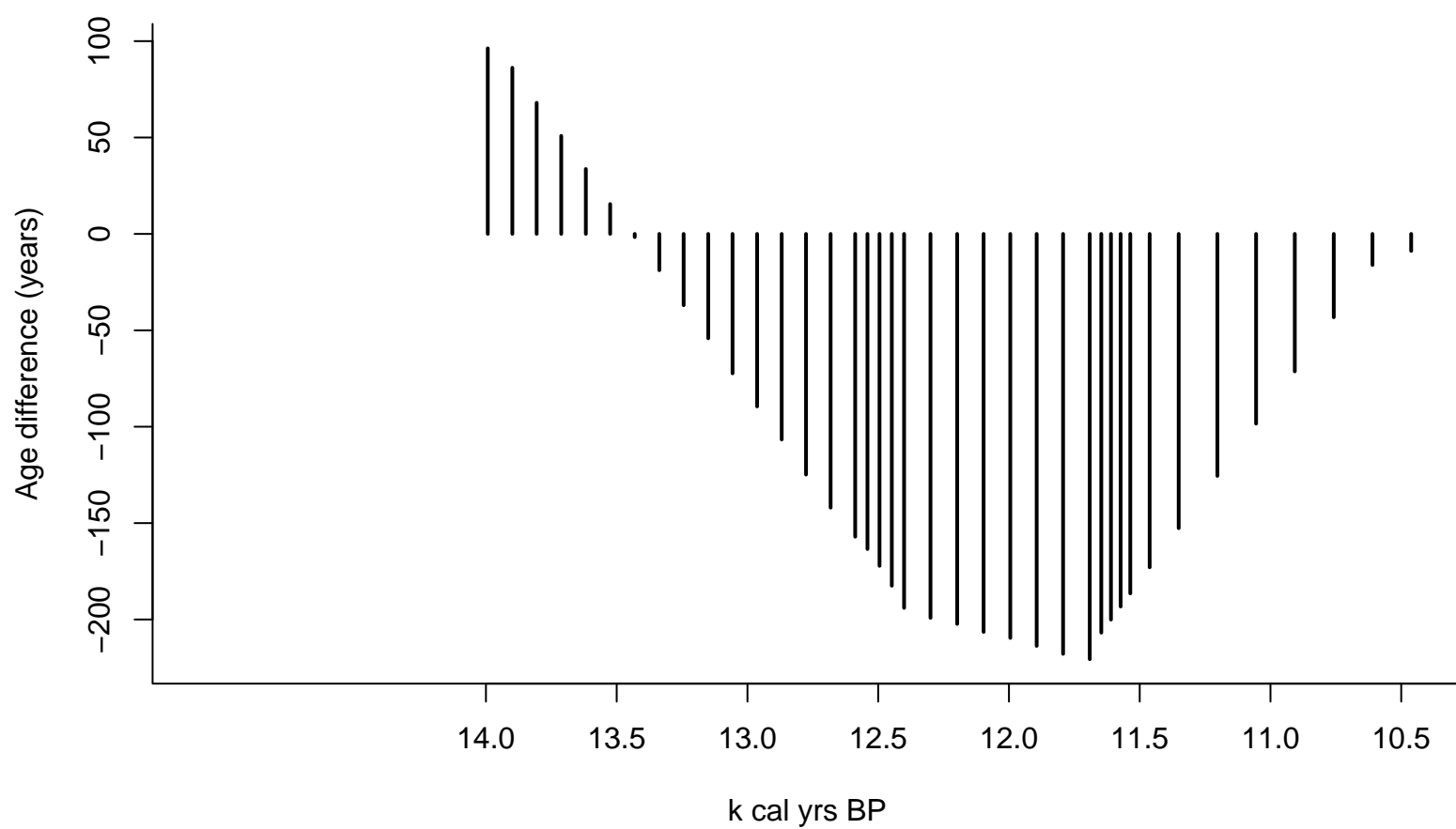
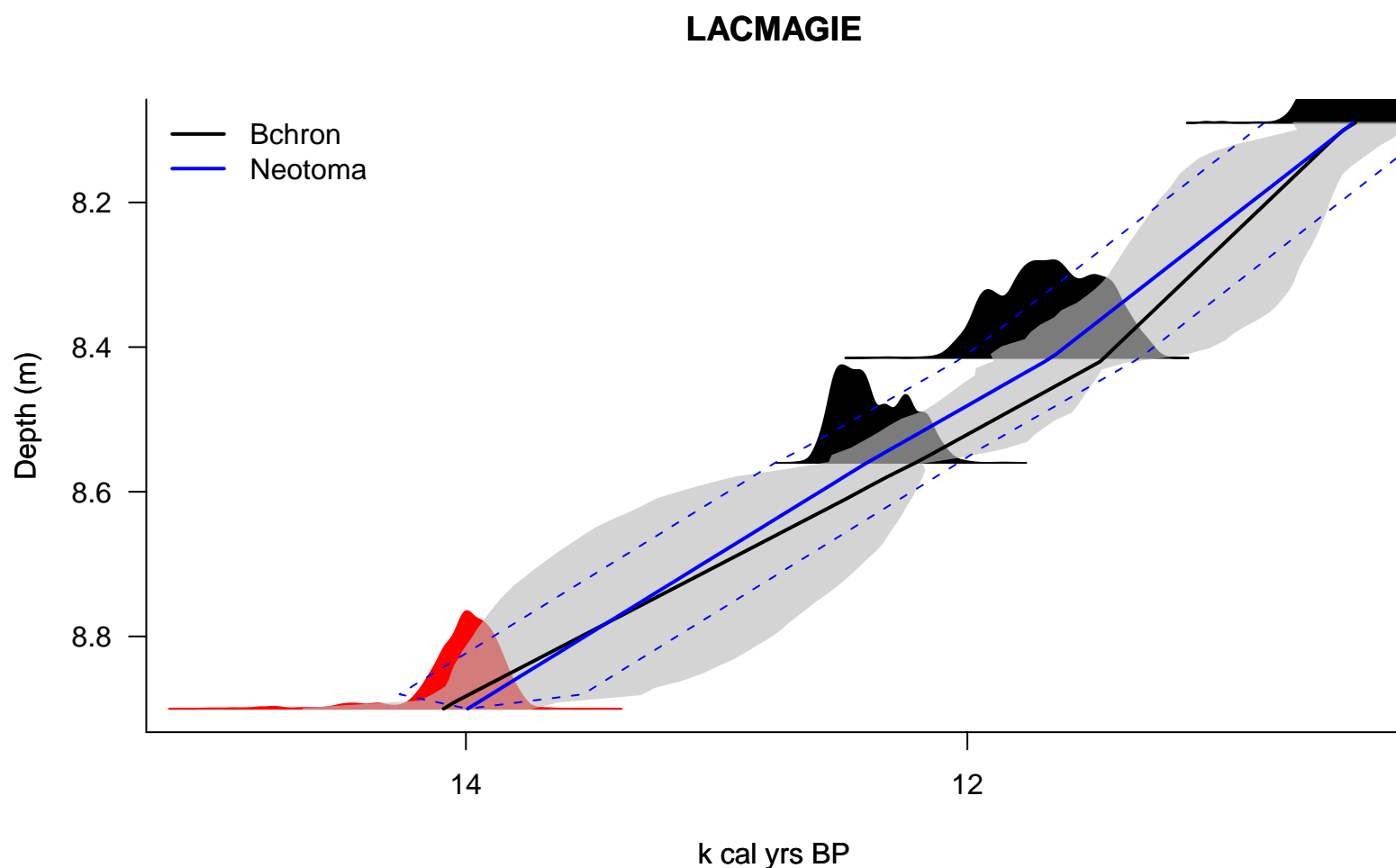


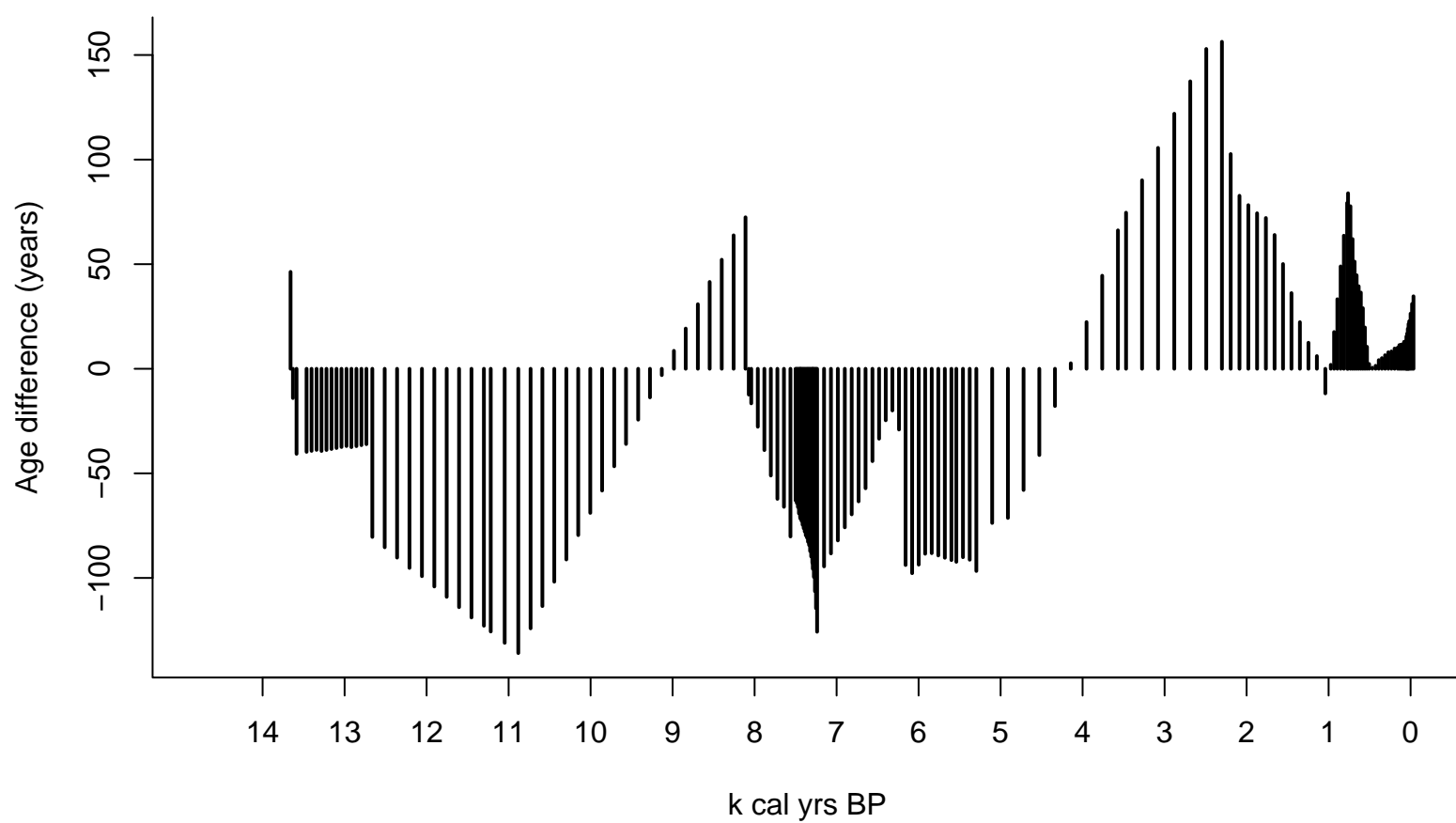
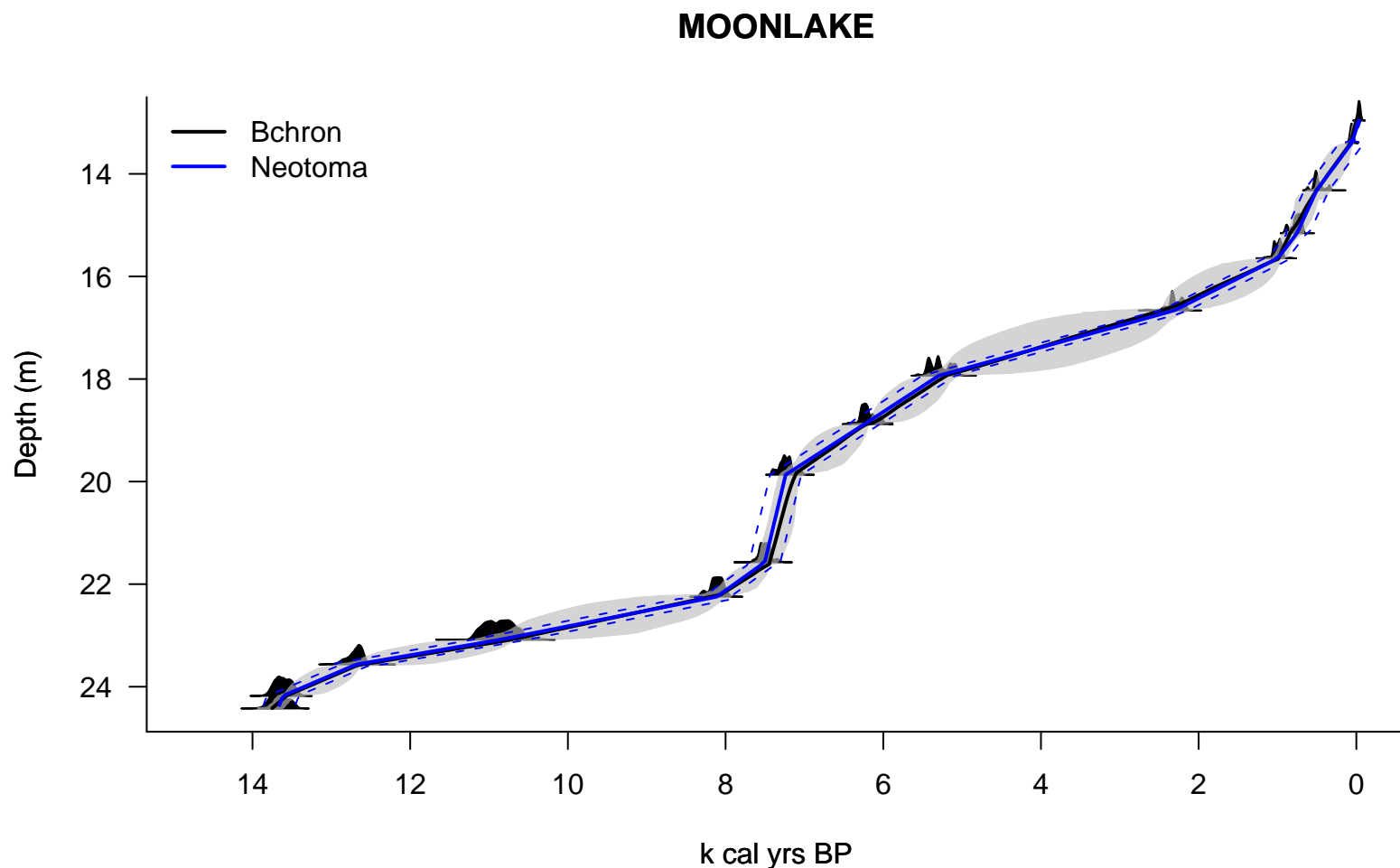




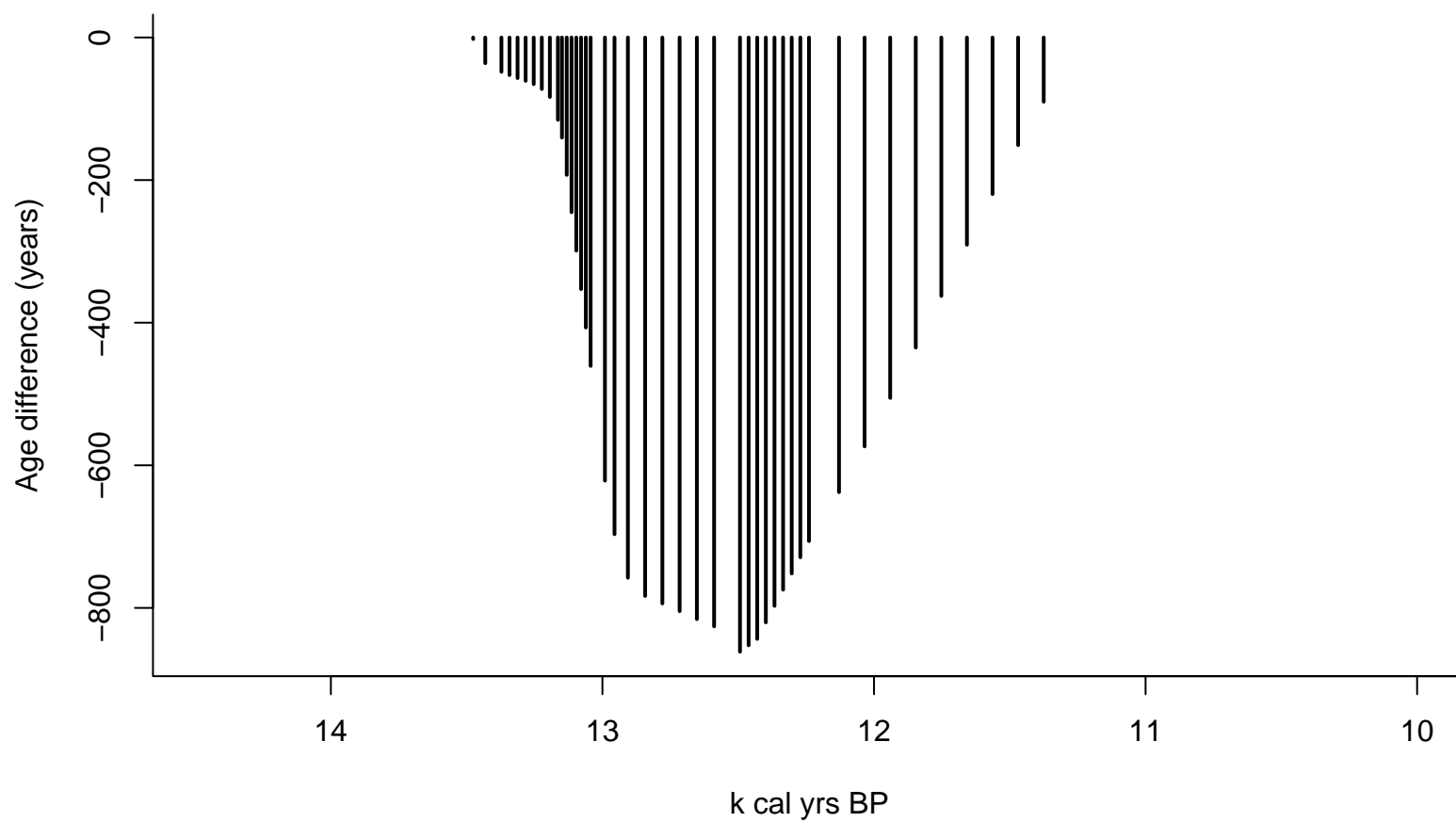
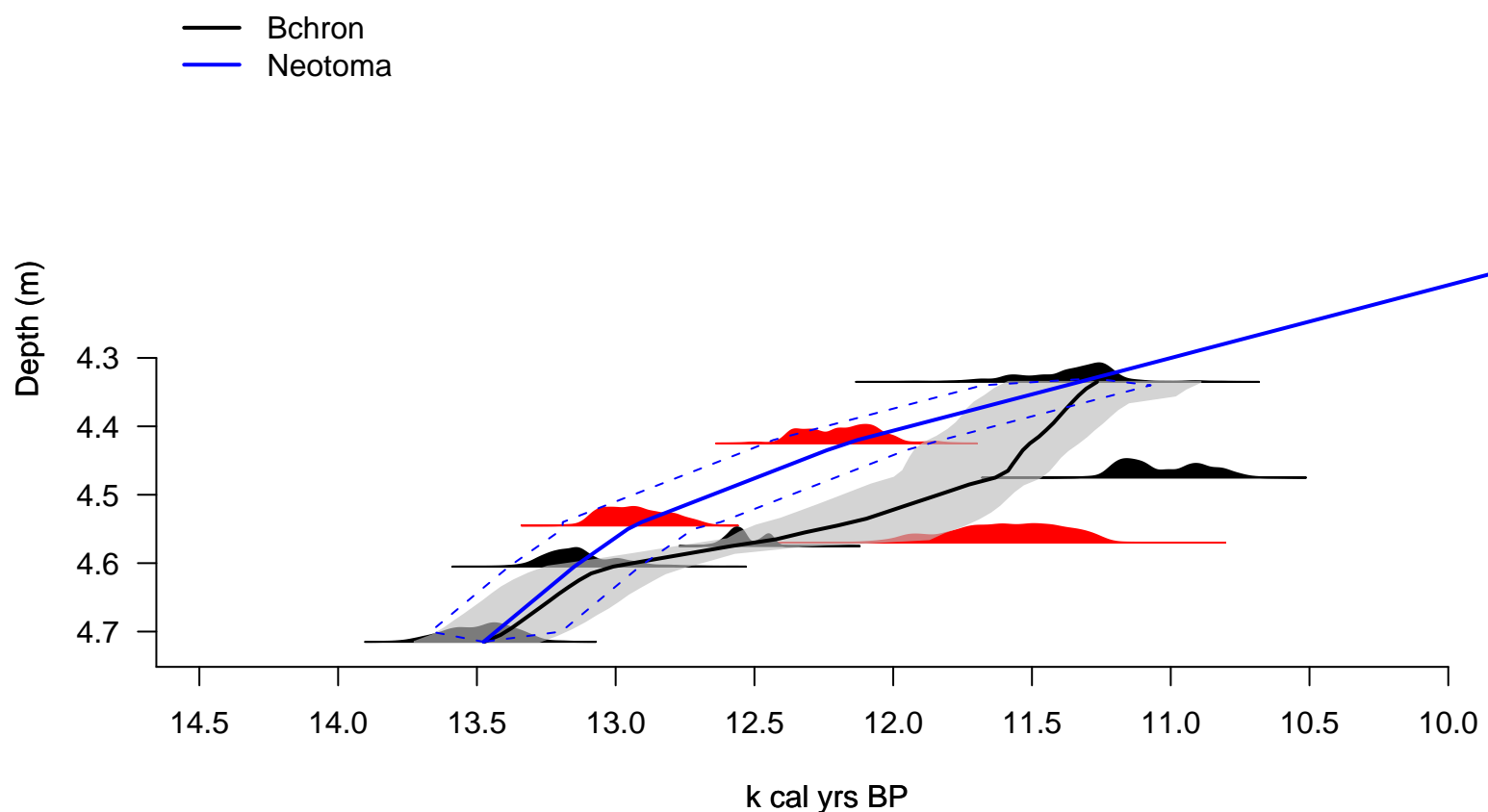
HISCOCK

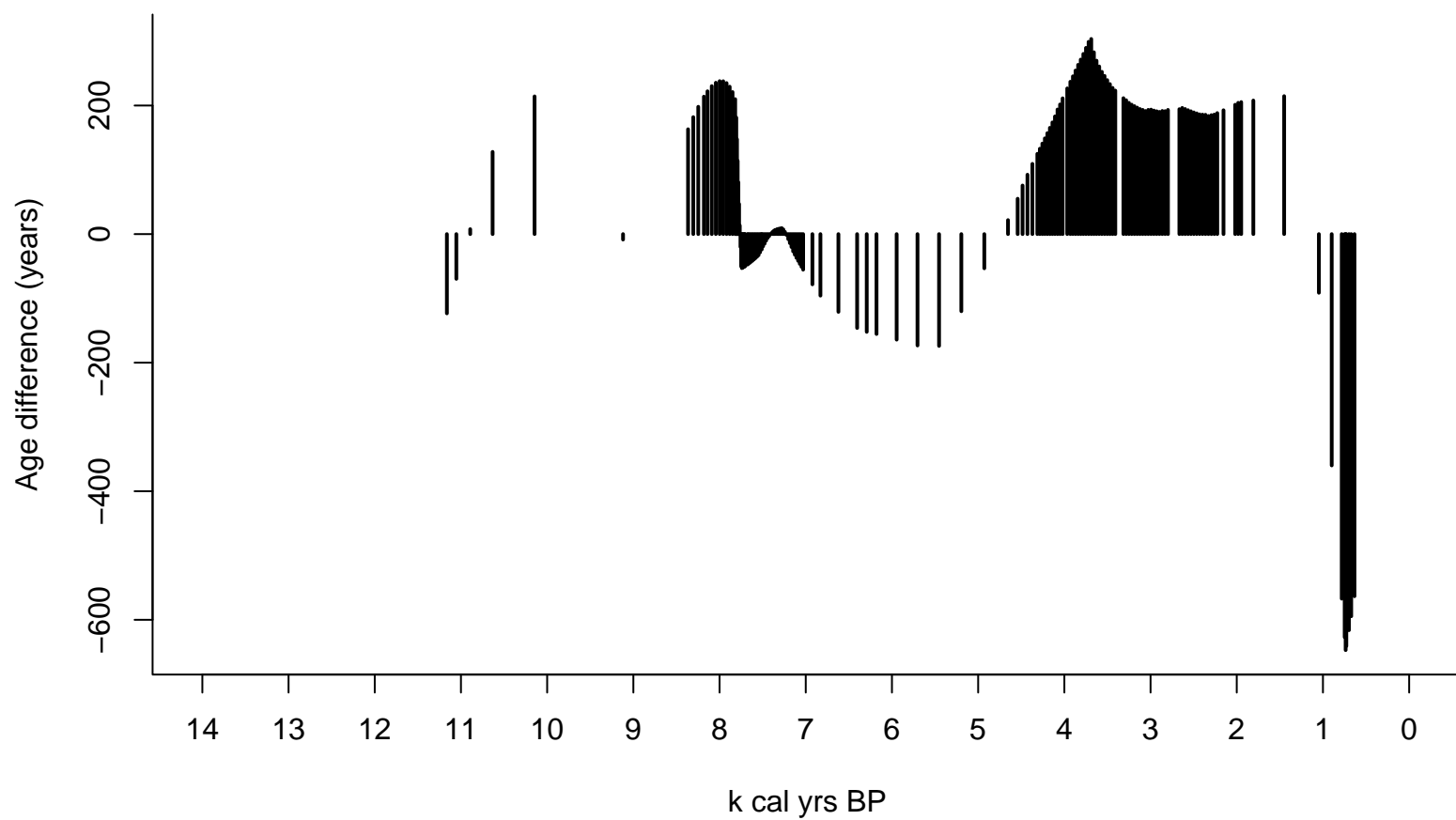
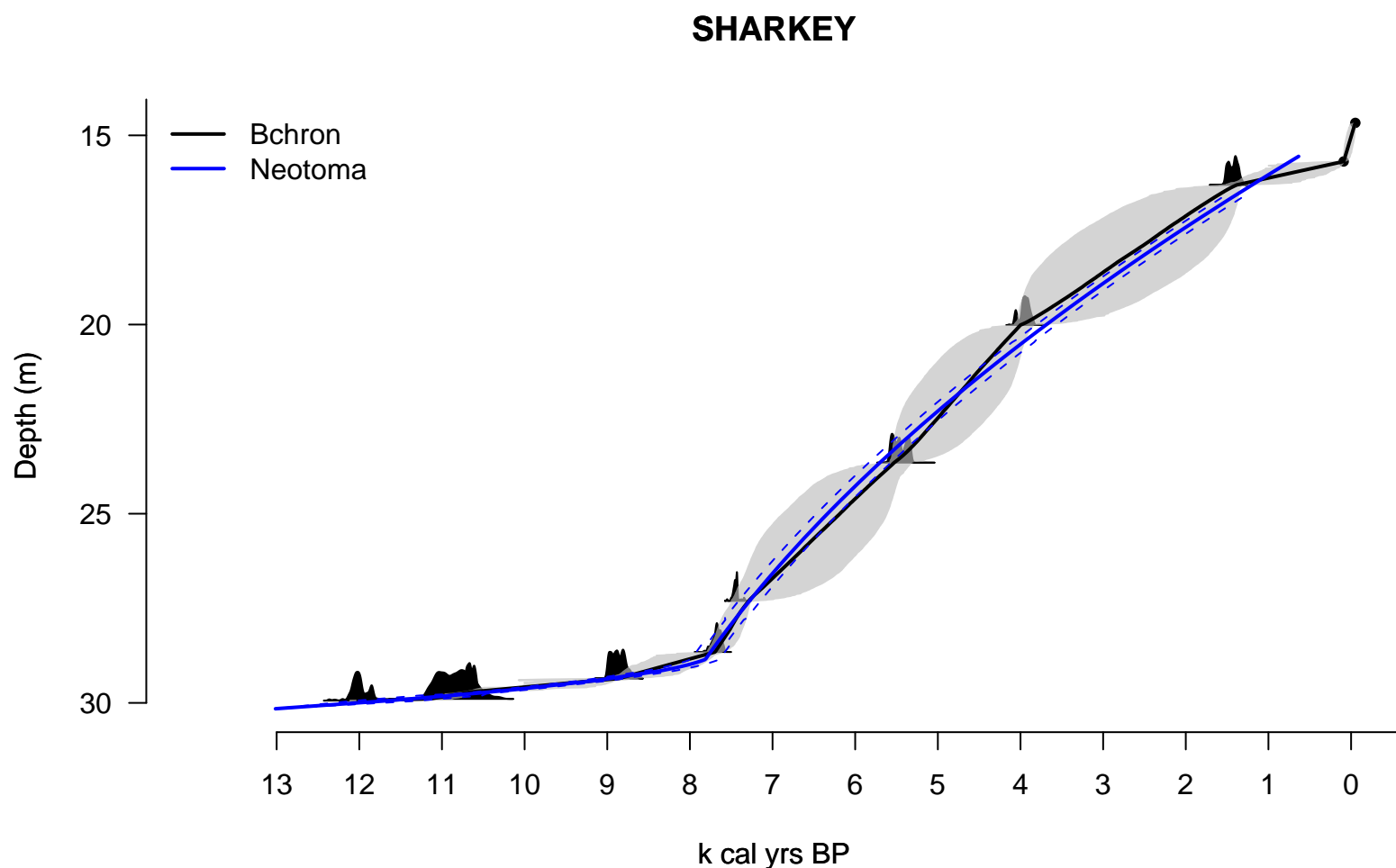


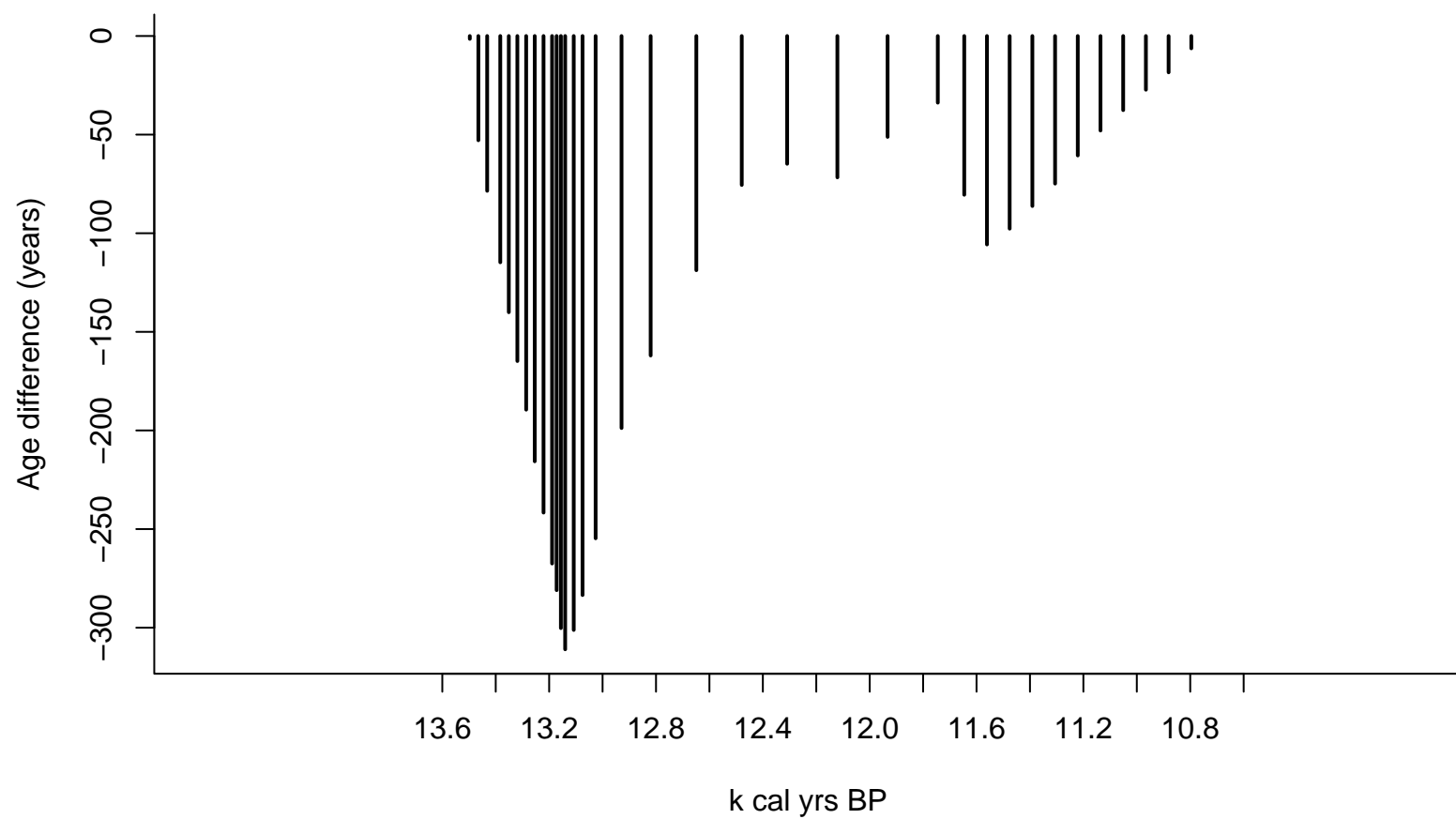
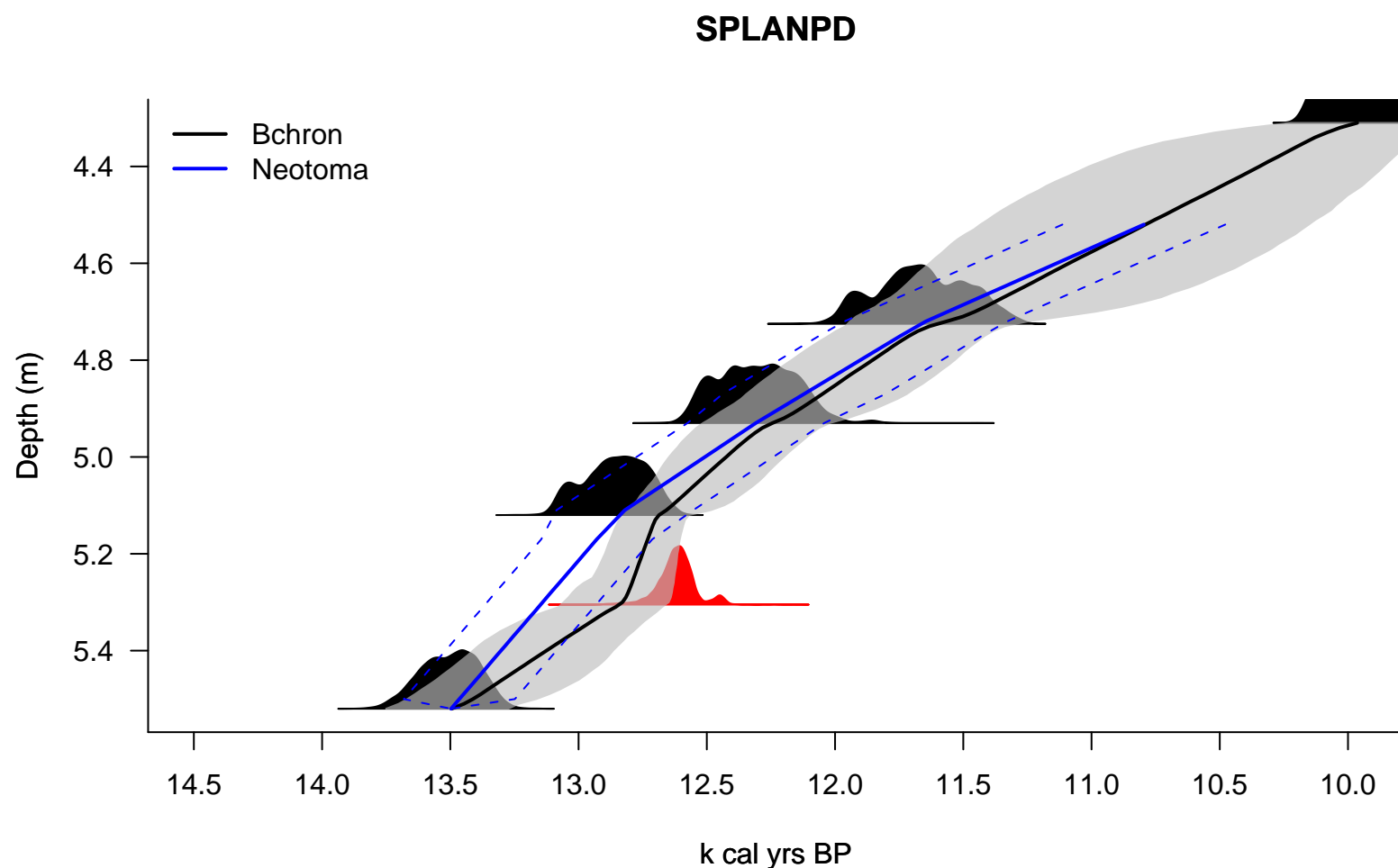


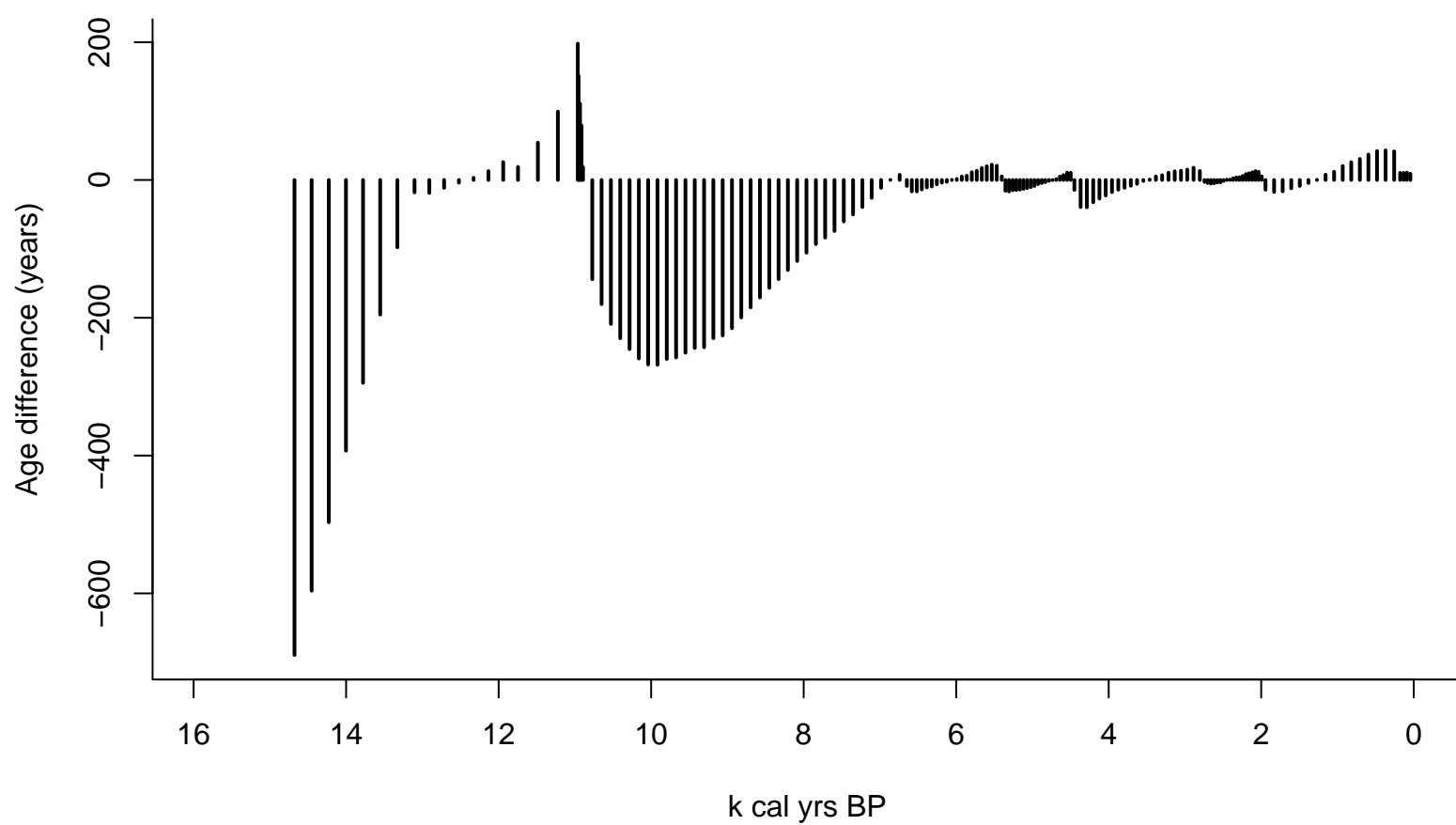
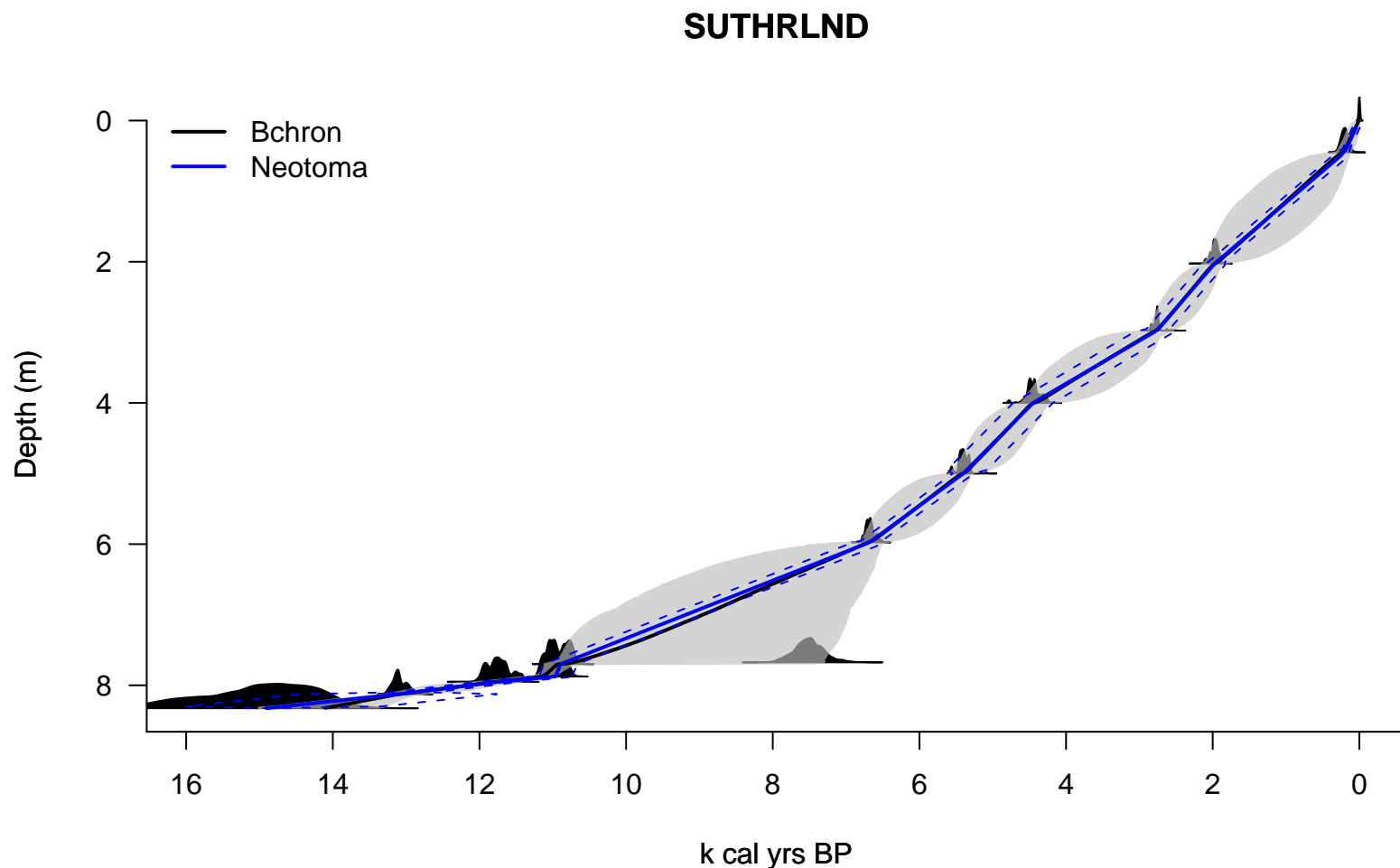


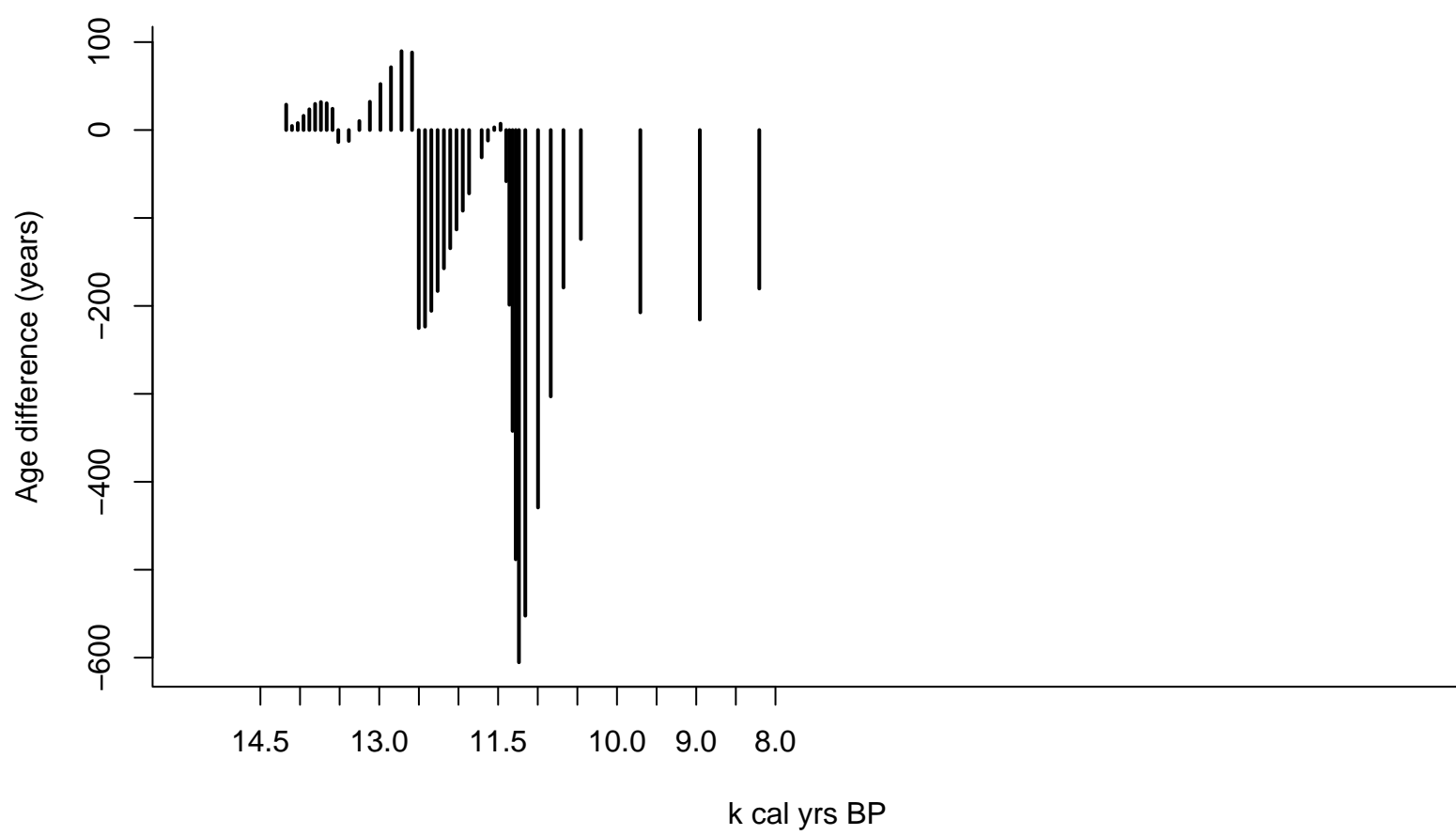
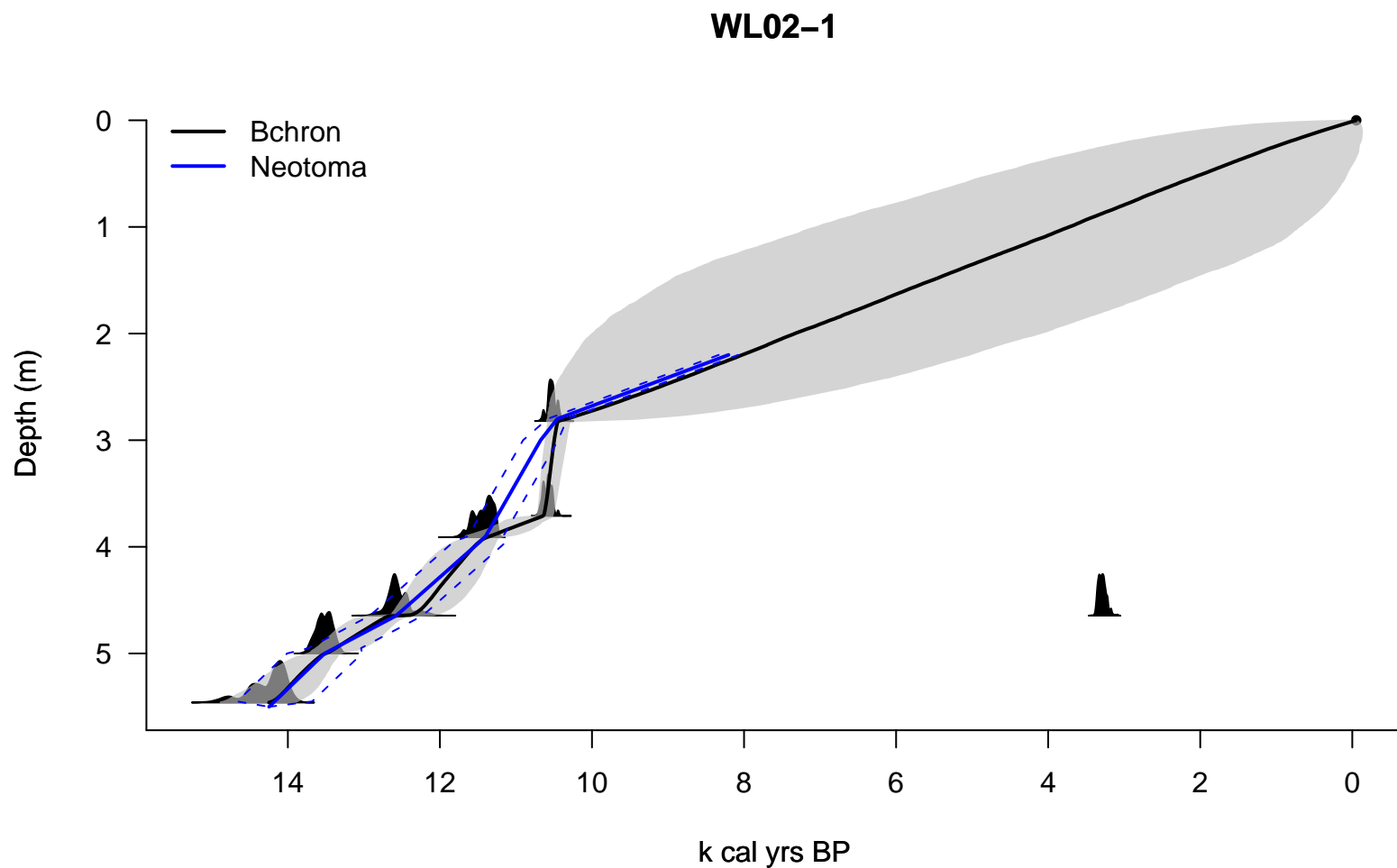
MUDPOND









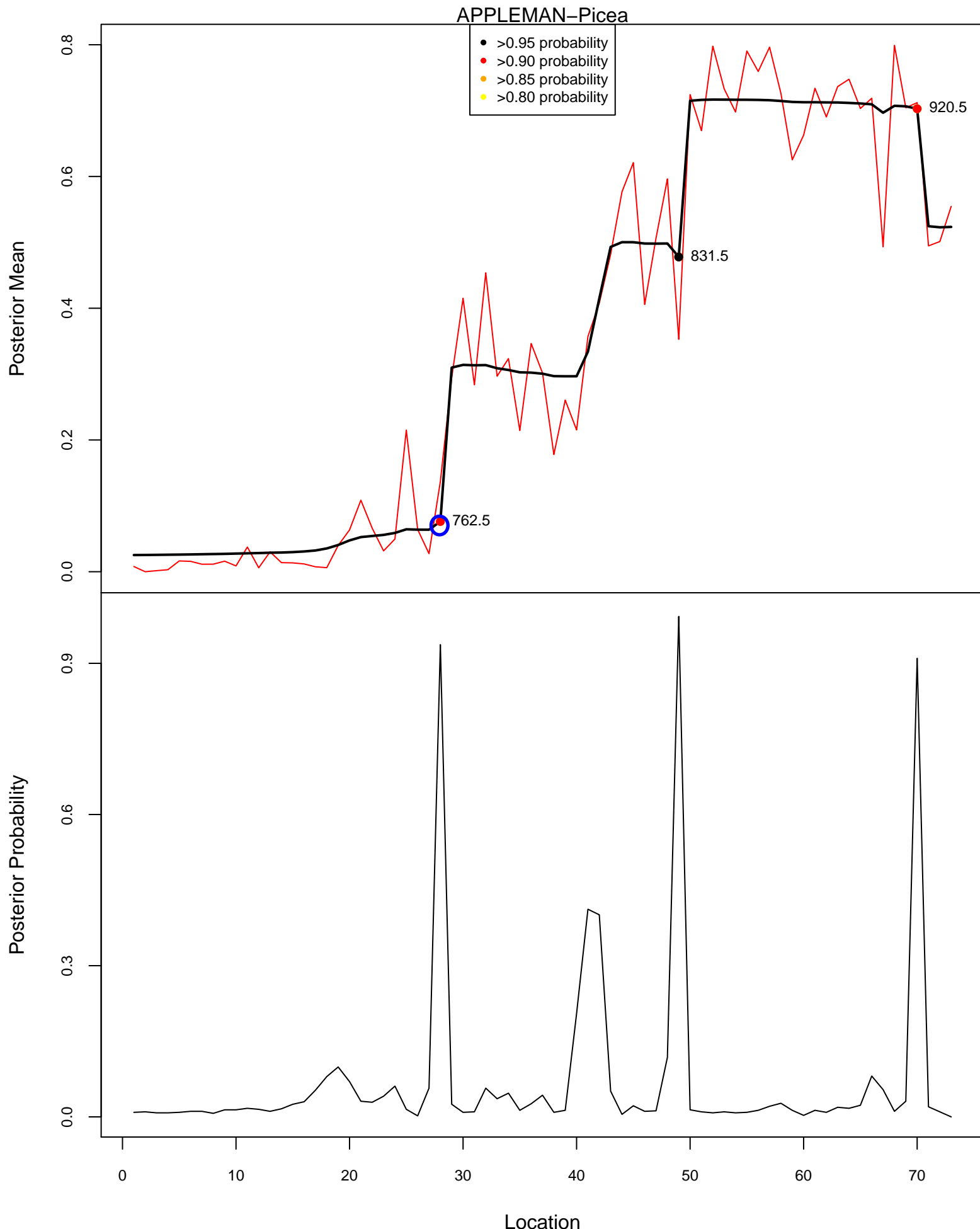


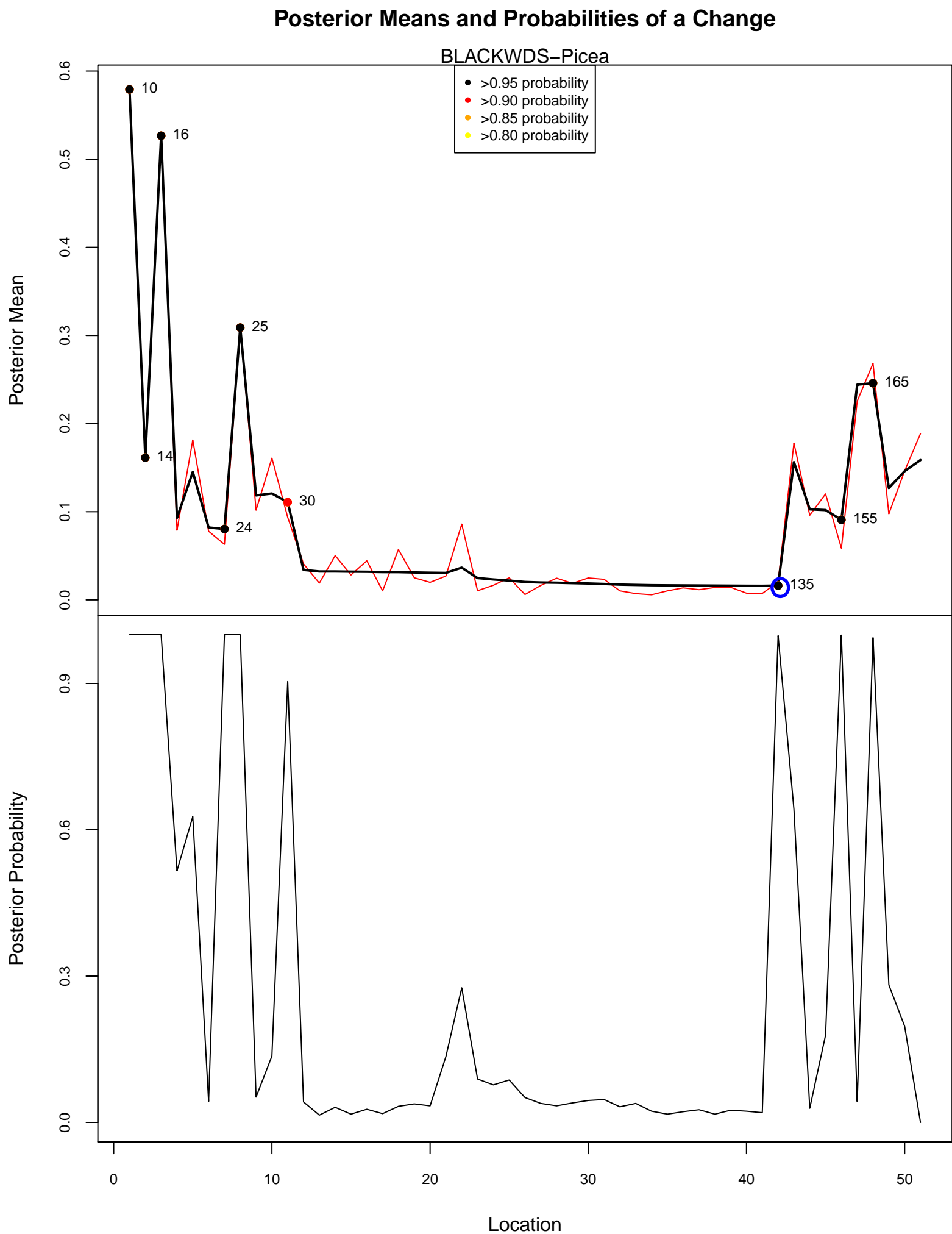
Supplementary Figure 3.

Change point plots for all benchmark sites for *Picea* decline, *Alnus* decline, and *Quercus* rise.

The upper graph shows the original relative abundance, as a proportion of the upland pollen sum (red line) and the posterior mean probability relative abundance (black line). Probable change points (based on BCP analysis) are indicated in filled circles and the change point that we identified as corresponding to each biostratigraphic event is circled. The number to the right of the change point is the sample depth. The bottom graph shows the posterior probability of a change point occurring at a particular sampling location along the core.

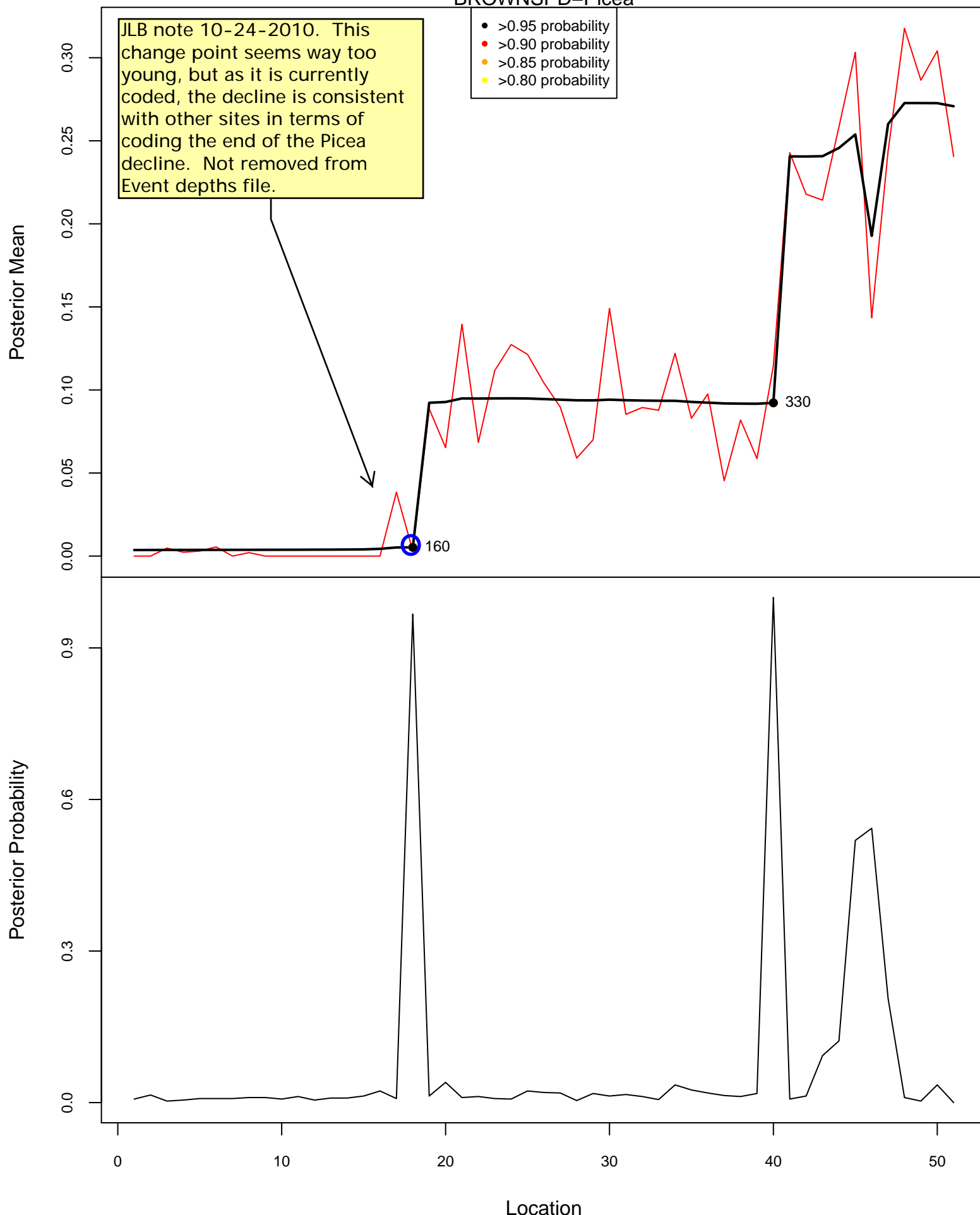
Posterior Means and Probabilities of a Change



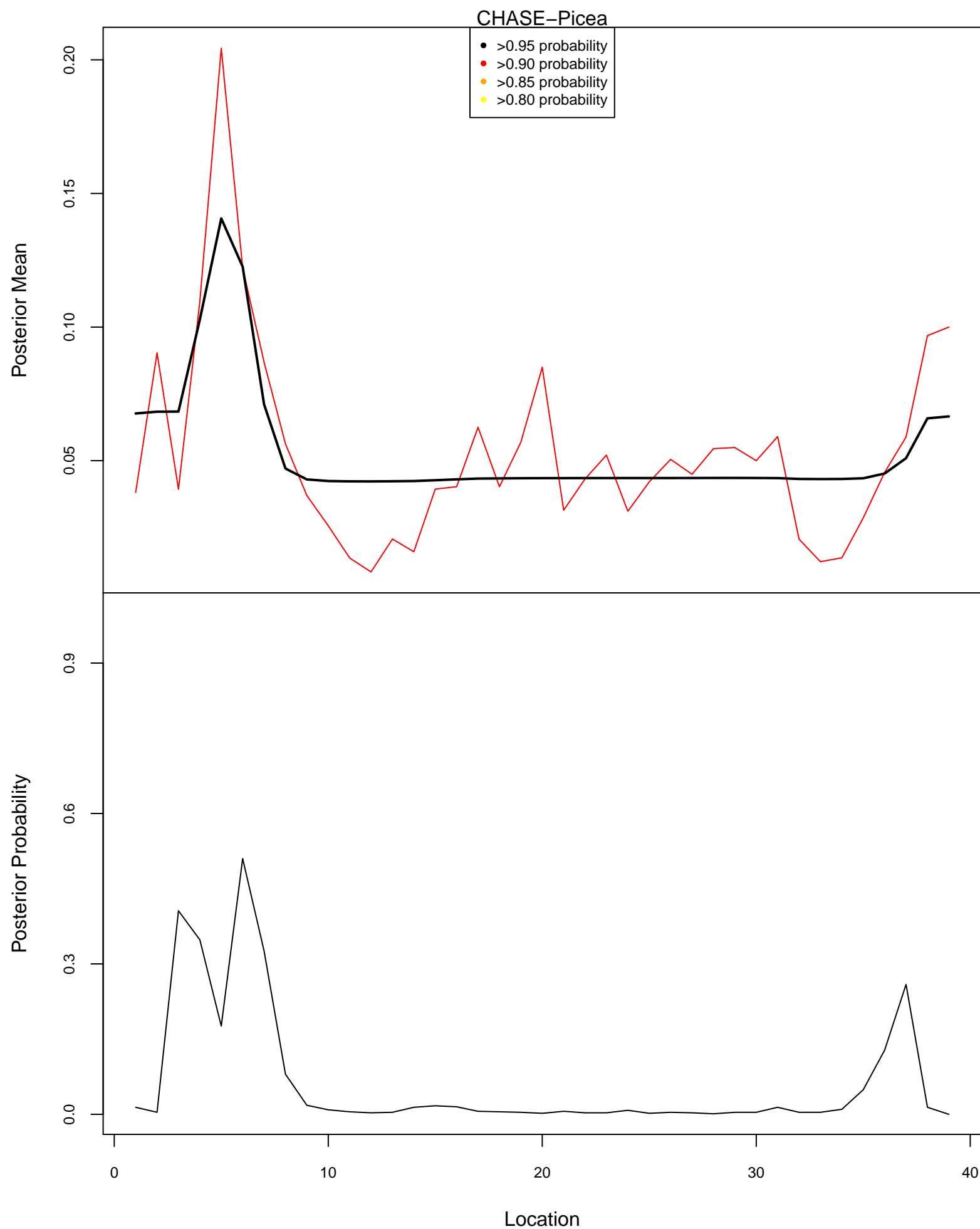


Posterior Means and Probabilities of a Change

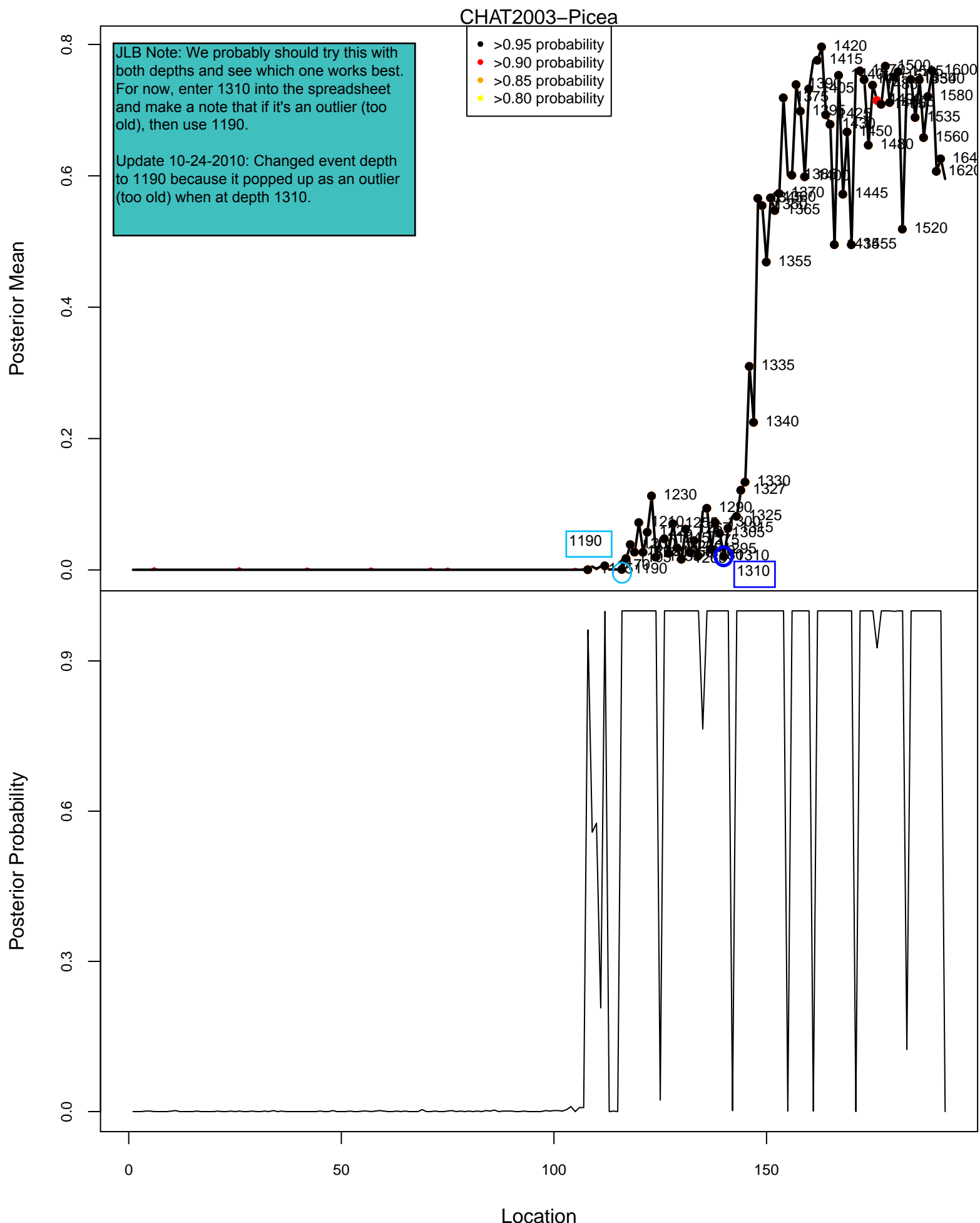
BROWNSPD–Picea



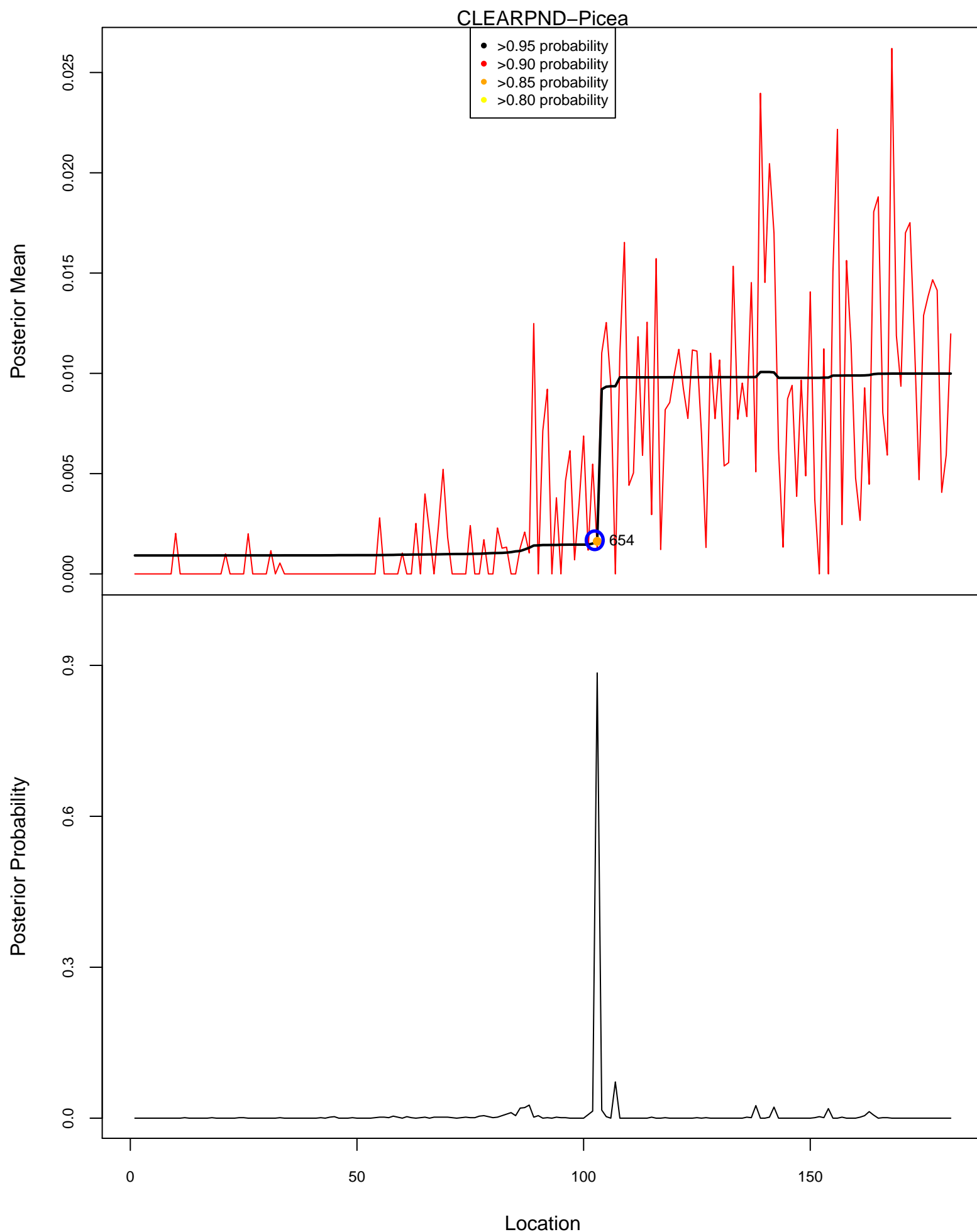
Posterior Means and Probabilities of a Change



Posterior Means and Probabilities of a Change

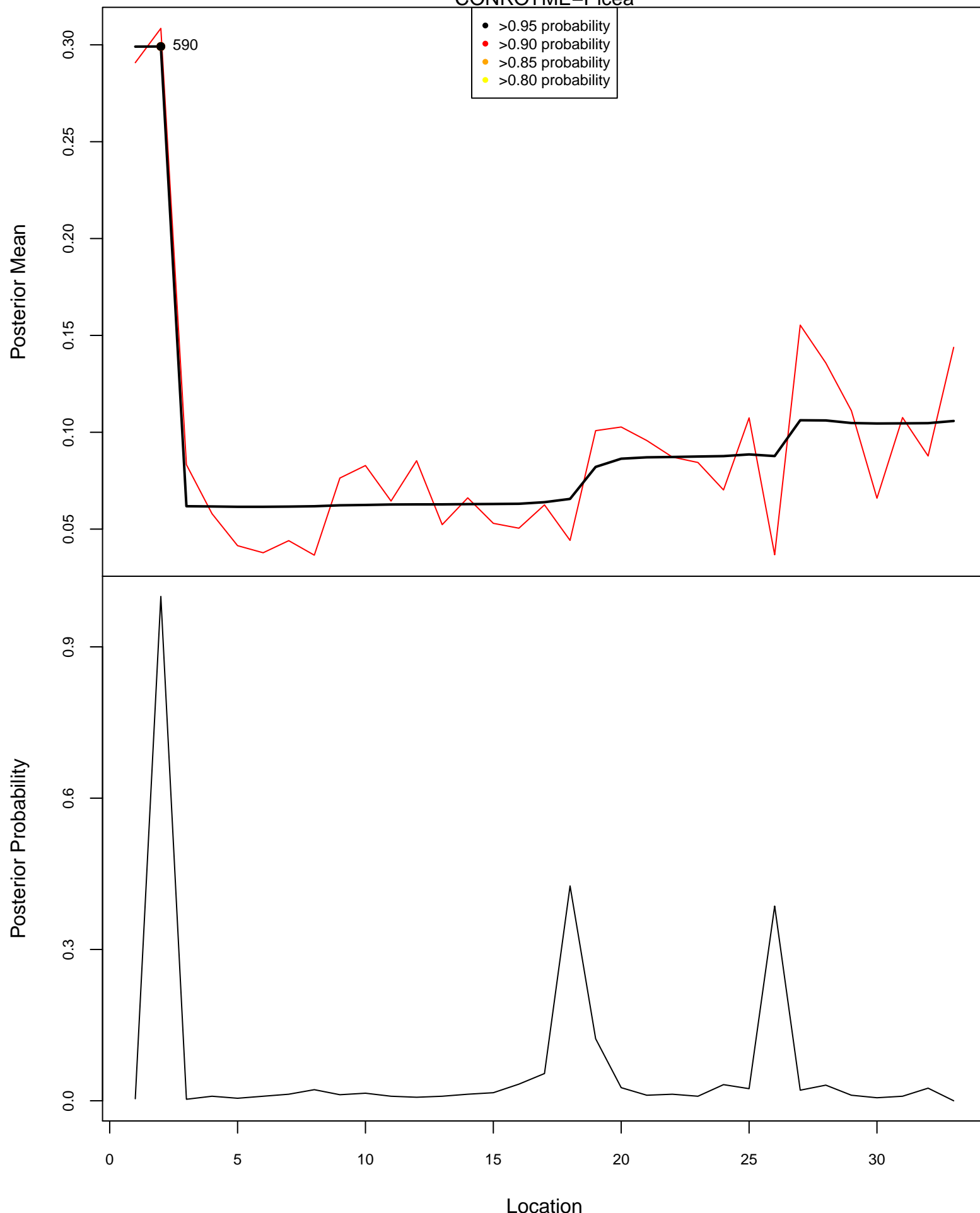


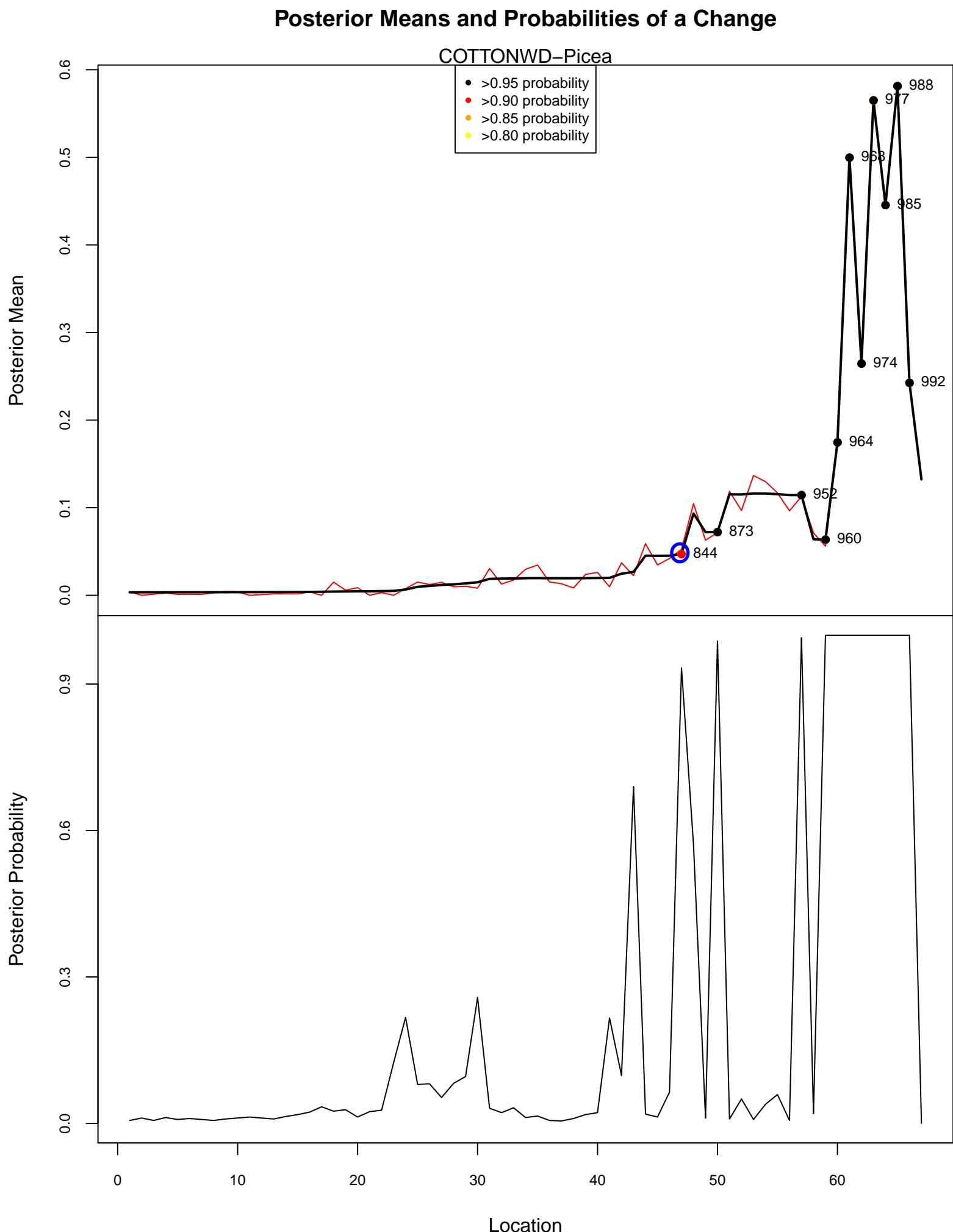
Posterior Means and Probabilities of a Change



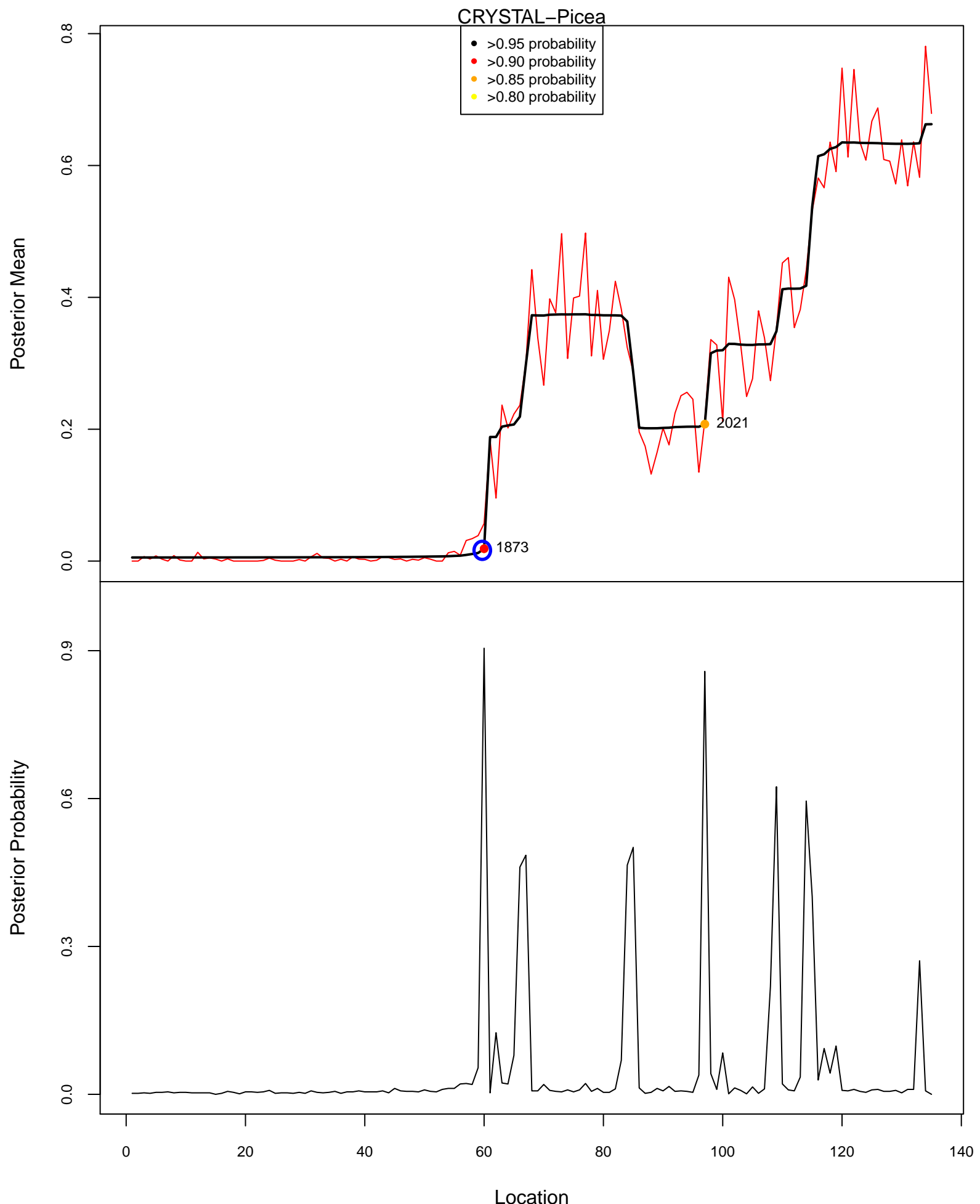
Posterior Means and Probabilities of a Change

CONROYME–Picea

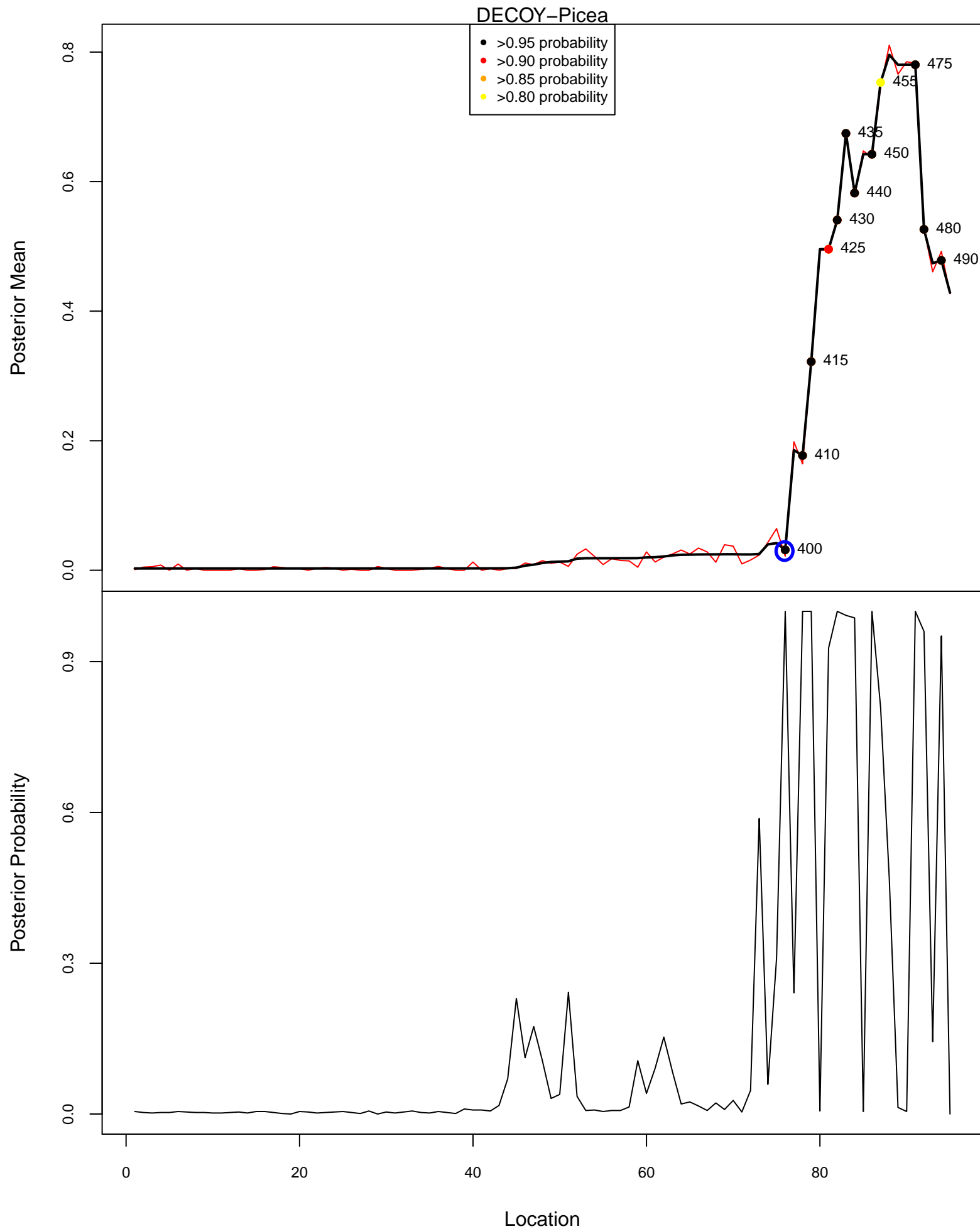


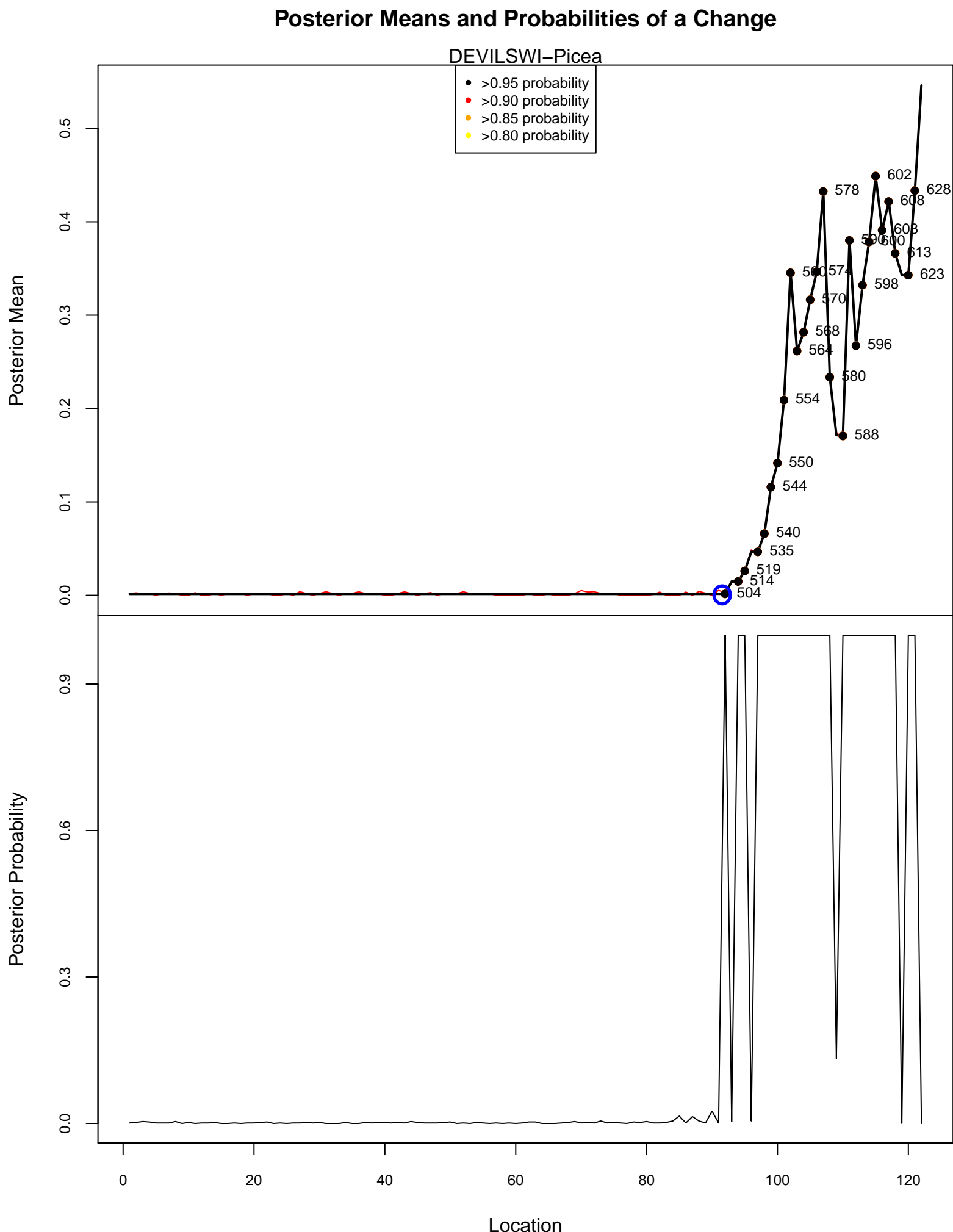


Posterior Means and Probabilities of a Change

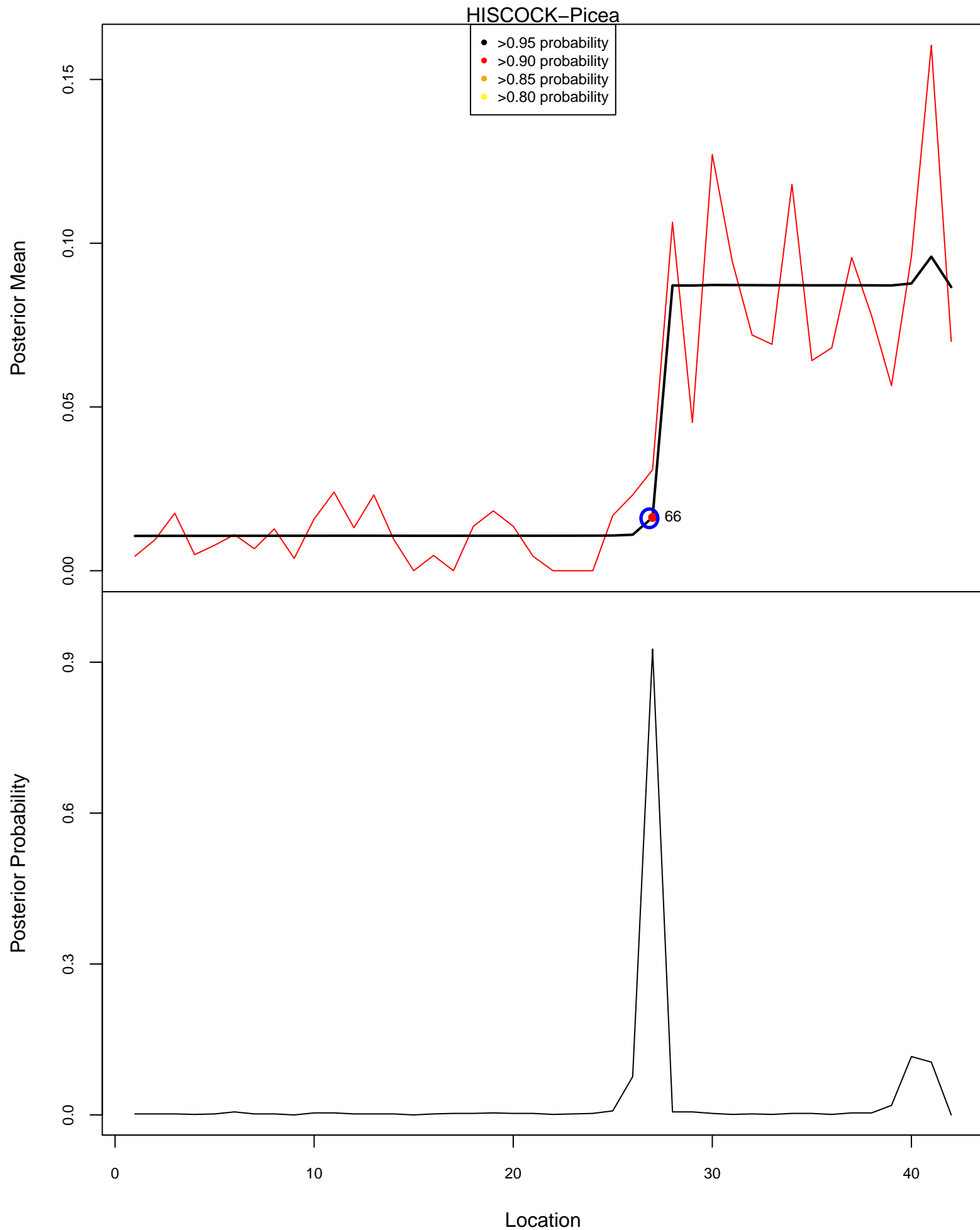


Posterior Means and Probabilities of a Change

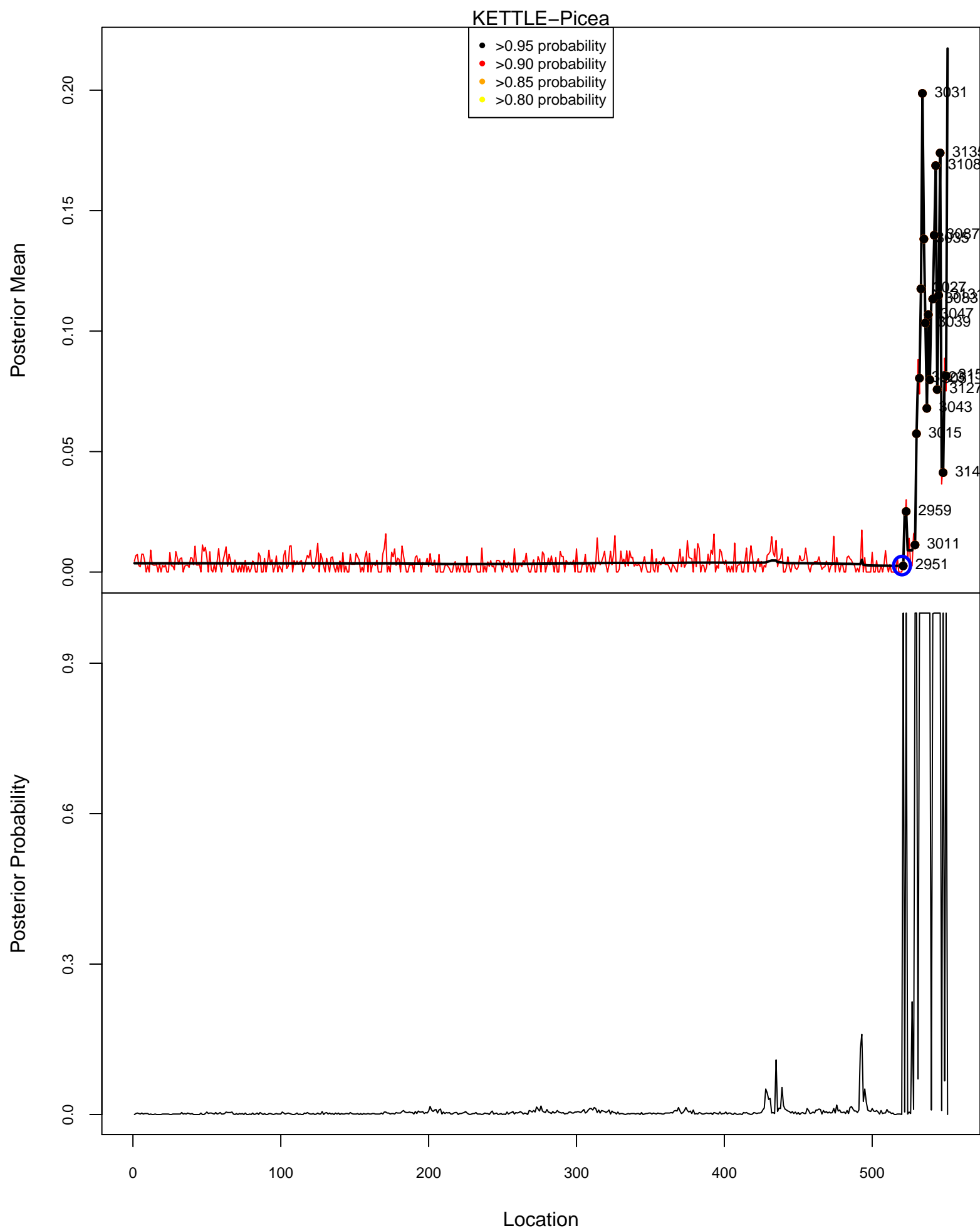




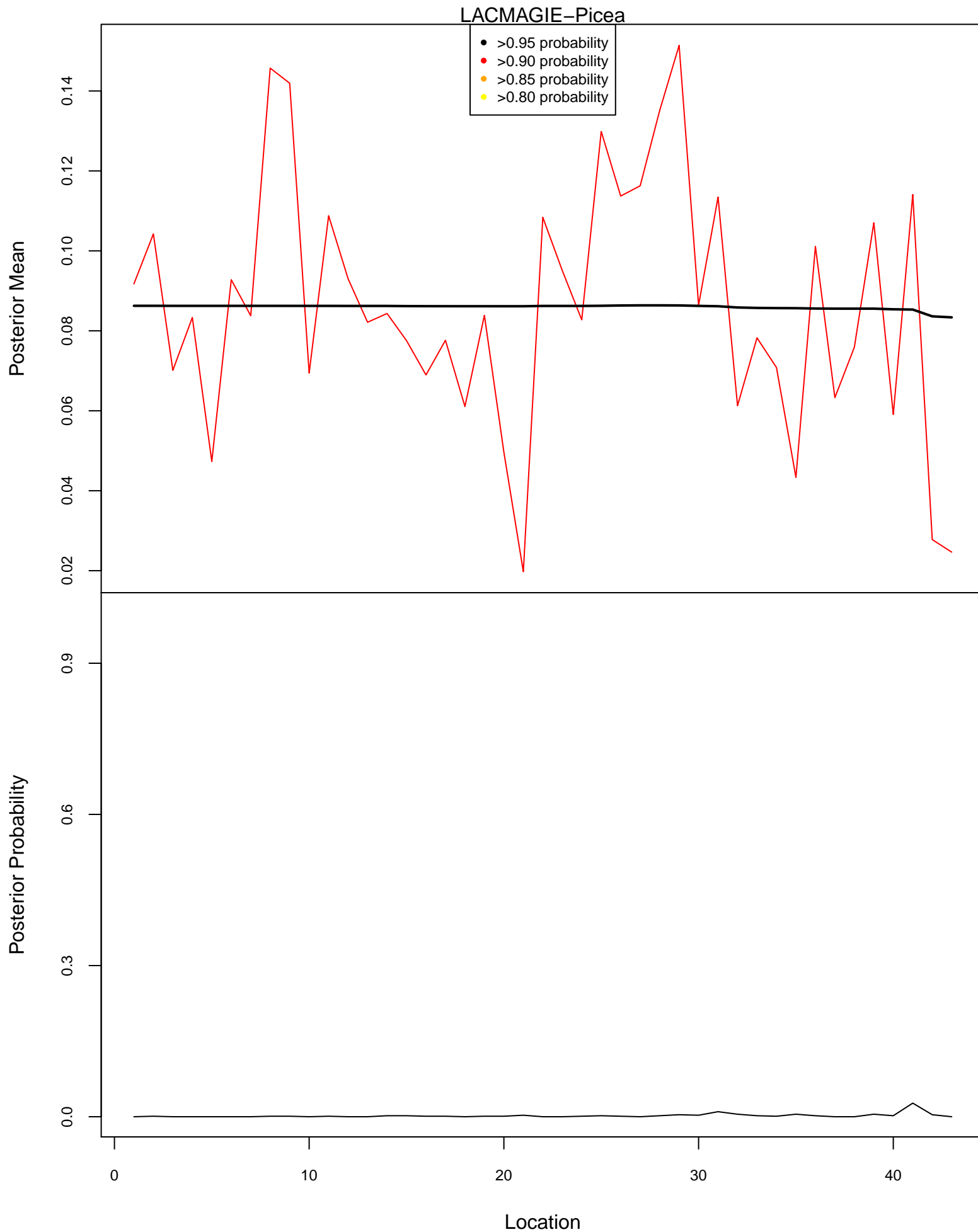
Posterior Means and Probabilities of a Change



Posterior Means and Probabilities of a Change

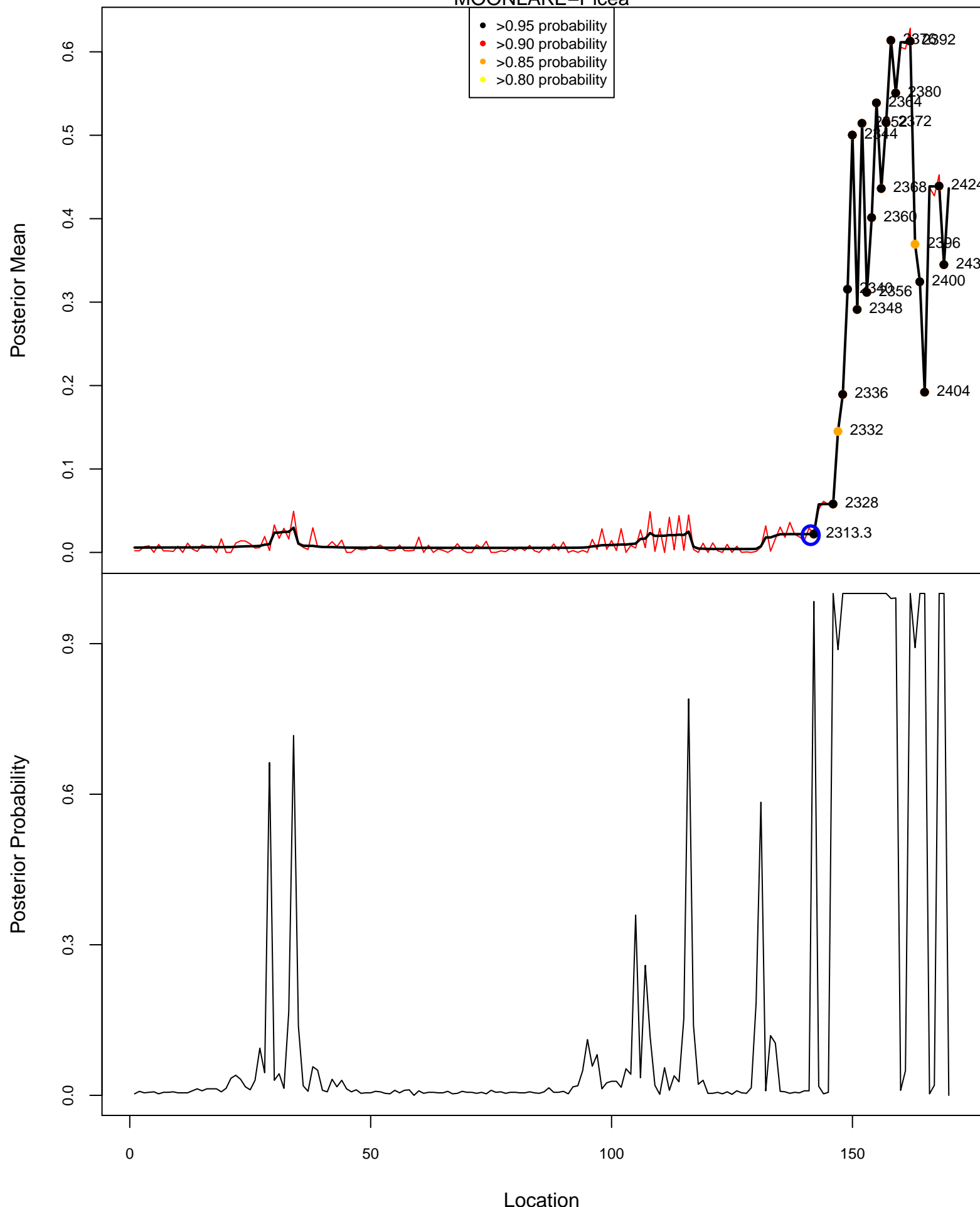


Posterior Means and Probabilities of a Change



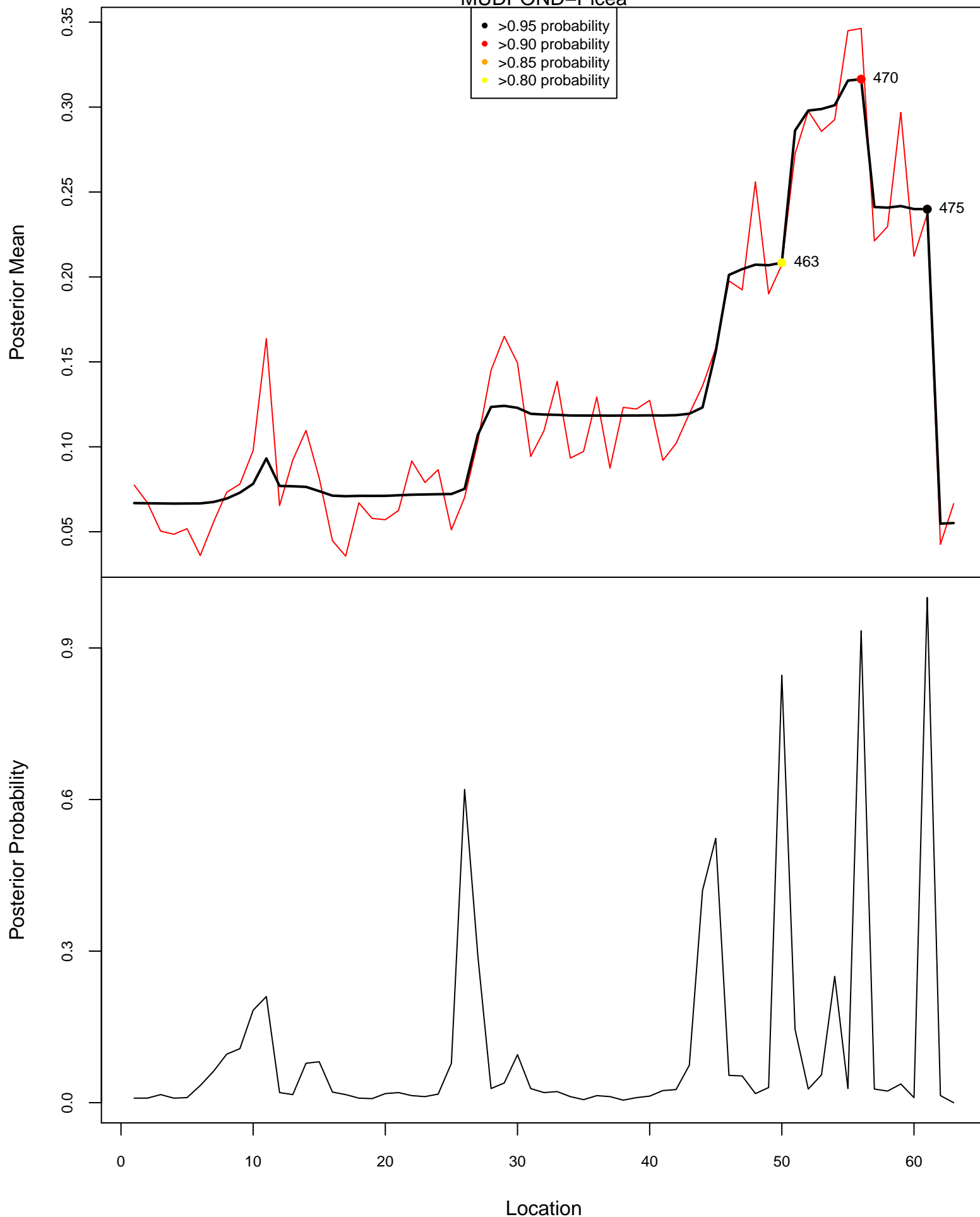
Posterior Means and Probabilities of a Change

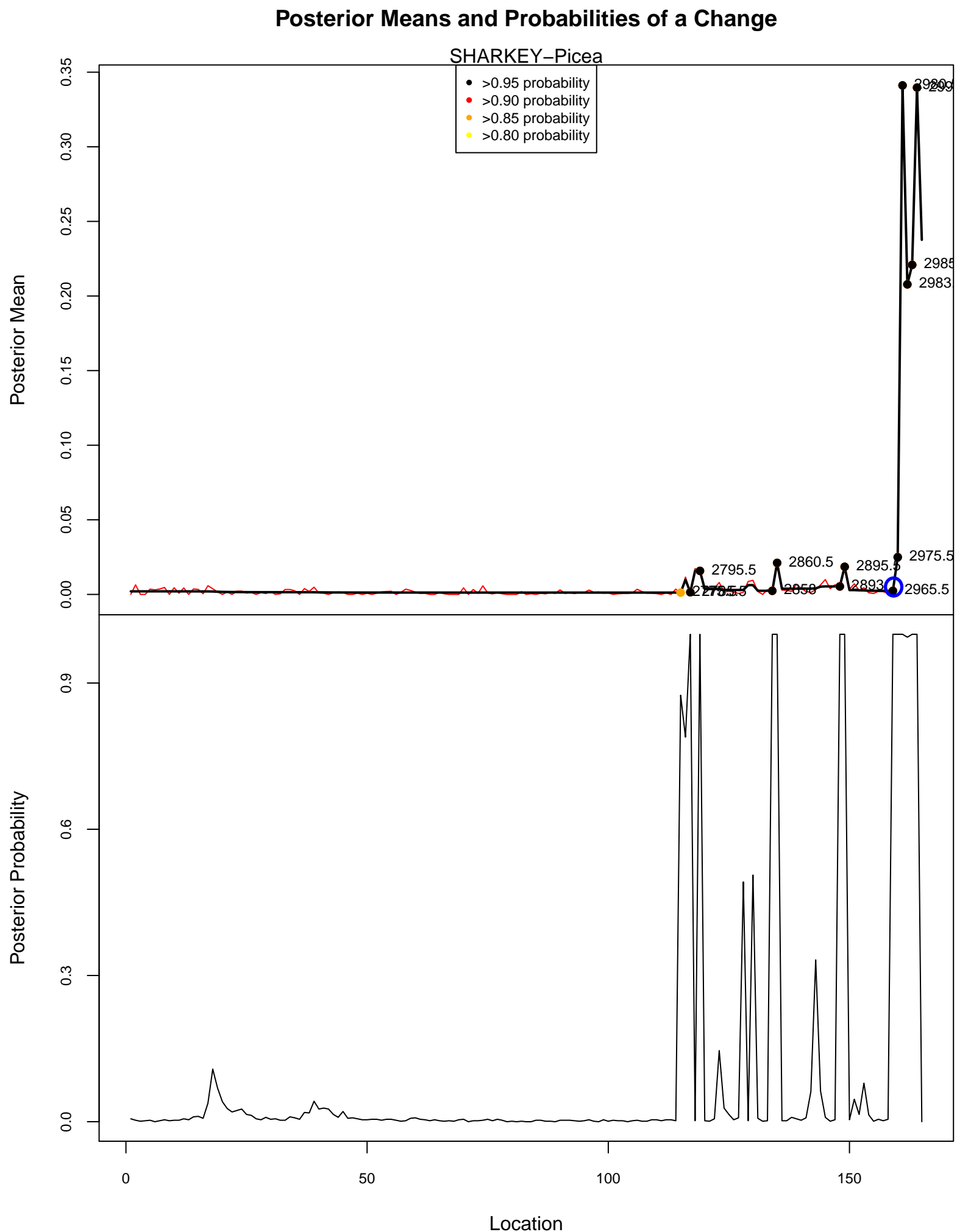
MOONLAKE–Picea

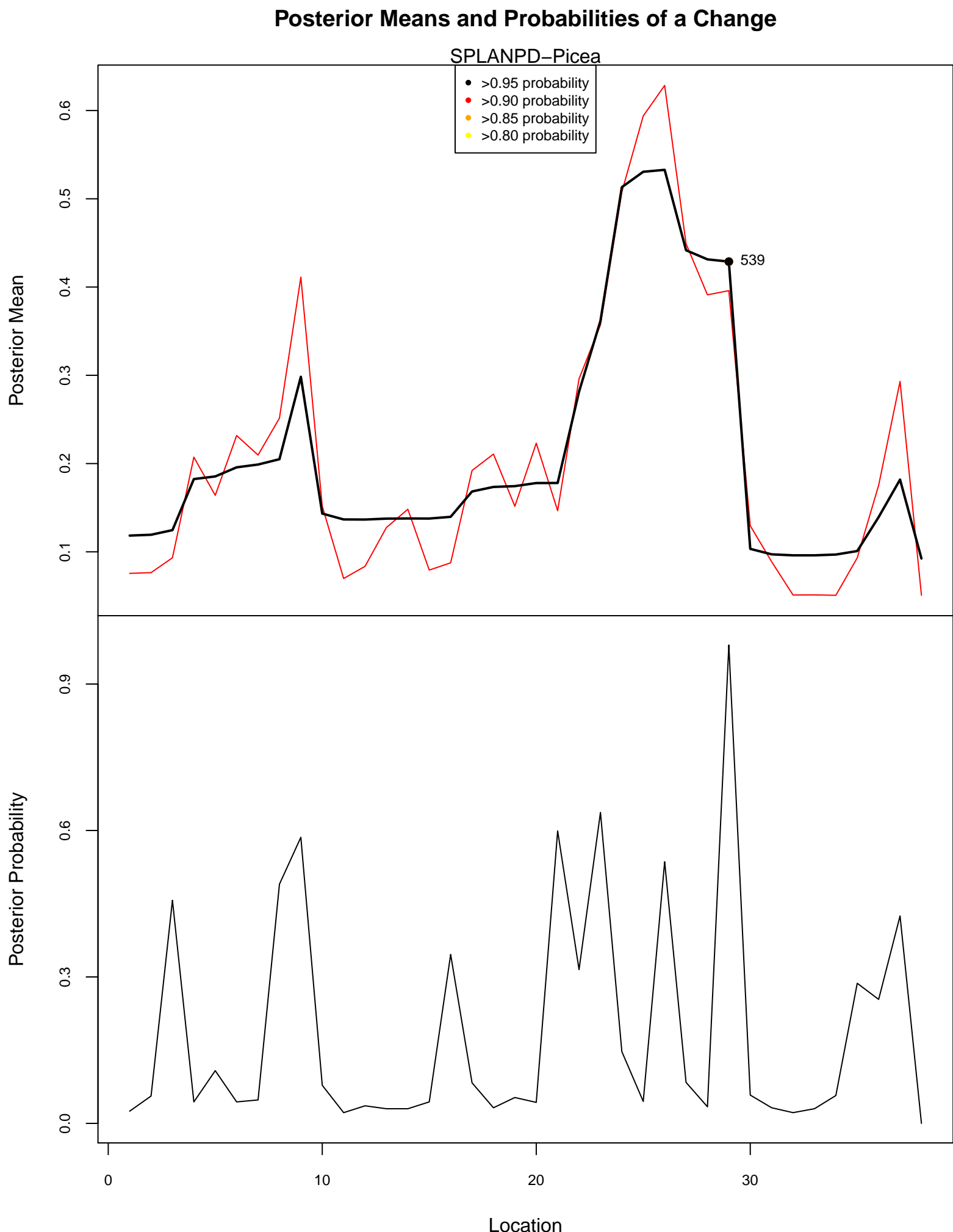


Posterior Means and Probabilities of a Change

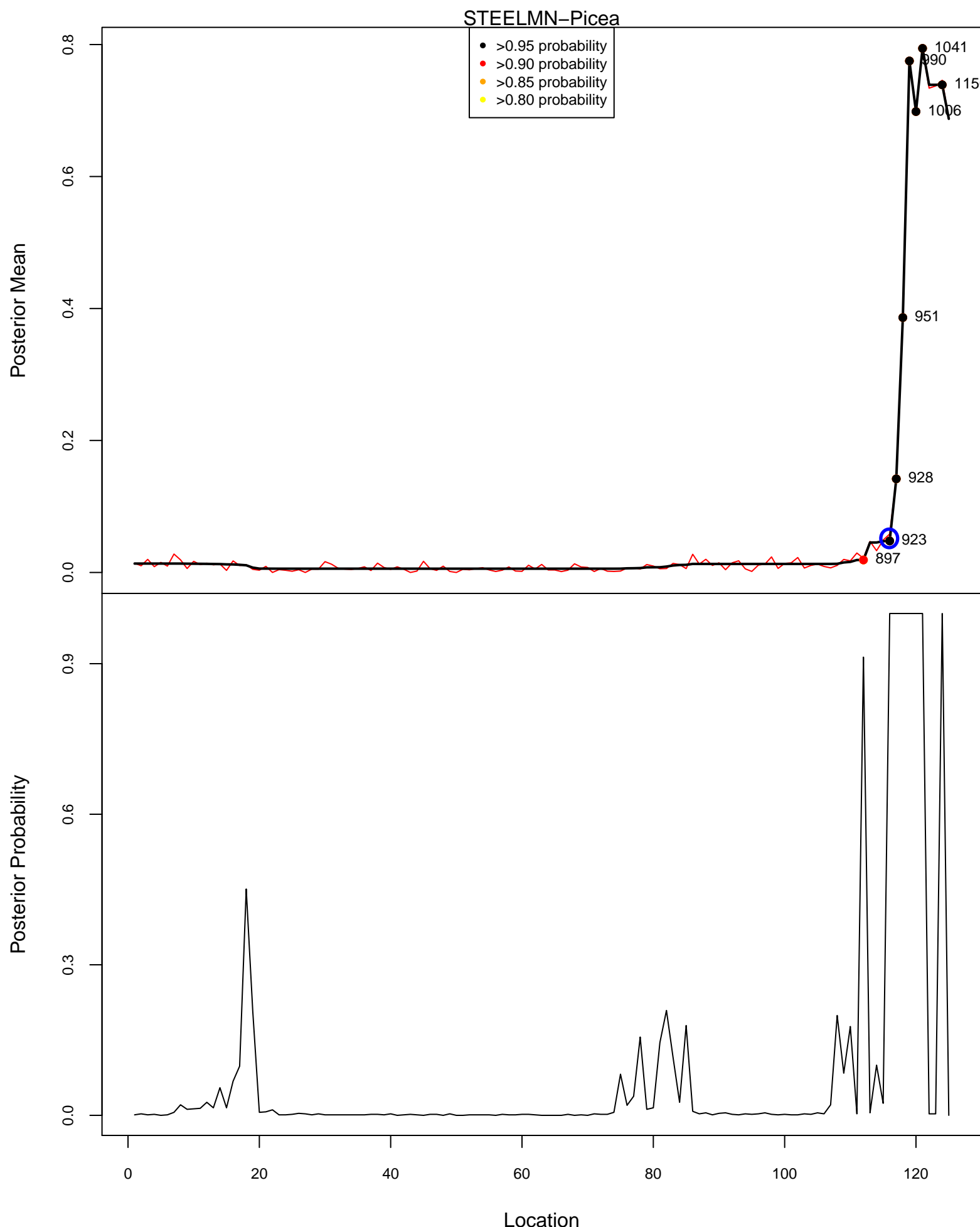
MUDPOND–Picea



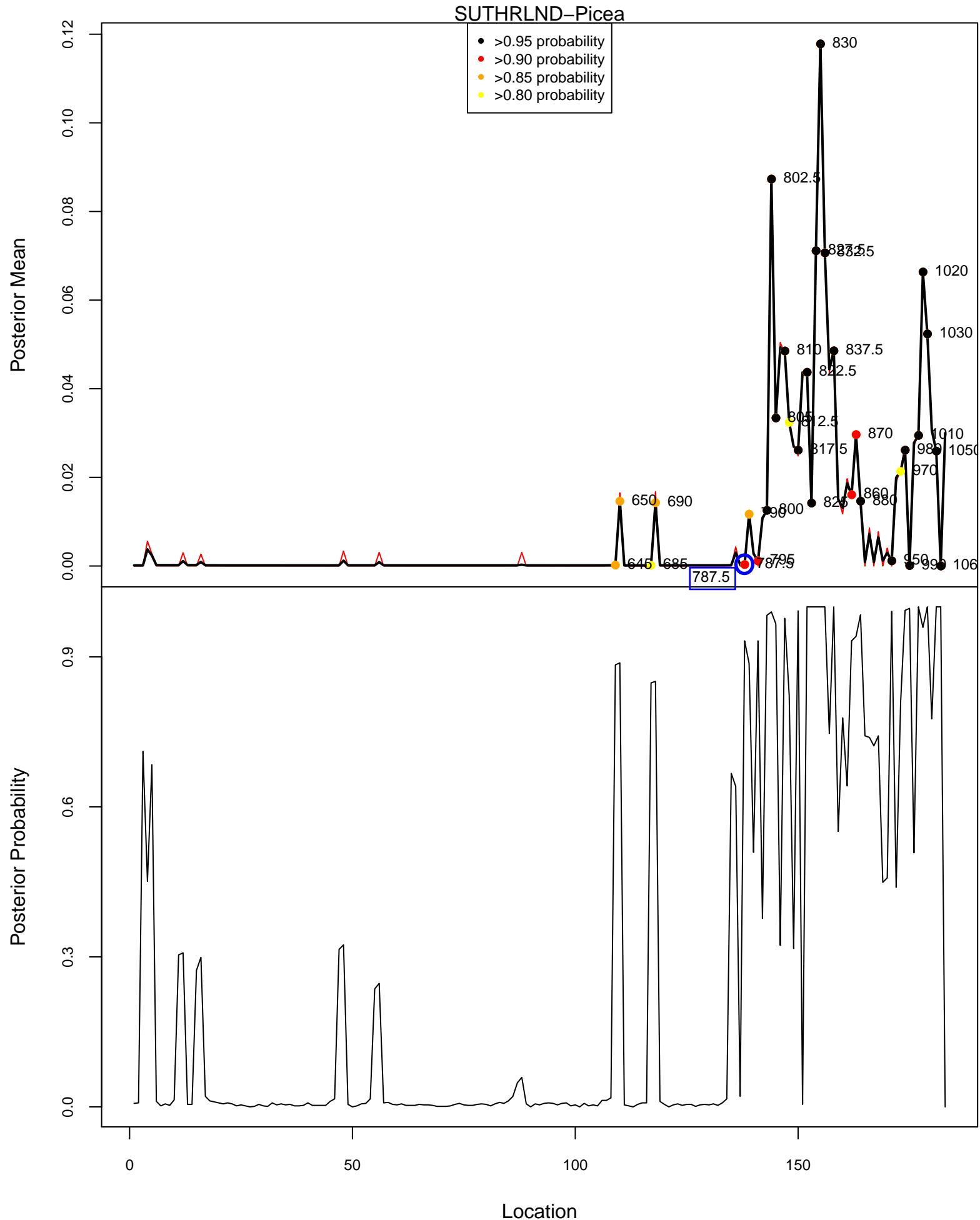




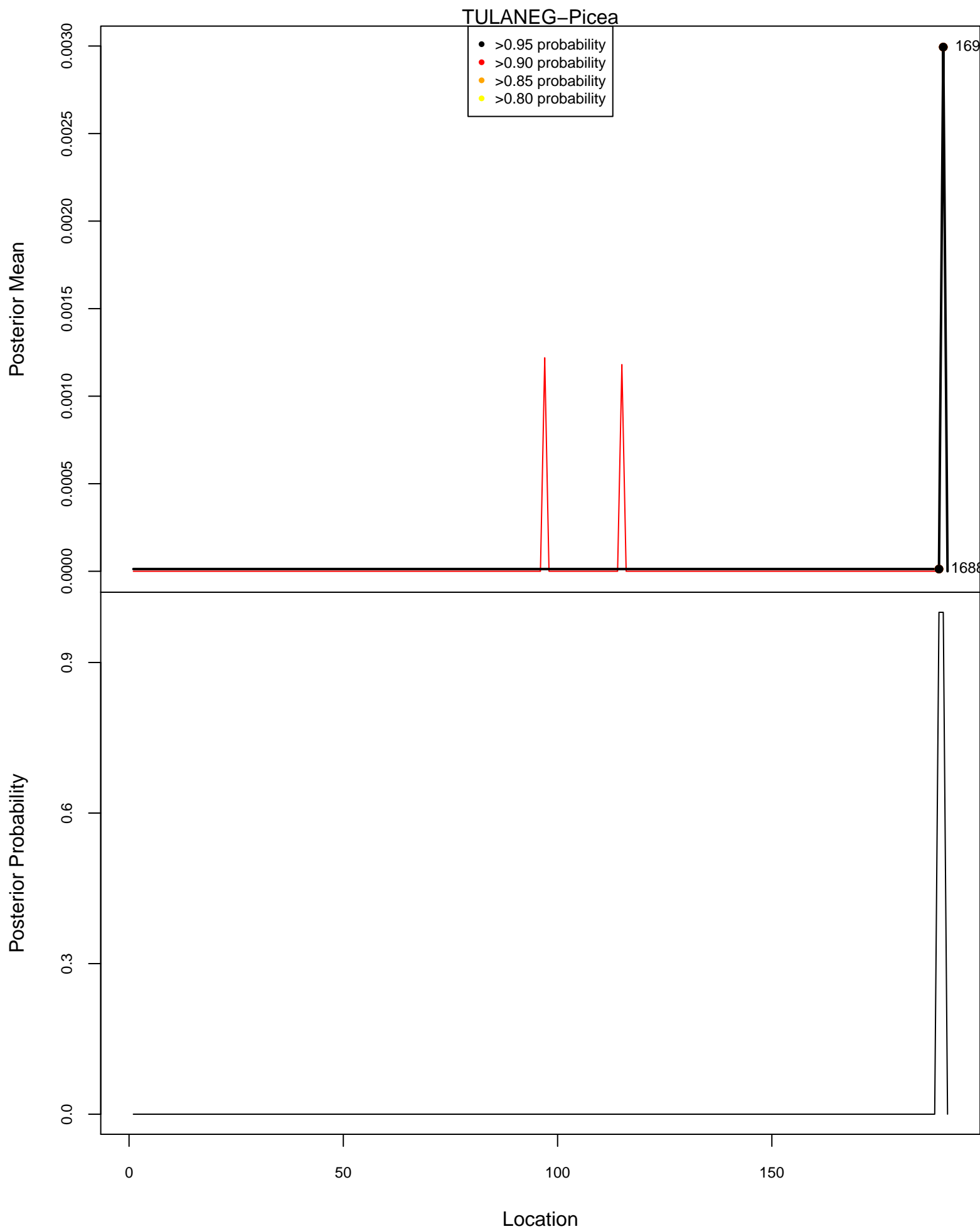
Posterior Means and Probabilities of a Change



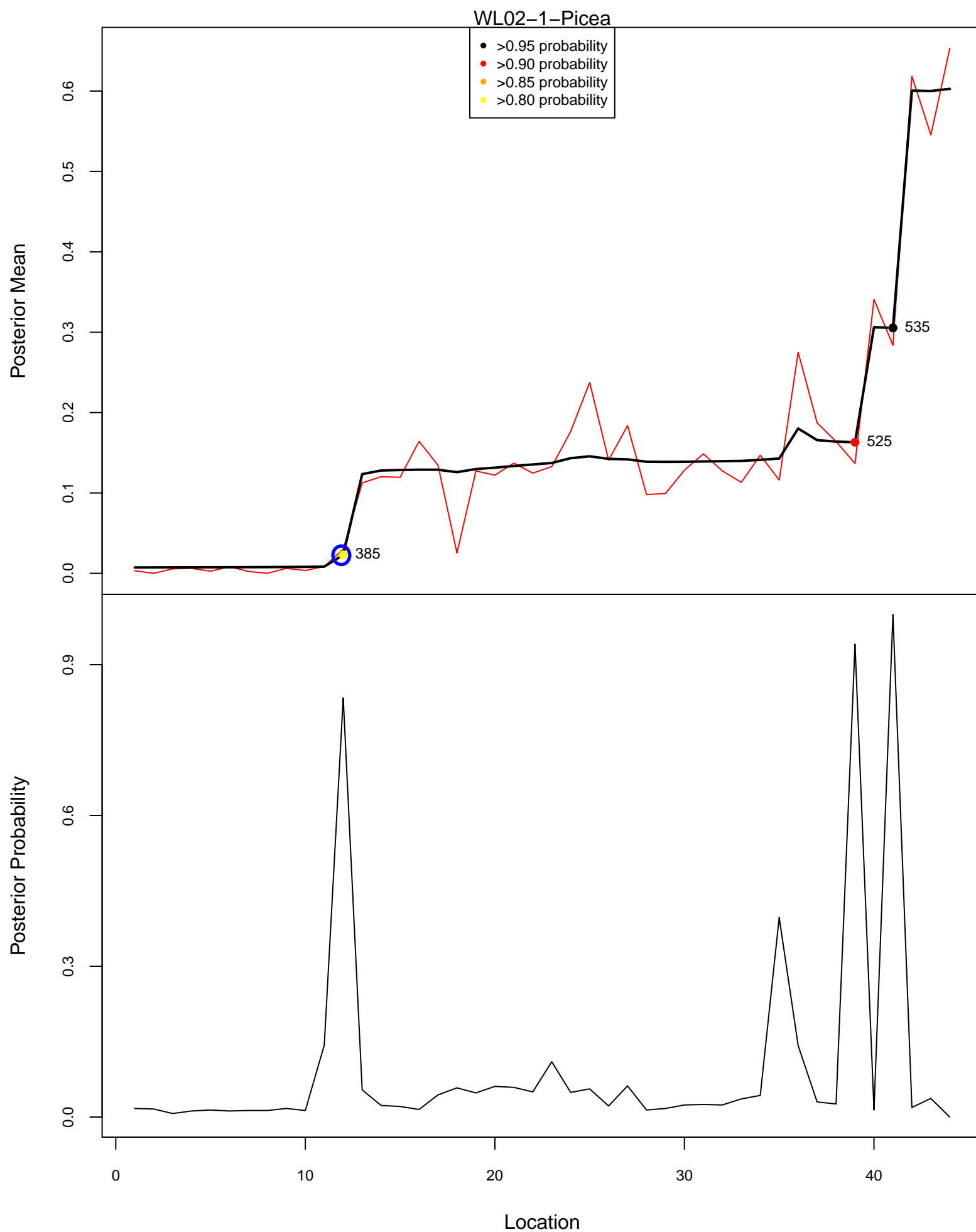
Posterior Means and Probabilities of a Change



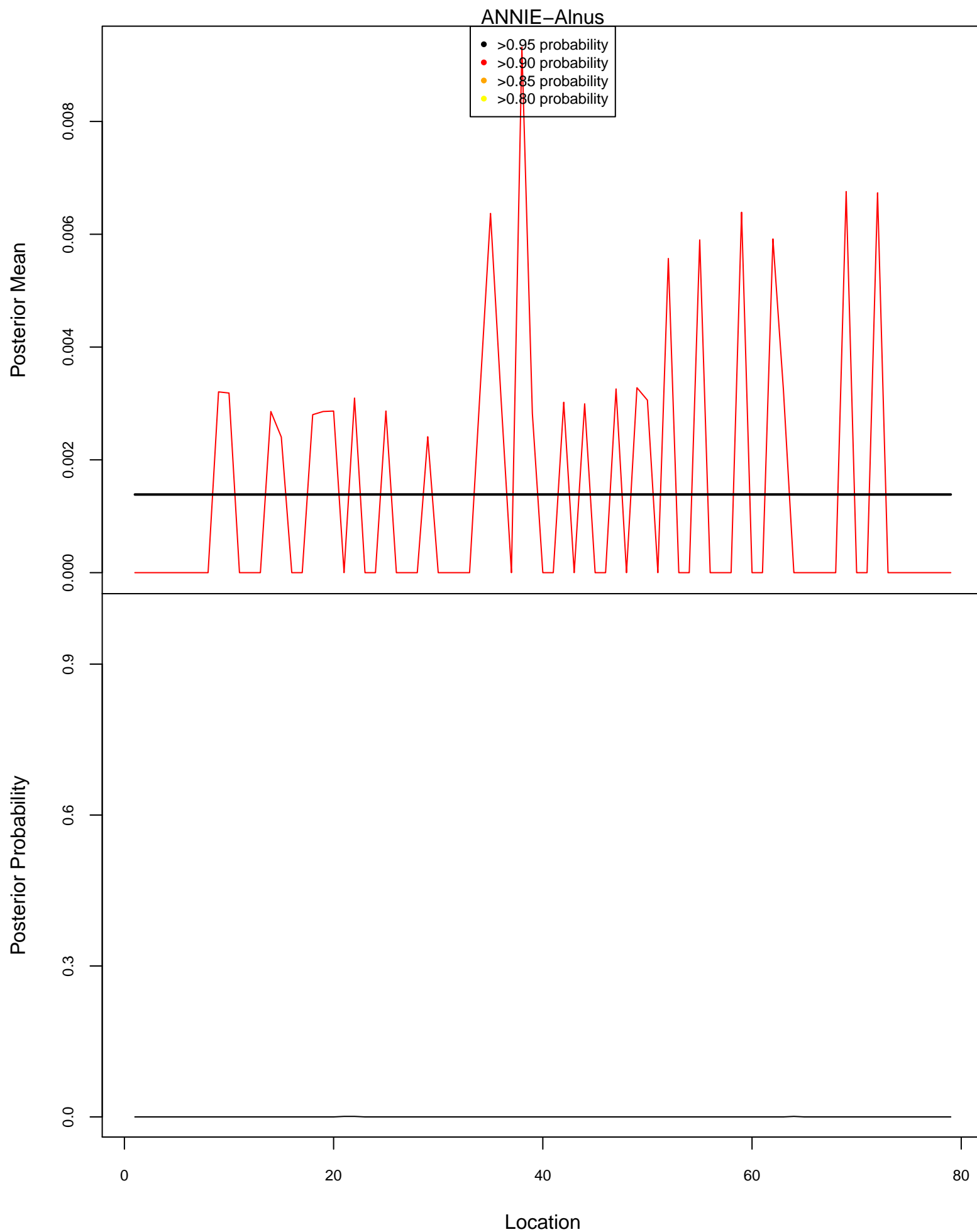
Posterior Means and Probabilities of a Change



Posterior Means and Probabilities of a Change

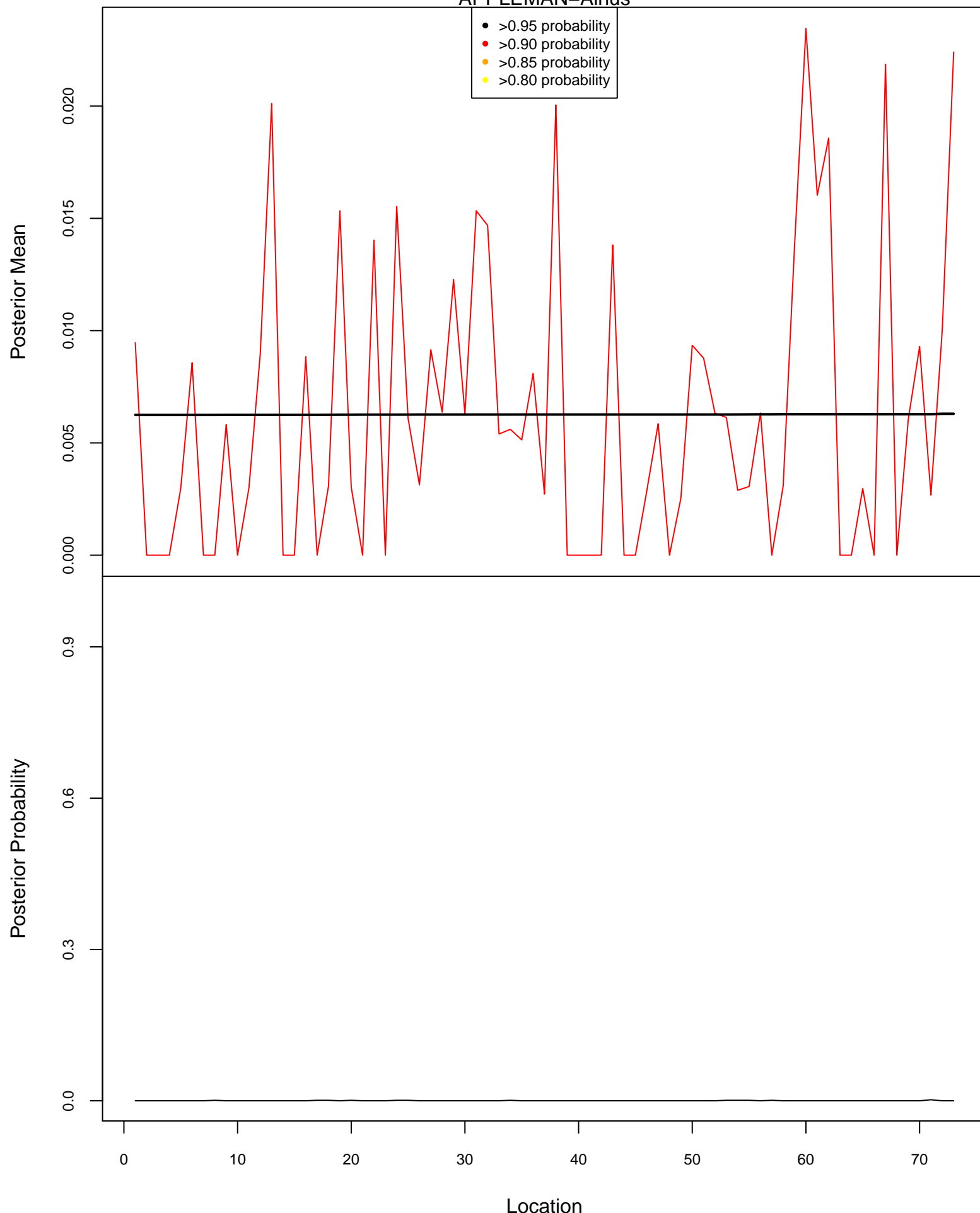


Posterior Means and Probabilities of a Change

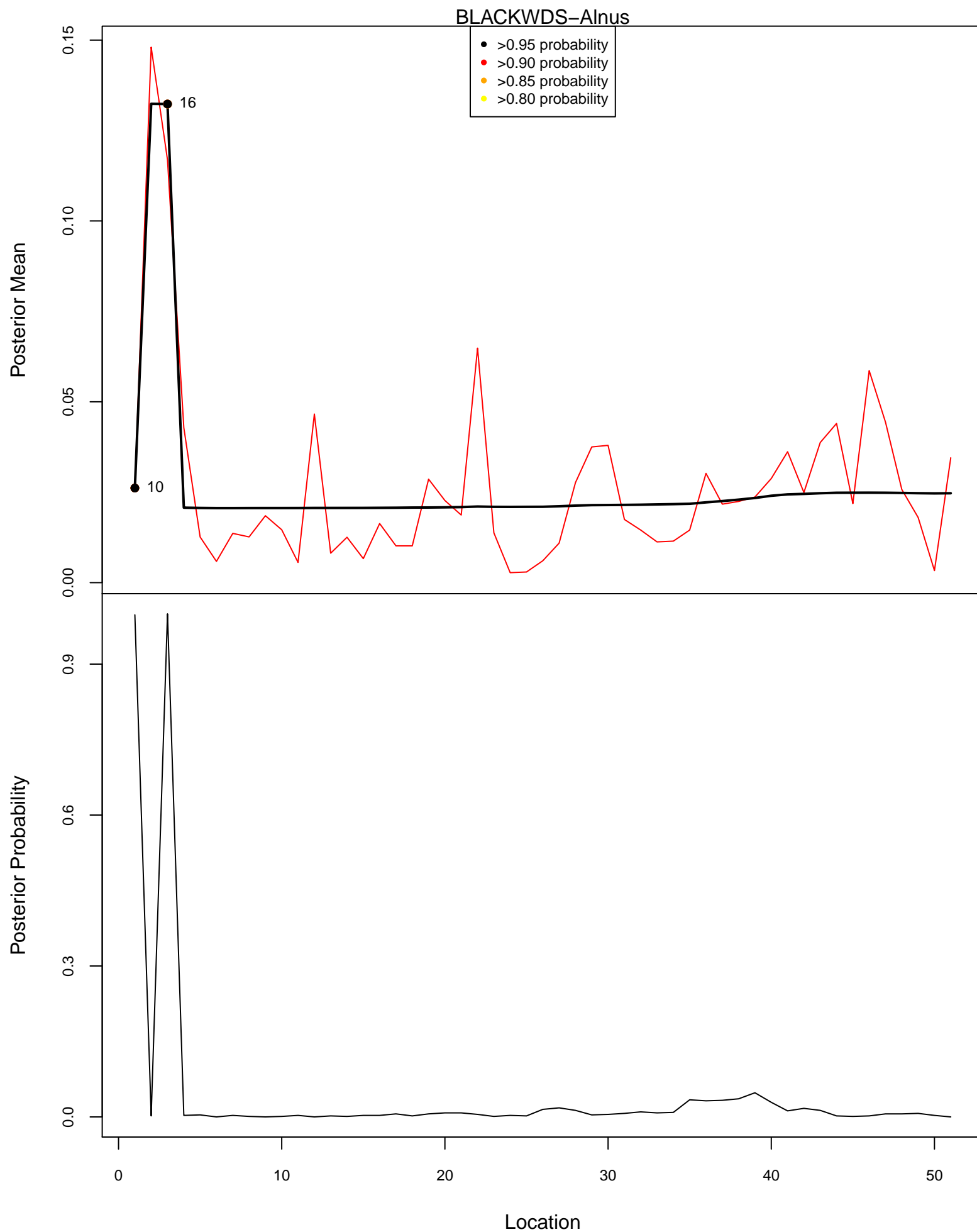


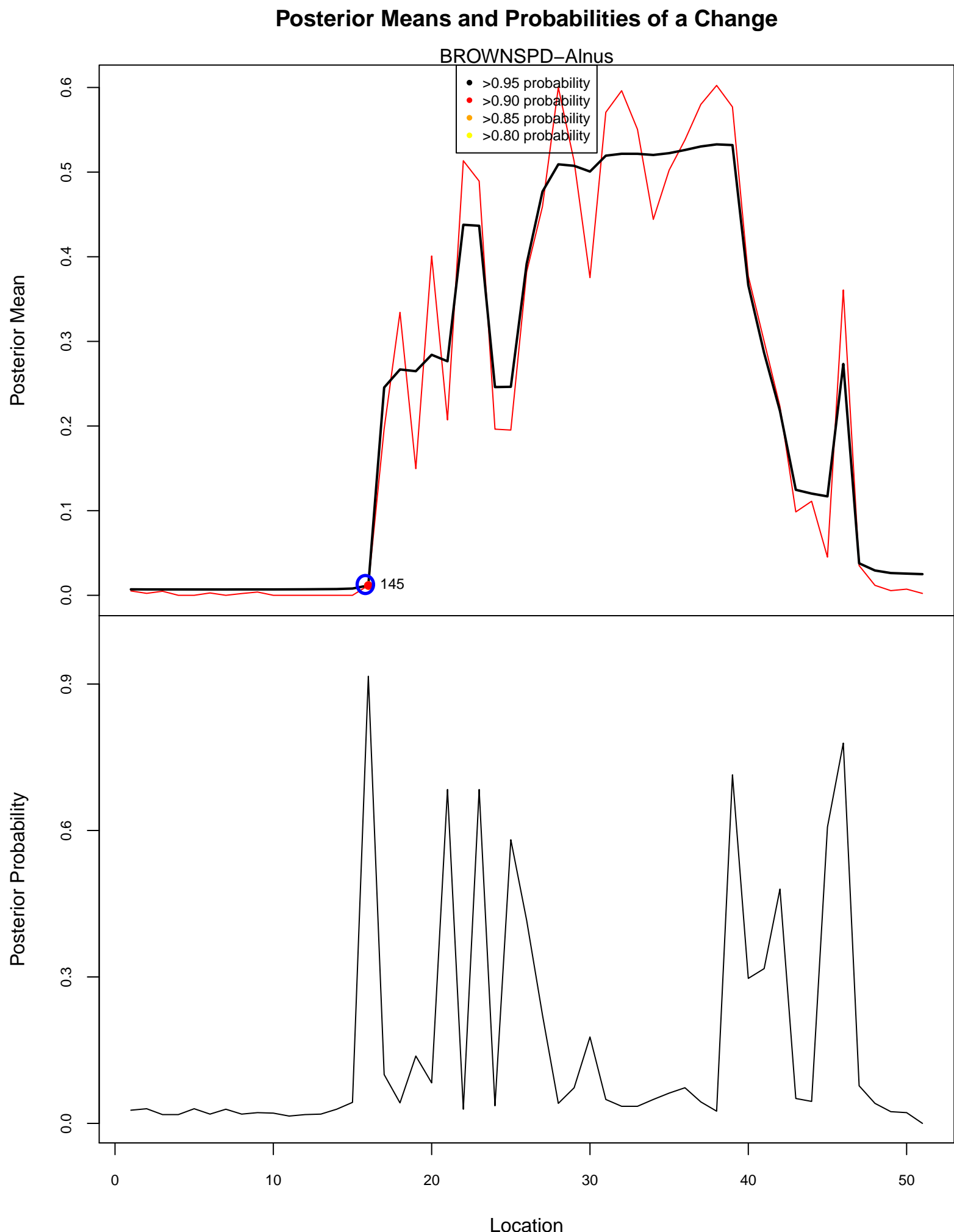
Posterior Means and Probabilities of a Change

APPLEMAN–*Alnus*

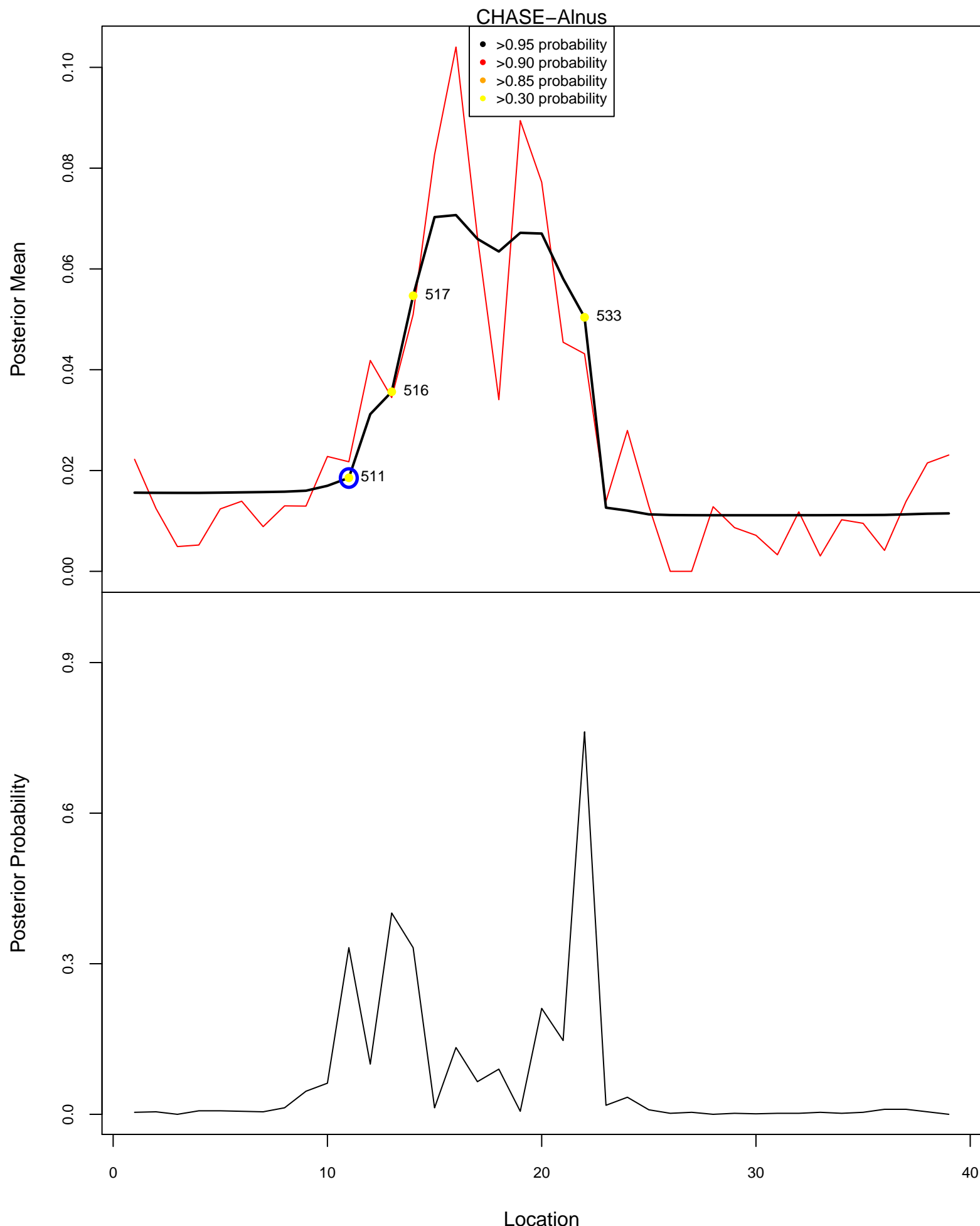


Posterior Means and Probabilities of a Change

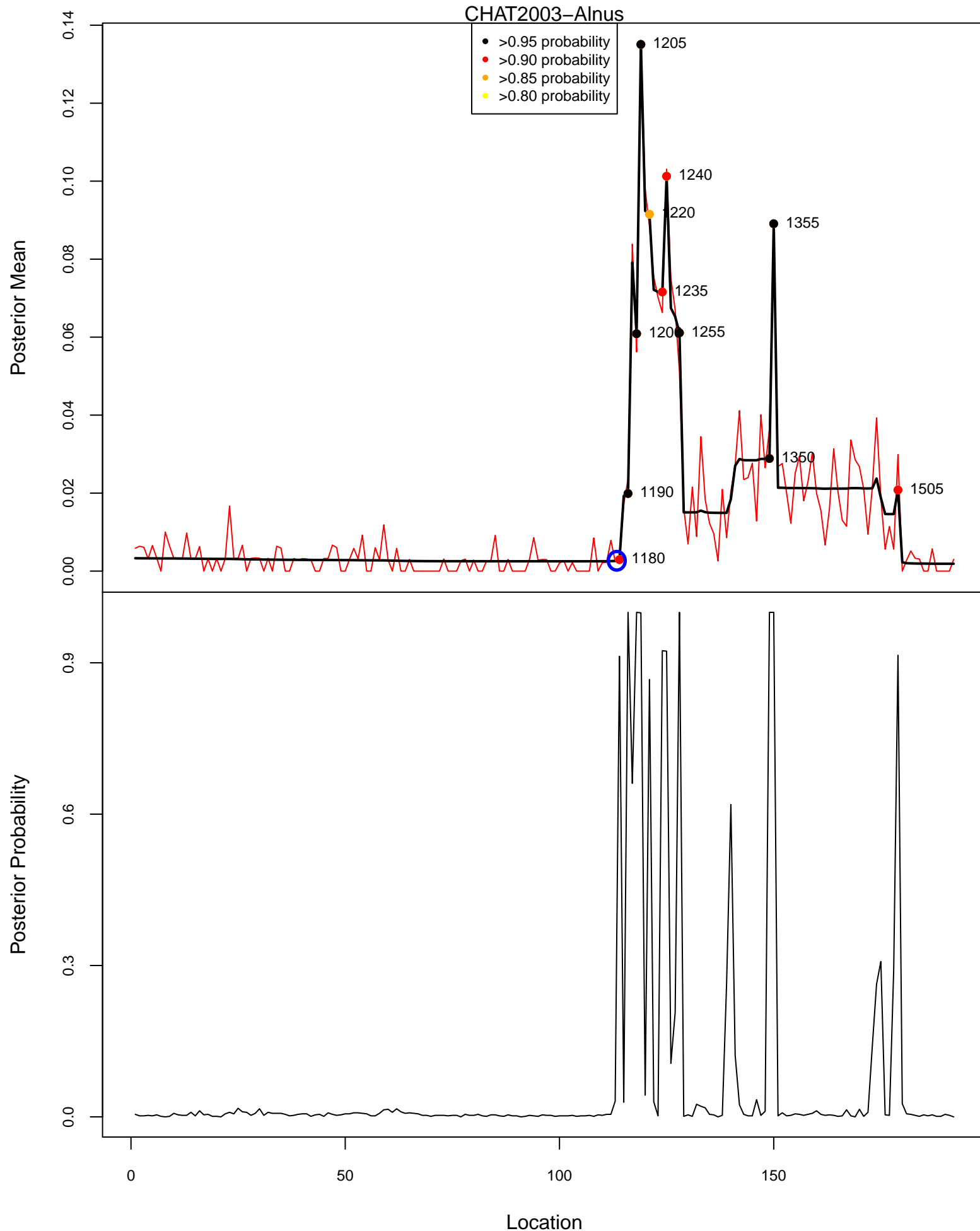




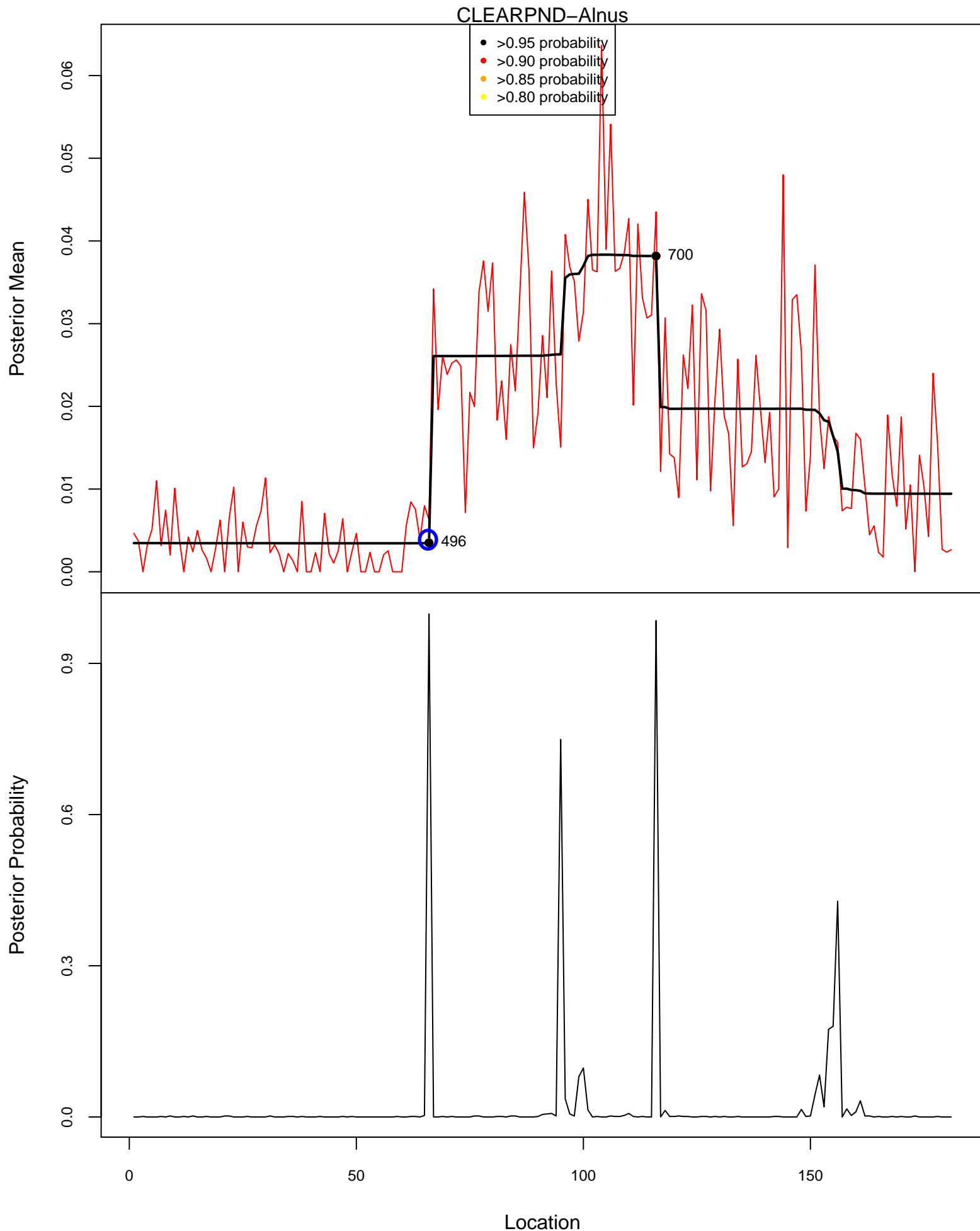
Posterior Means and Probabilities of a Change



Posterior Means and Probabilities of a Change

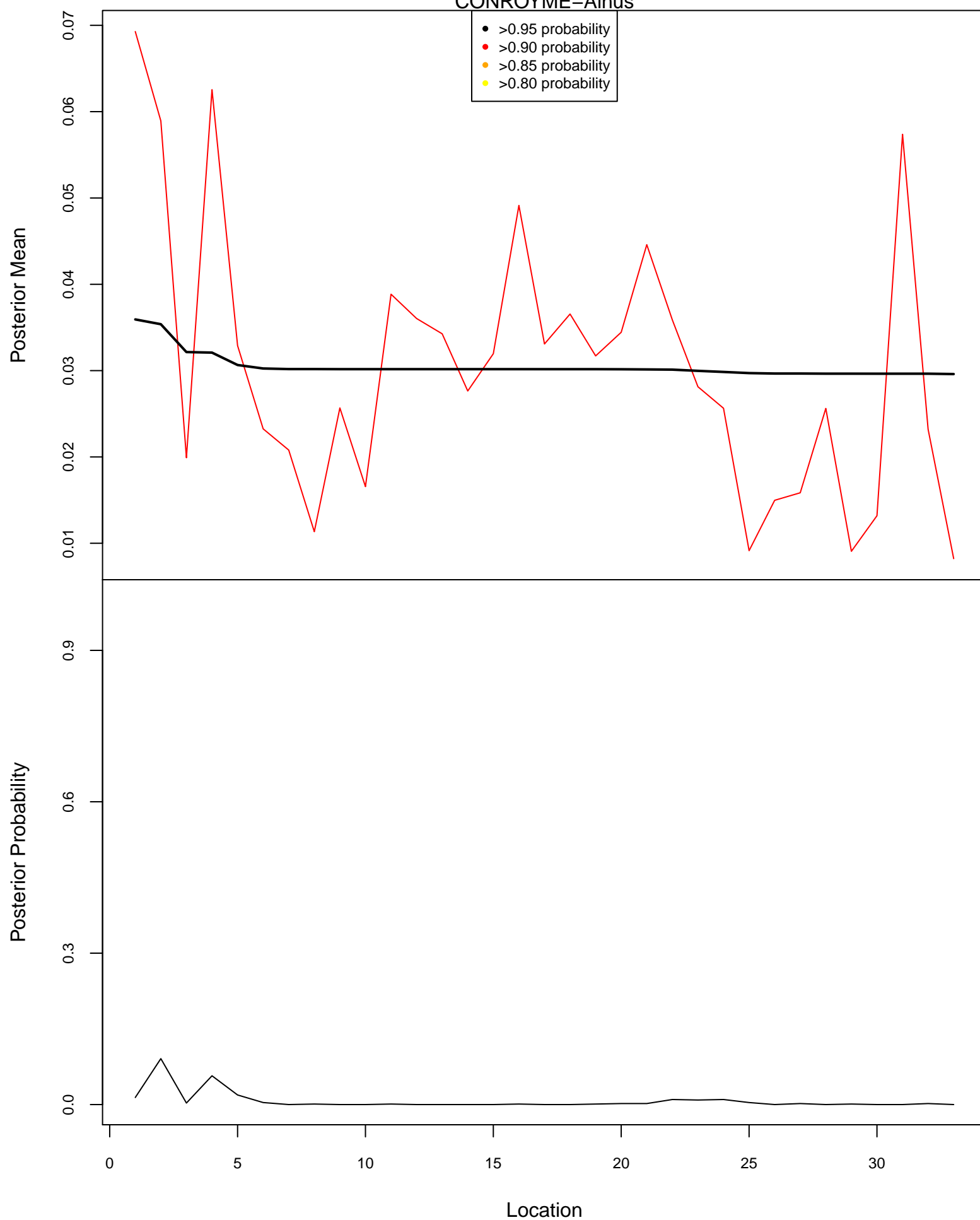


Posterior Means and Probabilities of a Change



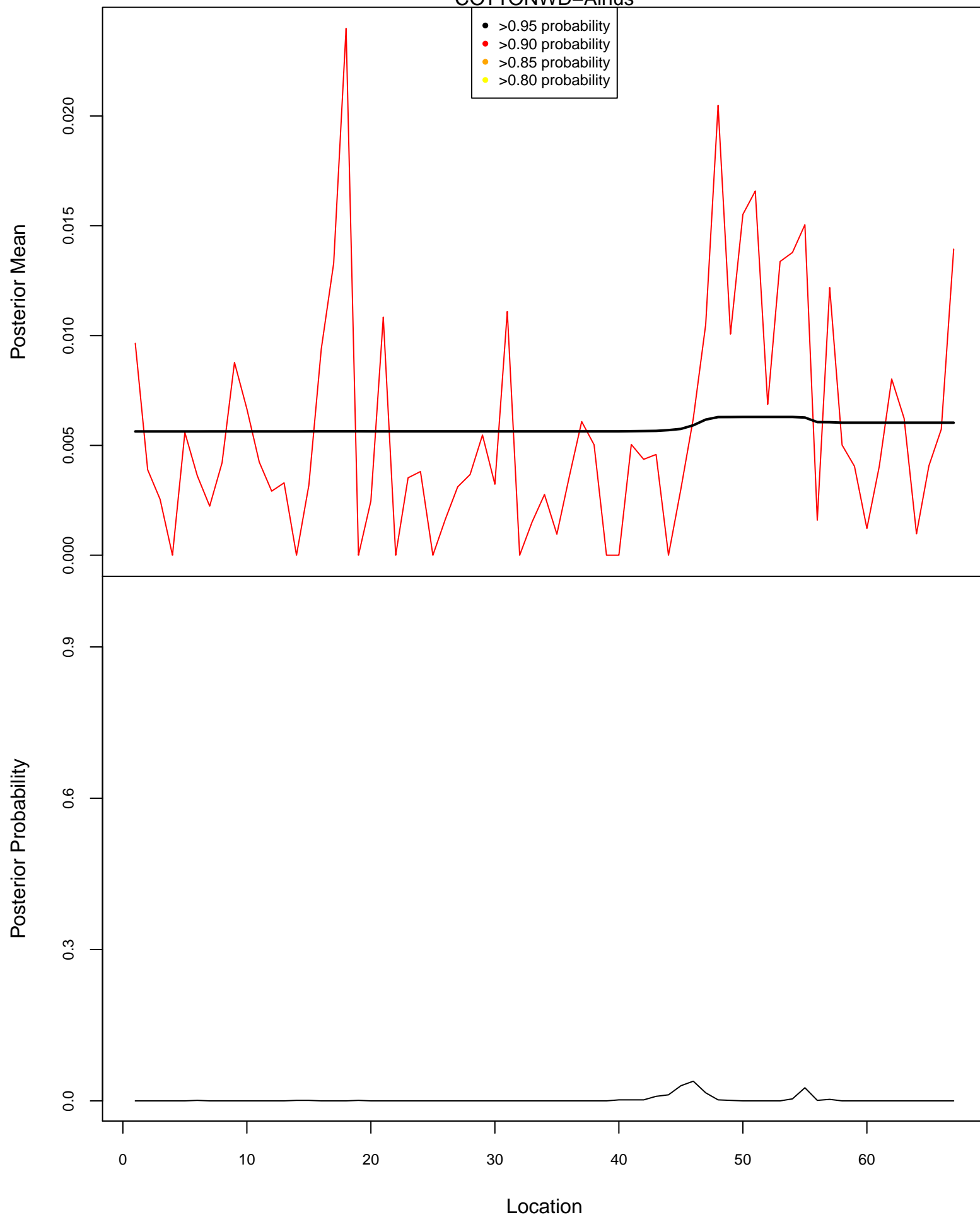
Posterior Means and Probabilities of a Change

CONROYME-Alnus

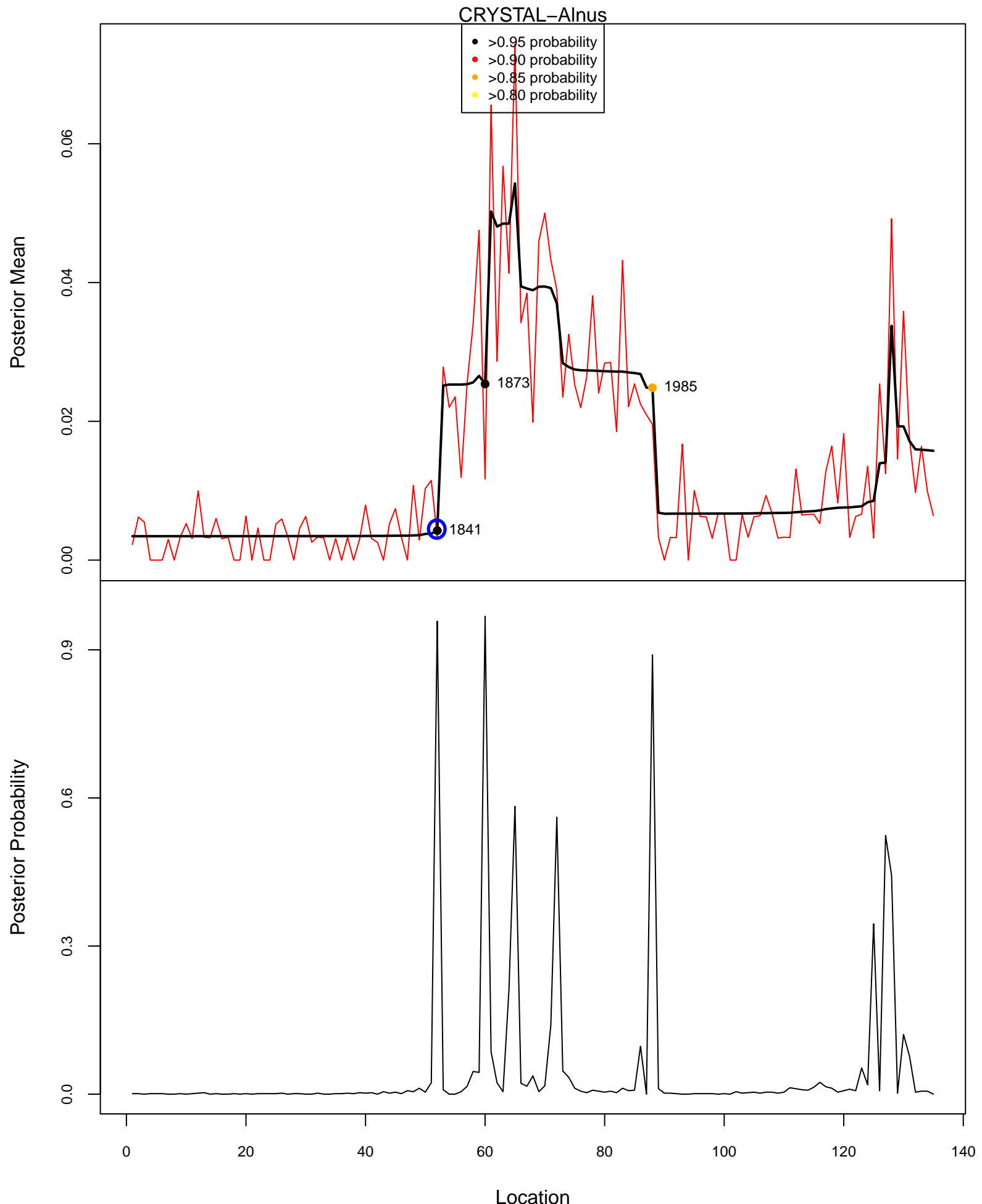


Posterior Means and Probabilities of a Change

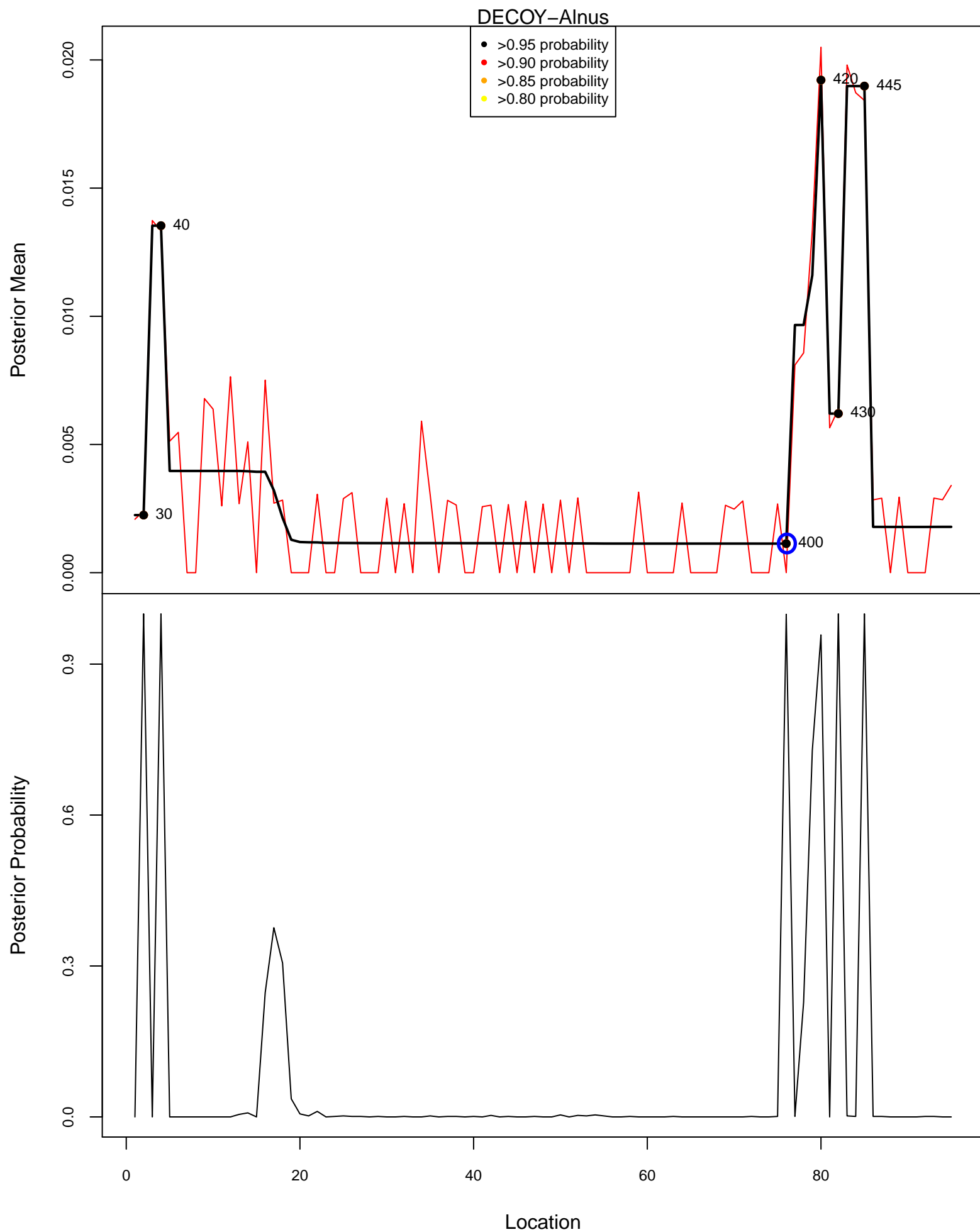
COTTONWD–Alnus



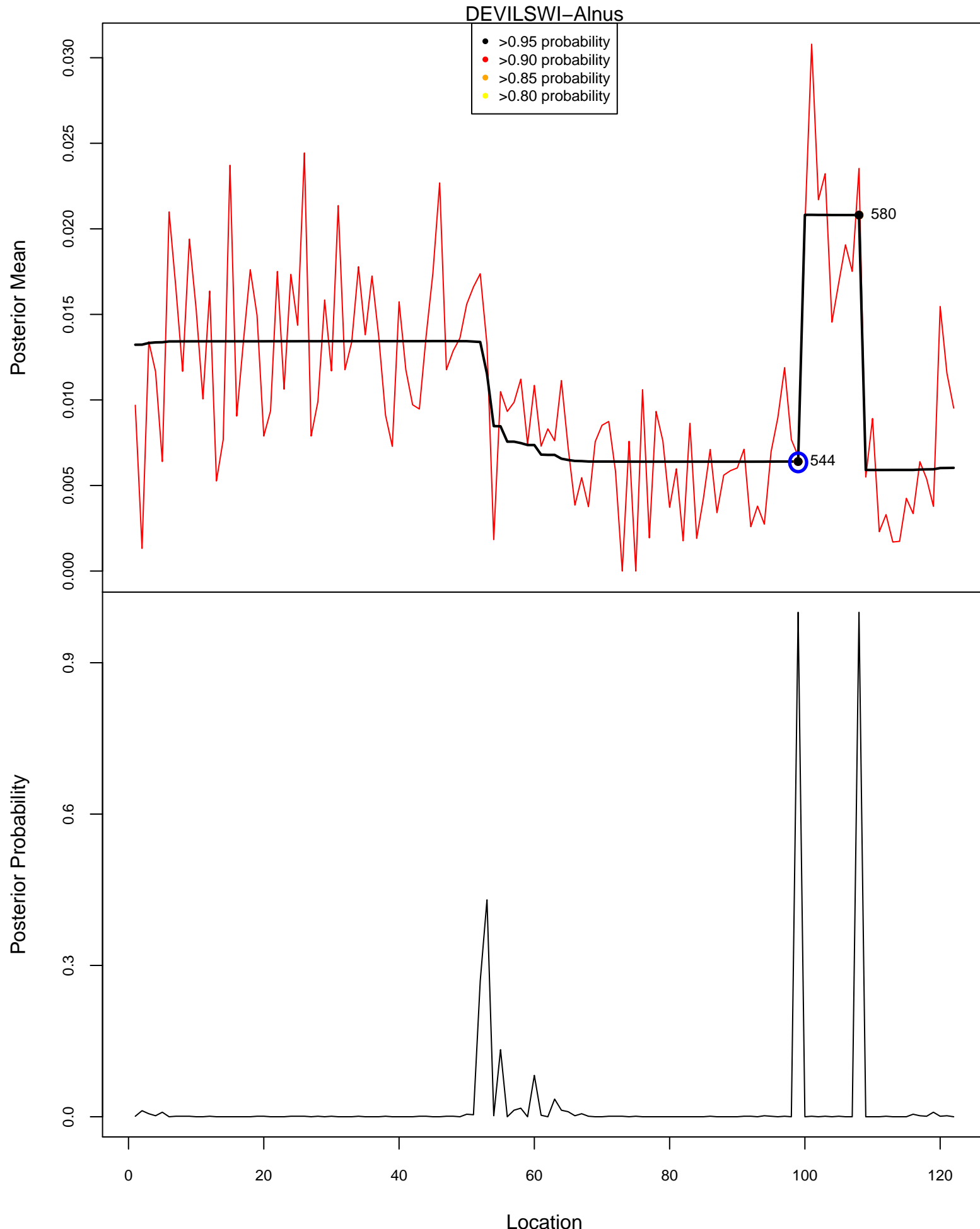
Posterior Means and Probabilities of a Change



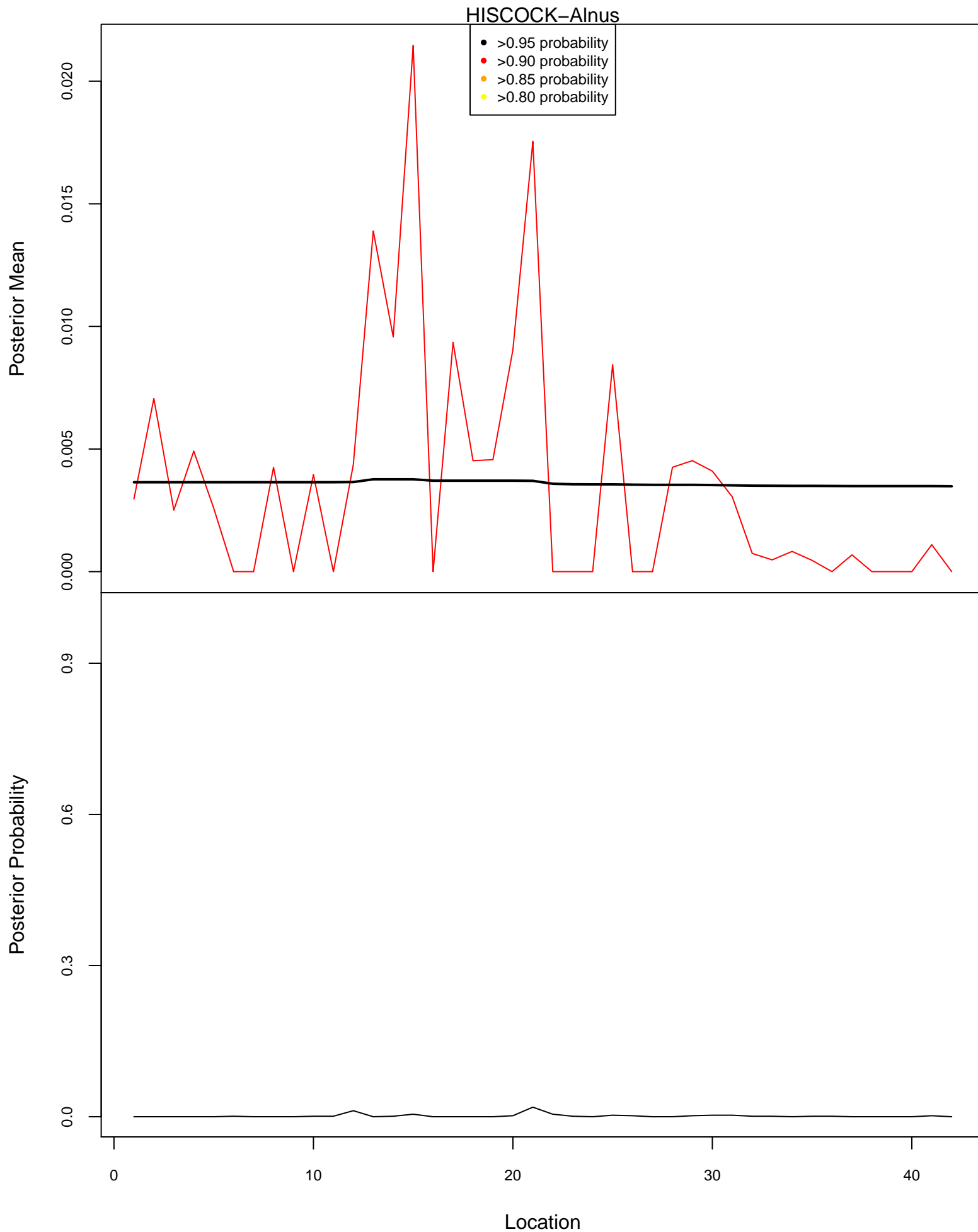
Posterior Means and Probabilities of a Change



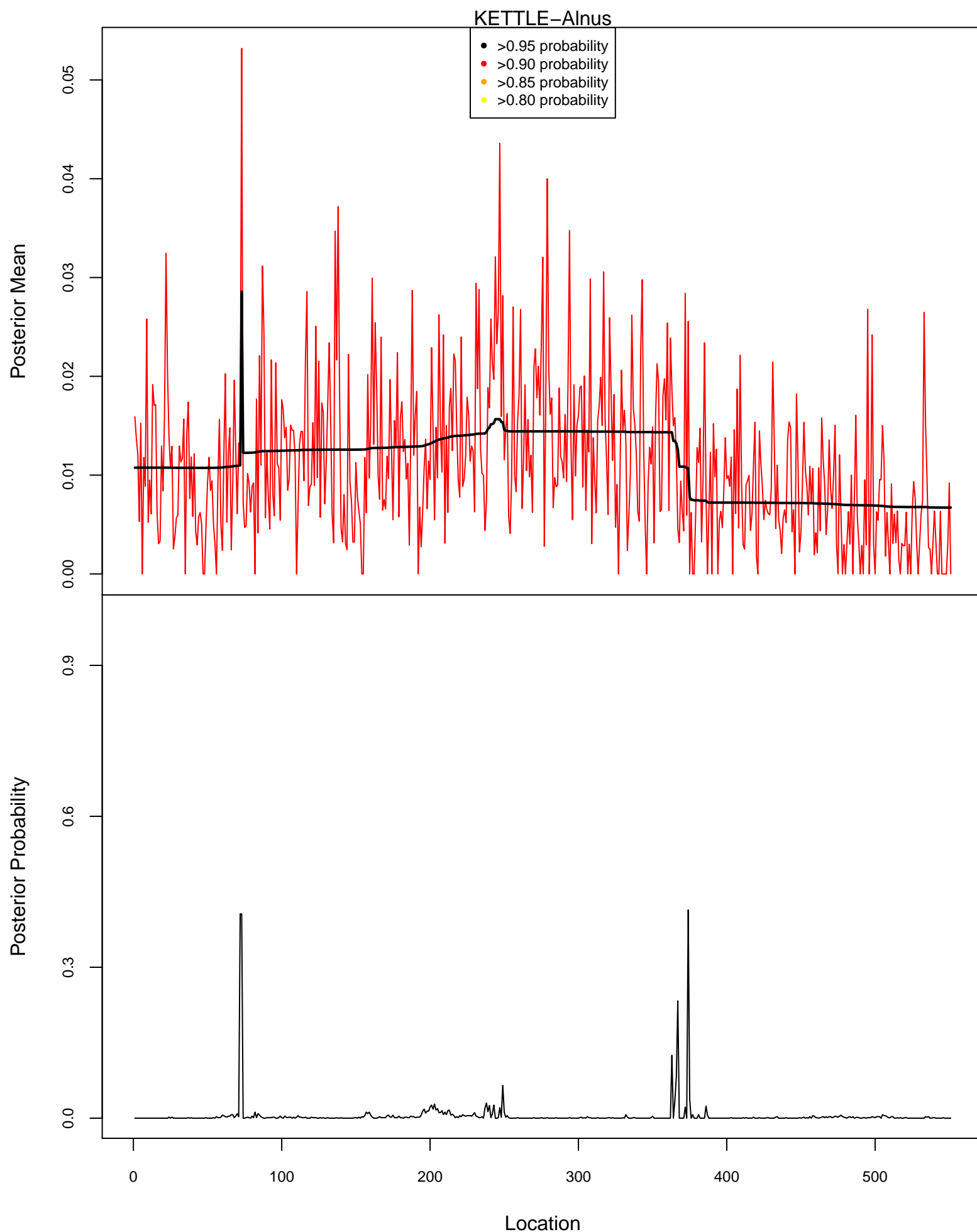
Posterior Means and Probabilities of a Change



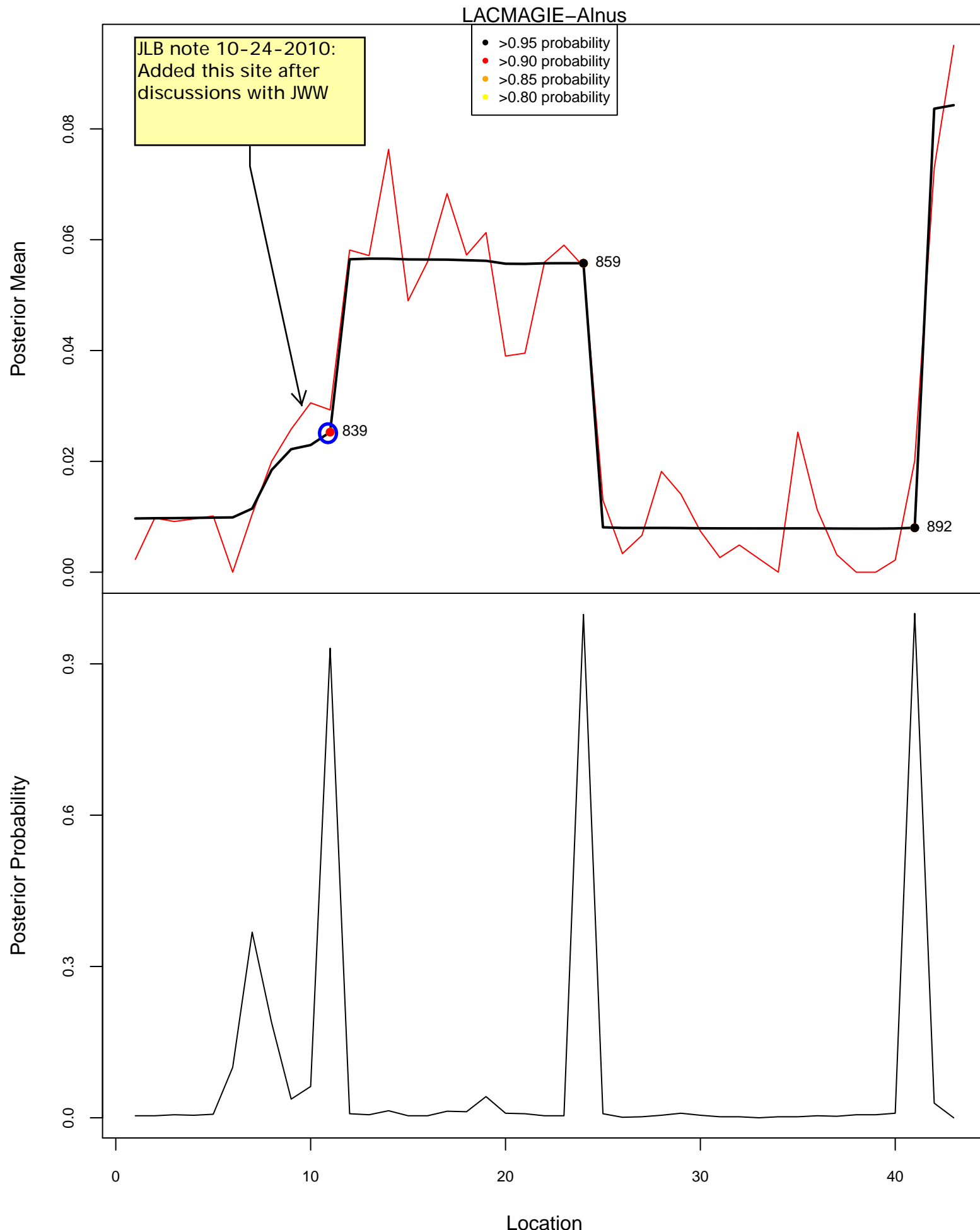
Posterior Means and Probabilities of a Change



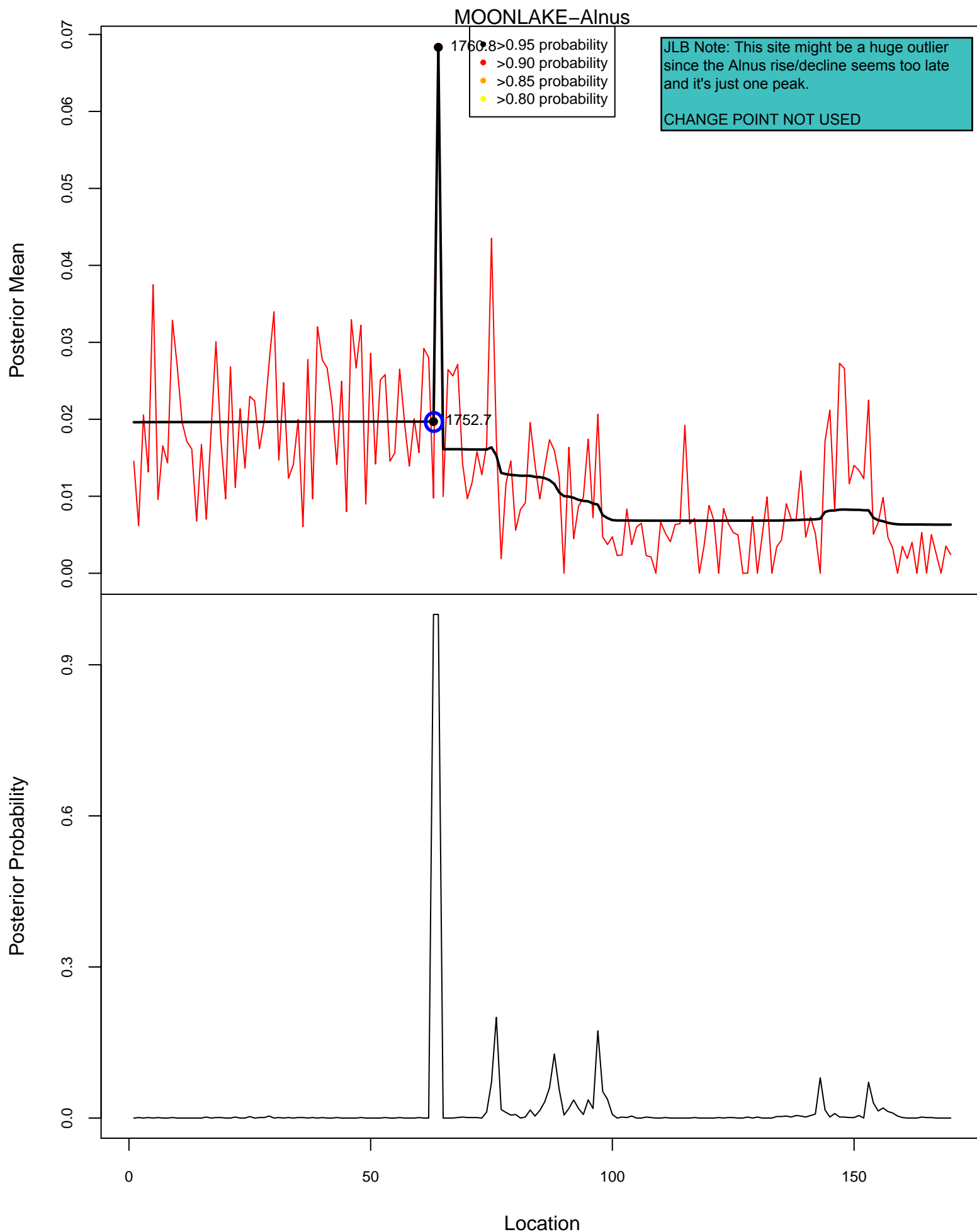
Posterior Means and Probabilities of a Change



Posterior Means and Probabilities of a Change

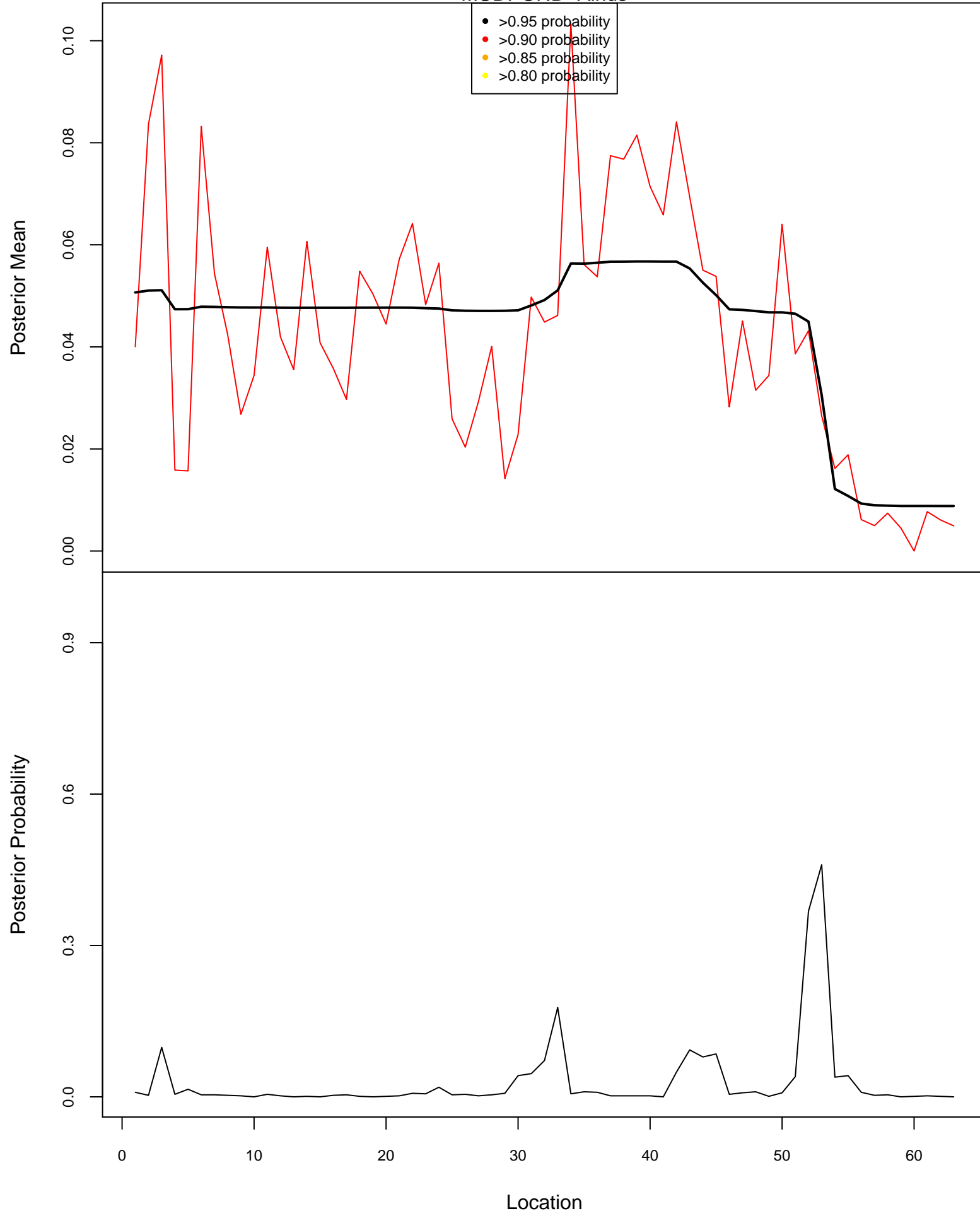


Posterior Means and Probabilities of a Change

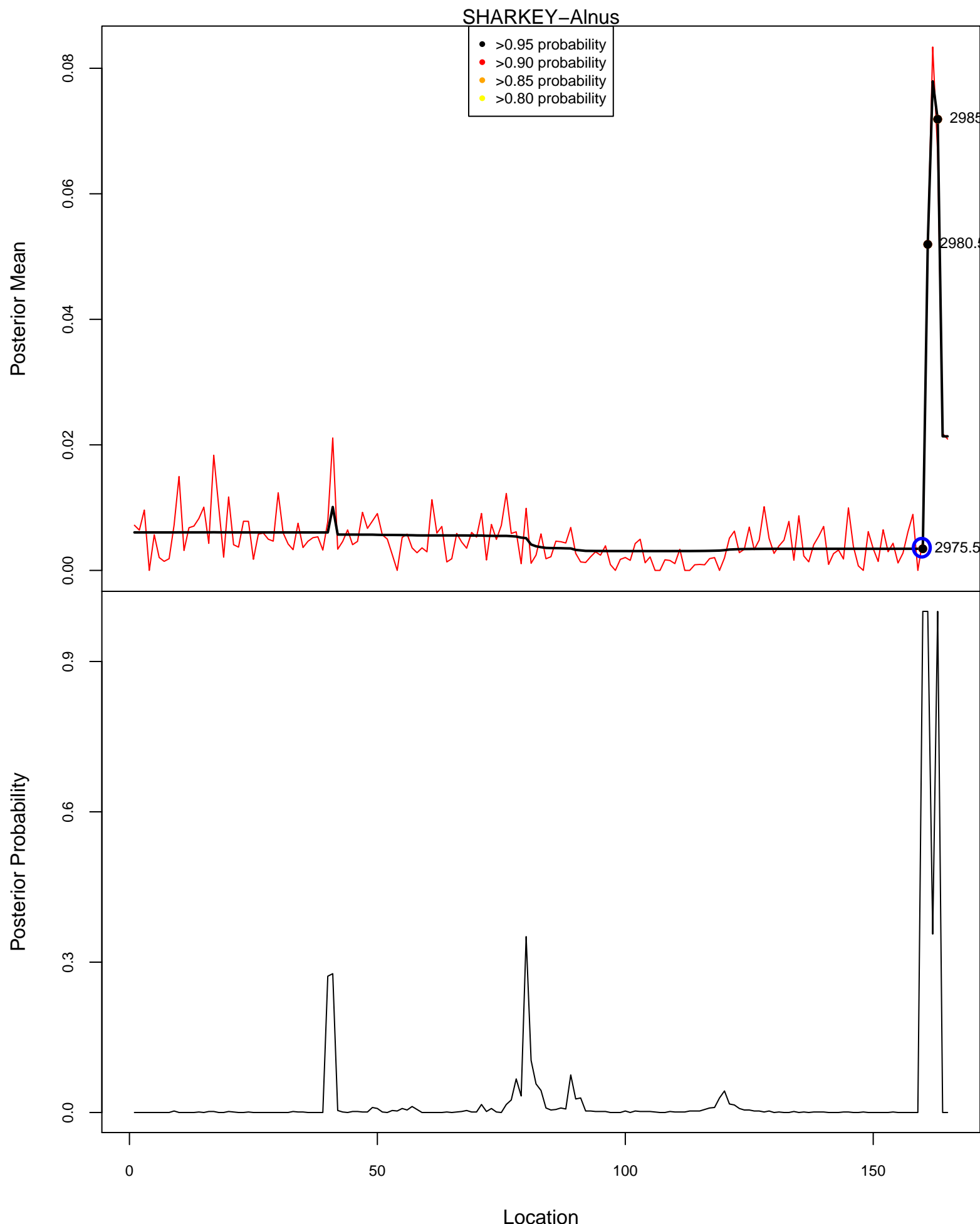


Posterior Means and Probabilities of a Change

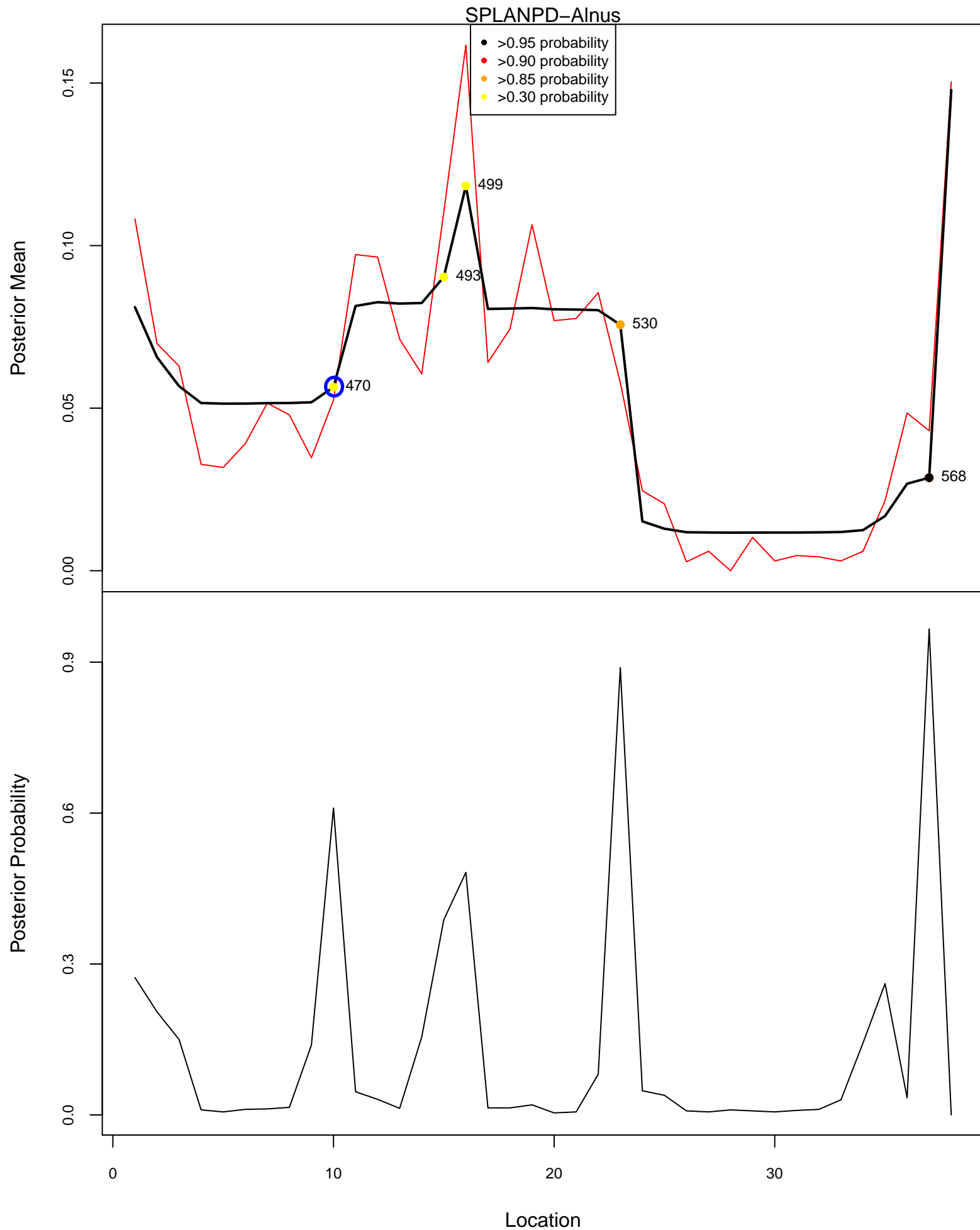
MUDPOND–Alnus



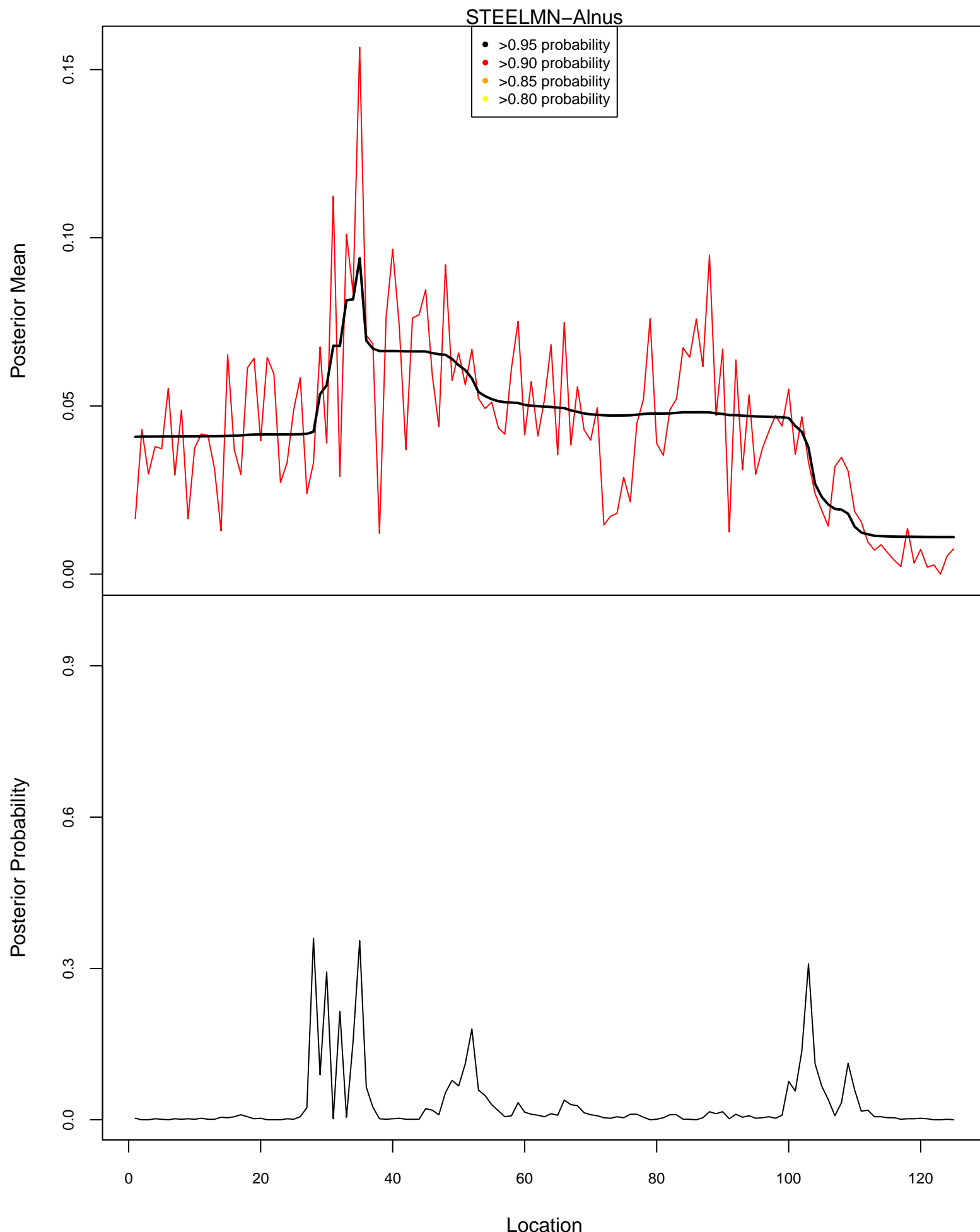
Posterior Means and Probabilities of a Change



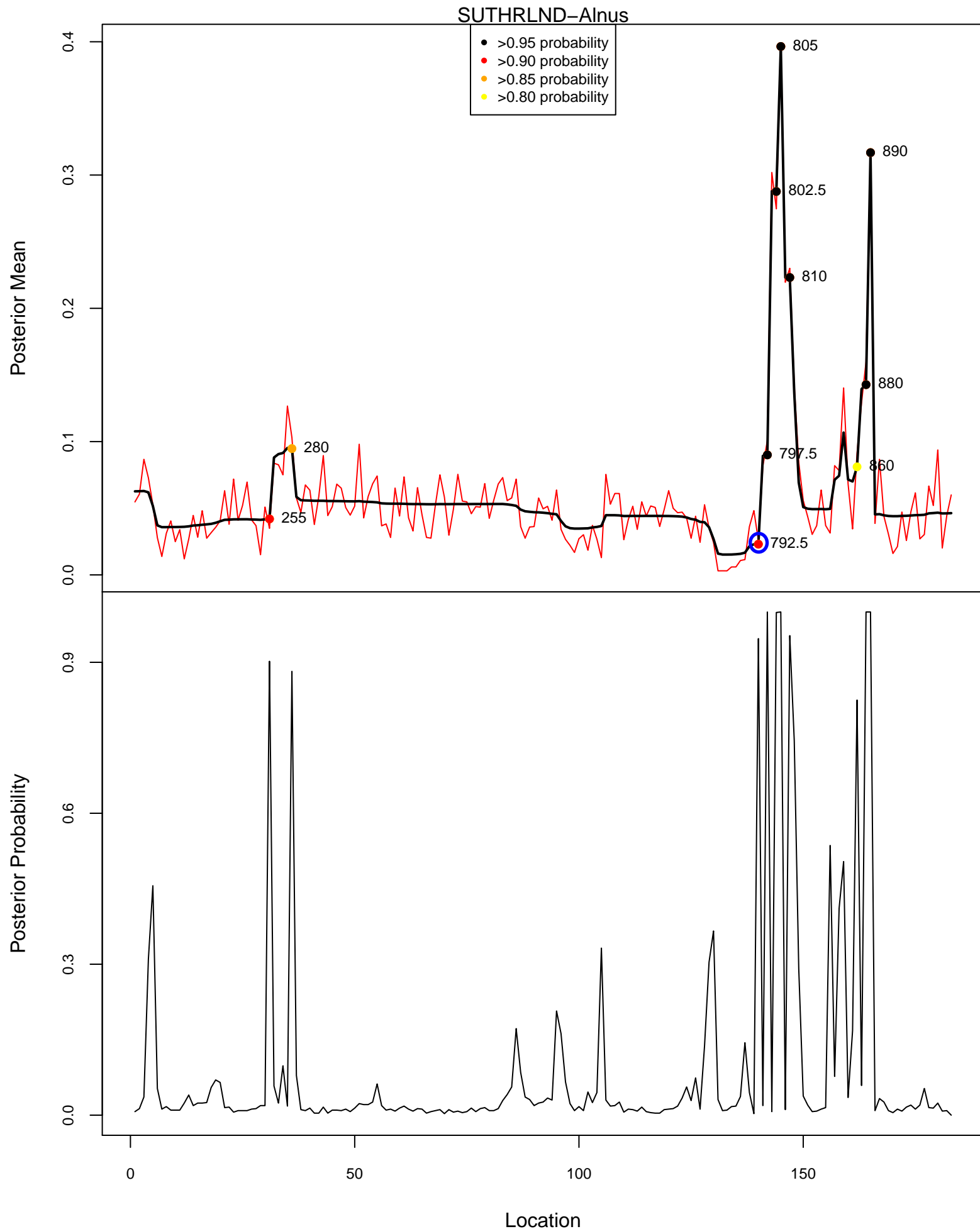
Posterior Means and Probabilities of a Change



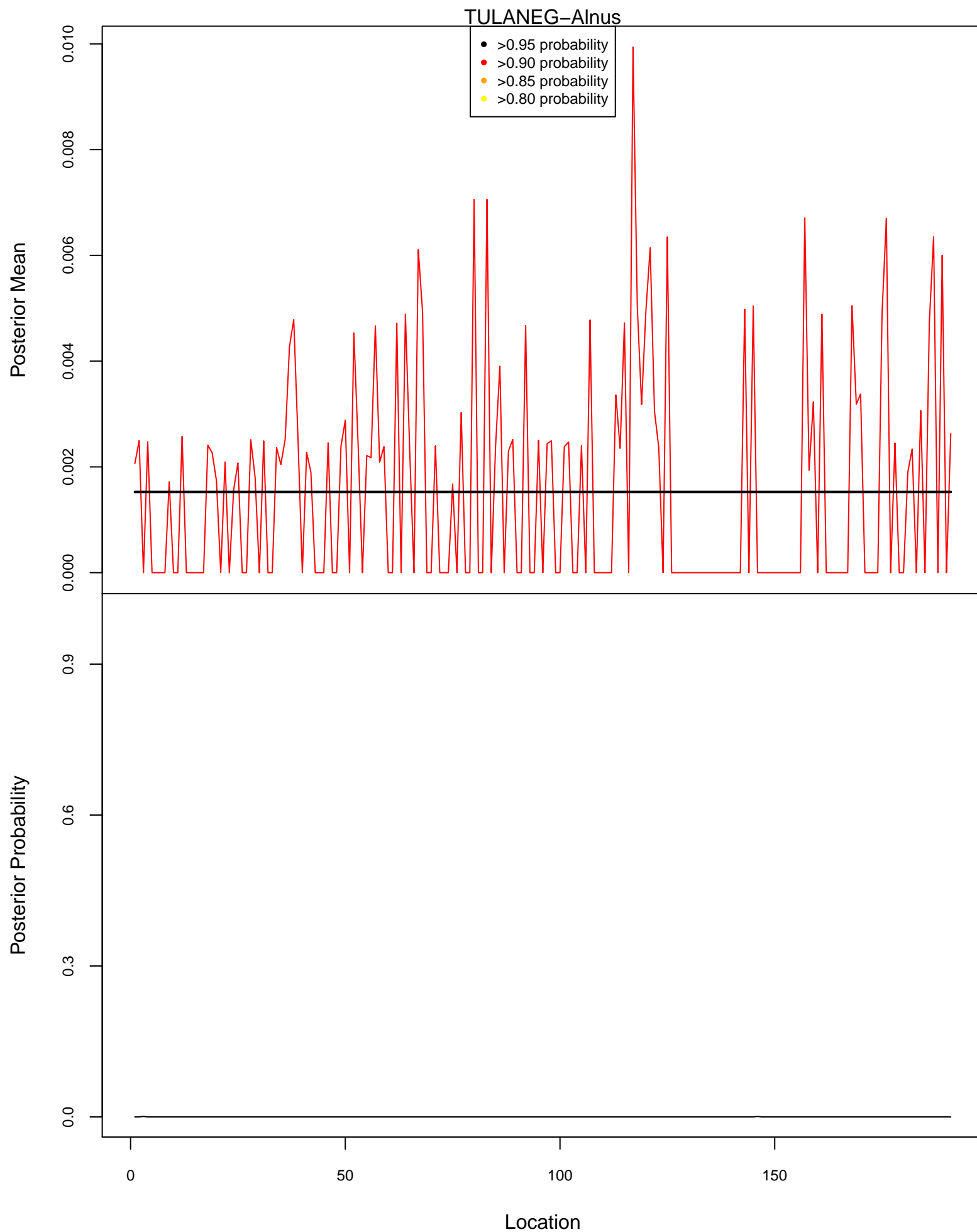
Posterior Means and Probabilities of a Change



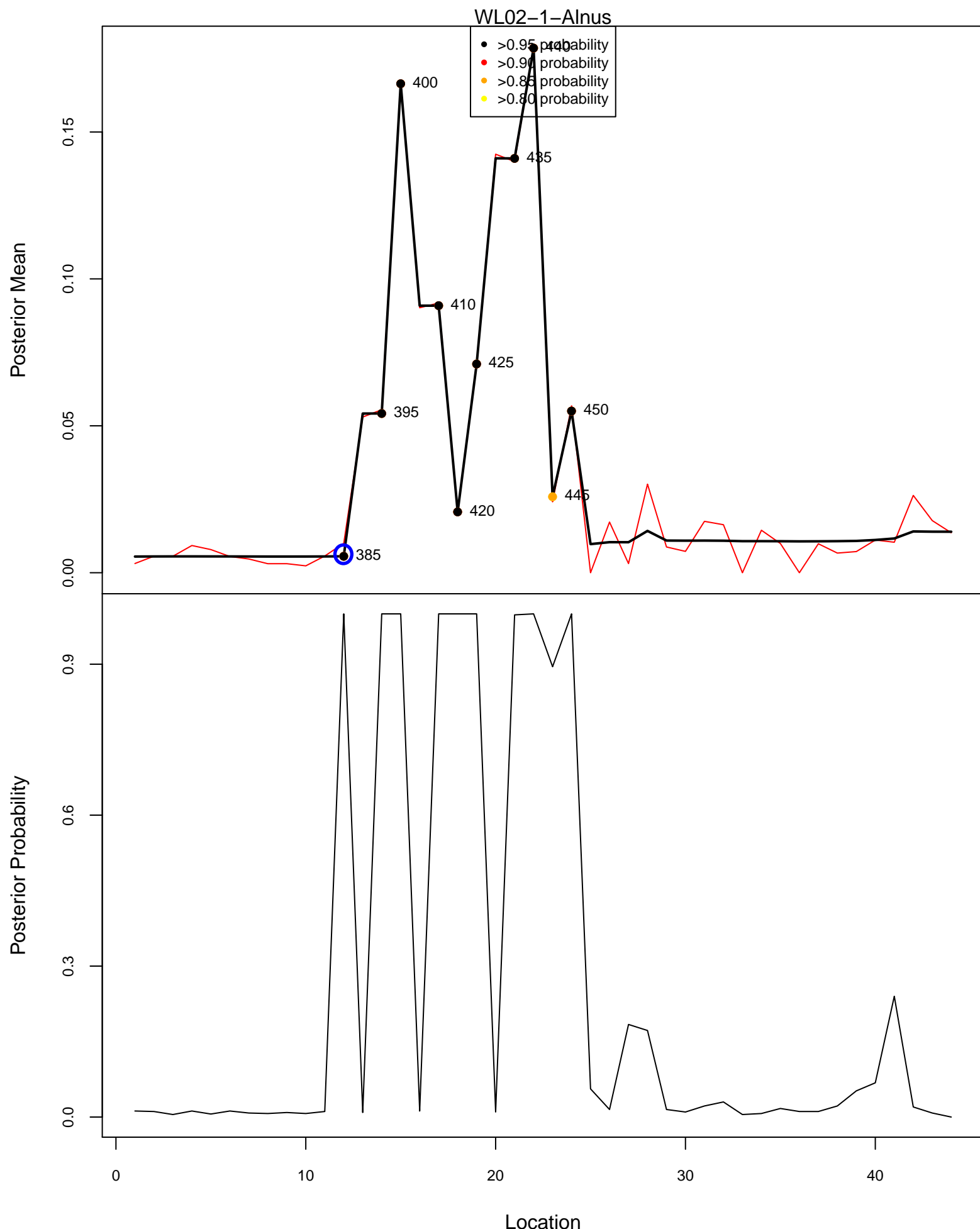
Posterior Means and Probabilities of a Change



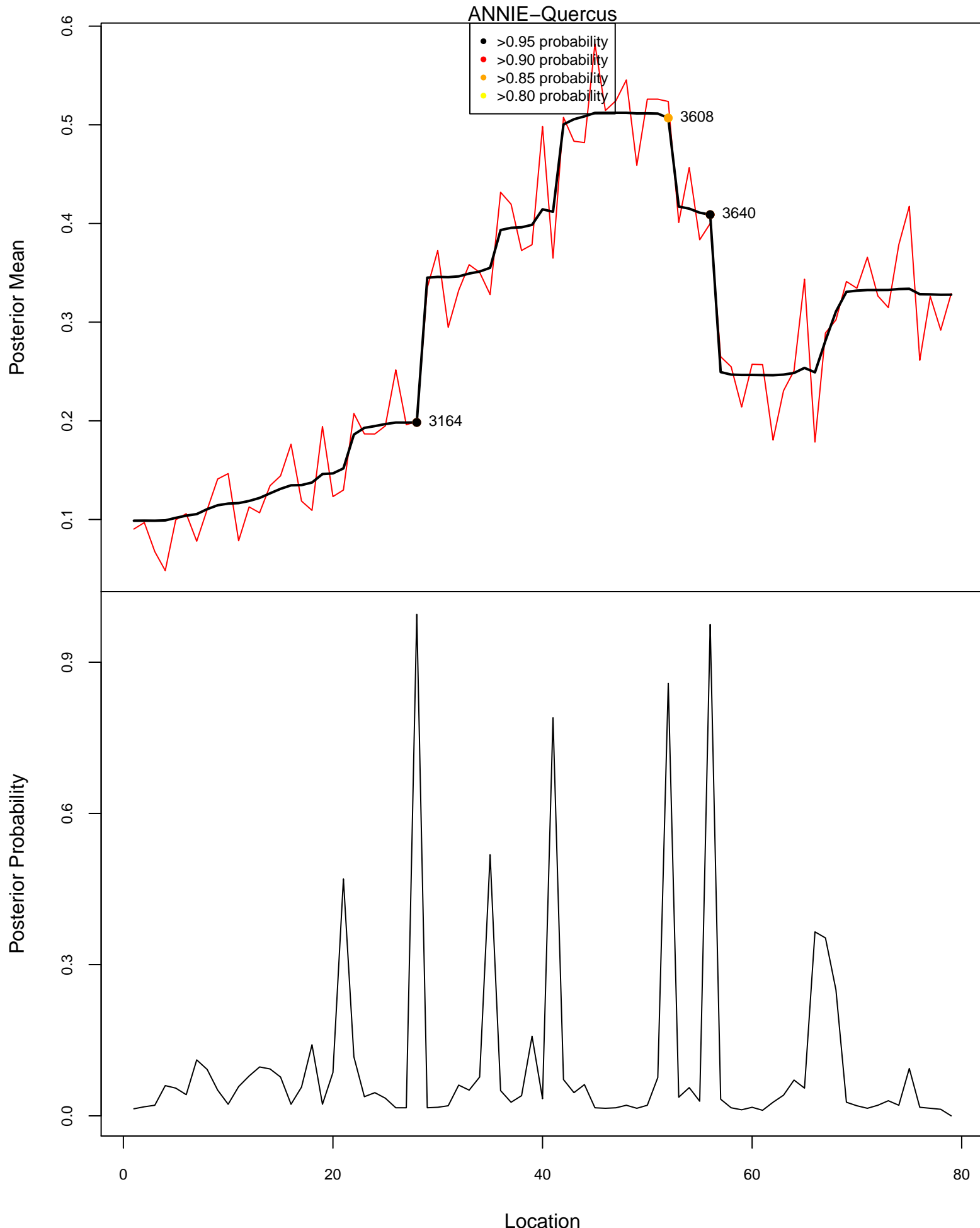
Posterior Means and Probabilities of a Change



Posterior Means and Probabilities of a Change

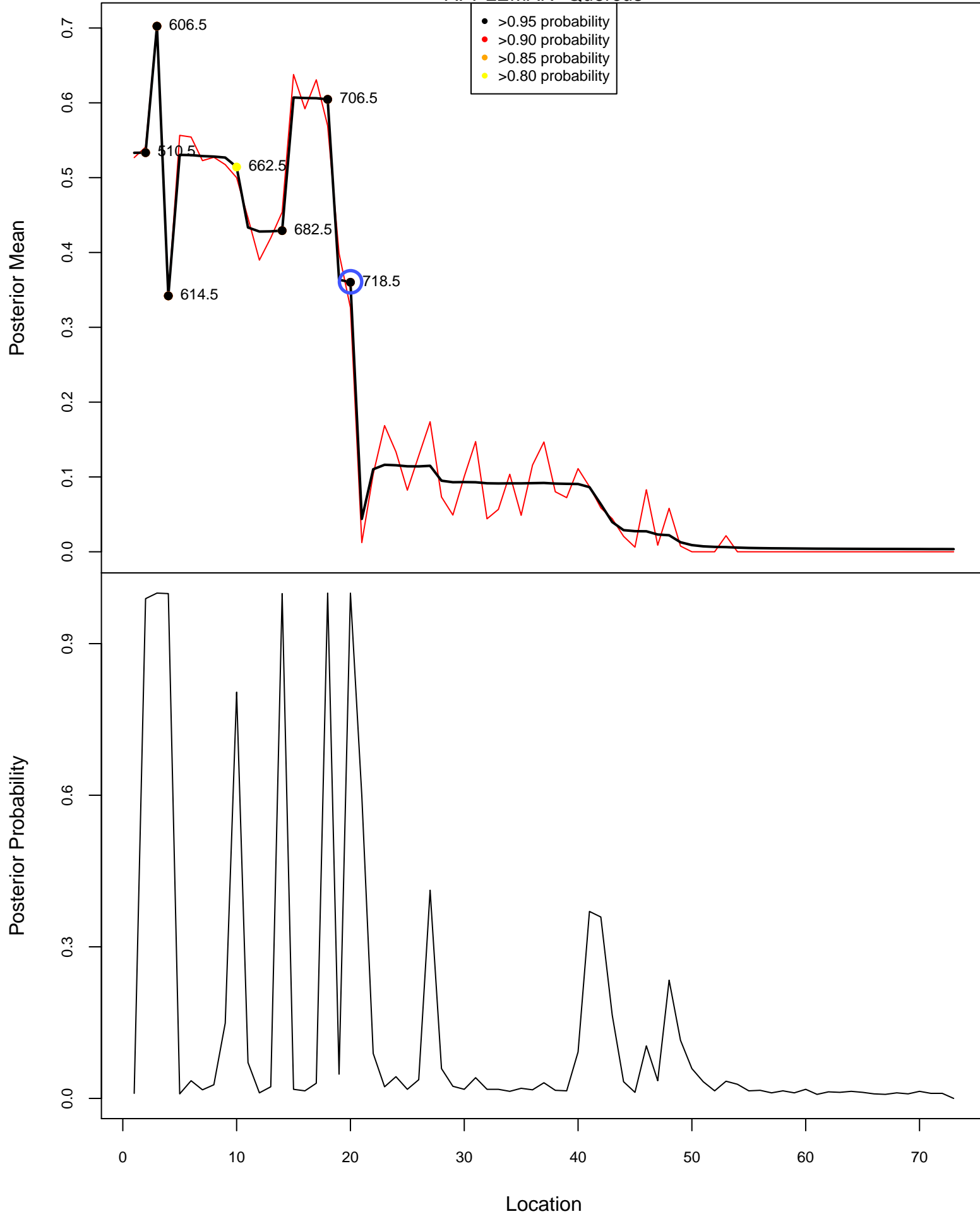


Posterior Means and Probabilities of a Change

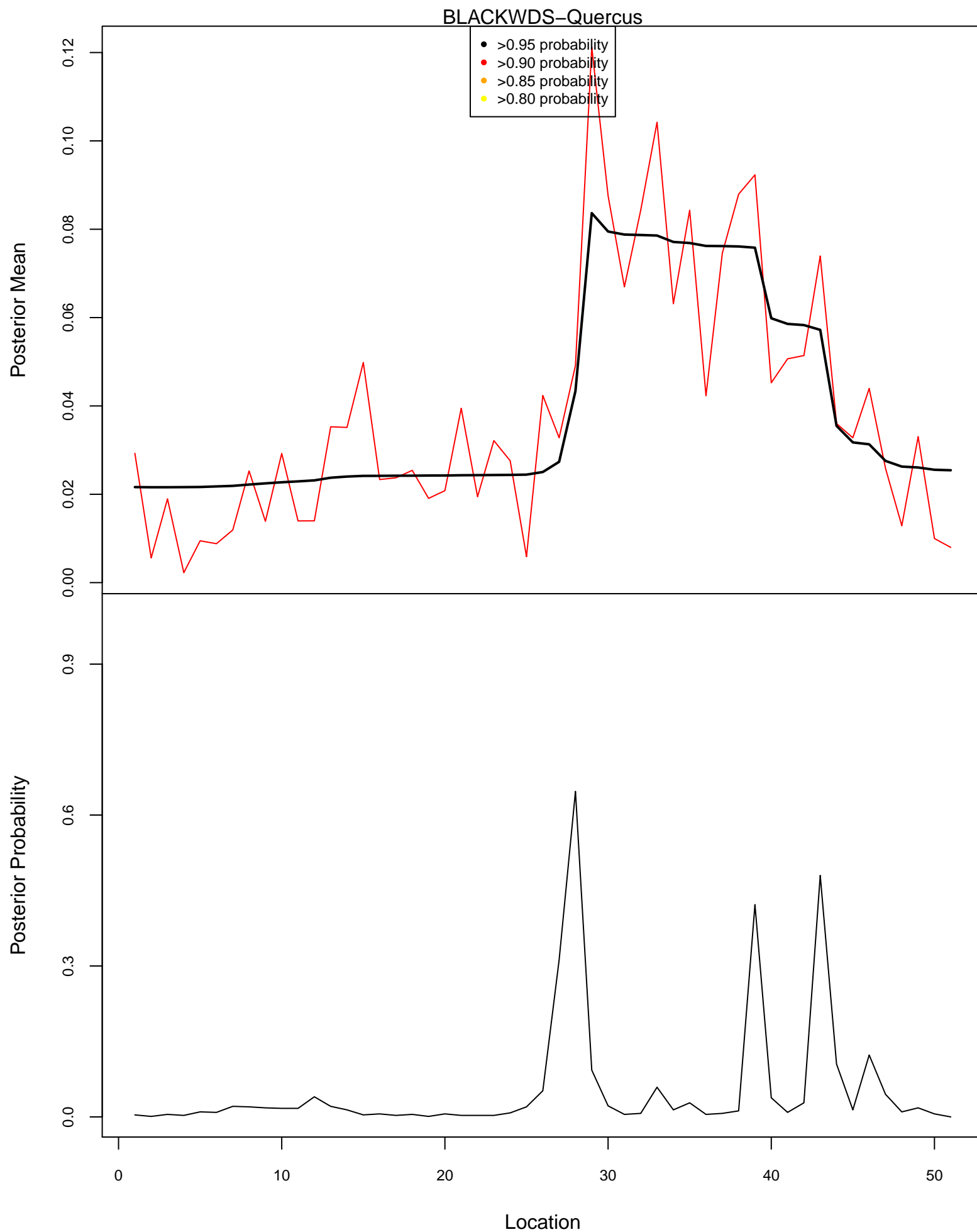


Posterior Means and Probabilities of a Change

APPLEMAN–Quercus

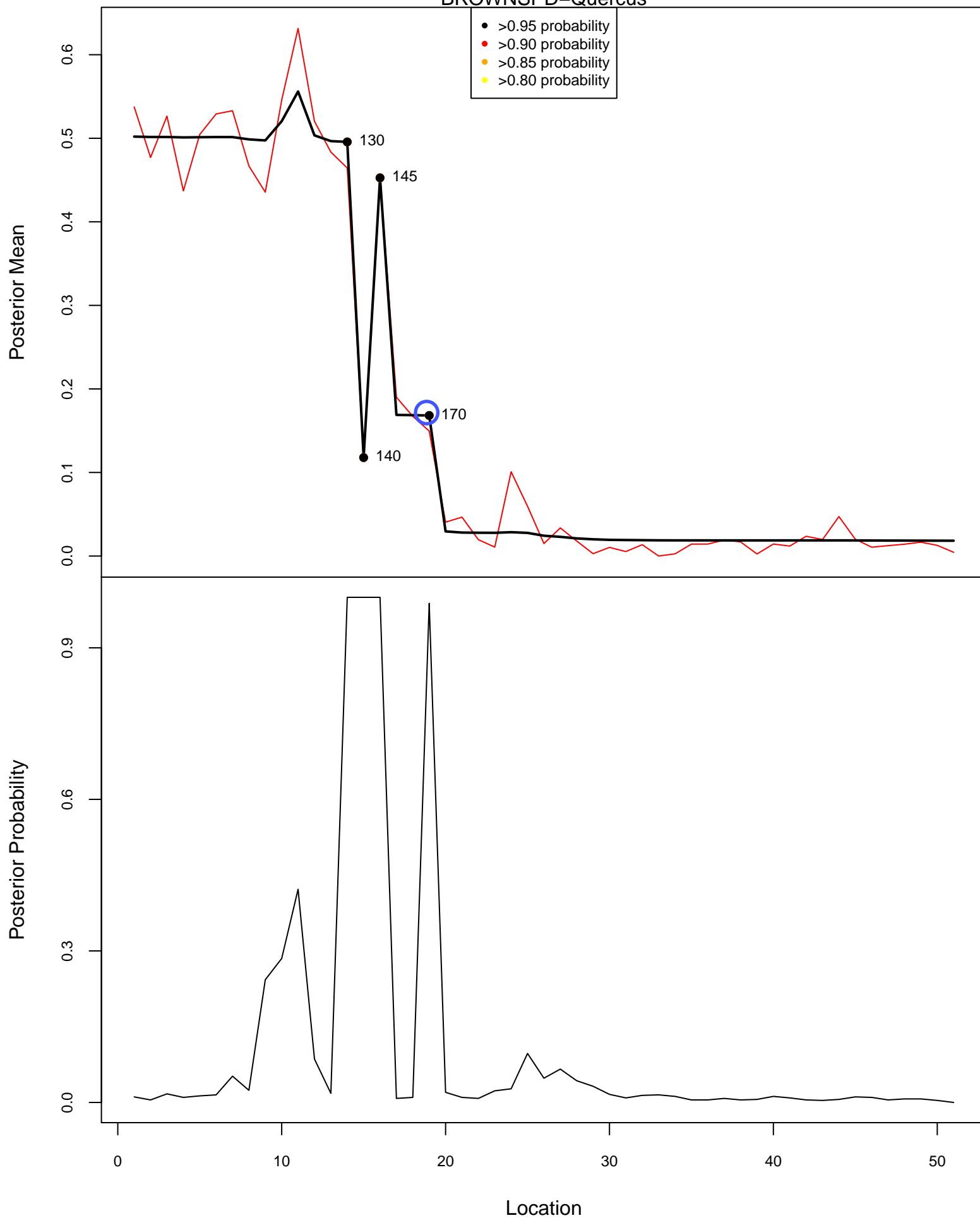


Posterior Means and Probabilities of a Change

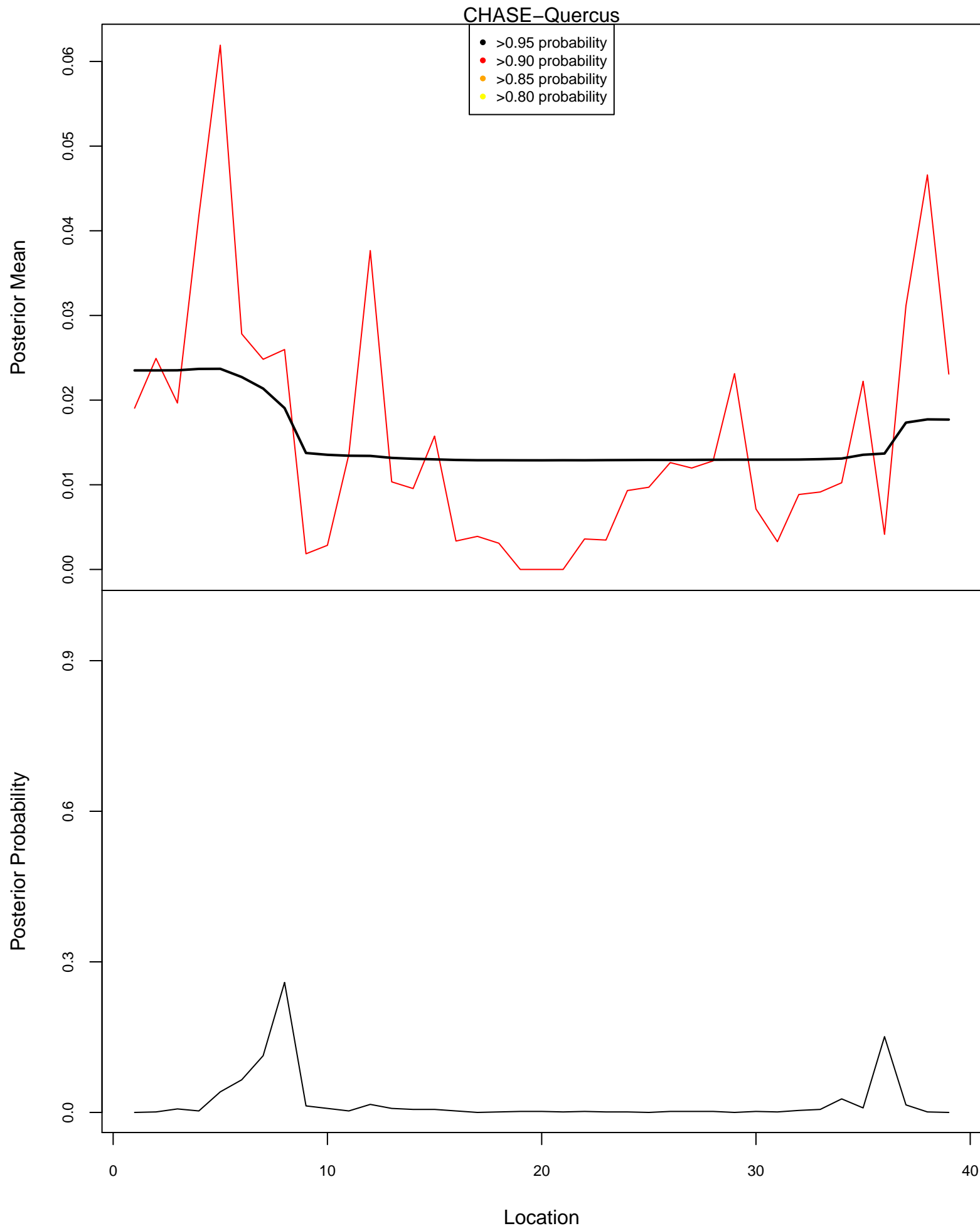


Posterior Means and Probabilities of a Change

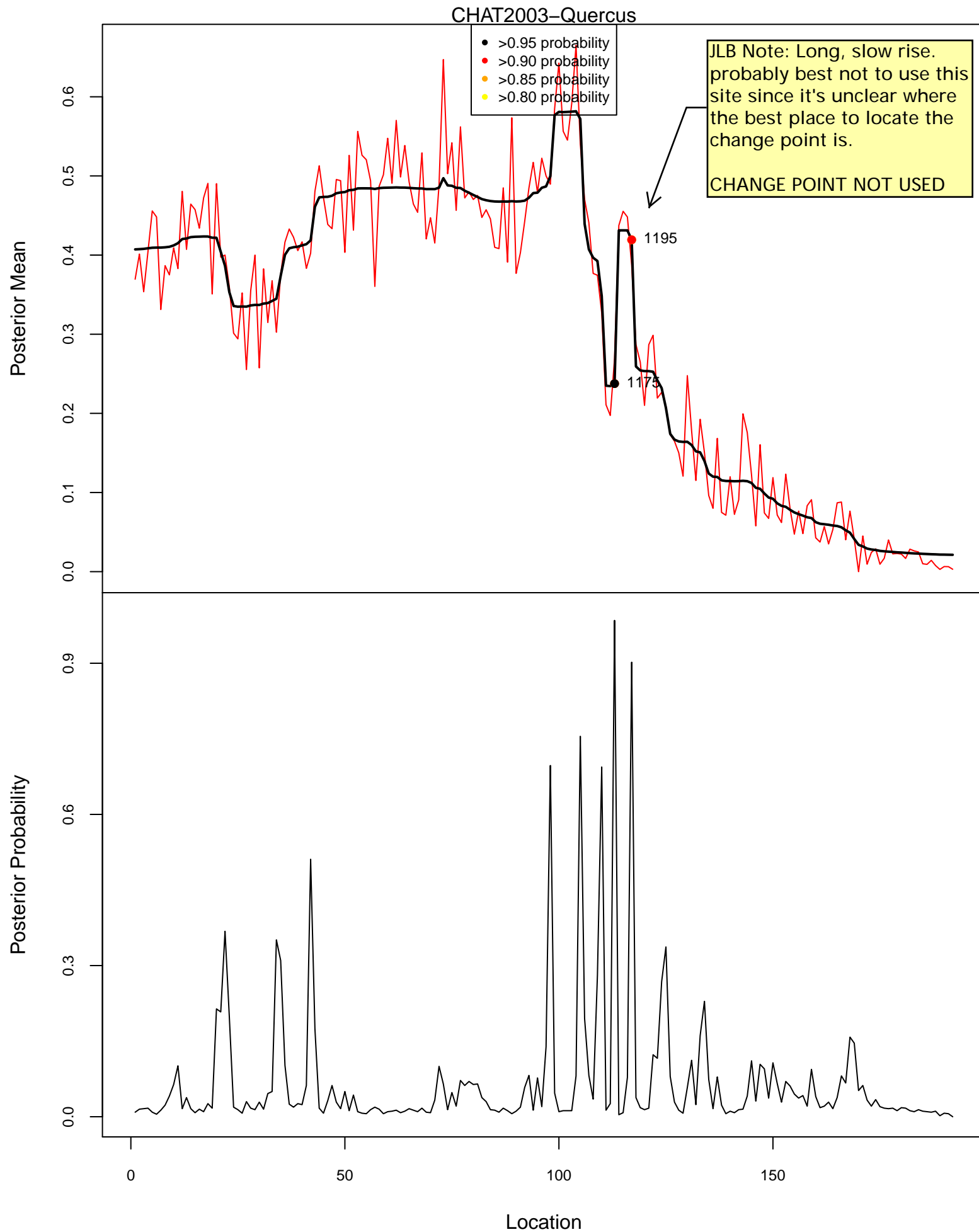
BROWNSPD–Quercus

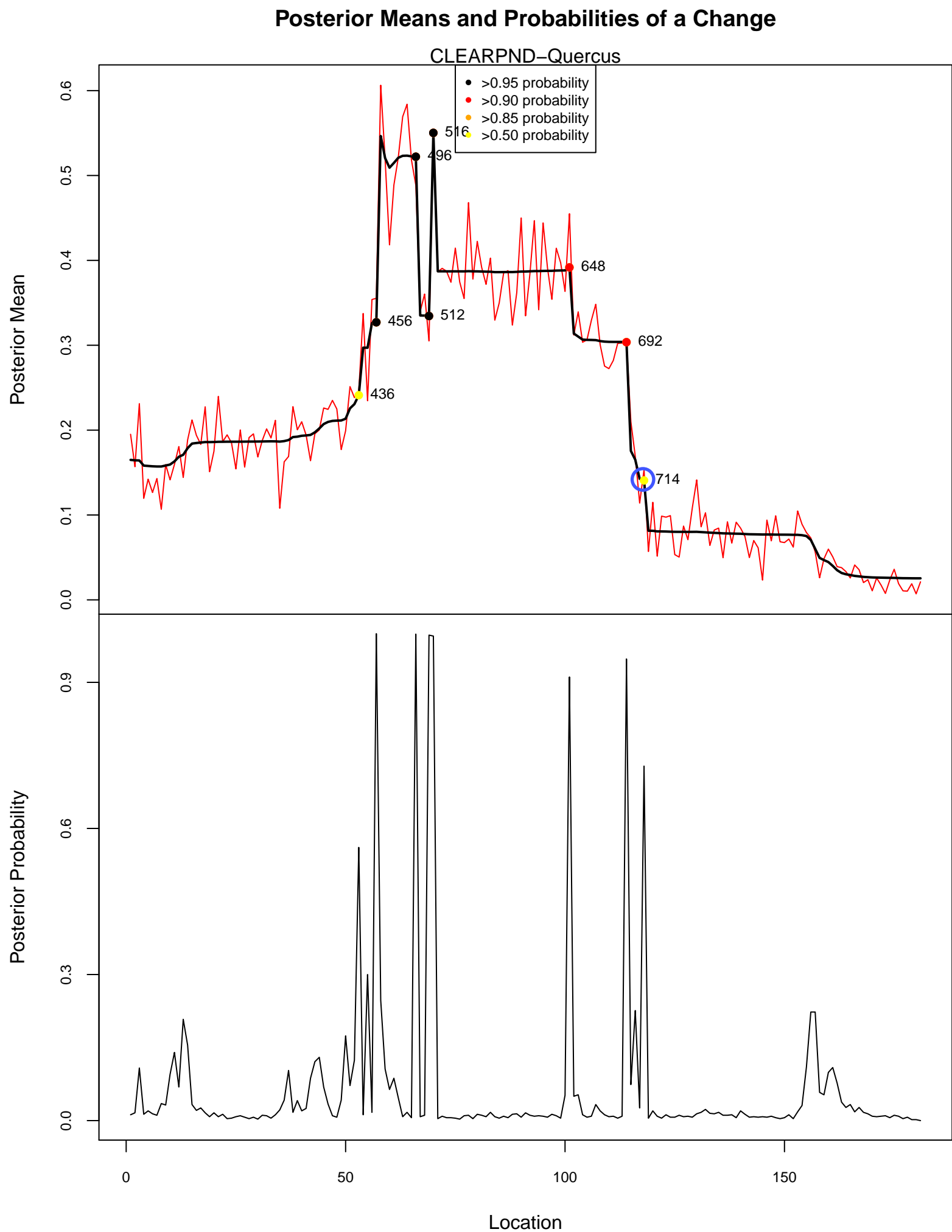


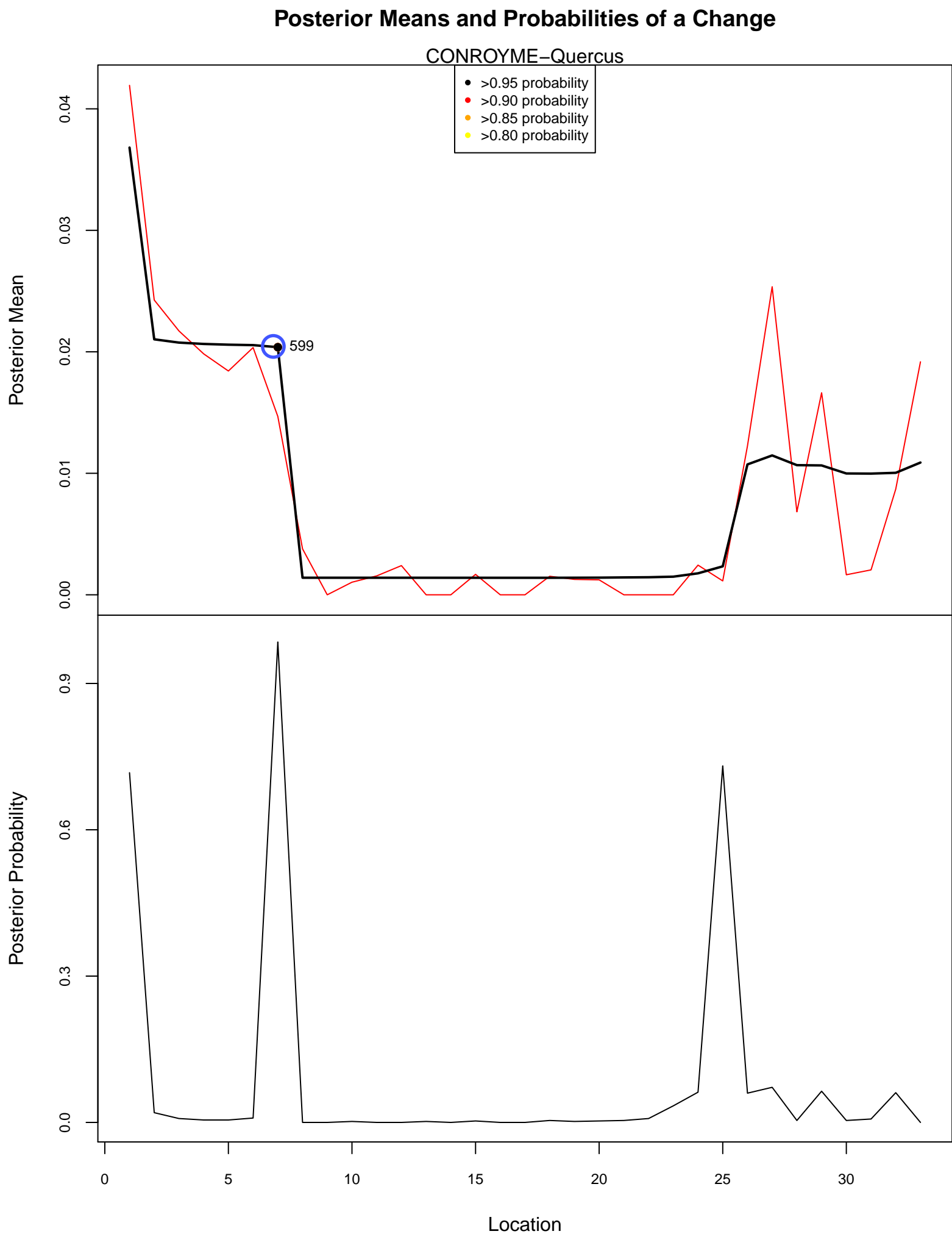
Posterior Means and Probabilities of a Change



Posterior Means and Probabilities of a Change

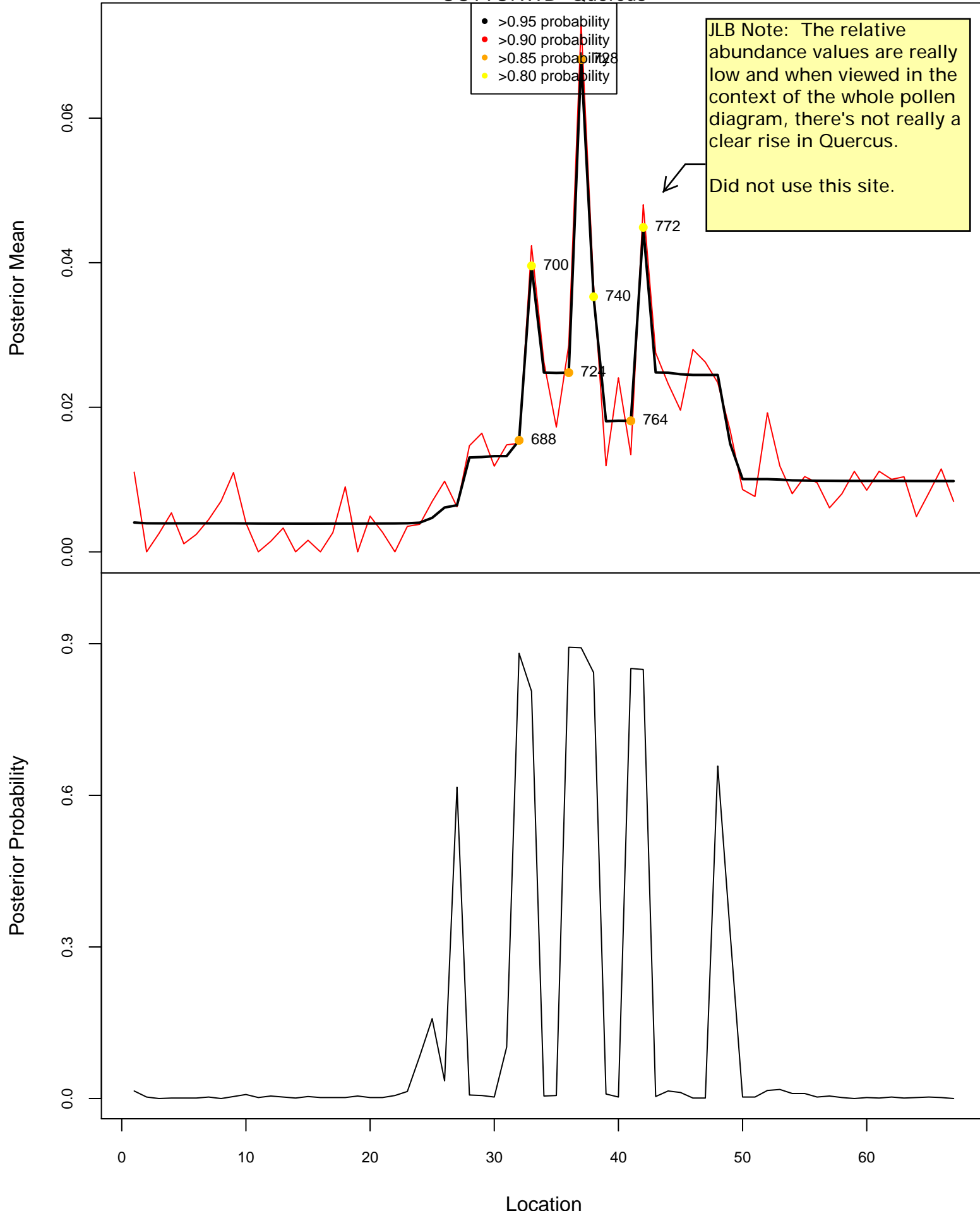






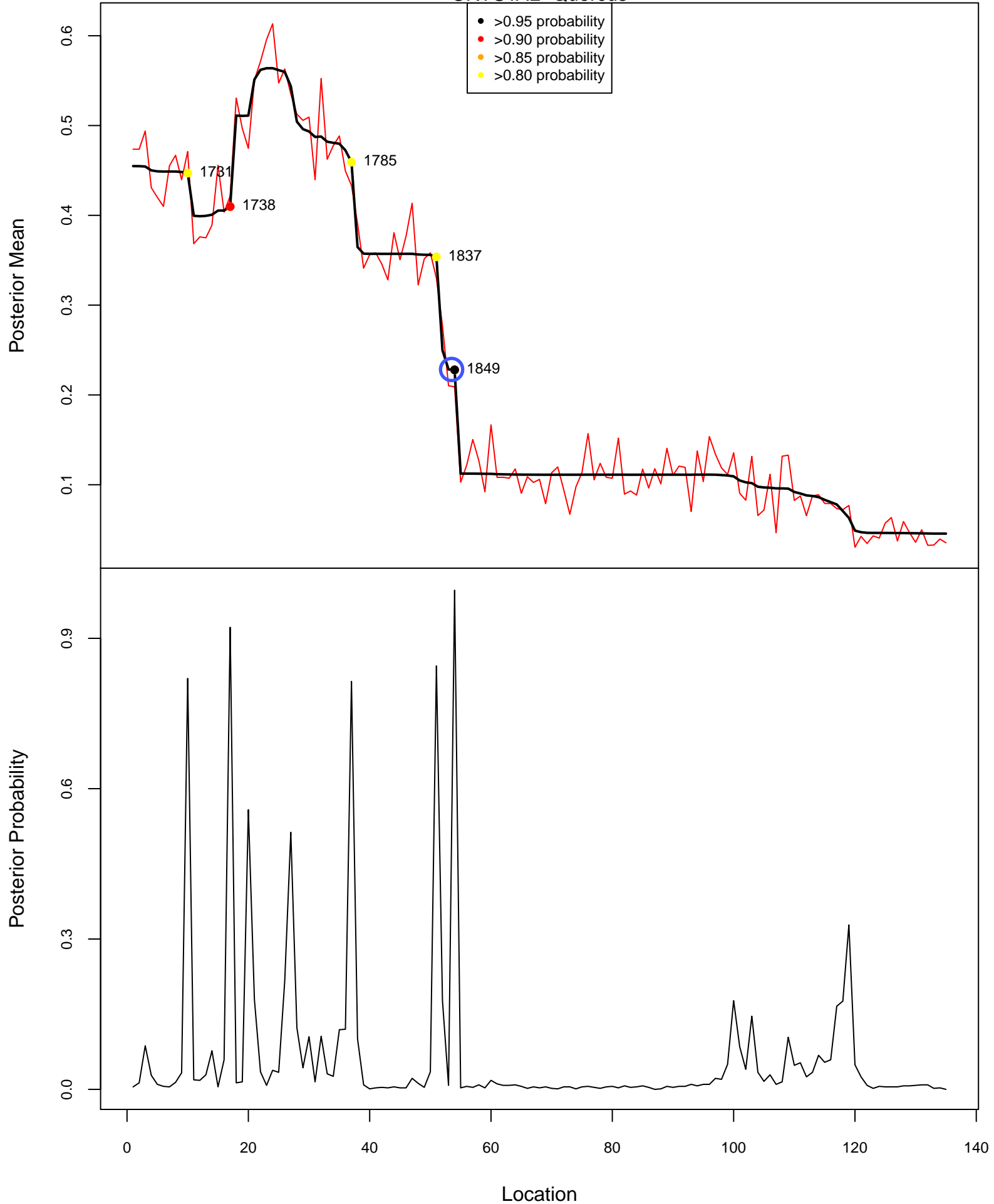
Posterior Means and Probabilities of a Change

COTTONWD–Quercus

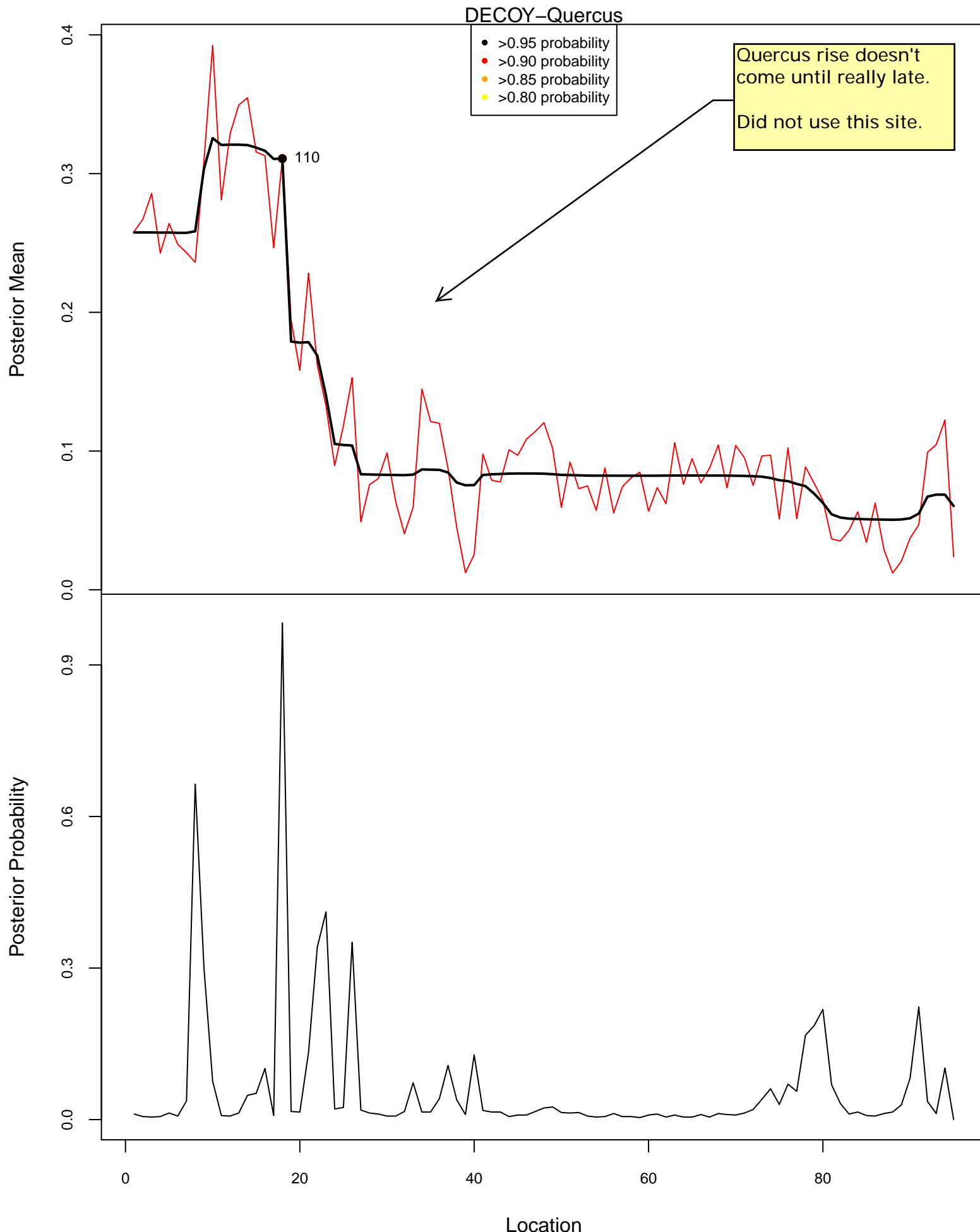


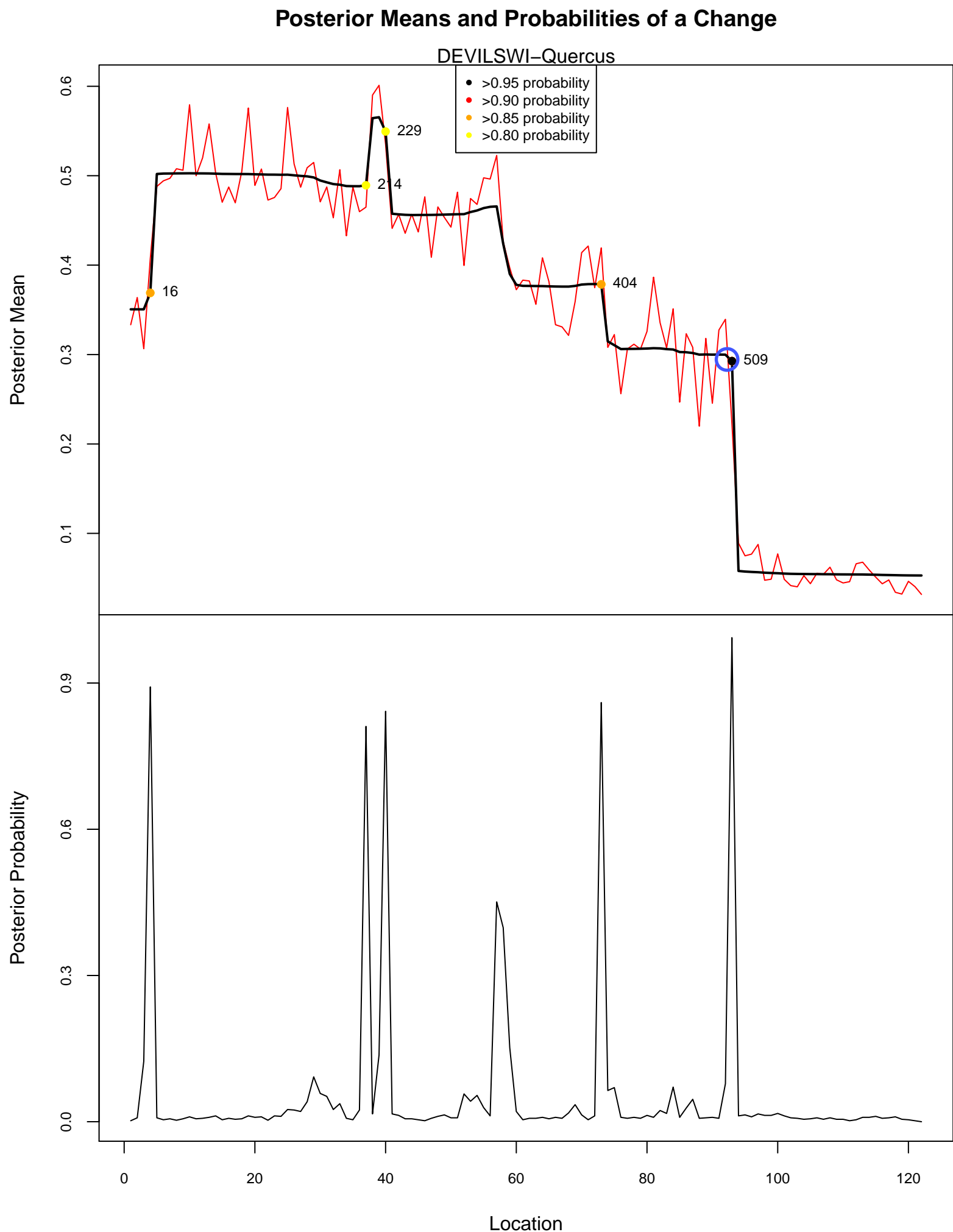
Posterior Means and Probabilities of a Change

CRYSTAL–Quercus



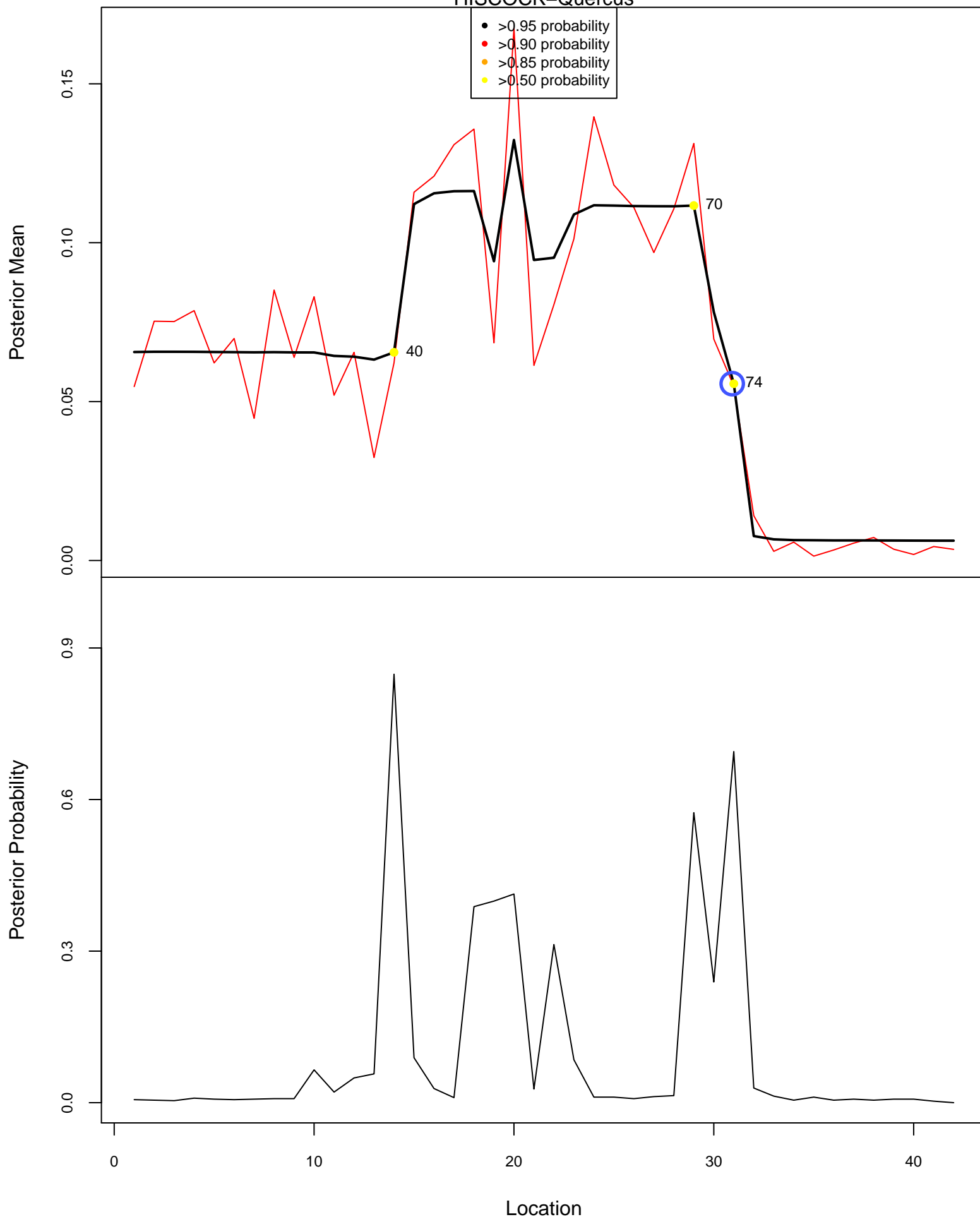
Posterior Means and Probabilities of a Change



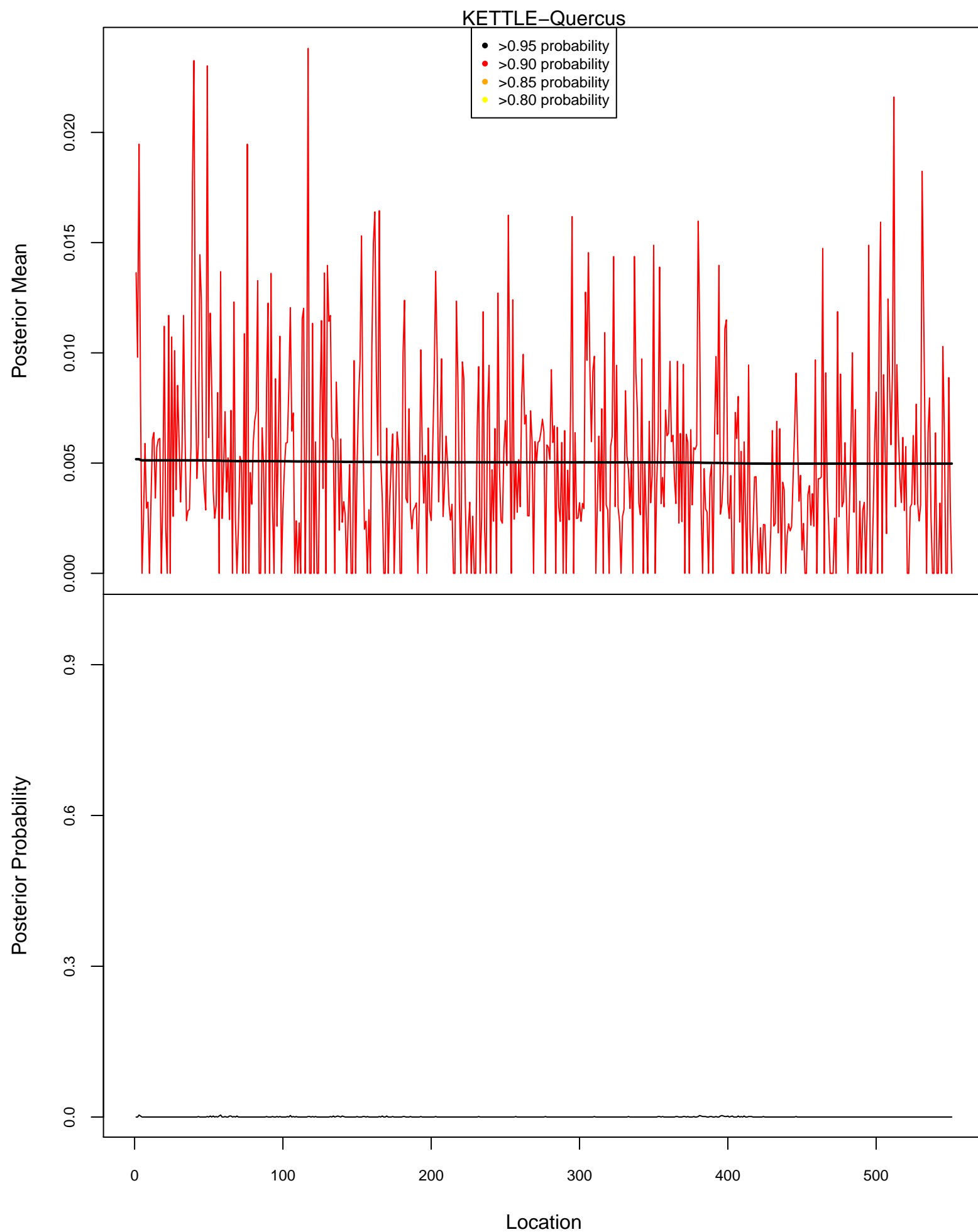


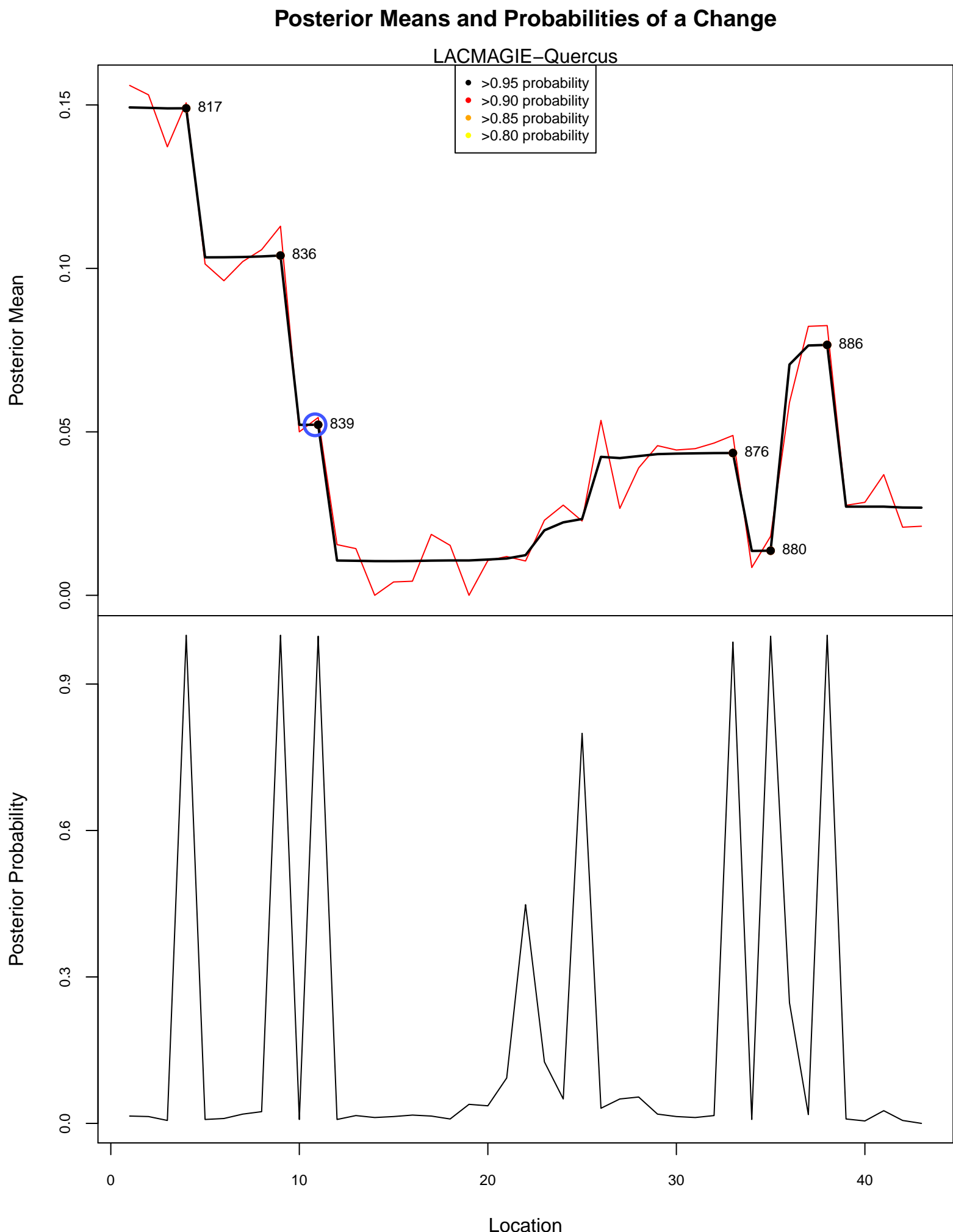
Posterior Means and Probabilities of a Change

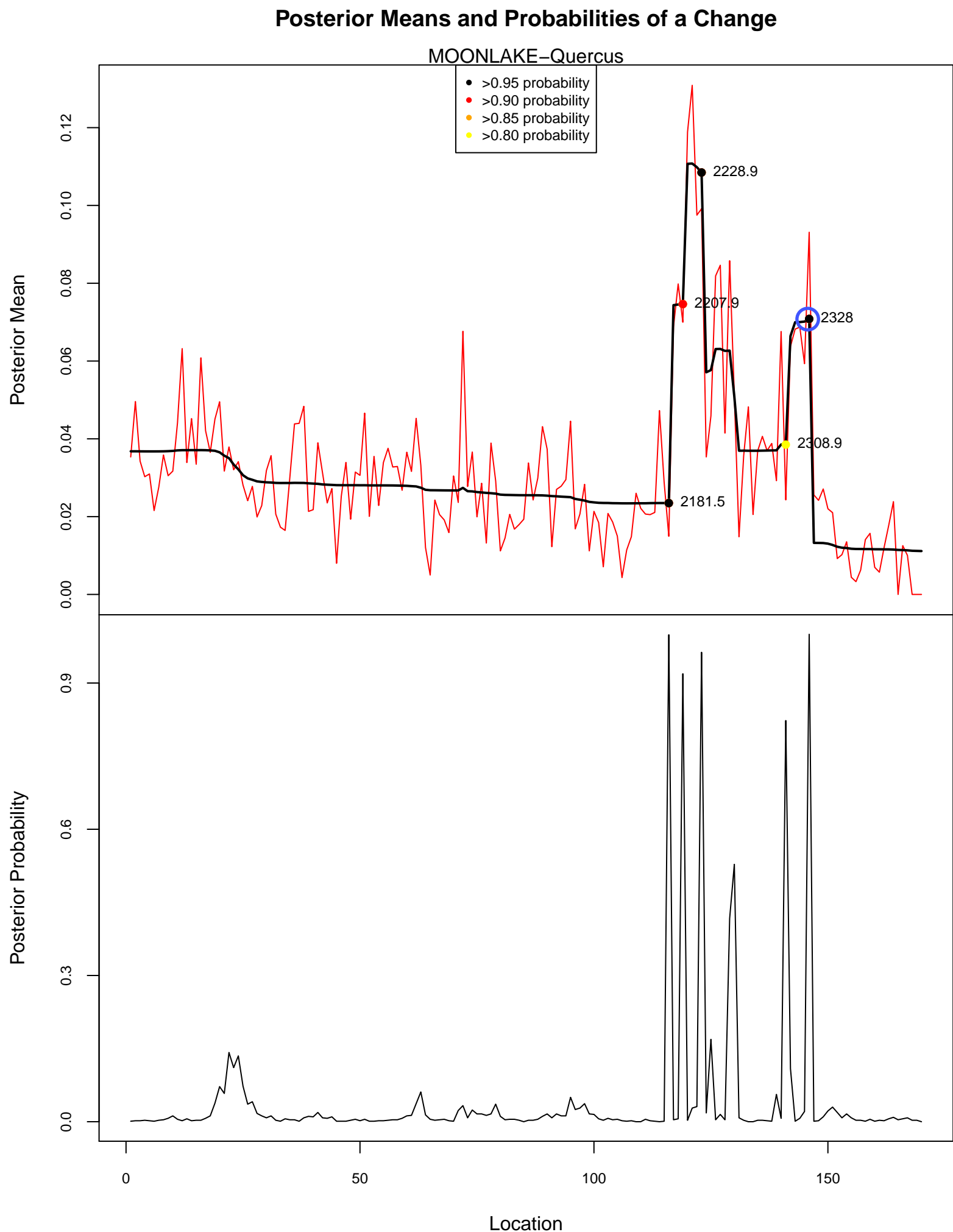
HISCOCK–Quercus

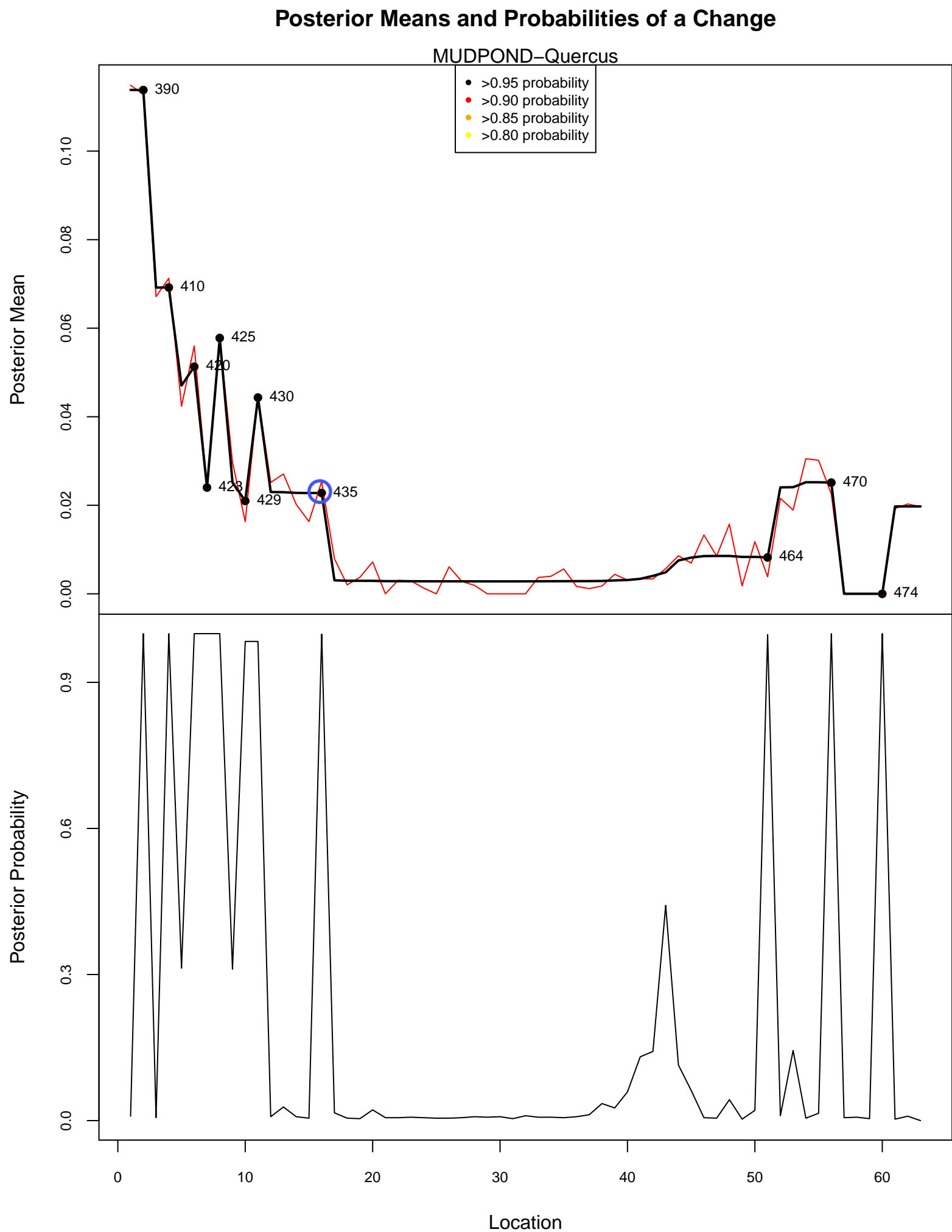


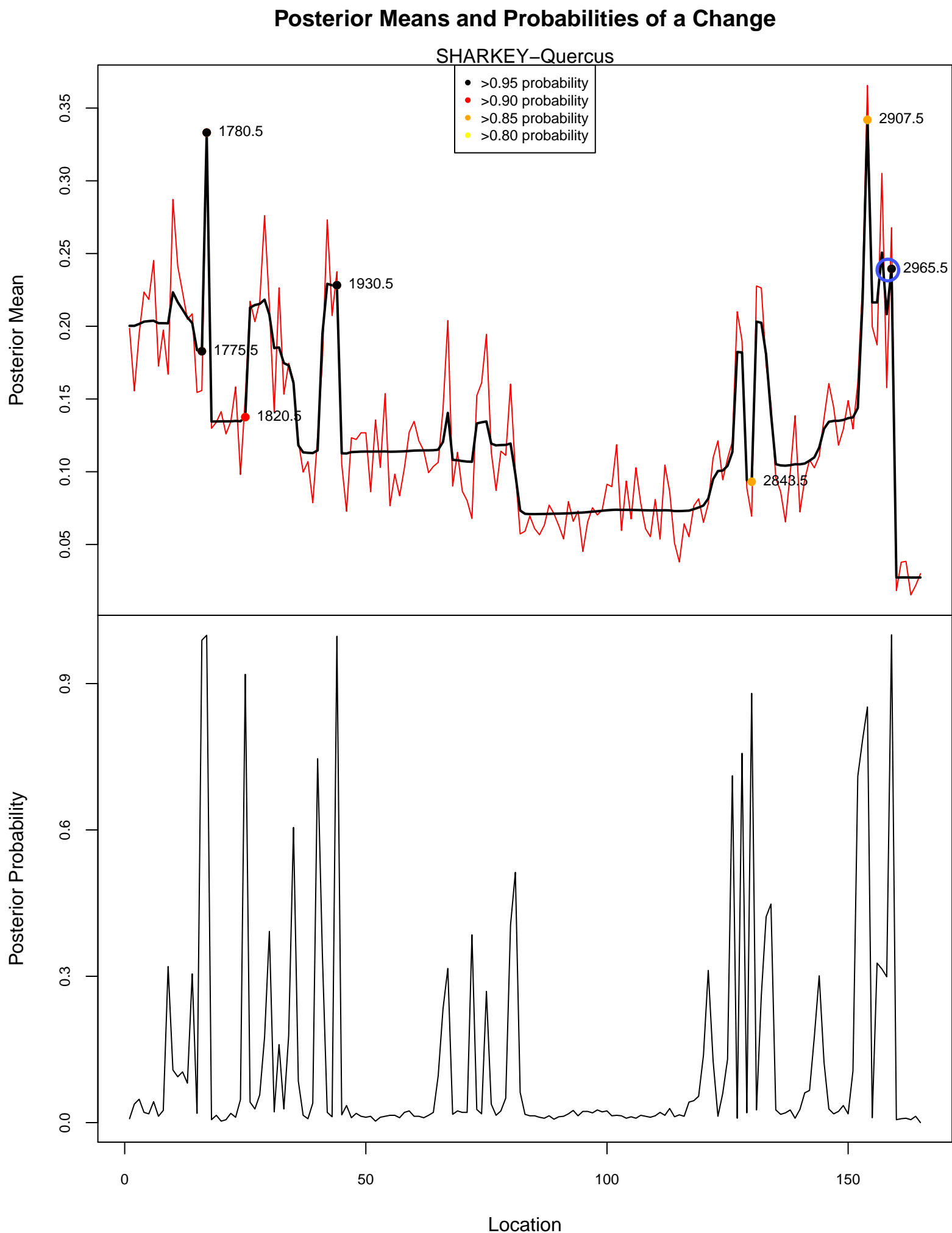
Posterior Means and Probabilities of a Change

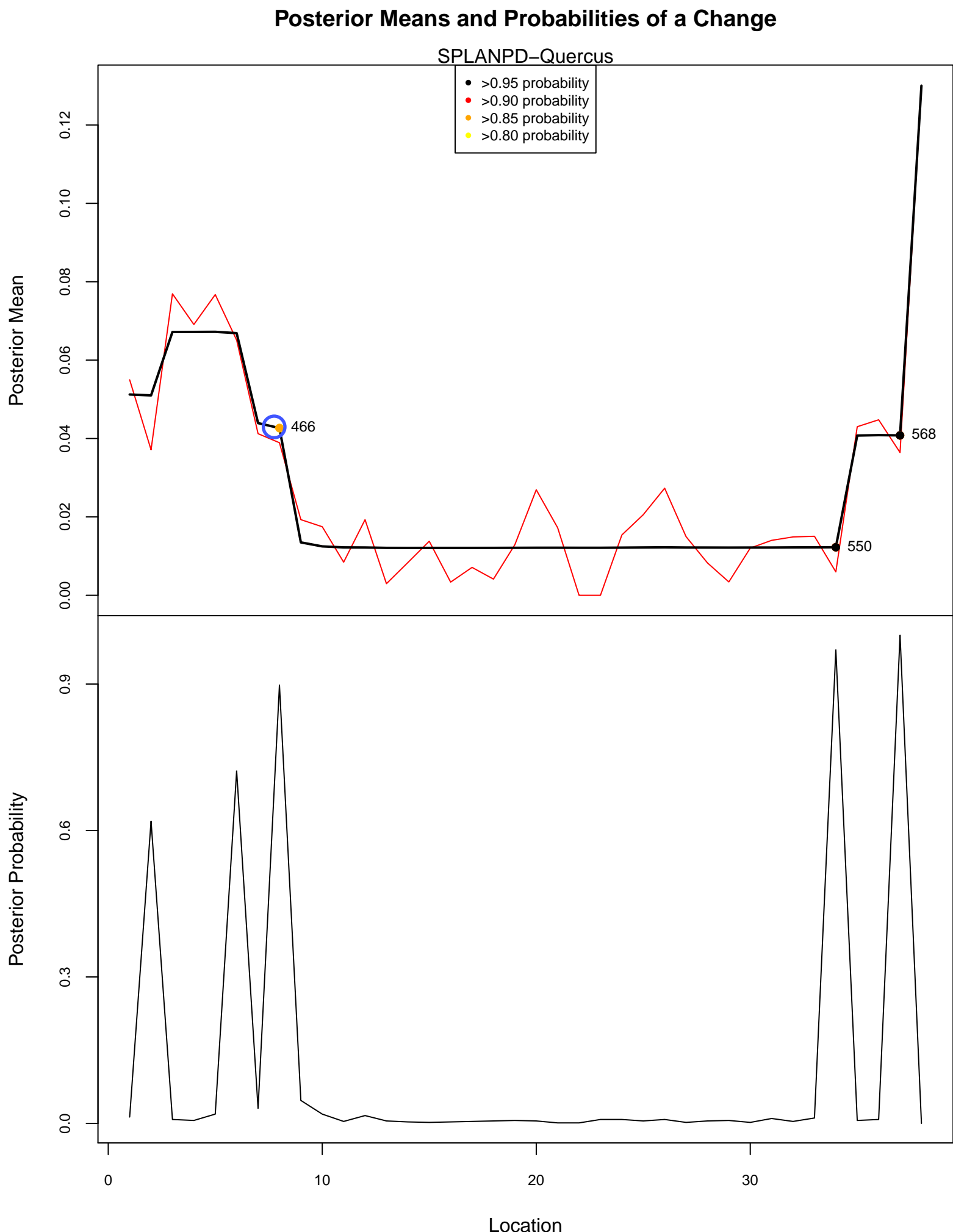


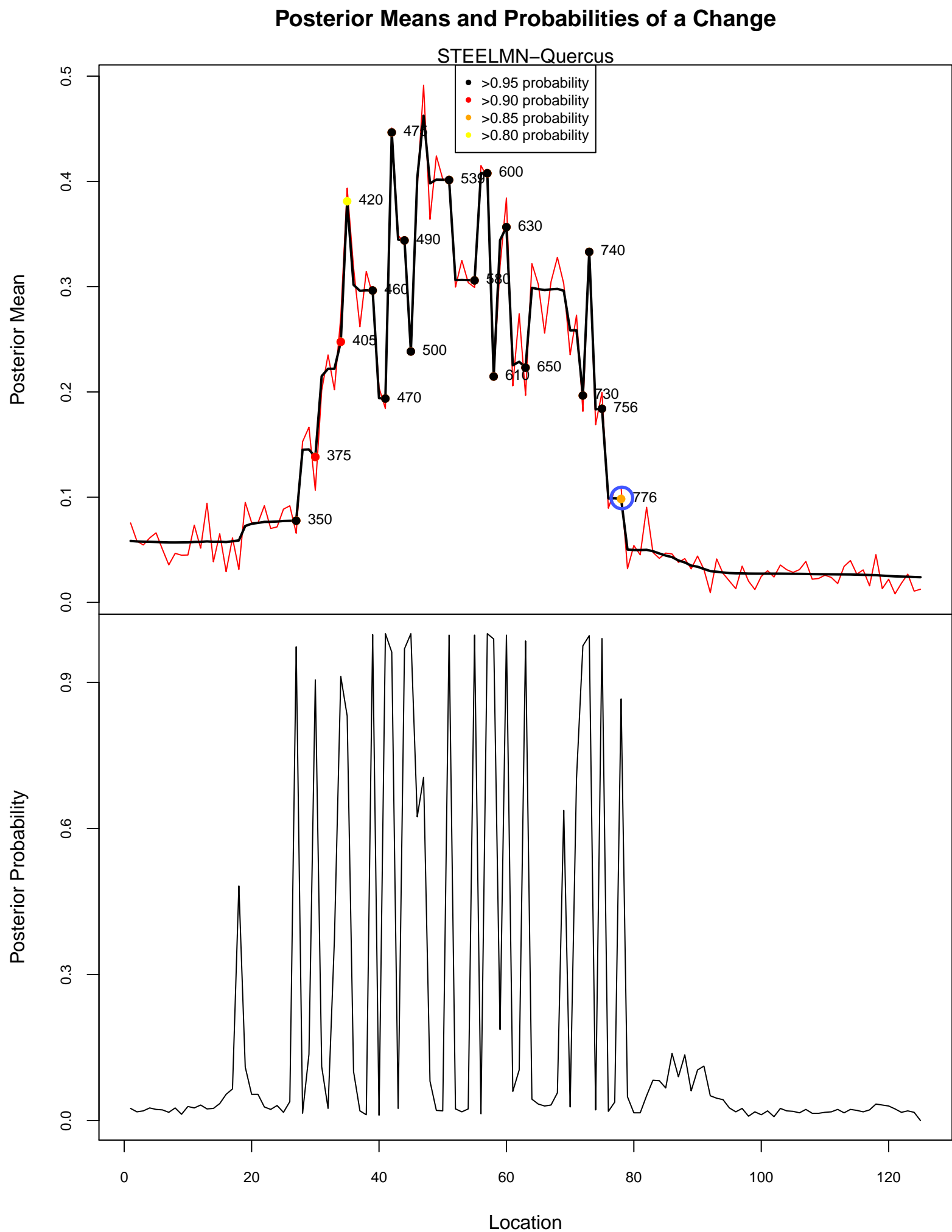




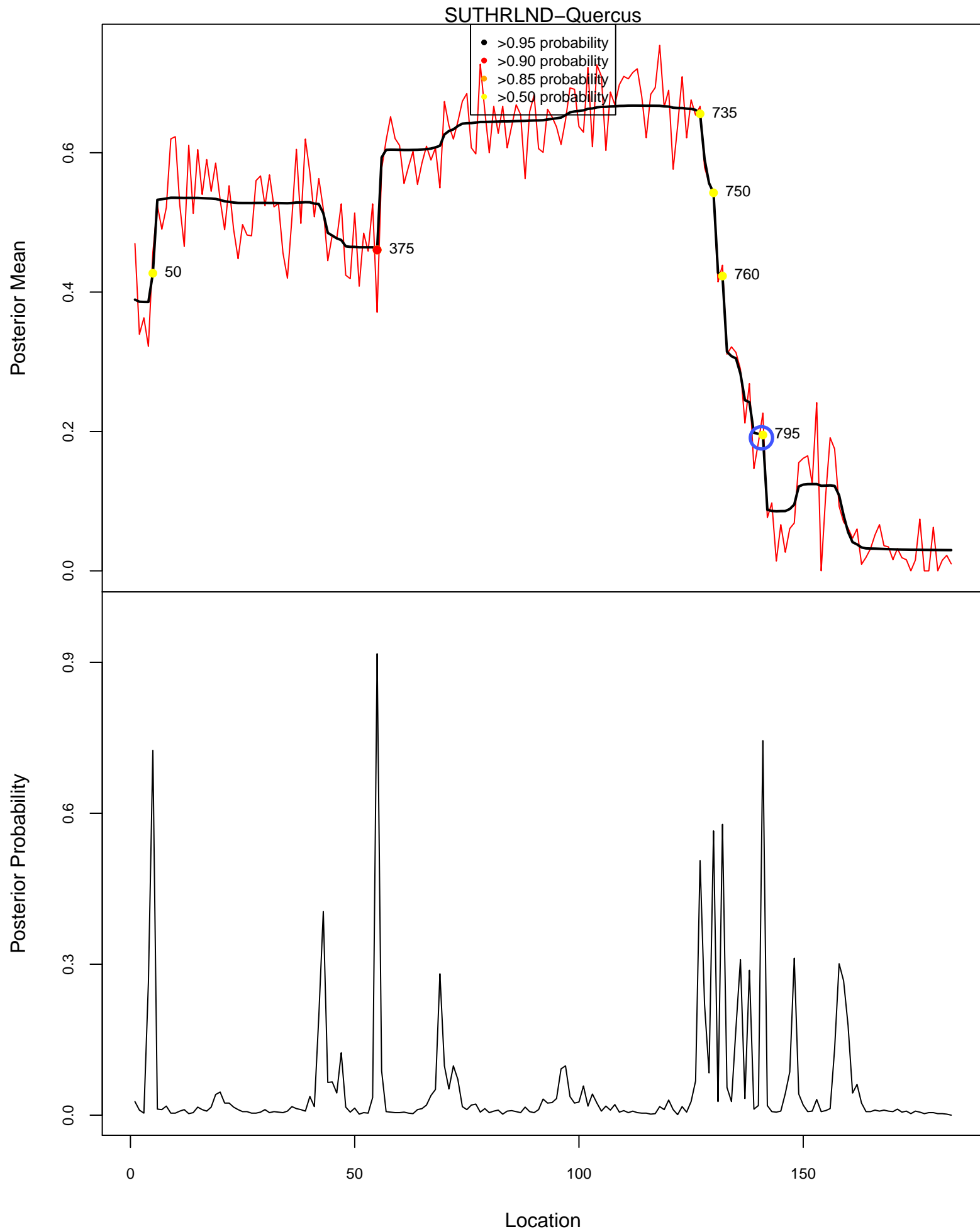






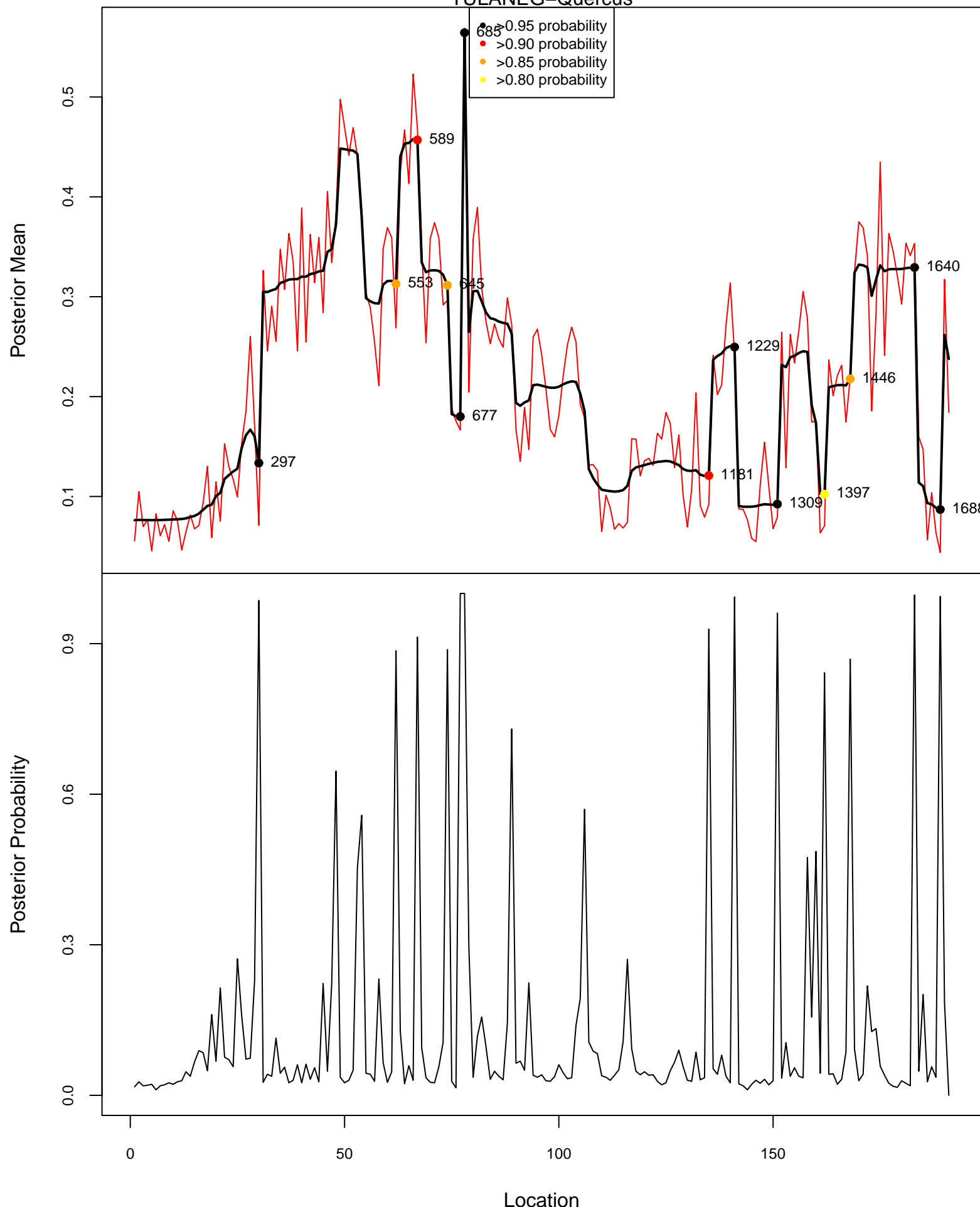


Posterior Means and Probabilities of a Change

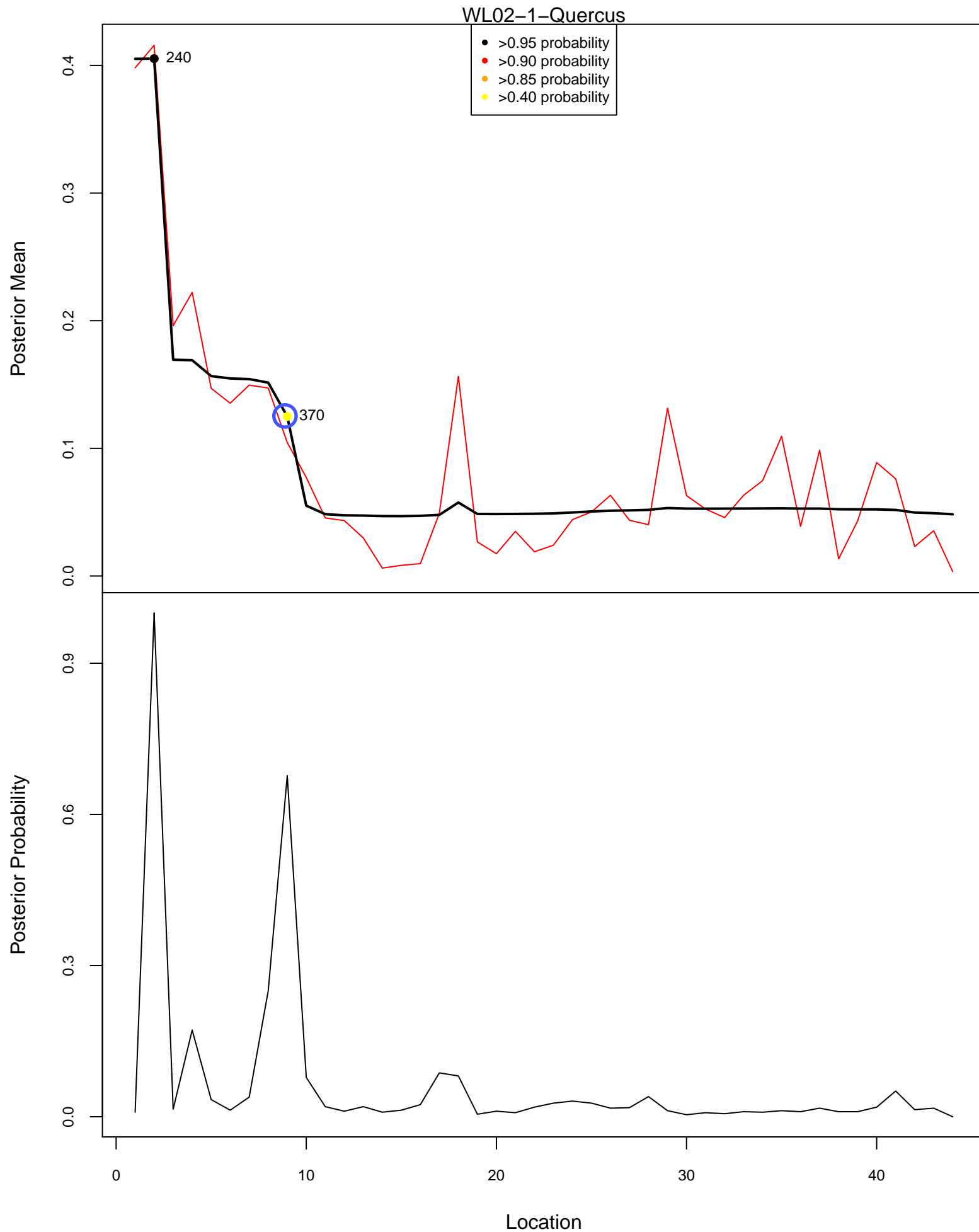


Posterior Means and Probabilities of a Change

TULANE—Quercus



Posterior Means and Probabilities of a Change



Supplementary Code

R code for change point determination, modified change point plots (by depth and by age) and event age interpolation. Please contact the corresponding author for non-pdf versions of these scripts.

```

1 ######
2 ##### READ ME #####
3 #####
4
5 ## This code was written by Jessica Blois for the paper "A methodological framework for ass
6 # This code:
7 # scrolls through the relative abundance dataframe for each site
8 # finds all columns that store the specified taxon
9 # sums the columns if appropriate (eg., you are looking at Pinus spp., it sums data from I
10 # performs Bayesian change point analysis using the R program bcp
11 # plots the resultant change points (using modified code- see annotated files for plot.bcp
12
13 #clear out all objects
14 rm(list=ls(all=TRUE))
15
16 #load necessary libraries
17 library(bcp)
18 library(foreach)
19 library(iterators)
20
21 #Change to the appropriate base directory
22 setwd("X:/HoloceneGoldenSpikes/ChangePoint/change point plots/OtherSites")
23
24 #Set the base directory object
25 wd.base<- "Z:/Research/Williams/blois/NEOTOMA_working/"
26
27 #un-comment depending on whether you want to plot by depth or age
28 source(paste(wd.base, "Rscripts/plot.bcp.mod-depth.r", sep="")) #call bcp.mod
29 #source(paste(wd.base, "Rscripts/plot.bcp.mod-age.R", sep="")) #call bcp.mod3
30
31 sites<- c('BROWNSPD', 'CHASE', 'CHAT2003', 'CLEARPND', 'CONROYME', 'COTTONWD', 'CRYSTAL', 'C
32 taxa<- c("Ulmus", "Picea") #set the taxa you want to plot
33
34 ## code for the benchmark sites, to do it by depth
35 #to do it by age, change pdf file name and change to call bcp.mod3 (line 90)
36
37 for (j in 1:length(taxa)){
38 pdf(file=paste(Sys.Date(), taxa[j], "by.depth.pdf", sep="-"), height=8.5, width=5) #creat
39
40     for (i in 1:length(sites)){
41
42         #read in the data
43         #This uploads the relative data (data as a proportion of the upland sum)
44         #format: sample.depths, sample.ages, taxon1, taxon2, etc.
45         data<- read.csv(paste(wd.base, "SiteFiles/Neotoma1/", sites[i], ".rel.data.csv", se
46
47         #cut out rows with NA values (ie, upland sum=0, so rel.data = 0/0 = NA)
48         rows<- vector(length=0)
49         t<- data[,-(1:2)]
50         for (k in 1:dim(t)[1]){
51             if (all(is.na(t[k,]))) {
52                 rows<- c(rows, k)
53             }
54         }
55
56         #if there are rows with NAs, remove them
57         if (length(rows)>0) {
58             data<- data[-rows,]
59         }
60

```

```

61 #find all columns that contain the taxon name (e.g. Pinus banksiana/P. resinosa, Pi
62 c<- grep(taxa[j], colnames(data), ignore.case=T)
63
64 if (length(c)>0) { #only plot the site if the taxon is found
65
66     #if only one column of data per taxon
67     if (length(c)==1){
68         abund<- data[,grep(taxa[j], colnames(data), ignore.case=T)]
69     }
70
71     #if more than one column of data per taxon, sum the different taxa
72     if (length(c)>1){
73         abund<- rowSums(data[,grep(taxa[j], colnames(data), ignore.case=T)])
74     }
75
76     #Set y limits for plotting
77     lim<- 1
78     if (max(abund, na.rm=T)<=0.25){
79         lim<- 0.5
80     }
81     if (max(abund, na.rm=T)>0.5){
82         lim<- 2
83     }
84
85     #perform the change point analysis
86     probs<- bcp(abund, burnin=100, mcmc=1000, w0=var(abund))
87
88     #plot the change points
89     #use bcp.mod for depth and bcp.mod3 for age
90     plot.bcp.mod(probs)
91     mtext(paste(sites[i], taxa[j], sep="-"), side=3)
92 }
93
94 }
95 dev.off()
96 }
97
98 ## Save the workspace image
99 workspace.file= gsub(":", "-", paste("Workspace-", Sys.time(), ".Rdata", sep=""))
100 save.image(file=workspace.file)

```

```

1 #this creates change point plots that plot the x axis with depth
2 #some other modifications made to separate out the significance levels of different change
3
4 plot.bcp.mod<-
5 function (x, ...)
6 {
7   posterior.prob <- x$posterior.prob
8   posterior.prob[length(posterior.prob)] <- 0
9   op <- par(mfrow = c(2, 1), col.lab = "black", col.main = "black")
10  op2 <- par(mar = c(0, 4, 4, 2), xaxt = "n", cex.axis = 0.75)
11  plot(data$sample.depths, x$data, type="l", col = "red", pch = 20, lwd=2, xlab = "",
12    ylab = "Posterior Mean", main = "Posterior Means and Probabilities of a Change",
13    ...)
14  lines(data$sample.depths, x$posterior.mean, lwd = 1.5) #modified this line to plot by c
15
16 #added this section to add the points to the plot and labels to the points, plus a figure
17 points(data$sample.depths[which(x$posterior.prob>0.80)], x$posterior.mean[which(x$poster
18 points(data$sample.depths[which(x$posterior.prob>0.85)], x$posterior.mean[which(x$poster
19 points(data$sample.depths[which(x$posterior.prob>0.90)], x$posterior.mean[which(x$poster
20 points(data$sample.depths[which(x$posterior.prob>0.95)], x$posterior.mean[which(x$poster
21
22 labs<- paste(data$sample.depths[which(x$posterior.prob>0.80)], data$sample.ages[which(x
23 if (length(labs) > 0) { text(data$sample.depths[which(x$posterior.prob>0.80)], x$poster
24 legend("top", c(">0.95 probability", ">0.90 probability", ">0.85 probability", ">0.80 p
25
26 par(op2)
27 op3 <- par(mar = c(5, 4, 0, 2), xaxt = "s", cex.axis = 0.75)
28 plot(1:length(x$posterior.mean), posterior.prob, yaxt = "n",
29   type = "l", ylim = c(0, 1), xlab = "Location", ylab = "Posterior Probability",
30   main = ""))
31 axis(2, yaxp = c(0, 0.9, 3))
32 par(op3)
33 par(op)
34 }

```

```

1 #this creates change point plots that plot the x axis with age
2
3 plot.bcp.mod3<-
4 function (x, ...)
5 {
6   posterior.prob <- x$posterior.prob
7   posterior.prob[length(posterior.prob)] <- 0
8   op <- par(mfrow = c(2, 1), col.lab = "black", col.main = "black")
9   op2 <- par(mar = c(0, 4, 4, 2), xaxt = "n", cex.axis = 0.75)
10  plot(data$sample.ages, x$data, type="l", col = "red", pch = 20, lwd=2, xlab = "",
11        ylab = "Posterior Mean", main = "Posterior Means and Probabilities of a Change",
12        ...)
13  lines(data$sample.ages, x$posterior.mean, lwd = 1.5) #modified this line to plot by age
14
15 #added this section to add the points to the plot and labels to the points, plus a figure
16 points(data$sample.ages[which(x$posterior.prob>0.60)], x$posterior.mean[which(x$posterior.prob>0.60)])
17 points(data$sample.ages[which(x$posterior.prob>0.70)], x$posterior.mean[which(x$posterior.prob>0.70)])
18 points(data$sample.ages[which(x$posterior.prob>0.80)], x$posterior.mean[which(x$posterior.prob>0.80)])
19 points(data$sample.ages[which(x$posterior.prob>0.90)], x$posterior.mean[which(x$posterior.prob>0.90)])
20
21
22 labs<- paste(data$sample.depths[which(x$posterior.prob>0.60)], data$sample.ages[which(x$posterior.prob>0.60)])
23 if (length(labs) > 0) { text(data$sample.ages[which(x$posterior.prob>0.60)], x$posterior.mean[which(x$posterior.prob>0.60)], labs, pos = 15, offset = 0.5, cex = 0.75) }
24 legend("top", c(">0.60 probability", ">0.70 probability", ">0.80 probability", ">0.90 probability"))
25
26 par(op2)
27 op3 <- par(mar = c(5, 4, 0, 2), xaxt = "s", cex.axis = 0.75)
28 plot(data$sample.ages, posterior.prob, yaxt = "n",
29       type = "l", ylim = c(0, 1), xlab = "Age", ylab = "Posterior Probability",
30       main = "")
31 axis(2, yaxp = c(0, 0.9, 3))
32 par(op3)
33 par(op)
34 }
```

```

1 ##########
2 ##### READ ME #####
3 ##############
4
5 ## This code was written by Jessica Blois for the paper "A methodological framework for ass
6 ## This code was superseded by simpler code for the Holocene benchmark site interpolation.
7
8 ## This code pulls data from all sites in the dataset
9 ## performs interpolation between all benchmark sites (note that gs = golden spike, which i
10 ## uses both thin-plate spine (TPS) and inverse-distance weighting (IDW) methods
11 ## calculates the cross-validation error statistics
12 ## matches the inferred age
13
14 ## Inputs: gs.events, ie, lp.sites
15
16 ## gs.events (read in on lines 131, 133, 135)
17 # this is the main file for analysis
18 # it contains all of the benchmark sites for an event, with the change point depth and age
19 # Format:
20 # id      Handle   Source   golden_spike     Altitude     lon_alb_km   lat_alb_km   depth     age age
21
22 # id= number of site
23 # handle= site name in short form
24 # source= internal column for my own reference (eg. access vs excel)
25 # golden_spike = Is this a benchmark site? holdover column, all are yes
26 # Altitude= altitude in m
27 # lon_alb_km= albers equal area longitude
28 # lat_alb_km= albers equal area latitude
29 # depth= depth of event change point
30 # age= age of event change point
31 # age.range.younger= age range of the younger bounding chron control
32 # age.range.older= age range of the older bounding chron control
33
34 ## ie (Internal-external look-up table) (read in on lines 132, 134, 136)
35 # Format:
36 # Handle i_e
37
38 # Handle= site name
39 # i_e = "i" or "e". Is the benchmark site an "internal" or "external" site?
40
41 # lp.sites (read in on line 143)
42 # this file contains both benchmark and non-benchmark sites
43 # this object is used to establish the interpolation grid (lines 147-150)
44 # it has been trimmed down so that only those sites that meet interpolation criteria remain
45 # site has some chronology information, chronology extends at least partway into the window
46
47 # Format:
48 # id      SiteName     Handle   Longitude    Latitude     Altitude     GeoPolitic   Chronology   Age
49
50 # id= number of site
51 # SiteName= site name
52 # Handle= site name in short form
53 # Longitude= WGS84
54 # Latitude= WGS84
55 # Altitude= meters
56 # GeoPolitic= country
57 # Chronology= Chronology ID from Neotoma (or NA)
58 # AgeType= Radiocarbon vs calibrated years
59 # AgeModel= shape of age model (ie, linear interpolation, 2nd degree polynomial, etc)
60 # AgeBoundYo= younger age bound for the core

```

```

61 # AgeBound0l= older age bound for the core
62 # 21_18= does the chronology extend into the time period 21-18 calibrated years bp? "y" or
63 # 18_145= does the chronology extend into the time period 18-14.5 calibrated years bp? "y"
64 # 145_129= does the chronology extend into the time period 14.5-12.9 calibrated years bp? '
65 # 129_115= does the chronology extend into the time period 12.9-11.5 calibrated years bp? '
66 # 115_105= does the chronology extend into the time period 11.5-10.5 calibrated years bp? '
67 # Source= internal column for my own reference (eg. access vs excel)
68 # lon_alb_km= albers equal area longitude
69 # lat_alb_km= albers equal area latitude
70 # alt_km= altitude, scaled to be comparable to lat/long (see line X)
71
72 ## Outputs:
73
74 # Raw tps ages- the interpolated ages for tps.2d and tps.3d
75 # tps-interpolated.ages.2d.nreps.csv (created on line 217)
76 # tps-interpolated.ages.3d.nreps.csv (created on line 218)
77 # tps-interpolated.ages.csv (created on line 247)
78
79 # Raw idw.ages- the interpolated ages for idw.2d and idw.3d
80 # idw-interpolated.ages.2d.nreps.csv (created on line 219)
81 # idw-interpolated.ages.3d.nreps.csv (created on line 220)
82 # idw-interpolated.ages.csv (created on line 252)
83
84 # Raw cross validation statistics
85 # tps-comparison.csv (created on line 326)
86 # idw-comparison.csv (created on line 327)
87 # tps-comparison-diffs.csv (created on line 339)
88 # idw-comparison-diffs.csv (created on line 352)
89
90 # Error statistics and plots for each method
91 # overall-comparison.csv (created on line 397)
92 # overall-means-comparison.csv (created on line 499)
93 # table2.csv (created on line 517)
94 # pdf: error~orig-parameters.pdf (created on line 421)
95
96
97 ##### START OF CODE #####
98 ##### START OF CODE #####
99 #####
100
101 ## Load required libraries
102   library(sp)
103   library(maptools)
104   library(maps)
105   library(mapproj)
106   library(gstat)
107   library(lattice)
108   library(fields)
109   library(RODBC)
110
111 ## Remove all objects from your workspace
112 rm(list=ls(all=TRUE))
113
114 ##### CHANGE PARAMETERS AND LOAD FILES #####
115 ##### Set the base and gis directories for later use in file names
116   wd<- "X:/Drafts/Framework paper/Analysis/change point/2010-1215/" #path to the working
117   setwd(wd)
118   gis.wd<- "Y:/R plotting/"    #set the path to the gis directory for plotting
119
120 ## set the number of bootstrap replicates for sensitivity analysis

```

```

121 nreps=1000
122
123 ## Set the event you want to look at
124 all.events<- c("picea_decline", "alnus_decline", "quercus_rise")
125 m=1    # 1="picea_decline" 2="alnus_decline" 3="quercus_rise"
126 event<- all.events[m]
127
128 ##### LOAD FILES #####
129
130 ##Load gs.events and Internal-external look-up table
131 if (m==1){gs.events<- read.delim("picea.txt", header=T, sep="\t")
132           ie<- read.csv("PiceaDecline-ext-int-lookup.csv", header=T)}
133 if (m==2){gs.events<- read.delim("alnus.txt", header=T, sep="\t")
134           ie<- read.csv("AlnusDecline-ext-int-lookup.csv", header=T)}
135 if (m==3){gs.events<- read.delim("quercus.txt", header=T, sep="\t")
136           ie<- read.csv("QuercusRise-ext-int-lookup.csv", header=T)}
137
138 ## Convert Altitude from meters to km (*1/1000) and then convert to the space equivalent us
139   gs.events[,5]<-gs.events$Altitude*(1/1000)*600      # this column has already been added
140   colnames(gs.events)[5]<- "alt_km"
141
142 # Load trimmed lp sites from previous save (already has altitude converted)
143 lp.sites<- read.csv("X:/Site files/2010-10-30-trimmed.lp.sites.csv", header=T)
144
145 ##### Set the GS ages file #####
146 #####
147 ## Establish the grid to interpolate the ages to
148 grid<- cbind(lp.sites$id, lp.sites$lon_alb_km, lp.sites$lat_alb_km, lp.sites$alt_km)
149 colnames(grid)<- c("ID", "lon_alb_km", "lat_alb_km", "alt_km")
150 grid<- as.data.frame(grid)
151
152 gs.events.orig<- gs.events  #rename gs.events so I can always access the original data, ev
153
154 ## Pare down the grid to just those sites within the range of the benchmark sites
155 event.grid<- grid[which((grid[, 2] >= (range(gs.events$lon_alb_km)[1]-1)) & (grid[,2] <
156 event.grid<- as.data.frame(event.grid)
157
158 #Create the age limits for the event (the uniform interval)
159   interval.95<- apply(cbind(gs.events$age.range.younger, gs.events$age.range.older), 1, m
160   age.younger<- gs.events$age-interval.95/2
161   age.older<- gs.events$age+interval.95/2
162
163   nmax<- dim(gs.events)[1]
164
165 #####
166 ##### Interpolation #####
167 #####
168
169 #create the blank dataframes to store the replicate tps.ages
170 tps.ages.2d<- matrix(data=0, nrow=dim(event.grid)[1], ncol=nreps)
171 tps.ages.3d<- matrix(data=0, nrow=dim(event.grid)[1], ncol=nreps)
172
173 idw.ages.2d<- matrix(data=0, nrow=dim(event.grid)[1], ncol=nreps)
174 idw.ages.3d<- matrix(data=0, nrow=dim(event.grid)[1], ncol=nreps)
175
176 for (i in 1:nreps){
177
178   #generate a set of ages by sampling from U(age.younger, age.older)
179   ages<- vector(length= dim(gs.events)[1])
180   for (k in 1:dim(gs.events)[1]){

```

```

181     ages[k]<- runif( 1, age.younger[k], age.older[k])
182 }
183
184 ##### TPS INTERPOLATION #####
185 ## Create the basic model and apply to all sites within the lat/long or lat/long/alt limi
186
187     #2D TPS Interpolation with Lat/Long
188 fit.tps .2d<- Tps(cbind(gs.events$lon_alb_km,gs.events$lat_alb_km), ages)
189     #summary(fit.tps.2d)
190
191     #3D TPS Interpolation with Lat/Long/Alt
192 fit.tps .3d<- Tps(cbind(gs.events$lon_alb_km,gs.events$lat_alb_km, gs.events$alt_km), ac
193     #summary(fit.tps.3d)
194
195     ## Predict the tps model to all sites, both benchmark sites and non-benchmark sites
196 tps.ages .2d[,i]<- predict(fit.tps.2d, event.grid[,2:3])
197 tps.ages .3d[,i]<- predict(fit.tps.3d, event.grid[,2:4])
198
199 ##### IDW INTERPOLATION #####
200 ## Create the basic model
201 gs.events.temp<- gs.events
202 gs.events.temp$age<- ages
203
204     #2D IDW Interpolation with Lat/Long
205 fit.idw.2d<- gstat(id= "age", formula = age ~ 1, locations = ~ lon_alb_km + lat_alb_km
206
207     #3D IDW Interpolation with Lat/Long/Alt
208 fit.idw.3d<- gstat(id= "age", formula = age ~ 1, locations = ~ lon_alb_km + lat_alb_km
209
210     ## Predict to all sites within the range of the gs sites
211 idw.ages.2d[,i] <- predict(fit.idw.2d, event.grid[,2:3])$age.pred
212 idw.ages.3d[,i] <- predict(fit.idw.3d, event.grid[,2:4])$age.pred
213
214 }
215
216 #save the raw bootstrap files
217 write.table(tps.ages.2d, file=paste(Sys.Date(), event, "tps-interpolated.ages.2d.nreps.csv")
218 write.table(tps.ages.3d, file=paste(Sys.Date(), event, "tps-interpolated.ages.3d.nreps.csv")
219 write.table(idw.ages.2d, file=paste(Sys.Date(), event, "idw-interpolated.ages.2d.nreps.csv")
220 write.table(idw.ages.3d, file=paste(Sys.Date(), event, "idw-interpolated.ages.3d.nreps.csv")
221
222 #calculate the 95% interval for each row
223 lower.tps.2d<- vector(length=dim(event.grid)[1])
224 upper.tps.2d<- vector(length=dim(event.grid)[1])
225 lower.tps.3d<- vector(length=dim(event.grid)[1])
226 upper.tps.3d<- vector(length=dim(event.grid)[1])
227 lower.idw.2d<- vector(length=dim(event.grid)[1])
228 upper.idw.2d<- vector(length=dim(event.grid)[1])
229 lower.idw.3d<- vector(length=dim(event.grid)[1])
230 upper.idw.3d<- vector(length=dim(event.grid)[1])
231
232 for (j in 1:dim(event.grid)[1]){
233 lower.tps.2d[j]<- quantile(tps.ages.2d[j,], probs = seq(0, 1, 0.025))[2] #corresponds to lo
234 upper.tps.2d[j]<- quantile(tps.ages.2d[j,], probs = seq(0, 1, 0.025))[40] #corresponds to hi
235 lower.tps.3d[j]<- quantile(tps.ages.3d[j,], probs = seq(0, 1, 0.025))[2] #corresponds to lo
236 upper.tps.3d[j]<- quantile(tps.ages.3d[j,], probs = seq(0, 1, 0.025))[40] #corresponds to hi
237 lower.idw.2d[j]<- quantile(idw.ages.2d[j,], probs = seq(0, 1, 0.025))[2] #corresponds to lo
238 upper.idw.2d[j]<- quantile(idw.ages.2d[j,], probs = seq(0, 1, 0.025))[40] #corresponds to hi
239 lower.idw.3d[j]<- quantile(idw.ages.3d[j,], probs = seq(0, 1, 0.025))[2] #corresponds to lo
240 upper.idw.3d[j]<- quantile(idw.ages.3d[j,], probs = seq(0, 1, 0.025))[40] #corresponds to hi

```

```

241 }
242 
243 ## Determine mean and sd, store these ages in 'tps.ages' and "idw.ages" and write to folder
244 tps.ages<- cbind(event.grid, apply(tps.ages.2d, 1, mean), apply(tps.ages.2d, 1, sd), lowe
245 tps.ages<- as.data.frame(tps.ages)
246 colnames(tps.ages)<- c( "ID", "longitude", "latitude", "altitude", "mean.tps.age.2d", "s
247 write.table(tps.ages, file= paste(Sys.Date(), event, "tps-interpolated.ages.csv"), sep="-"
248 
249 idw.ages<- cbind(event.grid, apply(idw.ages.2d, 1, mean), apply(idw.ages.2d, 1, sd), lowe
250 idw.ages<- as.data.frame(idw.ages)
251 colnames(idw.ages)<- c( "ID", "longitude", "latitude", "altitude", "mean.idw.age.2d", "s
252 write.table(idw.ages, file= paste(Sys.Date(), event, "idw-interpolated.ages.csv"), sep="-")
253 
254 #####
255 ##### Cross-validation #####
256 #####
257 
258     ## Create storage matrix for the tps comparison
259 comparison.tps<- matrix(nrow=nmax, ncol=9)
260 comparison.tps<- as.data.frame(comparison.tps)
261 comparison.tps[,1:4]<- tps.ages[match(gs.events$id, tps.ages$ID),1:4]
262 comparison.tps[,5]<- gs.events$age
263 comparison.tps[,6:7]<- tps.ages[match(gs.events$id, tps.ages$ID), c(5,9)]
264 colnames(comparison.tps)<- c(colnames(tps.ages)[1:4], "original.age", colnames(tps.ages)
265 
266     ## Create storage matrix for the idw comparison
267 comparison.idw<- matrix(nrow=nmax, ncol=9)
268 comparison.idw<- as.data.frame(comparison.idw)
269 comparison.idw[,1:4]<- idw.ages[match(gs.events$id, idw.ages$ID),1:4]
270 comparison.idw[,5]<- gs.events$age
271 comparison.idw[,6:7]<- idw.ages[match(gs.events$id, idw.ages$ID),c(5,9)]      #the mean
272 colnames(comparison.idw)<- c(colnames(idw.ages)[1:4], "original.age", colnames(idw.ages)
273 
274 ## Perform cross-validation by sequentially dropping each site
275 for (i in 1:nmax){
276 
277     #drop the site
278     gs.cv<- gs.events[-i,]
279 
280     #generate a set of ages by sampling from U(age.younger.temp, age.older.temp)
281     age.younger.temp<- age.younger[-i]
282     age.older.temp<- age.older[-i]
283     ages<- vector(length= dim(gs.cv)[1])
284     for (k in 1:dim(gs.cv)[1]){
285         ages[k]<- runif( 1, age.younger.temp[k], age.older.temp[k])
286     }
287 
288     #create the blank dataframes to store the replicate tps.ages
289     tps.ages.2d.cv<- matrix(nrow=dim(event.grid)[1], ncol=nreps)
290     tps.ages.3d.cv<- matrix(nrow=dim(event.grid)[1], ncol=nreps)
291     idw.ages.2d.cv<- matrix(nrow=dim(event.grid)[1], ncol=nreps)
292     idw.ages.3d.cv<- matrix(nrow=dim(event.grid)[1], ncol=nreps)
293 
294     for (j in 1:nreps){      #repeat the cv procedure using different ages
295 
296         ## Create the tps model
297         #tps 2D cv
298         fit.tps.2d.cv<- Tps(cbind(gs.cv$lon_alb_km,gs.cv$lat_alb_km), ages)
299         tps.ages.2d.cv[,j]<- predict(fit.tps.2d.cv, event.grid[,2:3])
300         comparison.tps[i,8]<- mean(tps.ages.2d.cv[match(gs.events$id[i], event.grid$ID)

```

```

301
302     if (nmax>6){          #3D TPS CV only works is gs.cv dataframe is longer than 5 sites !
303         #tps 3D cv
304         fit.tps  .3d.cv<- Tps(cbind(gs.cv$lon_alb_km, gs.cv$lat_alb_km, gs.cv$alt_km), 
305             tps.ages  .3d.cv[,j]<- predict(fit.tps.3d.cv, event.grid[,2:4])
306             comparison.tps[i,  9]<- mean(tps.ages.3d.cv[match(gs.events$id[i], event.grid$II
307             }]
308
309     ## Create the idw model
310     gs.cv.temp<- gs.cv
311     gs.cv.temp$age<- ages
312
313     #idw 2D cv
314         fit.idw.2d.cv <- gstat(id= "age", formula = age ~ 1, locations = ~ lon_alb_km
315             idw.ages.2d.cv[,j] <- predict(fit.idw.2d.cv, event.grid[,2:3])$age.pred
316             comparison.idw[i,8]<- mean(idw.ages.2d.cv[match(gs.events$id[i], event.grid$II
317
318     #idw 2D cv
319         fit.idw.3d.cv <- gstat(id= "age", formula = age ~ 1, locations = ~ lon_alb_km
320             idw.ages.3d.cv[,j] <- predict(fit.idw.3d.cv, event.grid[,2:4])$age.pred
321             comparison.idw[i,9]<- mean(idw.ages.3d.cv[match(gs.events$id[i], event.grid$II
322
323     }
324 }
325
326 write.table(comparison.tps, file=paste(Sys.Date(), event, "tps-comparison.csv", sep="-"
327 write.table(comparison.idw, file=paste(Sys.Date(), event, "idw-comparison.csv", sep="-"
328
329     ## Calculate differences between original age and cross-validation age
330     diffss.tps<- matrix(nrow=nmax, ncol=6)
331     diffss.tps<- as.data.frame(diffss.tps)
332     diffss.tps[,1]<- comparison.tps$ID
333     diffss.tps[,2]<- comparison.tps$original.age
334     diffss.tps[,3]<- comparison.tps$original.age - comparison.tps$mean.tps.age.2d
335     diffss.tps[,4]<- comparison.tps$original.age - comparison.tps$mean.tps.age.3d
336     diffss.tps[,5]<- comparison.tps$original.age - comparison.tps$mean.tps.CV.age.2d
337     diffss.tps[,6]<- comparison.tps$original.age - comparison.tps$mean.tps.CV.age.3d
338     colnames(diffss.tps)<- c("ID", "original.age", "tps.age.2d.diff", "tps.age.3d.diff", "t
339     write.table(diffss.tps, file=paste(Sys.Date(), event, "tps-comparison-diffs.csv", sep='
340
341     ## Calculate differences between original age and cross-validation age
342     diffss.idw<- matrix(nrow=nmax, ncol=6)
343     diffss.idw<- as.data.frame(diffss.idw)
344     diffss.idw[,1]<- comparison.idw$ID
345     diffss.idw[,2]<- comparison.idw$original.age
346     diffss.idw[,3]<- comparison.idw$original.age - comparison.idw$mean.idw.age.2d
347     diffss.idw[,4]<- comparison.idw$original.age - comparison.idw$mean.idw.age.3d
348     diffss.idw[,5]<- comparison.idw$original.age - comparison.idw$mean.idw.CV.age.2d
349     diffss.idw[,6]<- comparison.idw$original.age - comparison.idw$mean.idw.CV.age.3d
350
351     colnames(diffss.idw)<- c("ID", "original.age", "idw.interp.age.2d.diff", "idw.interp.ac
352     write.table(diffss.idw, file=paste(Sys.Date(), event, "idw-comparison-diffs.csv", sep='
353
354 ##########
355 ##### Method Comparison #####
356 #####
357
358     ## calculate the difference between the original age and the interpolated/cross-validate
359     overall<- cbind(
360         gs.events$Handle, comparison.tps[, 1:4],                                # 1-5,

```

```

361 comparison.tps$original.age, # 6, "original.age"
362 comparison.tps$mean.tps.age .2d, # 7, "tps.2d"
363 (comparison.tps$mean.tps.age .2d - comparison.tps$original.age), # 8, "tps.2d"
364 comparison.tps$mean.tps.CV.age .2d, # 11, "tps.CV.2d"
365 (comparison.tps$mean.tps.CV.age .2d - comparison.tps$original.age), # 12, "tps.CV.2d"
366 comparison.idw$mean.idw.CV.age .2d, # 13, "idw.CV.2d"
367 (comparison.idw$mean.idw.CV.age .2d - comparison.idw$original.age), # 14, "idw.CV.2d"
368 comparison.tps$mean.tps.age .3d, # 9, "tps.age.3d"
369 (comparison.tps$mean.tps.age .3d - comparison.tps$original.age), # 10, "tps.age.3d"
370 comparison.tps$mean.tps.CV.age .3d, # 15, "tps.CV.3d"
371 (comparison.tps$mean.tps.CV.age .3d - comparison.tps$original.age), # 16, "tps.CV.3d"
372 comparison.idw$mean.idw.CV.age .3d, # 17, "idw.CV.3d"
373 (comparison.idw$mean.idw.CV.age .3d - comparison.tps$original.age), # 18, "idw.CV.3d"
374 (comparison.tps$mean.tps.CV.age .2d - comparison.idw$mean.idw.CV.age.2d), # 19, "tps-j"
375 (comparison.tps$mean.tps.CV.age .3d - comparison.idw$mean.idw.CV.age.3d) # 20, "tps-j"
376 )
377
378 colnames(overall)<- c(
379   "site", "ID", "lon_alb_km", "lat_alb_km", "alt_km", #1-5
380   "original.age", #6
381   "tps.age.2d", #7
382   "tps.2d.interp.error", #8
383   "tps.CV.age.2d", #9
384   "tps.CV.2d.error", #10
385   "idw.CV.age.2d", #11
386   "idw.CV.2d.error", #12
387   "tps.age.3d", #13
388   "tps.3d.interp.error", #14
389   "tps.CV.age.3d", #15
390   "tps.CV.3d.error", #16
391   "idw.CV.age.3d", #17
392   "idw.CV.3d.error", #18
393   "tps-idw-2d.diff", #19
394   "tps-idw-3d.diff" #20
395 )
396 ## write comparison file to folder
397 write.table(overall, file=paste(Sys.Date(), event, "overall-comparison.csv", sep="-"),
398
399
400 ##Create the final dataframes for the appropriate error metrics
401
402 error<- c("idw.CV.2d.error", "idw.CV.3d.error", "tps.CV.2d.error", "tps.CV.3d.error")
403
404 #store the p values for later use in table2
405 pval<- matrix(nrow=5, ncol=4)
406 pval<- as.data.frame(pval)
407 colnames(pval)<- c("IDW-2d", "IDW-3d", "TPS-2d", "TPS-3d")
408 rownames(pval)<- c("P: original age", "P: age range", "P: latitude", "P: longitude", "I")
409
410 # Create "table2" for paper
411 table2<- matrix(nrow=5, ncol=4)
412 table2<- as.data.frame(table2)
413 colnames(table2)<- c("IDW-2d", "IDW-3d", "TPS-2d", "TPS-3d")
414 rownames(table2)<- c("ME", "RMSE", "MAE", "External MAE", "Internal MAE")
415
416 if (nmax<=6){
417   error<- error[1:3]
418 }
419
420 #plot each error statistic against the original age, age range, lat, long, alt to examine

```

```

421 pdf(file=paste(Sys.Date(), event, "error~orig-parameters.pdf", sep="-"), height=8, width=10)
422 orig.error<- interval.95
423 par(mfrow=c(5,1), pch=19)
424
425 for (i in 1:length(error)){
426
427 #Original Age
428 lm<- lm(overall[,grep(error[i], colnames(overall))]-overall$original.age)
429 plot(overall[,grep(error[i], colnames(overall))]-overall$original.age, main=paste("P=", round(anova(lm)$Pr[1], 4)))
430 abline(lm(overall[,grep(error[i], colnames(overall))]-overall$original.age))
431 pval[1,i]<- round(anova(lm)$Pr[1], 4)
432
433 #Original Age Range
434 lm<- lm(overall[,grep(error[i], colnames(overall))]-orig.error)
435 plot(overall[,grep(error[i], colnames(overall))]-orig.error, main=paste("P=", round(anova(lm)$Pr[1], 4)))
436 abline(lm(overall[,grep(error[i], colnames(overall))]-orig.error))
437 pval[2,i]<- round(anova(lm)$Pr[1], 4)
438
439 #Latitude
440 lm<- lm(overall[,grep(error[i], colnames(overall))]-overall$lat_alb_km)
441 plot(overall[,grep(error[i], colnames(overall))]-overall$lat_alb_km, main=paste("P=", round(anova(lm)$Pr[1], 4)))
442 abline(lm(overall[,grep(error[i], colnames(overall))]-overall$lat_alb_km))
443 pval[3,i]<- round(anova(lm)$Pr[1], 4)
444
445 #Longitude
446 lm<- lm(overall[,grep(error[i], colnames(overall))]-overall$lon_alb_km)
447 plot(overall[,grep(error[i], colnames(overall))]-overall$lon_alb_km, main=paste("P=", round(anova(lm)$Pr[1], 4)))
448 abline(lm(overall[,grep(error[i], colnames(overall))]-overall$lon_alb_km))
449 pval[4,i]<- round(anova(lm)$Pr[1], 4)
450
451 #Altitude
452 lm<- lm(overall[,grep(error[i], colnames(overall))]-overall$alt_km)
453 plot(overall[,grep(error[i], colnames(overall))]-overall$alt_km, main=paste("P=", round(anova(lm)$Pr[1], 4)))
454 abline(lm(overall[,grep(error[i], colnames(overall))]-overall$alt_km))
455 pval[5,i]<- round(anova(lm)$Pr[1], 4)
456
457 }
458 dev.off() #close the pdf
459
460 ##### Separate out error at external vs internal sites
461 #Pull out statistics for external and internal sites
462 overall.e<- overall[match(ie$Handle[which(ie$site=="e")], overall$site),]
463 overall.i<- overall[match(ie$Handle[which(ie$site=="i")], overall$site),]
464
465 #calculate error statistics for each separate dataset
466 dataset<- c("overall", "overall.e", "overall.i")
467
468 for (h in 1:length(dataset)){
469   temp<- get(dataset[h])    #temporary dataframe corresponding to overall, overall.e, or overall.i
470   temp.error<- temp[,match(error, colnames(temp))]    #temporary dataframe that just contains error fields
471
472 ## Calculate the mean statistics for the error fields
473 mean.error<- round(colMeans(temp.error), 0)
474
475 abs.mean.error<- round(colMeans(abs(temp.error)), 0)
476
477 abs.sd<- round(apply(abs(temp.error), 2, sd), 1)
478
479 rmse<- vector(length=length(error))
480 for (i in 1:length(error)){

```

```

481     rmse[i]<- round(sqrt(mean((temp.error[i])^2)),1)
482 }
483
484     range<- apply(temp.error ,2, range)
485     range<- t(as.data.frame(range))
486     colnames(range)<- c("min", "max")
487
488     overall.stats<- as.data.frame(cbind(mean.error, rmse, abs.mean.error, abs.sd, range))
489
490 #add a row for consistency if TPS 3d does not work
491 if (nmax<=6){
492 overall.stats<- rbind(overall.stats, rep("NA",5))
493 }
494
495 # assign the overall.stats object to its own name per dataset
496 assign(paste(event, dataset[h], "overall.stats", sep=".") , overall.stats)
497
498 # write comparison files to folder
499     write.table(overall.stats, file=paste(Sys.Date(), event, dataset[h], "overall-means-cc"))
500
501 # store the correct values in table2
502 if (dataset[h] == "overall"){
503     table2[1:3,]<- t(overall.stats[,1:3])
504 }
505 if (dataset[h] == "overall.e"){
506     table2[4,]<- overall.stats$abs.mean.error
507 }
508 if (dataset[h] == "overall.i"){
509     table2[5,]<- overall.stats$abs.mean.error
510 }
511
512 }
513
514 ##add on the p values
515 table2<- rbind(table2, pval)
516
517 write.table(table2, file=paste(Sys.Date(), event, "table2.csv", sep="-"), sep=",", row.names=F)

```